NASA CR-[illegible]

N72-27878

Contract NAS1-10873

Final Report

A Study of System Requirements for Phobos/Deimos Missions

Volume III - Phase II Results - Satellite Sample Return Missions & Satellite Mobility Concepts

June 1972

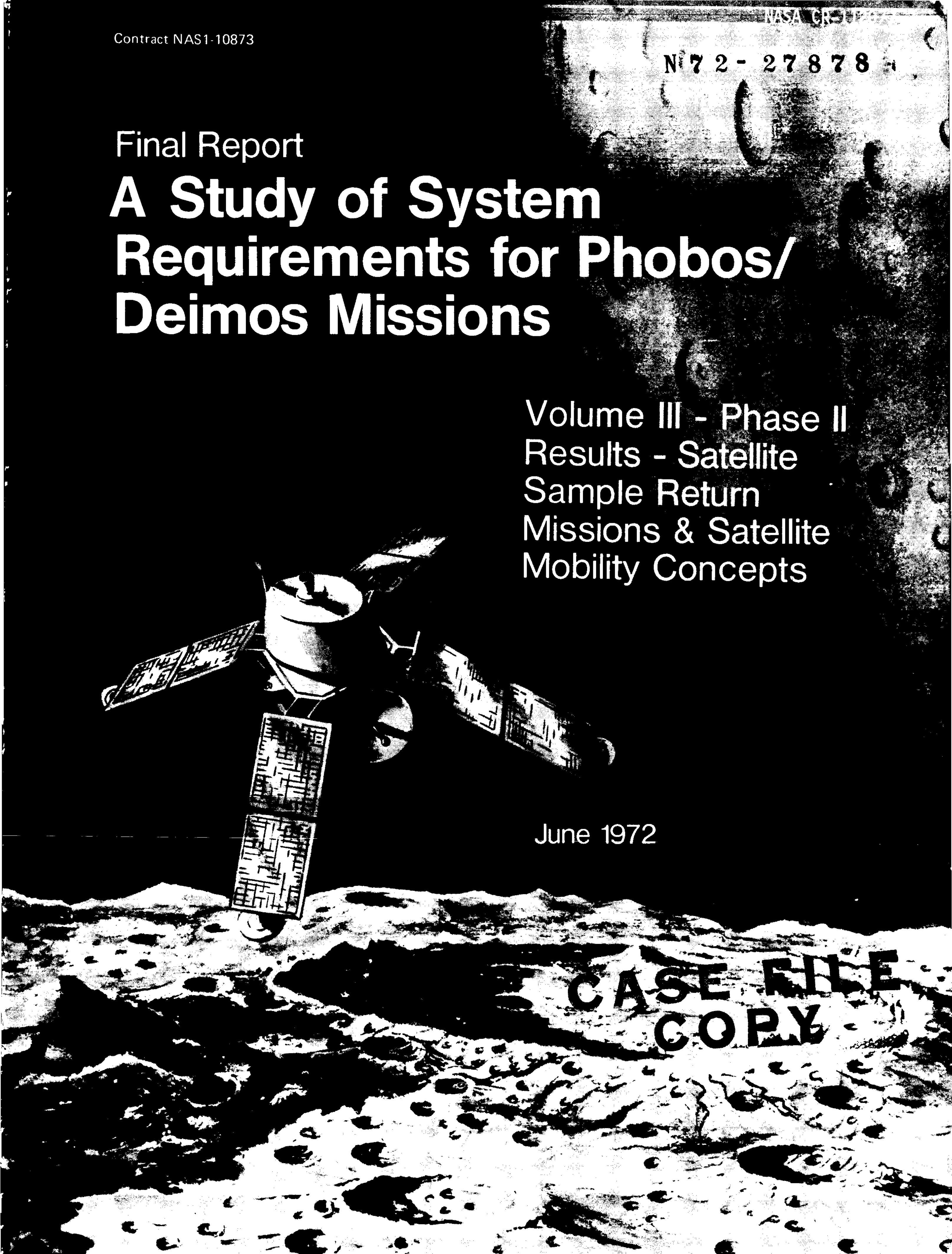

CASE FILE COPY

Contract NAS1-10873

A STUDY OF SYSTEMS REQUIREMENTS FOR PHOBOS/DEIMOS MISSIONS

FINAL REPORT

Volume III

Phase II Results - Satellite Sample Return Missions and Satellite Mobility Concepts

Approved

W. T. Scofield

William T. Scofield
Program Manager

MARTIN MARIETTA CORPORATION
DENVER DIVISION
Denver, Colorado 80121

FOREWORD

This is Volume III of the Final Report on A Study of Systems Requirements for Phobos/Deimos Missions, conducted by the Martin Marietta Corporation.

This study was performed for the Langley Research Center, NASA, under Contract NAS1-10873, and was conducted during the period 4 June 1971 to 4 June 1972. Mr. Edwin F. Harrison of Langley Research Center, NASA, was the Technical Representative of the Contracting Officer. The study was jointly sponsored by the Advanced Concepts and Mission Division of the Office of Aeronautics and Space Technology (OAST) and the Planetary Programs Division of the Office of Space Sciences (OSS) in NASA Headquarters.

This Final Report, which summarizes the results and conclusions of the three-phase study, consists of four volumes as follows:

Volume I	- Summary
Volume II	- Phase I Results - Satellite Rendezvous and Landing Missions
Volume III	- Phase II Results - Satellite Sample Return Missions and Satellite Mobility Concepts
Volume IV	- Phase III Results - Combined Missions to Mars and Its Satellites

ACKNOWLEDGEMENT

Martin Marietta wishes to recognize the contributions of the following NASA individuals to this study:

Edwin F. Harrison of the NASA Langley Research Center, Technical Representative of the Contracting Officer, for NASA management and direction.

E. Brian Pritchard of the NASA Langley Research Center, for general guidance and direction.

James J. Taylor and Nickolas L. Faust of the NASA Manned Spacecraft Center, for information on broken-plane trajectory performance characteristics.

George F. Lawrence of OSS, NASA Headquarters, for technical monitoring and general guidance.

Robert H. Rollins, II of OAST, NASA Headquarters, for technical monitoring and general guidance.

Donald L. Young of the Jet Propulsion Laboratory, (JPL) for supplying data on JPL's space storable propulsion studies.

TABLE OF CONTENTS

PAGE

Foreword ii
Acknowledgements iii
Contents iv
Abbreviations and Symbols xiv

I. Objectives and Study Results I-1
  A. Introduction I-1
  B. Study Objectives and Guidelines I-4
  C. Study Approach I-7
  D. Study Results . . . . I-9 thru I-16

II. Mission Science Objectives and Recommended Payloads . . . II-1
  A. Scientific Objectives II-1
  B. Minimal Science Payloads. II-3
  C. Scientific Significance of Sample Return. . . . . . . II-5 thru II-9

III. Mission Analysis and Design III-1
  A. Performance Analysis III-1
  B. Navigation Analysis . . . . III-18 thru III-56

IV. Phobos/Deimos Phase II-Concept Trade Studies. IV-1
  A. Trade Study Ground Rules and Guidelines IV-2
  B. Earth Return Vehicle Definition IV-3
  C. Sample Return Mission Integration IV-7
  D. Mission Evaluations . . . . IV-10 thru IV-18

Page

V. System Description V-1
- A. System Overview V-1
- B. Sample Return Guidance and Control V-12
- C. Structural Design V-31
- D. Thermal Control V-55
- E. Propulsion V-65
- F. Telecommunication V-83
- G. Power. V-102

VI. Phobos/Deimos Rover Concepts VI-1
- A. Phobos/Deimos Wheeled Rover VI-4
- B. Phobos/Deimos Flying Rover. VI-19
- C. Deployable Boom Instrument Mobility VI-23
- D. Phobos/Deimos Rover Navigation Concept VI-28
- E. Phobos/Deimos Rover Communications VI-35
- F. Mobility Study Conclusions . . . . VI-43 thru VI-46

VII. Program Costs . . . . VII-1 thru VII-4

VIII. Program Schedule . . . . VIII-1 thru VIII-2

IX. Conclusions . . . . IX-1 thru IX-5

Appendix A . . . . A-1 thru A-2

LIST OF FIGURES

Figure		Page
I-1	Comparative ΔV Requirements for Sample Return Missions	I-3
I-2	Baseline Sample Return Configuration	I-10
I-3	Baseline Sample Sequence	I-12
I-4	Preferred Alternate Sample Return Configuration	I-14
I-5	Preferred Alternate Sample Return Sequence	I-15
III-1	Overview of Sample Return Mission	III-7
III-2	Dual Satellite Mission Description	III-17
III-3	Definition of ZAE Angle and DEC Angle	III-22
III-4	Launch/Encounter Variations of ZAE, DEC Angles	III-29
III-5	Sigma vs Sample Histogram	III-52
III-6	Sigma vs Sample Histogram	III-53
III-35	Total Return to Earth ΔV_{STAT} Budget	III-55
V-1	Baseline Sample Return Configuration	V-3
V-2	Preferred Alternate Sample Return Configuration	V-8
V-3	Deflection Maneuvers (Spin Stabilized)	V-13
V-4	Spin Stabilized G&C Subsystem	V-16
V-5	Vehicle Attitudes During Orbital Deflection Maneuver	V-19
V-6	Map of Stars Greater Than Third Magnitude	V-20
V-7	Time Profile of Deflection Maneuver (Three-Axis)	V-23
V-8	Flight Control Subsystem Block Diagram (Three-Axis)	V-26
V-9	Methods of Minimizing Landing Site Alteration	V-30
V-10	Baseline Sample Return Configuration	V-33
V-11	Modified Planetary Explorer Earth Return Vehicle	V-38
V-12	Earth Entry Module	V-41
V-13	Earth Entry Module	V-42

Figure | | Page
V-14 Soil Transfer Unit Installation V-45
V-15 Schematic Transfer Unit Drive V-46
V-16 Preferred Alternate Sample Return Configuration . . V-47
V-17 Earth Return Vehicle (Three-Axis) V-48
V-18 Alternate Sample Return Configuration V-51
V-19 Alternate Sample Return Configuration V-52
V-20 Baseline Thermal Schematic V-62
V-21 Preferred Alternate Thermal Schematic V-63
V-22 Model R-4B Bipropellant Rocket Engine V-67
V-23 Schematic of Modified P.E. Earth Return Propulsion System V-69
V-24 Attitude Control Schematic for Modified P.E. Earth Return Vehicle V-73
V-25 Modified Planetary Explorer Attitude Control Thruster V-75
V-26 Schematic of New Three-Axis Vehicle Propulsion System V-79
V-27 Engine and Gimbal Mounting Arrangement V-81
V-28 New Three-Axis Attitude Control Propulsion Schematic V-82
V-29 Return Vehicle Required Transmitter Power Output vs Antenna Half Power Beamwidth V-95
V-30 Return Vehicle S-Band Communication Subsystem . . . V-97
V-31 Electronically Despun Antenna Option. V-100
V-32 Round Trip Control Module/Lander Configuration. . . V-101
V-33 Solar Panel Output Landed Orbiter V-105
V-34 RTG Power System V-110
V-35 Recovery Package Power Supply V-115
VI-1 Baseline Lander for Phase III Mobility Studies. . . VI-3
VI-2 Phobos/Deimos Wheeled Roving Lander VI-5
VI-3 Wheel Storage/Deployment. VI-7
VI-4 Mobility Configurations VI-6

Figure Page

VI-5 Problem Configuration for Digital Simulation. . . . VI-16

VI-6 Velocity and Slip Outputs VI-17

VI-7 Yaw Perturbations at Obstacle VI-18

VI-8 Phobos/Deimos Flying Rover VI-20

VI-9 Velocity/Altitude Time Curves for Phobos/Deimos Flying Rover VI-21

VI-10 Flying Rover Example. VI-22

VI-11 Extendable Boom Characteristics VI-27

VI-12 Rover Navigation System Block Diagram VI-30

VI-13 Sample of Celestial Sphere From Phobos Surface. . . VI-32

VI-14 Rover Navigation Functional Description VI-34

VI-15 Communication System Geometry, Constraints, and Assumptions VI-36

VI-16 Candidate Communication System Performance. VI-37

VI-17 Phobos Mobility/Communication Interaction VI-39

VI-18 Lander/Orbiter Communication System Performance . . VI-40

VI-19 Communication Profile/Phobos Rover. VI-44

LIST OF TABLES

Table Page

I-1 Study Milestones I-2

I-2 Phase II Study Tasks I-5

I-3 LRC Directed Study Ground Rules I-6

I-4 MMC Derived Study Ground Rules I-6

III-1 Event Sequences and Timing (Earth to Phobos) . III-2

III-2 ΔV Budget (Earth to Phobos). III-3

III-3 Weight Profile (Earth to Phobos) III-4

III-4 Mission Profile Trade Studies. III-6

III-5 Event Sequences and Timing (Phobos to Earth) . III-9

III-6 ΔV Budget (Phobos to Earth). III-10

III-7 Weight Profile (Phobos to Earth) III-12

III-8 Sample Return Payloads for Alternate Years . . III-13

III-9 Earth Orbital Capture vs Direct Entry. III-14

III-10 Solar Electric Propulsion Alternative III-16

III-11 Dual Satellite Payload Capability. III-19

III-12 Rendezvous Dependence on Launch/Encounter Date III-21

III-13 In-Orbit DSN Tracking Errors (1σ) for. . . . . the Baseline Rendezvous to Phobos III-24

III-14 Variation of Knowledge and Control for 1977, 1979 III-25

III-15 Sensitivity of Rendezvous to Encounter . . . . Knowledge and Control Dispersions III-26

III-16 Effect of Control and Knowledge Variations . . on ΔV_{STAT} for Observation Orbit and for Deimos Interception III-28

III-17 Sensitivity of Rendezvous to Phasing and . . . Observation Orbit Knowledge III-31

III-18 Conclusions - Rendezvous Dependence on . . . . Launch/Encounter Date III-32

III-19 Sensitivity to Ephemeris Error III-34

Table Page

III-20 Case Description of 1σ Satellite Ephemeris Errors III-34

III-21 **Maneuver ΔVs for Largest Total ΔV Cases** III-36

III-22 Effect of Execution Error III-36

III-23 Baseline Execution Error Model III-36

III-24 Standard Deviations for Nominal Baseline Maneuvers . . . III-37

III-25 Maneuver Size vs Level of Execution Error. . . III-37

III-26 Rendezvous Sensitivity III-38

III-27 Standard Deviations of Vehicle and Satellite Error After First TV Tracking Arc III-40

III-28 Standard Deviations of Relative State Error After First TV Tracking Arc III-40

III-29 Rendezvous Dependence on Filter Type III-41

III-30 Return to Earth ΔV Budget: Spin vs 3-Axis . . III-43

III-31 Control Velocity Dispersions for Various TEI Pointing Misalignments . . . III-46

III-32 Midcourse Correction ΔV_{STAT} and Control Dispersions: Spin/3-Axis III-47

III-33 1σ Control and Knowledge Dispersions* at Deflection Times . . . III-49

III-34 99.6 Percentile Flight Path Angle (γ) and/ΔV/Dispersions: Spin/3-Axis III-51

IV-1 Earth Return Vehicle Subsystem Trades. IV-4

IV-2 Earth Return Vehicle Trade Results IV-6

IV-3 Sample Return Configurations for Earth Return Vehicle Types IV-8

IV-4 Sample Return Configuration Evaluation IV-11

IV-5 Sample Return Basic Configurations IV-14

IV-6 Overall Relative Cost Comparison by Year . . . IV-16

IV-7 Modified Viking Orbiter Cost Trade Due to Propulsion Options IV-18

Table		Page
V-1	Subsystem Weight & Power Requirements . . . . (Spin Stabilized)	V-18
V-2	Attributes of Three-Axis vs Spin Attitude . . Stabilized Spacecraft	V-22
V-3	Subsystem Weight and Power Requirements . . . (Three-Axis)	V-27
V-4	Round Trip Control Module/Lander. . . . . . . Configuration Weights	V-28
V-5	Baseline Configuration Weight Summary, KGS. .	V-34
V-6	Modified Planetary Explorer Earth Return. . . Vehicle Weight Summary, KGS	V-40
V-7	Earth Entry Module Design Characteristics . .	V-43
V-8	Three-Axis Stabilized Earth Return Vehicle. . Weight Summary, KGS	V-49
V-9	Preferred Alternate Weight Summary, KGS . . . (Round Trip Control Module/Lander)	V-50
V-10	Alternate Configuration Weight Summary, KGS	V-53
V-11	Alternate Configuration Weight Summary, KGS	V-54
V-12	Landing Dynamics Analysis	V-56
V-13	Baseline Thermal Control Approach	V-61
V-14	Sample Return Mission Thermal Control . . . . Summary	V-64
V-15	Modified P.E. Return Vehicle Propulsion . . . System Weight Statement	V-70
V-16	Maneuver Budget & Required Propellant . . . . Expenditure Weight for Modified P.E. Earth Return Vehicle	V-76
V-17	Modified P.E. Attitude Control System Weight	V-77
V-18	New Three-Axis Earth Return Attitude Control System Weight	V-84
V-19	New Three-Axis Attitude Control Gas . . . . . Requirements	V-85
V-20	Required Communication Links	V-86

Table		Page
V-21	Video Transmission Capability	V-89
V-22	Video Transmission Capability	V-90
V-23	Antenna/Transmitter Power Trade-Offs	V-91
V-24	Telemetry Design Control	V-93
V-25	Telemetry Design Control	V-94
V-26	Telemetry Design Control	V-96
V-27	P.E. Type Return Vehicle Communications . . . Subsystem	V-98
V-28	Baseline Configuration.	V-103
V-29	Baseline (Spin-Stabilized) Configuration. . . Power Summary (Watts) Mars to Earth	V-107
V-30	Alternate Configuration	V-109
V-31	Preferred Alternate Configuration Power . . . Summary (Watts) Earth to Mars	V-111
V-32	Preferred Alternate Configuration Landed. . . Operations Power Summary (Watts)	V-112
V-33	Preferred Alternate Configuration . . . . . . (Three-Axis Stabilized) Power Summary (Watts) Mars to Earth	V-113
VI-1	Rover Operating Environment	VI-2
VI-2	Rover Digital Simulation Model - Inputs . . .	VI-15
VI-3	Extendable Boom Parameters	VI-24
VI-4	Communication System Characteristics	VI-41
VI-5	Comparison of Direct Link vs Relay . . . . . Through Orbiter Communication System Performance	VI-42
VII-1	Costing Ground Rules.	VII-2
VII-2	Cost Summary-Baseline Sample Return Mission	VII-3
VII-3	Cost for One Flight Article With . . . . . Minimum Spares ($ in Millions)	VII-4
VIII-1	Phobos Sample Return Mission	VIII-2
IX-1	Recommendations for Supporting Research . . and Technology	IX-1

ABBREVIATIONS AND SYMBOLS

a	orbit semi-major axis
ACS	attitude control system
ARU	attitude reference system
Ax, Ay, Az	body acceleration
Az	azimuth angle
bps	bits per second
CC&S	control computer and sequencer
cg	center of gravity
db	decibel
DLA	declination of launch asymptote
DSN	Deep Space Net
DSS	Deep Space System
EL	elevation angle
ETC	engineering test capsule
$F1_c$, $F2_c$, $F3_c$, FN_c	lander engine thrust command
FOV	field of veiw
g	acceleration due to gravity, Earth
G&C	guidance and control
GCSC	guidance, control and sequencing computer
grms	gravity (rms)
HZ	hertz
i	orbit inclination
IRU	inertial reference unit
JPL	Jet Propulsion Laboratory
kbps	kilobits per second
km	kilometers
L/E	launch/encounter

LOS	line-of-sight
LPCA	lander pyrotechnic control assembly
LRC	Langley Research Center
mbps	megabits per second
MCC	midcourse correction
MLI	multilayer insulation
MMC	Martin Marietta Corporation
MOI	Mars orbit insertion
NASA	National Aeronautics and Space Administration
NW	net load factor times weight
OSR	optical solar reflector
p, q, r	body attitude rates
PTC	proof test capsule
PTO	proof test orbiter
R	range
$\dot{R}$	range rate
RCS	reaction control system
RF	radio frequency
RSS	root-sum-of-squares
RTG	radioisotope thermoelectric generator
R99	99 percentile closest approach radius
S/C	spacecraft
TA	orbit true anomaly
TEI	trans-Earth injection
T/M	thrust-to-mass
TMI	trans-Mars injection
TWTA	traveling wave tube amplifier
UHF	ultra-high frequency
UV	ultraviolet
VHE	hyperbolic excess velocity

VM	velocity meter
VO	Viking Orbiter
VRU	velocity reference unit
W	weight

α	solar absorptivity
ΔV	delta velocity
ΔV_{STAT}	navigation uncertainty delta velocity
ε	orbit eccentricity
θ	pitch attitude angle
π	3.1416
ρ	density
σ	standard deviation
ϕ	roll attitude angle
ψ	yaw attitude angle
μ_{MARS}	Mars central gravity potential constant
Ω	Mars longitude of ascending node
ω	Mars argument of periapsis
$\sim$	approximately

I. Objectives and Study Results

I. OBJECTIVES AND STUDY RESULTS

A. INTRODUCTION

This report, in four volumes, contains the results of a nine-month, three-phase study conducted for the Langley Research Center to evaluate the systems requirements to accomplish Phobos/Deimos missions in the 1977-1983 time period.

The study was initiated in June 1971, under NASA Contract NAS1-10873. The study milestones are summarized in Table I-1. The study was based on a succession of three phases that allowed a logical progression from the straight-forward rendezvous and landing satellite mission conducted during Phase I to a more meaningful sample return mission performed during Phase II, and finally culminating in a highly cost effective combined Mars landing and Phobos/Deimos mission studied during Phase III. Each succeeding phase effort built upon the results of the previous phase to a large degree. For example, the original concept of missions to the Martian satellites was developed by Messrs. Pritchard and Harrison of the NASA Langley Research Center. They demonstrated the technical feasibility of such space missions in a preliminary mission design that became the basis for the system study performed during Phase I. Using this basic knowledge then, we generated basic data on mission analysis and spacecraft system requirements during Phase I which we applied to alternate mission concepts during Phases II and III in a search for the most cost effective Phobos/Deimos exploration approach.

Table I-1 Study Milestones

Preliminary Mission Design by NASA/LRC-MAAB	January 1971
Systems Definition Study Contract to MMC	June 4, 1971
Phase I - Landing Roving Mission	June 4, 1971 thru September 9, 1971
First Presentation	September 9 & 10, 1971
Phase II - Sample Return Mission	September 13, 1971 December 9, 1971
Second Presentation	December 9 & 10, 1971
Phase III-Combined Mars and Phobos/Deimos Mission	December 13, 1971 thru April 6, 1972
Third Presentation	April 6 & 7, 1972
Final Report	May 5, 1972

Since the results of the Phase I study demonstrated that a Phobos/Deimos mission was both technically feasible and practicable, requiring only minimal modifications to be made to the Mars Viking spacecraft, the Phase II study effort addressed itself to studying a more potentially valuable mission to the Martian satellites. The contract Technical Monitor reasoned that a Phobos or Deimos sample return mission, if it could be accomplished in a cost effective manner, might be a very attractive element in a balanced NASA program of planetary exploration. There are several reasons why this might be true: as Mr. Harrison, our Technical Monitor pointed out in Reference I-1, it is the easiest sample return mission to perform, in terms of propulsive performance, in our solar system. This comparison is shown in Figure I-1. The second reason is that an understanding of the origin and evolution of the Mars satellites is very difficult if not impossible to answer by conducting only in-situ science investigations. Another reason for considering these missions is that

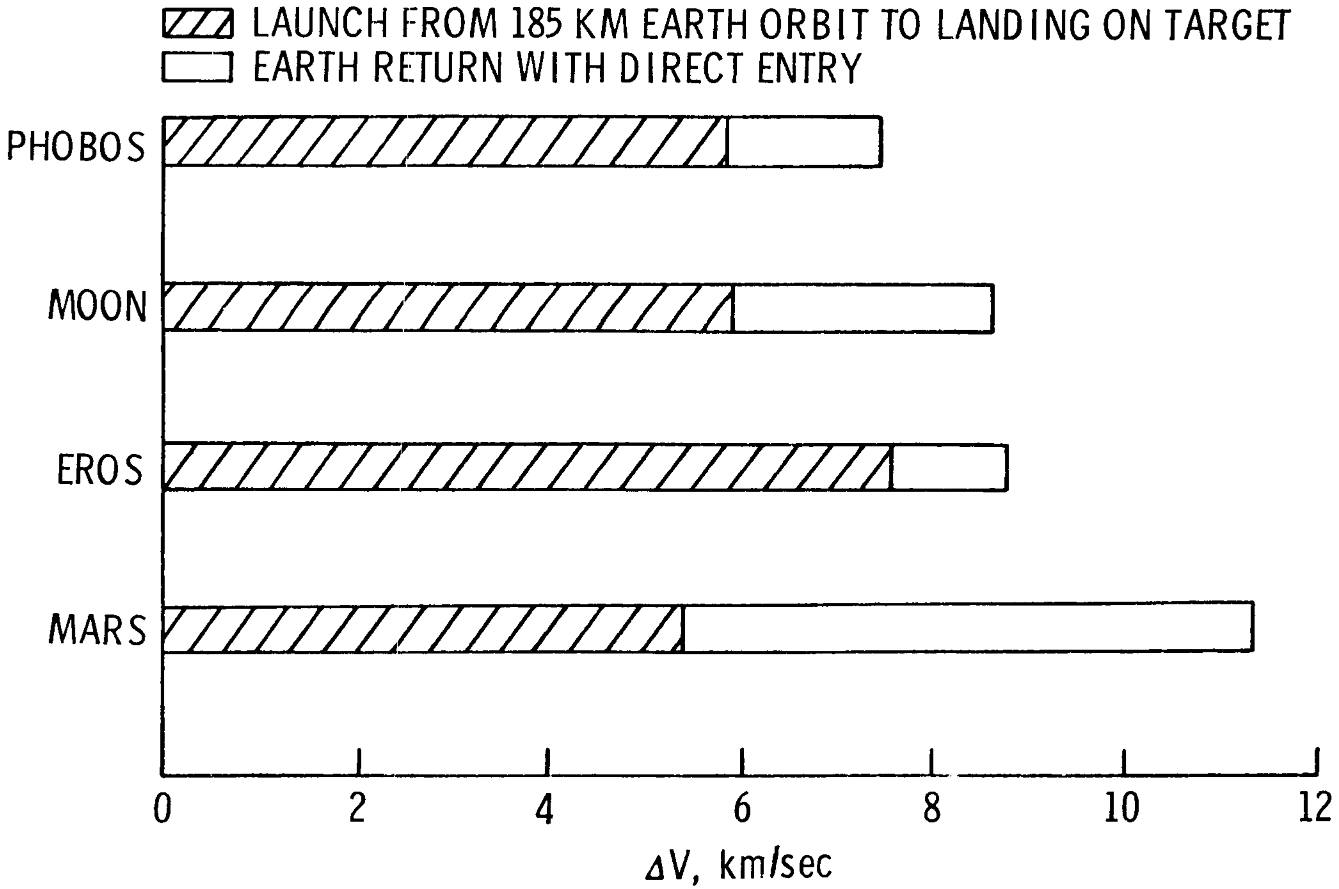

Figure I-1 Comparative ΔV Requirements for Sample Return Missions

the probability of back-contamination of the Earth's biosphere with extraterrestrial organisms is much lower for this mission than for a Mars sample return while the results could still provide good insight into the origin and evolution of Mars.

Throughout the Phase II study effort, numerous mission and system options were considered and either a trade study was used to determine the best option, or the relevant factors were considered and a conscious decision was made to use that particular mode. These studies and analyses are documented in the appropriate study phases in which they were performed.

The result of the mission and system trade studies led to the definition of a recommended baseline system and a leading alternate system. Both systems are described in detail in the following chapters. Associated cost and schedule data were also generated for the baseline mission.

B. STUDY OBJECTIVES AND GUIDELINES

The objective of the Phase II study effort was to establish relative cost, performance and development risk estimates, and subsystem implementation requirements for a number of alternate mission/system concepts and to select a baseline concept for further definition. In configuring the individual subsystems, our approach, in concert with our Phase I studies, was to use existing qualified systems and hardware from programs already in being or in the planning stage, wherever feasible, and the Viking systems in particular. Associated costs and schedule data were then formulated around the baseline design.

At the conclusion of the Phase I studies, several areas--in particular the navigation strategy and the definition of what the minimum Phobos/Deimos science requirements would be--appeared to offer potential for further optimization. Accordingly, these areas were examined in more detail during this study phase.

Some of the more detailed study tasks that were performed in meeting the study objectives are summarized in Table I-2.

Table I-2 Phase II Study Tasks

- Analyze sample return performance and navigation requirements.
- Re-examine minimum Phobos/Deimos science requirements.
- Complete Phase I navigation analyses.
- Compare application of solar electric propulsion (performance capability only) for sample return missions.
- Examine possibility of conducting dual satellite mission.
- Compare alternate satellite landing schemes.
- Perform trade-off studies of spacecraft configuration concepts.
- Develop landed mobility concepts.
- Define systems and subsystems for baseline configuration.
- Develop schedule and cost estimates.

Ground rules and guidelines were jointly established by the Langley Research Center and the MMC Phobos/Deimos study team just prior to the initiation of the Phase II study. These ground rules are summarized in Table I-3. Also, as preliminary results of the study were developed, a series of study generated ground rules evolved. These ground rules are tabulated in Table I-4.

Table I-3 LRC Directed Study Ground Rules

- Launch vehicles considered: Titan IIIC, Titan IIIE/Centaur, Titan IIIE7/Centaur and Shuttle/Centaur.
- Launch opportunities shall be from 1977 to 1983.
- Type I and II transfer trajectories to be considered.
- Dual satellite missions to be considered.
- Alternate mobility concepts to be evaluated.
- Design mission around returning a sample weight of 5 kgs.
- Apply proven hardware and technology.
- Minimize overall program costs.

Table I-4 MMC Derived Study Ground Rules

- Titan IIIE/Centaur launch system.
- 1981 launch opportunity.
- Type II transfer trajectory for both Earth-Mars and Mars-Earth.
- Earth launch window of 30 days.
- Two launches with spare spacecraft.
- Sample recovery at Earth is direct entry with sea recovery.
- "Stretched" Viking '75 Orbiter (38% propellant increase).
- No sterilization requirement.

C. STUDY APPROACH

The overall approach in conducting the study effort followed very closely the methodology that was used in performing the Phase I study.

The automated Phobos/Deimos sample return mission is complex and demanding in concept. The mission objectives require a roundtrip to the surface of the Martian satellites with an automated spacecraft. The return spacecraft must be designed to perform perfectly after up to two years of "storage" in an interplanetary and remote satellite environment.

The trade studies that were conducted then, were aimed at meeting this challenge with lightweight, minimum cost, low risk technology systems. The large array of mission modes and system options available for consideration produce a very large number of potential mission/system approaches worthy of investigation. This required that the study approach be designed to provide early definition of the many potential mission/system approaches and a means for consistent screening and evaluation of alternates to arrive at the most promising concepts for further detailed analysis. Maximum utilization of our Phase I launch vehicle and Phobos/Deimos orbiter delivery system definitions was made which allowed us to concentrate our efforts on the definition of the earth return spacecraft during Phase II. Once the most promising mission/system approaches were identified, the remainder of the study was devoted primarily to systems analysis and conceptual design of these candidate baseline concepts. A comparative evaluation of the baseline mission/system candidates based on point design results was then used to select a recommended Phobos/Deimos sample return baseline concept and leading alternative.

A comprehensive analysis was performed to establish Phobos/Deimos sample return mission science objectives and requirements, and to select experiments and associated instrumentation for the system. The mission environmental criteria developed during the Phase I study (Appendix A of Volume II) were utilized to guide the mission/system design.

Another major effort during the Phase II studies was to study in detail the three mobility concepts that were defined during Phase I: wheeled rovers, flying rovers, and long furlable booms.

Wheeled systems are the most conventional of the three concepts considered. However, the low gravity makes possible the use of large diameter, lightweight wheels which give the rover high obstacle performance capability with a mobility subsystem weight (approximately 12 kg) well below that required for similar performance on a Lunar or Mars rover.

A flying rover is attractive since low ΔVs are required for ballistic hops in the low-g environment and no totally new subsystems must be added to achieve post-landed mobility. Weight charged to flying mobility would include larger tanks and fuel loads and reusable shock absorbers in the landing legs.

Furlable booms are the third concept considered, such systems having significantly greater range per unit weight than booms used in higher-g environments. Although booms only provide access to the lander's immediate surroundings, such science mobility may be desirable on a simple first mission or in the event extreme surface irregularities prevent lander mobility.

D. STUDY RESULTS

This section summarizes the baseline mission/system as developed during the Phase II studies. More detailed descriptions and discussions of the options and trade studies that were considered appear in the appropriate sections of this report.

1. Baseline Mission/System Concept Description

The selected baseline launch opportunity is a 1981 launch from Earth with a 1982 arrival at the vicinity of Mars. The launch vehicle is the Titan IIIE/Centaur. The Earth-to-Mars portion of the mission is basically the same as the 1979 launch of Phase I.

Type II trajectories were again selected for mission design purposes for both the outbound leg (Earth-to-Mars) and the inbound leg (Mars-to-Earth) of the mission.

The Phobos/Deimos sample return spacecraft as shown in Figure I-2 consists of two major components: a modified landed Viking Orbiter with a 38% propulsion system stretch, basically the same configuration as our alternate Phase I vehicle, and a modified Planetary Explorer earth return vehicle. The orbiter dry weight is 972.3 kg. This, together with 1928 kg of propellant, gives a total loaded weight of 2900 kg. The loaded weight of the modified Planetary Explorer earth return vehicle is approximately 197 kgs. This includes a 13.6 kg earth entry module. Total injected payload weight is 3374 kgs.

To accomplish the sample return mission the Viking Orbiter is modified to incorporate landing legs, landing radar, sampling subsystem, the earth return vehicle; and a 38% stretched propulsion system. Thermal control is also adjusted by adding flip covers over the existing thermal control louvers for the landed

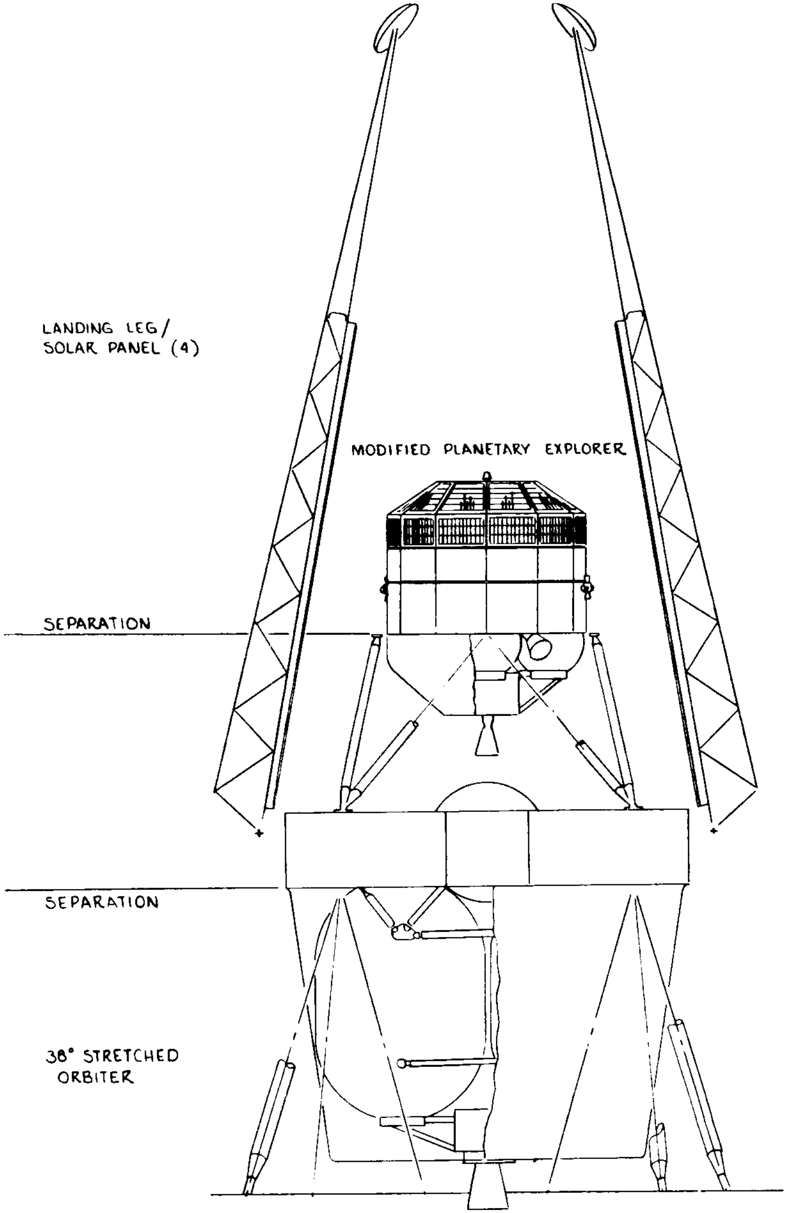
LANDING LEG/
SOLAR PANEL (4)
MODIFIED PLANETARY EXPLORER
SEPARATION
SEPARATION
38° STRETCHED
ORBITER

Figure I-2 Baseline Sample Return Configuration

mission. Solar panels have been integrated with the landing legs.

Modifications to the Planetary Explorer are primarily concentrated in the propulsion and structural areas. The structural modifications are necessary to achieve proper dynamic balance when the liquid propulsion and earth entry module are incorporated for sample return. The thermal control system has also been re-configured to emphasize heat retention instead of heat rejection.

The Mars orbit rendezvous and landing sequence is identical to that discussed in Phase I. The orientation of the spacecraft elements during various stages of the sample return sequence is depicted in Figure I-3.

Approximately thirteen (13) months after landing on the satellite's surface, the earth return vehicle is made ready for its return flight. The sequence of events for the return flight to Earth is very similar to the Mars arrival maneuvers, only performed in reverse. The transfer trajectory to Earth is a Type II trajectory. The launch window available is approximately twelve (12) days. The total velocity budget including navigation uncertainties, midcourse corrections, and a deflection maneuver at Earth is 1786 mps.

The sample return earth entry module is an Apollo shaped vehicle approximately 42.5 cm (16.75 inches) in diameter and is designed to survive the loads imposed during earth entry and impact. The capsule as designed can accommodate entry velocities up to 12.8 km/sec. This configuration provides for the stowage, sealing and environmental protection of a 5 kg Phobos surface sample.

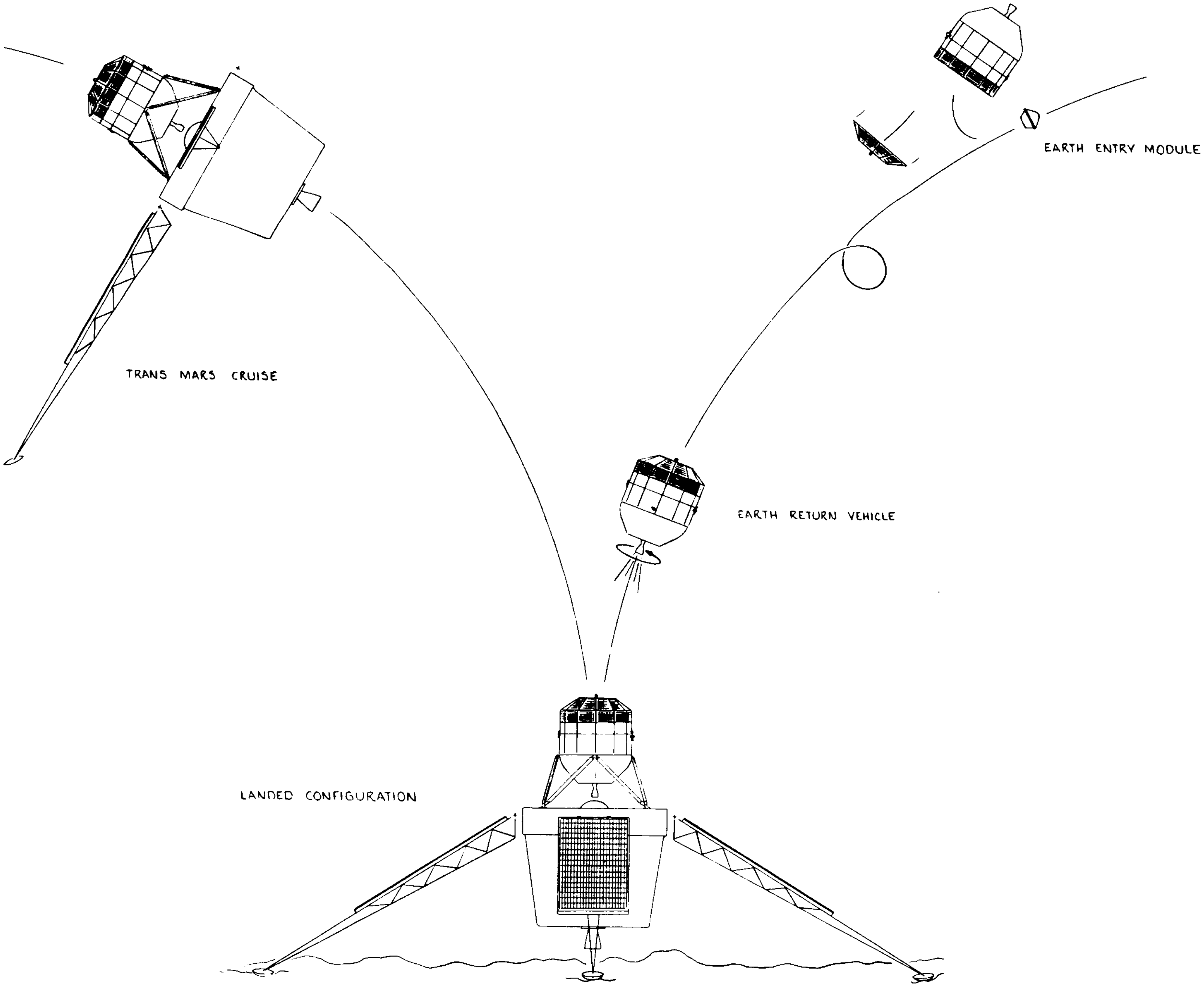
TRANS MARS CRUISE
EARTH ENTRY MODULE
EARTH RETURN VEHICLE
LANDED CONFIGURATION

Figure I-3 Baseline Sample Sequence

2. Alternative Concept

The alternate configuration shown in Figure I-4 consists of an integrated three-axis stabilized control module/lander with a propulsion module which is jettisoned prior to final closure and touchdown. The subsystems contained in the earth return vehicle function throughout the mission so that there is no duplication of hardware. The injected weight of the configuration is 2500 kg compared with 3375 kg for the baseline concept.

The earth return vehicle or control module, is a new lightweight three-axis stabilized vehicle composed of proven or currently identified interplanetary spacecraft subsystems.

The integrated lander module evolved from the Study Phase I lander/rover, houses the communications (20 watt TWTAs), primary power system (RTG and batteries), sampling subsystem, landing radar, tape recorders, and approach navigation TV cameras. The articulated 30" parabolic high gain antenna is located on the earth return vehicle.

The propulsion module which is jettisoned just prior to final closure and touchdown is the basic Viking '75 propulsion system. The terminal descent propulsion system which is an integral part of the control module structure is a hydrazine system.

The touchdown and return sequence for the alternate concept is shown in Figure I-5.

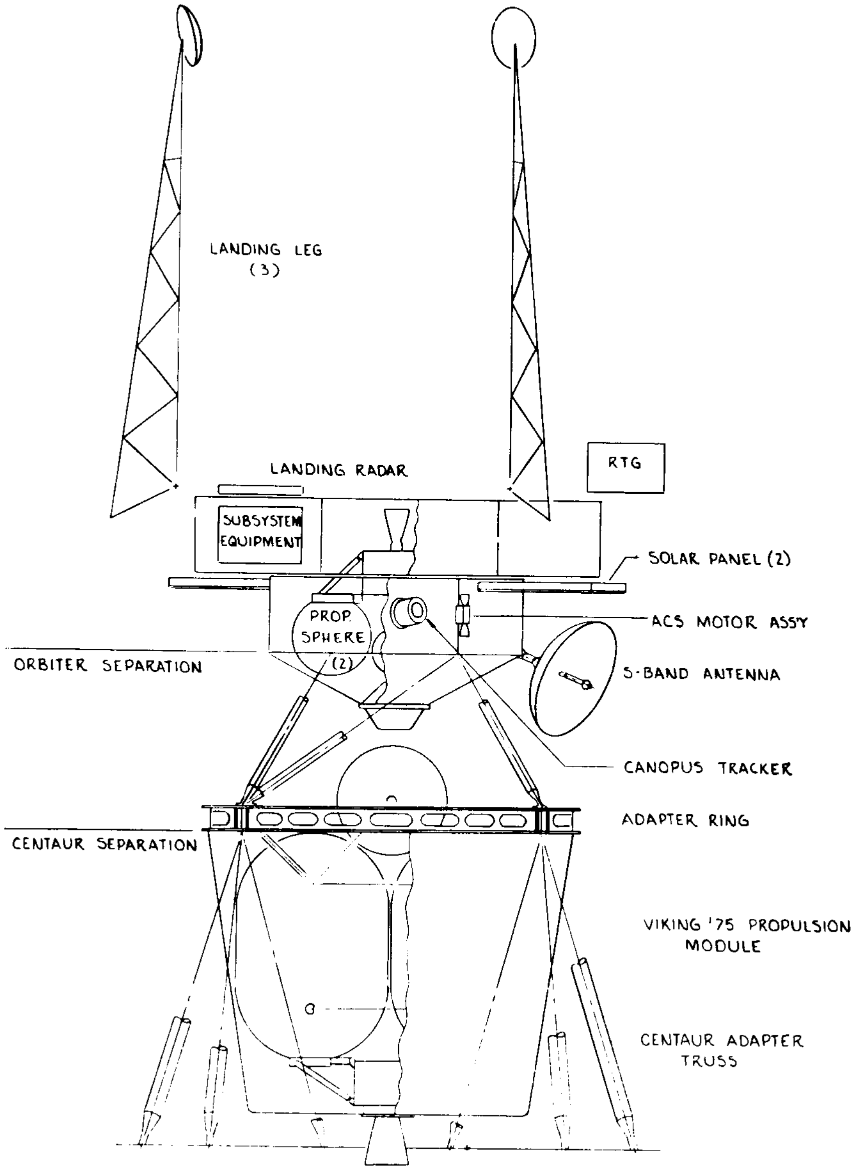
LANDING LEG
(3)
LANDING RADAR
RTG
SUBSYSTEM EQUIPMENT
SOLAR PANEL (2)
PROP. SPHERE (2)
ACS MOTOR ASSY
ORBITER SEPARATION
S-BAND ANTENNA
CANOPUS TRACKER
ADAPTER RING
CENTAUR SEPARATION
VIKING '75 PROPULSION MODULE
CENTAUR ADAPTER TRUSS

Figure I-4 Preferred Alternate Sample Return Configuration

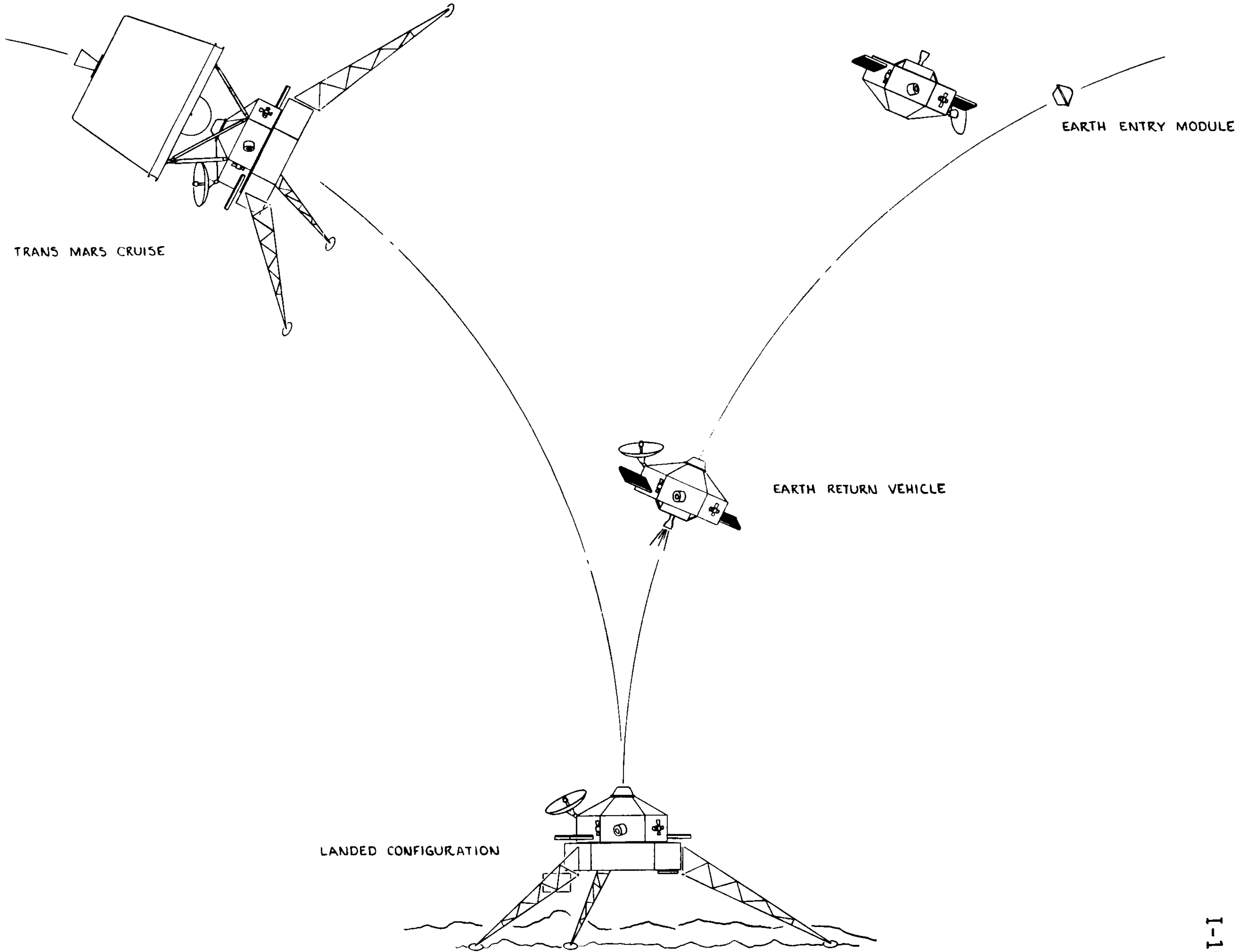
TRANS MARS CRUISE
EARTH ENTRY MODULE
EARTH RETURN VEHICLE
LANDED CONFIGURATION

Figure I-5 Preferred Alternate Sample Return Sequence

REFERENCES

I-1 Harrison, E. F., and J. W. Campbell: "Reconnaissance of Mars Satellites." J. of Spacecraft and Rockets, Vol 7, October 1970, p 1188.

II. Mission Science Objectives and Recommended Payloads

II. MISSION SCIENCE OBJECTIVES AND RECOMMENDED PAYLOADS

Our studies during Phase I were concerned with the rationale of selecting science instruments to complement a mission that was solely devoted to a landing on Phobos. From these studies we developed a baseline capable of delivering approximately 81.5 kgs (180 pounds) of science instruments. As part of our Phase II study activities we reconsidered the scientific objectives for performing a Phobos/Deimos mission and derived payloads which included what we felt to be a minimum useful instrument complement.

Next, the scientific rationale for a Phobos/Deimos sample return mission was developed, along with some thoughts on the science constraints and requirements on the acquisition of samples.

A. SCIENTIFIC OBJECTIVES

The avowed scientific goals of the space program are to enlarge our knowledge of

a) the origin and history of the solar system,
b) the origin and history of life,
c) the dynamic processes that shape man's terrestrial environment.

Although better knowledge of the Martian moons may shed some light upon goals (b) and (c), the real justification for exploring these moons is the high potential of adding significantly to our understanding of the birth of the solar system and the changes that may have occurred thereafter.

The bodies in the solar system (planets, satellites, asteroids, comets) are thought to have been formed mainly by condensation of a circumsolar gas cloud, although a few of these objects may have formed elsewhere in the universe and subsequently been captured by the Sun. One school of thought holds that the asteroid belt represents the debris of a broken-up planet. Others hold, however, that this debris is today in the process of accreting into a planet. If this second view is correct, the asteroid belt affords us our only real opportunity to study the genesis of a planet as it occurs. On the other hand, if the first view is correct, the asteroids provide us with material from all portions of a planet, right down to its innermost regions. In either case, the asteroids are therefore of great interest.

Satellites of the planets are important for similar reasons. Either they represent fragments of the central body, or they were formed elsewhere and subsequently captured. There is some evidence that the many satellites of Jupiter provide examples of both cases.

The Earth's moon remains an enigma. Even though the Apollo missions have vastly increased the available data, there remain three hypotheses concerning the Moon's origin. Singer still maintains the Moon could have been captured by the Earth. O'Keefe still favors a model by which the Moon is a fragment of the Earth split off as a result of a dynamic instability. Ringwood and Essene continue to propose that the Moon accreted from an assemblage of planetesimals which were left over during the accretion of the Earth itself. All increased knowledge of the chemical constitution, internal structure, and thermal history of the Moon is placing strong constraints upon each of these theories and by the completion of the Apollo 17 flight, we may have sufficient data to eliminate one or more of the possibilities.

These same theories may be invoked for the formation of the Martian satellites, but the details would be much different since our Moon is 10^{-2} of the Earth's mass whereas Phobos and Deimos comprise only 10^{-7} to 10^{-8} of Mars. The very small size of these satellites makes it highly probable that they are homogeneous. Even if not, it is likely that any heterogeneity would be simple compared to that of the Earth and the Moon. Furthermore, it would be susceptible to relatively straightforward experimental techniques.

B. MINIMAL SCIENCE PAYLOADS

The most important questions to be asked of Phobos and Deimos are, "What are they made of?" and "When were they formed?"

The first question can be answered directly by landing suitable equipment to conduct element composition analyses and to determine the mineralogy. Although remote analyses such as imagery and IR spectrometry have some value, these techniques do not have the capability of making the unambiguous measurements desired. Coupled with high-quality landed imagery, such as a quasi-microscope, an elemental analysis could provide sufficient information to derive the mineralogic composition, thus obviating the need for an X-ray diffraction instrument. A determination of the uranium and thorium contents is of real importance since these elements are low in abundance in meteorites and the Earth's interior, but high in abundance in the Earth's crust and lunar surface. The answer to the second question, viz., when the satellites were "formed" is certainly best answered by an isotope study to derive the age at which crystallization from molten rock occurred. No experimental apparatus yet exists for conducting this age investigation remotely. Therefore, allowing for such practicalities, the "minimal" mission to Phobos and/or Deimos would have as an instrument complement:

a) analyzer for major and minor elements (alpha backscattering spectrometer, x-ray fluorescence spectrometer, or other).

b) U, Th analyzer (gamma ray spectrometer).

c) mineralogic analyzer (quasi-microscope or x-ray diffractometer).

d) tracking beacon or other device (perhaps only communication system) to allow determination of the mass of the satellite.

This is the minimal instrument complement needed above and beyond the remote-sensing equipment used by Mariners 6, 7 and 9. A determination of the mass of the satellite is very valuable because when correlated with the observed volume, one can get the bulk density and thereby infer whether it is homogeneous and uniform, with a composition throughout which is the same as that at the surface, or whether some type of heterogeneity exists.

The outcome of the composition measurements will take us a long way toward deciding whether Phobos and Deimos are derived from Mars or elsewhere in the solar system. Note, however, that worthwhile comparisons can be made only if we know a good deal about the composition of Mars itself. Thus, exploration of the satellites of Mars presupposes a comprehensive geological study of the planet. Such missions are intimately related to one another, and might profitably be combined into one, single-purpose mission. Likewise, if the evidence points to an extra-Martian origin for the satellites, the asteroid belt could be investigated in detail to allow further progress. Therefore, Phobos/Deimos missions are potentially closely related to asteroid exploration.

More ambitious payload missions to Phobos and Deimos are probably only justified upon the basis of obtaining interesting results with the minimal payload given above. An appropriate advanced payload would be the 81.5 kg payload studied in Phase I. However, if a sample return mission proves feasible, it is likely that one would be willing to forego the 81.5 kg payload mission altogether in favor of obtaining samples of the body itself since on Earth one could analyze for trace elements, micro-mineralogic relationships, crystallization ages, cosmic ray exposure ages, remnant magnetization, etc.

C. SCIENTIFIC SIGNIFICANCE OF SAMPLE RETURN

The physical acquisition and return of samples from Phobos or Deimos has several advantages over remote examinations carried out on the satellite itself by automated landers and/or laboratories. Here on Earth, biologic and geologic scientists regularly return Earth samples to the laboratory for detailed analysis. Similarly, samples returned from Phobos or Deimos would permit comprehensive analytical procedures by scientists. Sequential experimentation and a heuristic approach to analyses would be made possible. Although in situ analytical procedures are feasible for advanced automated Phobos/Deimos landers, they are likely to be necessarily quite simple compared to those that are possible in Earth-based laboratories that are characterized by controlled environments and comprehensive analytical instrumentation. Such instrumentation often requires close human control that would severely burden the automated lander/laboratory's data system.

It is anticipated that the Phobos or Deimos landing sites will offer minimal hazards to a successful landing, yet will exhibit geologic features of sufficient diversity within the landing area to be representative of the satellite surface and warrant considerable stay time for investigation.

1. Surface Sampling

The sampling requirements involve consideration of several interrelated factors that include the minimum sample return, sampling radius about the landed vehicle, the effects of multiple sites, and the handling and storage requirements.

The minimum sample return involves collecting several different samples so that each type of accessible material is represented. Ideally, surface sampling will include a degree of selectivity; will be coordinated with television surveillance; and cover a sufficiently large horizontal area to define the immediate variations and assure that the samples are indeed representative of that portion of the satellite's surface.

The number and types of samples returned depend on the variety of surface materials that can be sampled within a reasonable distance of the landed vehicle and the requirements of the investigators who will examine the samples once they are returned to Earth. Following the practice established during the Apollo program it appears that the samples should be returned to a central laboratory, such as the lunar receiving laboratory, for preliminary analyses and systematic distribution to qualified investigators.

a. Sample Users - Each sample should provide for at least two users. It is assumed that one-half of each sample will be held in reserve for comparison with samples returned at a later date, second generation experiments, and to meet contingencies. The other half of the returned samples should be reserved for the physical scientists for extensive analyses. Based on the lunar sample analysis program, the physical sciences analyses will be largely geological in nature and may include: descriptive mineralogy and petrology, crystallography, microprobe investigations, radiation effects, shock effects, alpha particle autoradiography; chemical and isotope analysis including major elements, neutron activation, mass spectroscopy, rare-gas analysis, cosmic-ray induced and natural radioactivity and light stable isotopes; physical properties analysis such as magnetic measurements, elastic-mechanical measurements, electrical properties, and electromagnetic measurements.

b. Sample Weight - Several hundred scientists have requested lunar samples for 140 different investigation programs. It is expected that the Phobos or Deimos surface samples can be shared and that sequential distribution of individual samples will be carefully worked out so that early experiments will not destroy the samples' usefulness for later experiments. The samples would be returned to a central receiving laboratory after each off-site experiment for storage or redistribution. Exceptions would be where completely destructive tests are authorized. For purposes of this study 5 kg of samples was assumed to be brought back to the Earth for analyses.

c. Sample Variety - The variety of materials to be found at any particular landing site cannot be established without prior knowledge of the landing site; however, for purposes of this study assume that the following would be collected as a minimum:

1) surface dust from around the landing site;
2) loose rocks and/or crater ejecta;
3) subsurface sample from core hole;
4) bedrock drill chips from drill.

d. Sampling Radius - The minimum sampling radius relates to the geological variations in the surface, resolution and mapping scale of the Orbiter's imagery, and contamination from the terminal descent propulsion system rocket exhaust. Sampling should be as extensive as possible within the system constraints in order to sample across major lithologic boundaries if they exist. Some variations in the surface material can be expected at nearly any landing site although some will be considerably more complex than others. The sampling radius must also be coordinated with the Orbiter's imagery in order to establish the nature of the material and its distribution within an area that can be resolved. Once the nature of the material has been established at the landing site, the distribution patterns can be extended in interpreted over a much greater area on the orbital photographs.

It is recommended that a sample weight of at least one gram be returned from each of the locations sampled within the sampling radius.

e. Sample Handling and Storage Requirements - The primary objective in sample handling and storage is to return samples to a receiving laborabory for extensive scientific analyses without altering the samples or diminishing their scientific values. Therefore there are several factors that must be considered from the time the sample is collected from the satellite's surface until it is analyzed at the receiving laboratory. One of the primary considerations is for environmental control which should maintain the sample at or near its ambient satellite surface temperature and pressure. Other factors include: (1) each sample should be identified as to location and time of collection; preliminary analyses for identification or selection should be related to the sample; orientation and stratigraphic relationships should be preserved; depth in the corehole should be noted; (2) samples should be mechanically and biologically sealed in individual containers to prevent escape of chemical constituents or cross contamination; (3) the samples selected for return should be encapsulated within a biological barrier which is sterile or can be externally sterilized before return to Earth; (4) the encapsulated samples should be enclosed in an armored earth return capsule in order to assure survival even under catastrophic conditions; (5) a receiving laboratory analogous to the lunar receiving laboratory should be provided for the initial analysis on Earth.

III. Mission Analysis and Design

III. MISSION ANALYSIS AND DESIGN

A. PERFORMANCE ANALYSIS

The second phase of the Phobos/Deimos study was primarily concerned with developing a sample return concept from one of the two satellites of Mars. The baseline mission involves a launch from Earth in 1981 and a launch from Phobos in 1983 (more difficult than from Deimos). The Earth-to-Mars portion of the mission is basically the same as the 1979 launch in Phase I. The variations from that mission are primarily in the MOI ΔV and trip time.

The 1981 launch from Earth uses a Titan IIIE/Centaur and a Type II trajectory as in Phase I. The typical event sequences and timing are shown in Table III-1. The main difference from Phase I is the Earth-to-Mars transfer time of about 10 months which is about 1½ months shorter than the 1979 mission. The sequence of events for the Earth to Phobos mission is the same as the baseline from Phase I with the same delta time from Mars orbit insertion (MOI) to the landing. The baseline ΔV budget is shown in Table III-2 and is the same as the Phase I '79 mission except for the MOI and plane change maneuvers which are higher because of the higher Mars encounter VHE magnitude and declination in the 1981 opportunity. The weight profile for the Earth-to-Phobos mission is shown in Table III-3. This weight profile shows landed weight on Phobos of 1230 kg which includes the landed orbiter (Phase I considered a separate lander) and a sample return module as heavy as 259 kg (which is about 63 kg more than is required for the baseline sample return concept). This value of 259 kg is established by the orbiter propulsion limit which is a 38% stretch over the Viking '75 propellant load. The excess capability could be converted to landed science or sample return contingencies.

Table III-1 Event Sequences and Timing (Earth to Phobos)

EVENT	TIME
Earth Launch	Dec 9, 1981 (Nov 25, 1981 to Dec 25, 1981)
1st Midcourse Correction	Dec 19, 1981
2nd Midcourse Correction	Sept 2, 1982
Mars Orbit Insertion	Sept 12, 1982
Plane Change	Sept 18, 1982
Transfer to Phasing Orbit	Sept 24, 1982
Transfer to Observation Orbit	Sept 26, 1982
Transfer to Phasing Orbit for Phobos	Oct 10, 1982 (Typical)
Raise Periapse to Phobos Altitude	Oct 11, 1982
Transfer to Phobos Orbit	Oct 12, 1982
Rendezvous and Landing	Oct 13, 1982

Table III-2 ΔV Budget (Earth to Phobos)

EVENT	ΔV (MPS)
Midcourse Corrections	25
Mars Orbit Insertion	1245
Plane Change	95
Transfer to Phasing Orbit Transfer to Observation Orbit	300
Raise Periapsis to Phobos	200
Circularize at Phobos	430
Gravity and Steering Losses	100
Navigation Uncertainties	175
Rendezvous and Landing	100
TOTAL	2670

Table III-3 Weight Profile (Earth to Phobos)

EVENT	WEIGHT (kg)
Injected Weight	3373 (7438 lb)
Spacecraft Weight (Inj Wt-216 kg)	3157
After Midcourse Corrections	3123
After Mars Orbit Insertion	1916
After Plane Change Maneuver	1846
After Transfer to Observation Orbit	1641
After Maneuver to Raise Periapse to Phobos	1516
After Orbit Match with Phobos	1280
After Rendezvous & Landing	1230 *

* 668 kg Orbiter
303 kg Prop. Inerts
259 kg (571 lb) Return Vehicle

A series of trade studies were required to develop the sample return mission profile. Table III-4 indicates the major trades. The primary goal in optimizing the mission was to reduce the ΔV requirements for the trans-Earth injection. This injection is complicated by the inclination differences between the orbit of Phobos (or Deimos) and the required departure declination. A three-impulse transfer was selected in order to reduce the impact of the plane change on the ΔV requirements. The sequence of events is very similar to the Mars arrival maneuvers only in reverse. The first four listed trade studies involve the mechanics of the three-impulse transfer. The last two trades involve the midcourse correction strategy and entry mode as they impact the required propellants and the trajectory accuracy at Earth.

1. Mission Description

The overview of the sample return mission is shown in Figure III-1. The sequence of events for the departure from Phobos involves three major maneuvers after the initial lift off from the surface. The lift off is accomplished with a short burn of the main engine to achieve a separation velocity of approximately 10 mps. At the proper point in the orbit the engine is fired to lift the apoapsis to 95000 km. This maneuver requires a velocity increment of 746 meters per second. The line of apsides established by this maneuver is selected beforehand to allow the final transfer to occur at periapse. At apoapsis a small maneuver lowers periapsis to 1500 km to reduce the final trans-Earth injection ΔV. To prevent doing yaw steering during the final injection maneuver, a plane change maneuver is also done at apoapsis (95000 km) which rotates the orbital plane to include the required VHE vector for the trip to Earth. The final trans-Earth injection maneuver is done at the 1500 km periapsis and increases

Table III-4 Mission Profile Trade Studies

Phobos Lift-Off and Departure

Timing of Intermediate Orbit Injection

Sequence and Timing of Plane Change & Periapsis Lowering

Trans-Earth Injection Timing

Midcourse Correction Strategy

Direct Earth Entry vs Capture In Earth Orbit

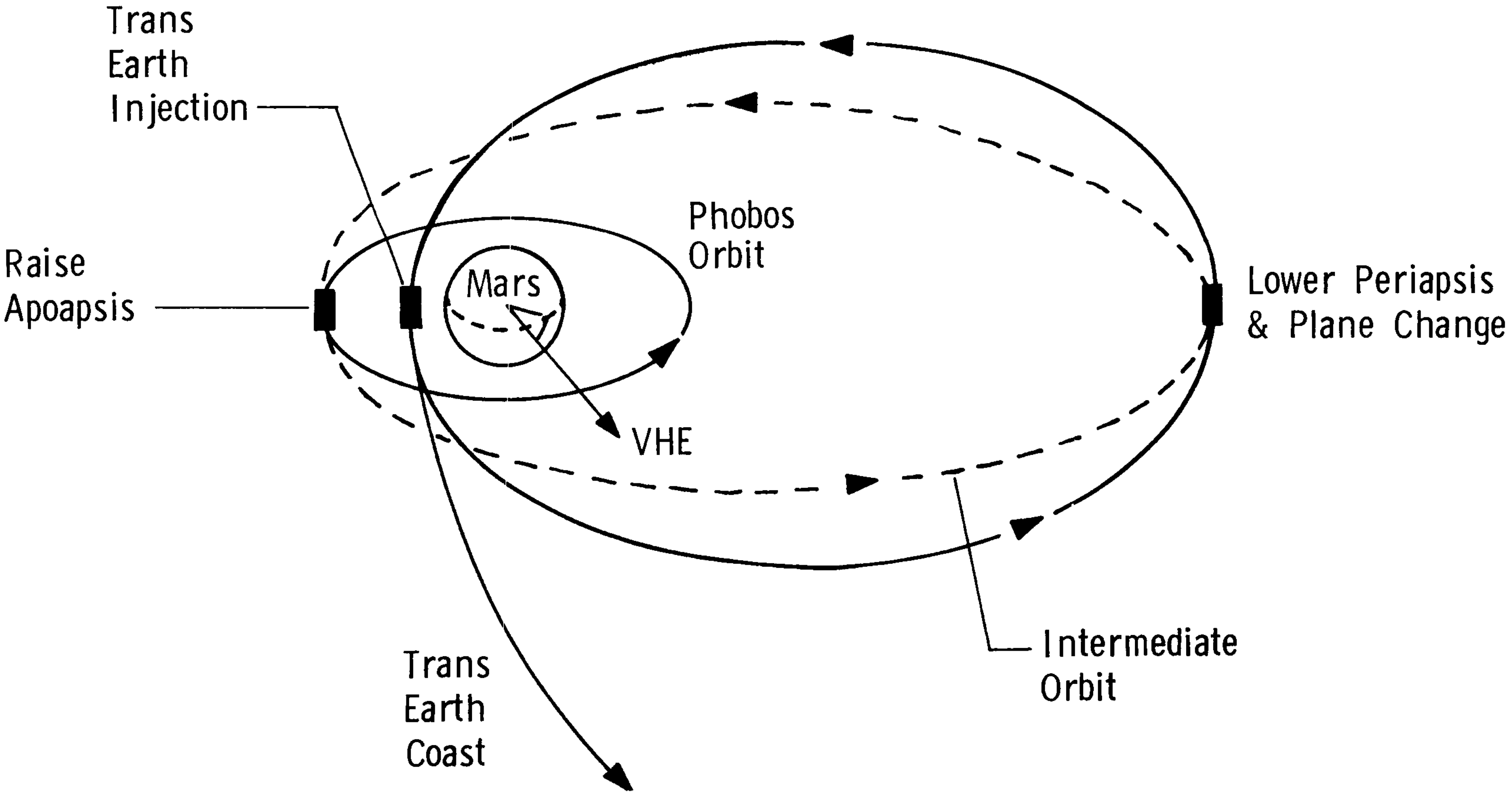
Trans
Earth
Injection
Raise
Apoapsis
Phobos
Orbit
Mars
VHE
Lower Periapsis
& Plane Change
Trans
Earth
Coast
Intermediate
Orbit

Figure III-1 Overview of Sample Return Mission

the velocity to the required VHE magnitude. For comparison, if this sequence of events is applied to a sample return from Deimos, the ΔV budget would be reduced by approximately 250 mps. This would yield a reduction in required propellant of approximately 10 kg. The SRTRK Program (Appendix A) was used to simulate these events.

2. Performance Characteristics

Table III-5 shows the event sequences and timing for the sample return mission. The trajectory to Earth is a Type II trajectory (greater than 180°). The actual launch window is twelve days. The 3 midcourse corrections are for correcting trajectory accumulated errors only and would not be required unless deviations from the nominal trajectory occur. The trajectory is biased slightly to provide a clear passage of Earth and a deflection maneuver is planned 1.5 days prior to entry to remove the bias and trim out the major portion of any flight path angle uncertainties. The nominal flight path angle at entry interface is $-7.25^{\circ} \pm .5^{\circ}$ to accommodate the higher entry velocities of approximately 12.6 km per second (41,500 fps). For comparison the Apollo flight path angle is -6.5° and entry velocity is 11 km/sec (36,300 fps).

The ΔV budget for the sample return mission is shown in Table III-6. This budget allows for a 12 day launch window and also for 3σ navigation uncertainties, midcourse correction and deflection maneuver. Later navigation analysis has reduced these values (see Section B of this chapter). The impulsive ΔV curve for the sample return mission is very flat as a function of launch day. For example, an additional kilogram of propellant would increase the width of the launch window by over 30 days. The 12 day window is considered adequate; however, since the only

Table III-5 Event Sequences and Timing (Phobos to Earth)

EVENT	TIME
Lift Off Surface of Phobos	Nov 19, 1983
Raise Apoapse to 95000 km	Nov 20, 1983
Lower Periapse to 1500 km & Plane Change	Nov 26, 1983
Trans-Earth Injection	Dec 2, 1983
1st Midcourse Correction	Dec 12, 1983
2nd Midcourse Correction	June 25, 1984
3rd Midcourse Correction	Sept 6, 1984
Deflection Maneuver	Oct 4, 1984
Separation	Oct 4, 1984
Entry and Landing	Oct 5, 1984

Table III-6 ΔV Budget (Phobos to Earth

EVENT	ΔV (MPS)
Liftoff From Surface	10
Raise Apoapsis to 95000 km	746
Lower Periapsis and Plane Change	110
Trans-Earth Injection	712
Gravity and Steering Losses	40
Navigation Uncertainties	85
Midcourse Corrections	68
Deflection Maneuver	15
TOTAL	1786 MPS

potential problem is the availability of the tracking network during the time of the three major maneuvers. Also included in the budget is 40 mps for gravity and steering losses. This loss value is substantially less than that needed for the trip to Mars since the thrust to mass ratio is over three times higher than the Mars orbit insertion ratio yielding significantly shorter burn durations and therefore less gravity and steering losses.

Table III-7 indicates the weight profile after each maneuver. As mentioned before, 3σ fuel allowances are used where applicable. Also shown is the separated entry module weight of 15 kg. The separated entry module concept has the effect of reducing the total spacecraft weight since the entire spacecraft does not have to be thermally and structurally protected from the effect of Earth entry. This trade study is shown in more detail below.

3. Trade Studies

Table III-8 shows the relative merits and maximum payload capabilities of sample return missions launching from Phobos between 1977 and 1990 for both Type I and Type II trajectories. An initial weight of 200 kg is used for this parametric study. The ΔV requirements include an additional 200 mps for navigation uncertainties, gravity and steering losses and midcourse corrections. Reasonably low ΔV requirements (less than 2000 mps) exist for returns to Earth between 1979 and 1986.

Before selecting the baseline mission it was required to determine the relative merits of the direct Earth entry mode and the Earth orbital capture. Table III-9 indicates the required initial weight for four cases of Earth sample retrieval. The Earth orbital capture requires ΔV expenditures of over 1300 mps to place the spacecraft in a 24 hour period orbit with a perigee altitude of 500 km. The Earth orbital capture of the entire

Table III-7 Weight Profile (Phobos to Earth)

EVENT	WEIGHT (kg)
On Surface	197.3 (435 lb)
After Liftoff From Phobos	196.6
After Raising Apoapsis to 95000 km	149.8
After Lowering Periapsis to 1500 km	145.8
After Plane Change	143.9
After Trans-Earth Injection	109.6
After Midcourse Corrections	106.9
After Deflection Maneuver	106.4 (234.6 lb)
Entry Capsule	15. (33 lb)

Table III-8 Sample Return Payloads for Alternate Years

(Assumes 200 kg Initial Weight on Phobos - Direct Earth Entry)

Launch Opportunity From Phobos	Trajectory Type	C3 (km/sec)^2	Departure Declination (Deg)	Fuel (kg)	ΔV* (MPS)	Burnout Weight (kg)	VHE (km/sec)
1977	I	11.22	-4.9	111.8	2318	88.2	4.32
	II	8.29	7.4	103.0	2051	97.0	2.82
1979	I	7.15	25.9	101.3	2004	98.7	4.73
	II	7.00	2.8	97.8	1901	102.2	3.20
1981	I	6.34	37.5	99.9	1961	100.1	5.83
	II	5.99	-0.1	93.6	1788	106.4	4.58
1983	I	5.77	31.4	97.0	1881	103.0	5.85
	II	5.44	-9.9	92.8	1767	107.2	5.73
1986	I	5.86	7.7	94.0	1804	106.0	3.76
	II	6.11	-18.4	96.6	1870	103.4	4.53
1988	I	10.03	-27.6	111.2	2301	88.8	3.24
	II	14.38	0.4	119.7	2588	80.3	4.26
1990	I	14.67	-21.9	122.8	2697	77.2	4.22
	II	12.06	2.3	113.8	2386	86.2	3.47

* Assumes An Excess ΔV Requirement of 200 MPS For Navigation Uncertainties, Gravity Losses, Steering Losses, and Midcourse Corrections

Table III-9 Earth Orbital Capture vs Direct Entry

Earth Orbital Capture* - Entire Spacecraft
Phobos Liftoff Weight - 422 kg (286 kg Propellant)

Earth Orbital Capture* - Small Separable Capsule
Phobos Liftoff Weight - 251 kg (112 kg Propellant)

Direct Entry - Entire Spacecraft
Phobos Liftoff Weight - 219 kg (101 kg Propellant)

Direct Entry - Small Separable Entry Module
Requires 91 kg Propellant and Total Phobos Weight of 197 kg
Phobos Liftoff Weight - 197 kg (91 kg Propellant)

* Capture In a 24 hr Period Orbit With 500 km Altitude of Periapsis

spacecraft requires a large amount of additional fuel. If a small unit is separated and put into the same earth capture orbit the additional fuel is reduced significantly. The direct entry cases require a 15% increase in basic structure weight for the heat shield and if the entire spacecraft is entered into the atmosphere an increase in total weight of 22 kg is required over the baseline case where a small separable entry module is used. As the table indicates, the two orbital capture cases require significantly heavier total spacecraft weights than do the two direct entry cases.

During this phase of the mission study we also investigated the capabilities of solar electric propulsion (SEP) for a round-trip mission to the Mars satellites. Table III-10 indicates the pertinent characteristics of this type of mission. Several constraints were applied to the SEP mission which prevented this from indicating a fully optimized case. The trip time was constrained to be equivalent to chemical propulsion trip time. It was also stipulated that a positive C_3 would be applied at Earth to bypass the Earth spiral departure problem. As can be expected the very high specific impulse of the SEP yields a significant increase in the payload capabilities over the chemical system. The current drawbacks involved with the SEP system are the high development costs, severe reliability requirements, and very difficult navigation problems.

The feasibility of rendezvousing with both the satellites of Mars during the same mission was studied. Figure III-2 illustrates the sequence of events for this dual mission. The mission is the same as the baseline mission up to the observation orbit. After the observation orbit is established, the spacecraft is circularized at apoapsis when Deimos is also there. The rendezvous is accomplished and the spacecraft co-orbits with Deimos

Table III-10 Solar Electric Propulsion Alternative

Ground Rules: Phobos Sample Return Mission - Titan IIID/Centaur Launch in 1981

	SEP Mission	Orbiter Baseline Mission
Injection C3	16 km^2/sec^2	12 km^2/sec^2
Injected Weight	3700 Kg	3373 Kg (capable of 3940 Kg)
Payload* at Phobos	1630 Kg	756 Kg
Payload* at Earth	1150 Kg	88 Kg
Earth Arrival VHE	3.4 km/sec	5.8 km/sec
Total Mission Duration	1020 days	1031 days
Total Propellant Weight	1510 Kg	2018 Kg
Systems Weight	560 Kg**	230 Kg
SEP Power	20 KW	------
I sp	1880 sec	289 sec
Launch Day	Nov. 11, 1981	Dec. 9, 1981
Phobos Rendezvous	Jan. 5, 1983	Oct. 13, 1982
Phobos Departure	Jul. 6, 1983	Nov. 19, 1983
Earth Entry	Aug. 27, 1984	Oct. 5, 1984

* Payload excludes propulsion system

** SEP systems include solar array, power conditioning, propulsion, and tankage

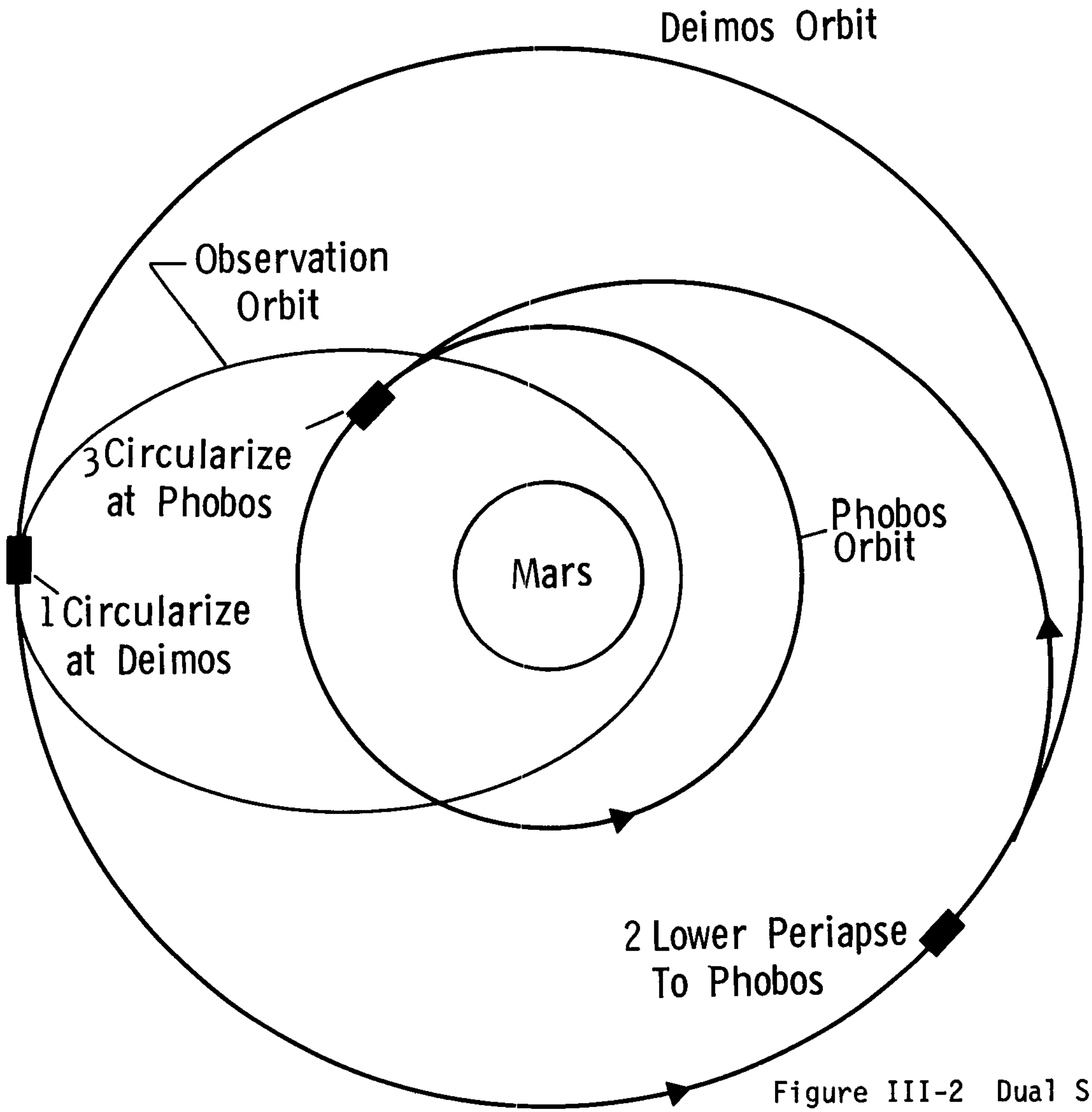
Deimos Orbit
Observation Orbit
3 Circularize at Phobos
1 Circularize at Deimos
Mars
Phobos Orbit
2 Lower Periapse To Phobos

Maneuvers Between Capture Orbit and Observation Orbit	300 mps
Circularize at Deimos	490
Lower Periapse to Phobos	330
Circularize at Phobos	420
Guidance & Steering Losses	100
Navigation Uncertainties	225
Dual Rendezvous	80
TOTAL	1945 mps

Phase 1 ΔV After MOI to Phobos is 1305 mps

Figure III-2 Dual Satellite Mission Description

for scientific observations and measurements. After this period the proper location in Deimos' orbit is determined to allow a Hohmann transfer to Phobos' orbit when Phobos is at the periapsis of the new orbit. The spacecraft circularizes at Phobos and rendezvous and co-orbit takes place as with Deimos. The ΔV for this type of mission is higher by 640 mps than a comparable Phobos landing mission. Table III-11 indicates the dual mission payload capability for various propulsion system concepts for launch opportunities in 1979, 1981 and 1983. The launch vehicle in all cases is the Titan IIIE/Centaur. Both the staged orbiter concept and the space storable concept are limited by the launch vehicle capability whereas the payload for the 38% and 60% growth orbiter propulsion systems are limited by the orbiter propellant. The total payload potential can be increased slightly if a portion is left behind in one of the earlier stages of the mission. For example, if half of the payload could be left co-orbiting Deimos while the rest of the spacecraft goes on to Phobos, the total payload capability would be increased by approximately 10%.

B. NAVIGATION ANALYSIS

The Phase II navigation work consisted of several studies dealing with: 1) the sensitivity of the baseline satellite rendezvous (Ref. III-1) to various mission parameters; and, 2) the characteristics of the Earth return leg of the Phobos/Deimos sample return mission. The material in this section of the report is presented as results of four studies. The rendezvous sensitivity to launch/encounter date, satellite ephemeris error, maneuver execution error, Mars gravity error and type of navigation filter are reported in Studies I and II. Studies III and

Table III-11 Dual Satellite Payload Capability

(Payload Available at Satellite in Addition to Basic Orbiter Weight)

CONFIGURATION	1979	1981	1983
38% Growth Orbiter	36 kg	None	None
60% Growth Orbiter	131	None	None
Staged Orbiter[1]	329	192 kg	11 kg
Space Storables[1]	710	577	353

1 - Launch Vehicle Limited

IV deal with the Earth return part of the mission. Study III examined the return-to-Earth ΔV budget including the out-of-Mars orbit ΔV_{STAT} and the trans-Earth midcourse correction ΔV_{STAT} for both a spin stabilized and 3-axis stabilized spacecraft. Study IV was concerned with the placement of the final deflection maneuver and the corresponding ΔV and entry flight path angle dispersions, again for both spin-stabilized and 3-axis machines. Separate conclusion sections are presented for each study.

1. Study I: Rendezvous Dependence on Launch/Encounter (L/E) Date

A parametric study of rendezvous sensitivity to navigation parameters which vary with L/E date was performed. These parameters characterize the encounter and in-orbit tracking accuracy obtainable with the Deep Space Network (DSN). The effect of nominal Mars orbit insertion (MOI) maneuver magnitude variation over the L/E window was not considered. This quantity is not expected to have a major effect on the rendezvous ΔV_{STAT} and has no effect on the ninety-nine percentile radius of closest approach to Phobos (R99).

a. Assumptions and Techniques - Specific assumptions made in this study are listed in Table III-12. The basic idea is to establish the likely range of variation of the encounter and in-orbit O.D. error statistics and then to test the effect of these variations on the rendezvous ΔV_{STAT} and R99. The maximum allowable 1σ encounter control and knowledge errors for the Viking '77 and '79 L/E windows are assumed to be the maximum allowable values for any Phobos/Deimos L/E window. Regions of the Phobos/Deimos windows where the Mars geocentric declination (DEC) is near 0° or where the spacecraft ZAE angle is near 90° will have to be avoided because they will yield unacceptable encounter dispersions. (These angles are defined in Figure III-3.) The range

Table III-12 Rendezvous Dependence on Launch/Encounter Date

ASSUMPTIONS

Only the Encounter Control and Knowledge Dispersions and In-Orbit Knowledge Dispersions Vary With Launch/Encounter Date

Mars Geocentric Equatorial Declination (DEC Angle) Near Zero in Control Tracking Arc (E-30 Days to E-10 Days) Implies That Encounter Control Dispersions Will Be Unacceptably Large

ZAE Angle Near 90° Implies That Encounter Knowledge Dispersions (Based on Tracking From E-30 Days to E-.5 Days) Will Be Unacceptably Large

Capture Orbit Knowledge Dispersions Not Strongly Affected By Mars Gravity Uncertainty and Hence Will Not Degrade Significantly With Launch/Encounter Date. Only Phasing and Observation Orbit Knowledge Need Be Considered

Standard Deviation of Phasing and Observation Orbit Knowledge Will Not Degrade by More Than Factor of 3 Over Launch/Encounter Windows (Orbits Are in Mars Equator and Hence Plane-of-Sky Angle Between 62° and 118°)

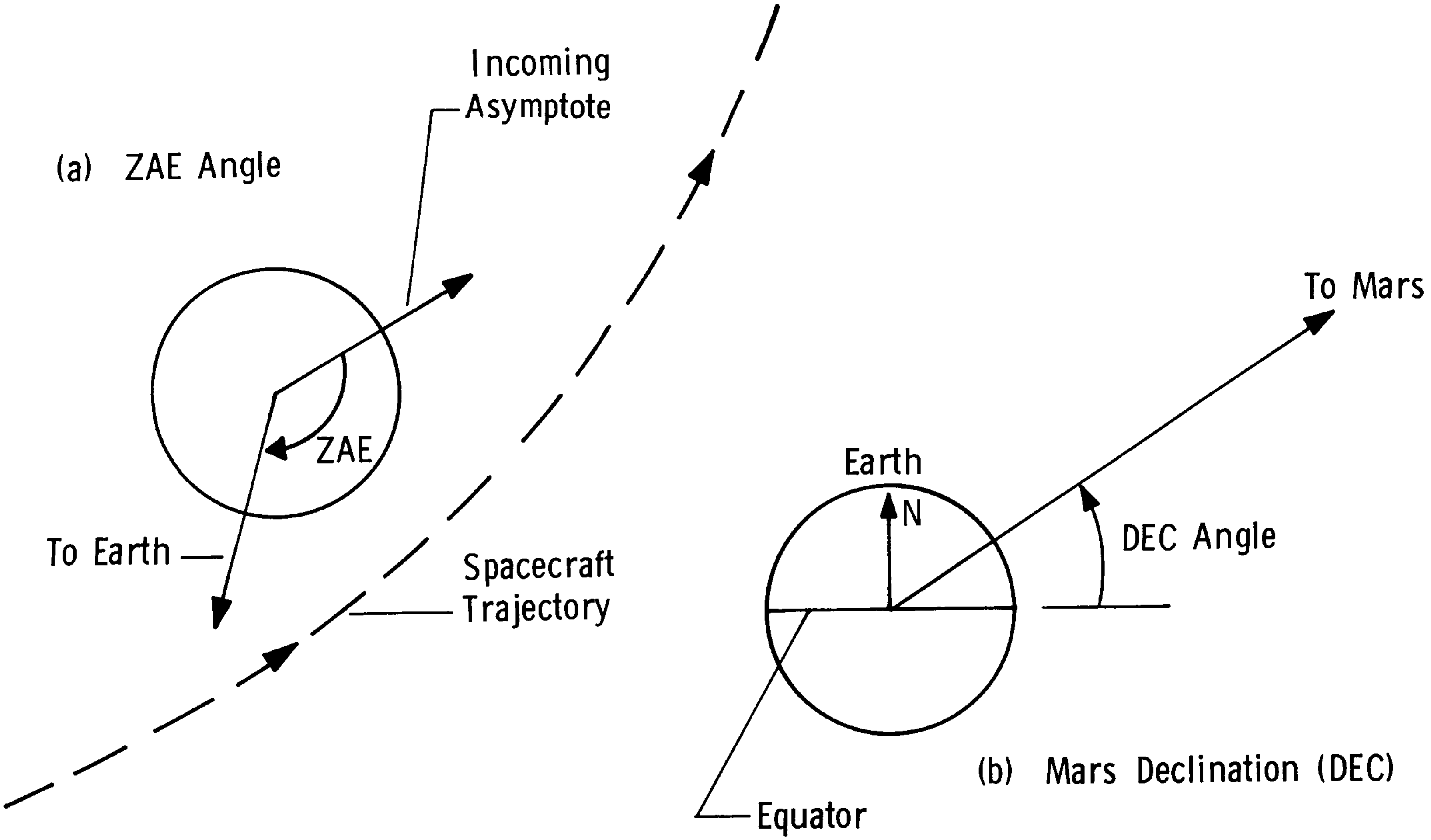
(a) ZAE Angle

(b) Mars Declination (DEC)

Incoming
Asymptote
ZAE
To Earth
Spacecraft
Trajectory
To Mars
Earth
N
DEC Angle
Equator

Figure III-3 Definition of ZAE Angle and DEC Angle

of variation of the in-orbit O.D. accuracy should not be extreme because the spacecraft is in the Mars equator and therefore the plane-of-the-sky (POS) angle lies between 62° and 118°. (This angle is measured between the Earth-Mars vector and the normal to the spacecraft orbit plane.) Since the POS angle is never 0°, in-plane degeneracy does not occur. The rendezvous on the other hand is not sensitive to out-of-plane degeneracy (which occurs for the DSN when POS = 90°) because the TV system is effective in determining the satellite out-of-plane angle. For this reason it was deemed sufficient to assume at worst a factor of three degradation in the in-orbit O.D. accuracy. This was done primarily to explore the sensitivity of the rendezvous to this quantity. Also, since the capture orbit O.D. accuracy is so much better than phasing and observation accuracies (Table III-13), the former will have a negligible effect on the rendezvous compared to the latter and hence is neglected in this study.

b. Results

1) Effect of Encounter Control and Knowledge Error Variations - Table III-14 shows the range of variation of the 1σ control and knowledge B-plane encounter dispersions for Viking '77 and '79 launch years. (Note that the knowledge results are for $\theta_{AIM} = 0^{o}$ because this is the θ_{AIM} required for Phobos/Deimos type approach trajectories.) The maximum control and knowledge ellipse semi-major axes are about 470 km and 300 km respectively for both launch years. This means that increases in the baseline control and knowledge SMAAs of about 100 km and 200 km respectively should be expected over a typical Phobos/Deimos window. The effect of these increases on the rendezvous ΔV_{STAT} and Deimos closest approach radius (R99) is shown in Table III-15. (A different sequence of random errors was used in generating these

Table III-13 In-Orbit DSN Tracking Errors (1σ) For the Baseline Rendezvous to Phobos

DSN UPDATE	VEHICLE STATE ERROR	
	RSS POSITION (KM)	RSS VELOCITY (M/S)
Capture Orbit - Prior to Plane Change	.472	.045
Capture Orbit - Prior to Phasing Maneuver	.337	.041
Phasing Orbit - Prior to Observation Orbit Maneuver	12.78	.814
Observation Orbit - Prior to Lambert Intercept Maneuver	12.78	.814

Table III-14 Variation of Knowledge and Control for 1977, 1979

	1977	1979
Min $SMAA_C$ Max $SMAA_C$	162. km 472. km	245 km 468 km
Min $SMAA_K$ ($\theta_{AIM}=0^\circ$) Max $SMAA_K$	92. km 216. km	108 km 304 km

Max. Control $SMAA_C \sim 470.$ km

Max. Knowledge $SMAA_K \sim 300.$ km

$$\left.\begin{array}{l} \text{Baseline } SMAA_K = 195.0 \\ \text{Baseline } SMAA_C = 279.7 \end{array}\right\} \begin{array}{l} \Delta SMAA_C \sim 100.\text{ km} \\ \Delta SMAA_K \sim 200.\text{ km} \end{array}$$

Table III-15 Sensitivity of Rendezvous to Encounter Knowledge and Control Dispersions

$SMAA_K = 195.0$ km

$SMAA_C = 279.7$ km

	$SMAA_K$	$SMAA_K + 100$	$SMAA_K + 200$
$SMAA_C$	104.3 m/s 109.1 km	107.9 m/s 109.3 km	111.3 m/s 109.6 km
$SMAA_C + 100$	105.8 m/s 108.5 km	111.6 m/s 108.8 km	182.3 m/s 108.9 km
$SMAA_C + 200$	123.4 m/s 108.0 km	131.6 m/s 108.2 km	170.7 m/s 108.4 km

results than was used in Reference III-1. Hence the nominal ΔV_{STAT} and R99 values are slightly different.) As expected, increasing the encounter errors has little or no effect on R99. The control perturbation only affects ΔV_{STAT} significantly when it is over the 100 km level regardless of the level of the effect of knowledge error. The knowledge perturbation on the other hand seems to be keyed to the magnitude of the control error. For nominal encounter control dispersions ΔV_{STAT} is relatively insensitive to increases in knowledge error up to the +200 level. In accordance with Table III-14, the maximum ΔV_{STAT} to be expected over the L/E window (corresponding to the $SMAA_C$ + 100, $SMAA_K$ + 200 case in Table III-15) is about 131.6 m/s--an increase of about 30%. This extra ΔV is required to establish the observation orbit as Table III-16 shows. This ΔV_{STAT} is for the sum of the maneuver ΔVs for the MOI maneuver, the PCM (Plane Change Maneuver), the POM (Phasing Orbit Maneuver), and the OOM (Observation Orbit Maneuver). The intercept ΔV_{STAT} is for the sum of the maneuver ΔVs for the LIM (Lambert Intercept Maneuver), the MCCM (Midcourse Correction Maneuver), and the VMM (Velocity Matching Maneuver). Note that the latter ΔV_{STAT} is approximately independent of launch/encounter control and knowledge errors and that the two orbit sequences are approximately statistically independent (i.e., the total ΔV_{STAT} is roughly the RSS of the observation orbit ΔV_{STAT} and the intercept ΔV_{STAT}).

As mentioned earlier, the range of encounter control and knowledge dispersions found in Table III-14 are expected only if the Mars DEC angle and the ZAE angle are acceptable (i.e., DEC $\neq 0^o$ and/or ZAE $\neq 90^o$). To be able to assert, therefore, that ΔV_{STAT} will not increase more than 30% over the L/E windows, it is necessary to exclude these regions of the L/E space where DEC = 0 and/or ZAE = 90°. Figure III-4 shows the DEC and ZAE

Table III-16 Effect of Control and Knowledge Variations on ΔV_{STAT} for Observation Orbit and for Deimos Interception

C/K	Observation Orbit ΔV_{STAT}	Intercept ΔV_{STAT}	Total ΔV_{STAT}	RSS of Observation Orbit and Intercept ΔV_{STAT}
+200/+200	103.0 m/s	112.3 m/s	170.7 m/s	152.6 m/s
+200/0	58.3 m/s	103.6 m/s	123.4 m/s	119.0 m/s
0/+200	44.3 m/s	97.7 m/s	111.3 m/s	107.3 m/s
0/0	32.1 m/s	102.2 m/s	104.3 m/s	107.0 m/s

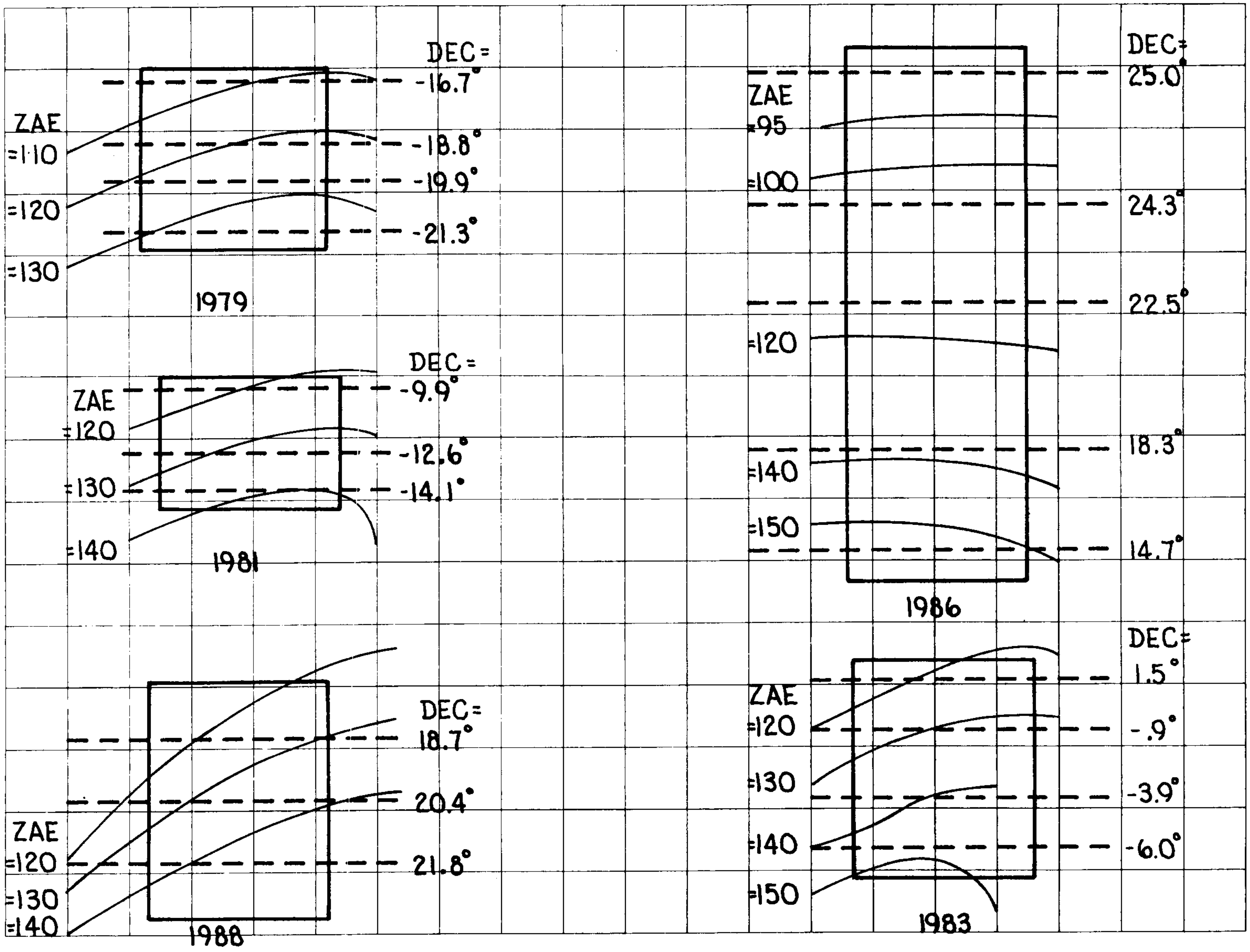

Figure III-4 Launch/Encounter Variations of ZAE, DEC Angles

contours for Phobos/Deimos missions (represented as L/E boxes) in '7[illegible], '81, '83, '86, '88. This figure shows that late encounters will have to be excluded in 1986 due to bad ZAE angles and in 1983 due to bad DEC angles.

2) Effect of In-Orbit Knowledge Error Variation with L/E Date - Table III-17 shows the effect of tripling the standard deviations of in-orbit DSN error. Note that R99 is affected considerably more than ΔV_{STAT}. The increase in R99 is due to the increased error in the satellite state relative to Mars as determined by the optical (TV) measurements. In other words, the degraded knowledge of the spacecraft state relative to Mars maps directly into a proportionately degraded knowledge for the satellite state relative to Mars once the satellite state is solved for using TV sightings. These results were obtained by Monte Carlo simulation of the baseline rendezvous (Reference III-1) using the baseline phasing and observation orbit DSN covariance matrices scaled by a factor of 10. The square root of the diagonal elements of the DSN covariance matrix, σ_x, σ_y, σ_z, $\sigma_{\dot{x}}$, $\sigma_{\dot{y}}$, $\sigma_{\dot{z}}$, are also shown in Table III-17. The same DSN covariance matrix is used for both the phasing and the observation orbit DSN updates (Reference III-1). Since an R99 of 100 km is acceptable, there apparently is considerable margin in the available DSN accuracies.

c. Conclusions - Basic conclusions are presented in Table III-18. In addition, late encounters in 1983 and 1986 must be excluded due to DEC and ZAE angle constraints respectively.

Table III-17 Sensitivity of Rendezvous to Phasing and Observation Orbit Knowledge

CASE	ΔV_{STAT}	R99
1σ * DSN Errors	97.9 m/s	18.1 km
3σ DSN Errors	109.9 m/s (Up~12%)	45.4 km (Up~150%)

* $\sigma_X = 4.47$ km

$\sigma_Y = .44$ km

$\sigma_Z = 10.12$ km

$\sigma_{\dot{X}} = .27$ m/s

$\sigma_{\dot{Y}} = .15$ m/s

$\sigma_{\dot{Z}} = .94$ m/s

Table III-18 Conclusions - Rendezvous Dependence on Launch/Encounter Date

ΔV_{STAT} Must Be Increased By 30% To Account For ZAE, DEC Variations and 12% For In-Orbit O. D. Variations Over the Possible Launch Windows

99 Percentile DCA Not Affected By Encounter Knowledge and Control Variations But Will Be 50 km When In-Orbit O. D. Variations Are Considered

	ΔV_{STAT}	99 DCA
Baseline Rendezvous	100. m/s	18.0 km
Updated For Encounter	130. m/s	18.0 km
Updated For Encounter And In-Orbit	150. m/s	45.3 km

2. Study II: Rendezvous Sensitivities

a. Assumptions and Technique - The sensitivity of the rendezvous ΔV_{STAT} and R99 to the level of satellite ephemeris error, maneuver execution error, Mars gravity error and to the type of navigation filter was explored. This type analysis helps to identify critical mission and hardware design parameters. The baseline rendezvous to Deimos was used as the reference mission. The study was carried out in most cases by merely varying the error standard deviations input to the Monte Carlo program. For the navigation filter dependence, however, it was necessary to recompute the tracking accuracy covariance matrices based on the weighted least squares filter. These matrices were then input to the rendezvous simulation.

b. Results

1) Satellite Ephemeris Error - The Phase I study considered ephemeris error in the satellite's semi-major axis (Δa), inclination (Δi), longitude of the ascending node ($\Delta \Omega$) and true anomaly (ΔTA). These errors were modeled as uncorrelated. Since, however, the orbital inclination and eccentricity are small, there is in actuality a high correlation between $\Delta \Omega$ and the argument of periapsis error, $\Delta \omega$. For the baseline this situation was simulated by using a small $1\sigma_{\Omega}$ and deleting the $\Delta \omega$ effect. Here, the $1\sigma_{\omega}$ and $1\sigma_{\Omega}$ are equal and a correlation of -1.0 ($\rho_{\omega\Omega}$) is assumed between $\Delta \omega$ and $\Delta \ell$. Results are shown in Table III-19. (The case descriptions are found in Table III-20.)

The more accurate model with $\rho_{\omega\Omega}=-1$ gives a slightly smaller ΔV_{STAT} and slightly larger R99 than the baseline case. The 3σ case on the other hand is unacceptable in terms of ΔV_{STAT} increase. Note, however, that R99 is relatively insensitive to the level of ephemeris error. This is because the TV system (sighting data)

Table III-19 Sensitivity to Ephemeris Error

ERROR MODEL	ΔV_{STAT}	R99
Baseline (1σ)	98.3 m/s	20.9 km
3σ	141.9 m/s	23.6 km
$\rho_{\omega\Omega} = -1$	88.4 m/s	22.1 km

Table III-20 Case Description of 1σ Satellite Ephemeris Errors

Error Model	σ_a	σ_i	σ_Ω	σ_ω	σ_{TA}	$\rho_{\omega\Omega}$
Baseline (1σ)	7.5 km	.1°	.005°	1.5°	.1(-3)°	0
3σ	22.5 km	.3°	.015°	4.5°	.3(-3)°	0
$\rho_{\omega\Omega} = -1$	7.5 km	.1°	1.5°	1.5°	.1(-3)°	-1

is very effective in solving for the ephemeris. Table III-21 is a description of the ΔV breakdown for the Monte Carlo case which yielded the largest total ΔV. Note that the increased ephemeris error is detected after the OOM and its effect is removed with the LIM and the MCCM. The $\rho_{\omega\Omega}$=-1 case yielded a smaller ΔV_{STAT} because it effectively represents less ephemeris error than the 1σ case due to cancellation of both $\Delta\omega$ and $\Delta\Omega$ errors with 1.5^o sigmas (i.e., the baseline case was somewhat conservative in this respect).

2) Execution Error - Table III-22 shows the effect of tripling the execution errors for the rendezvous maneuvers (other than MOI). Table III-23 contains the baseline execution error model and Table III-24 computes the standard deviations for the nominal maneuvers. Both ΔV_{STAT} and R99 roughly double due to increased error.

Table III-25 contains data on the individual maneuvers for the five largest total ΔV_{STAT} cases (#9, #48, #42, #39, #19) when the execution error is tripled. The corresponding 1σ values are shown for comparison.

Note that only the LIM, MCCM and VMM are significantly different. Execution errors in the PCM does not affect the POM because the former is primarily out-of-plane and the latter is in-plane. The out-of-plane error will have to be taken out later with the LIM, MCCM and VMM. The POM execution error causes an error in the phasing orbit period. This period error will increase the mismatch in vehicle/satellite timing at apoapsis on the observation orbit. Also contributing to the timing error at rendezvous is the OOM execution error which alters the period of the observation orbit. These errors are removed by the LIM, MCCM, and VMM maneuvers at considerable expense. The last case in Table III-22 is for no execution error after MOI. Note the R99 is

Table III-21 Maneuver ΔVs for Largest Total ΔV Cases

Error Model	PCM	POM + OOM	LIM	MCCM	VMM
Baseline (1σ)	53.3	287.6	40.7	47.0	523.2
3 σ	53.3	287.5	63.8	66.6	524.0
$\rho_{\omega\Omega} = -1$	62.2	289.0	34.8	18.1	521.8

Table III-22 Effect of Execution Error

Case	ΔV_{STAT}	R99
Baseline: 1σ MOI, 1σ rend.	98.3 m/s	20.9 km
1σ MOI, 3σ rend.	216.5 m/s	37.8 km
1σ MOI, 0σ rend.	63.1 m/s	21.6 km

Table III-23 Baseline Execution Error Model

MOI:

$\sigma_\alpha = \sigma_\delta = .476°$

$\sigma_{t_B} = 1.76$ sec

$\sigma_{TA} = .158°$

OTHER MANEUVERS:

$$\sigma_\alpha = \sigma_\delta = \left[(.3166)^2 + \left(\frac{.0001}{/\Delta V/} \times \frac{DEG}{RAD}\right)^2\right]^{\frac{1}{2}}$$

$$\sigma_{t_B} = \left[\left(\frac{.15}{1000}\right)^2 + (.005/\Delta V/)^2\right]^{\frac{1}{2}} \times \frac{MASS}{THRUST}$$

$\sigma_{TA} = .158°$

Table III-24 Standard Deviations for Nominal Baseline Maneuvers

POM (ΔV = .0548 km/s):

$$\sigma_{t_B} = \left[225 \times 10^{-10} + (.005 \times 54.8 \times 10^{-3})^2\right]^{\frac{1}{2}} \times \frac{.3207 \times 10^4}{1.334} \cong .75 \text{ sec}$$

$$\sigma_\alpha = \sigma_\delta \cong .45°$$

OOM (ΔV = .2332 km/s):

$$\sigma_{t_B} = 2.8 \text{ sec}$$

$$\sigma_\alpha = \sigma_\delta \cong .32°$$

Table III-25 Maneuver Size vs Level of Execution Error

Maneuver	3σ Execution					1σ Execution				
	Case # 9	Case #48	Case #42	Case #38	Case #19	Case # 9	Case #48	Case #42	Case #38	Case #19
PCM	53.7	54.1	49.4	51.7	61.0	53.3	52.6	51.0	51.0	61.4
POM	143.4	123.6	150.0	97.2	54.1	140.8	125.3	153.7	99.1	54.6
OOM	148.6	155.0	133.2	187.4	241.4	146.8	157.8	131.6	189.7	233.4
LIM	83.9	89.8	89.3	78.9	47.9	40.7	34.3	29.6	23.7	17.4
MCCM	97.1	99.6	75.7	85.2	43.9	47.0	26.6	20.9	20.4	11.8
VMM	543.2	513.7	528.0	510.3	551.0	523.2	507.5	512.7	510.1	531.8

essentially what it is for the baseline (i.e. the effect of execution error on R99 is swamped by other error sources, namely the tracking knowledge error). Table III-22 also shows that an appreciable ΔV penalty is paid in attempting to remove the effect of execution error (i.e., 35 m/s).

When all in-orbit maneuver execution errors are set to zero except for the burn time error, ΔV_{STAT} is 217.4 m/s and R99 is 26.4 km. Comparing these results with Table III-22 implies that the burn time error is by far the most important of the 4 execution errors, and as already noted, execution error does not have a prominent effect on R99. Specifically the burn time error arises from the .5% ΔV scale factor uncertainty.

3) Mars Gravity Error - As Table III-26 shows, the rendezvous is insensitive to uncertainty in the Mars gravity central potential constant, μ_{MARS}.

Table III-26 Rendezvous Sensitivity

σ_μ	ΔV_{STAT}	R99
0. km^3/sec^2	98.2 m/s	20.9 km
(nominal) .1 km^3/sec^2	98.3 m/s	20.9 km
10. km^3/sec^2	108.9 m/s	25.0 km

This error affects the propagation of all Mars centered state vectors. In particular, though, it does not degrade the rendezvous ΔV_{STAT} or R99 because it will not affect the accuracy of the relative vehicle/satellite state when the two are in similar orbits.

4) Choice of Navigation Filter - The "Kalman/Schmidt (K/S) optimal consider filter" used for the baseline analysis is a sequential filter which utilizes the presumed known statistics of systematic error parameters in the filtering process. It also down weights (i.e., increases) the state covariance matrix when the state is propagated from measurement to measurement in the presence of dynamic uncertainty. A less optimistic filter utilizes a weighted least squares (WLS) "fit" to a data arc. It does not presume to know the statistics of any systematic error parameters. An error analysis of this type of filter produces a state covariance matrix which considers the operation of the filter in the presence of unknown systematic errors. The resultant state covariance matrix for the WLS filter will be "larger" than the K/S covariance matrix (i.e., the WLS estimate is likely to be more in error than the K/S estimate). Table III-27 shows the resultant vehicle and satellite standard deviations for the K/S and the WLS filters with and without μ_{MARS} and TV angle biases. Note that when biases are not present the K/S and WLS filters give comparable results but that when biases are present, the K/S filter can minimize their effect--if the "actual" bias error statistics are known. (These data are for the first TV tracking arc.) Table III-28 presents the relative state error standard deviations. The effect of these different filters (or errors) on the rendezvous is shown in Table III-29. Obviously from this data, the choice of navigation filter is critical to mission feasibility.

Table III-27 Standard Deviations of Vehicle and Satellite Error After First TV Tracking Arc

σ	With Biases		Without Biases	
	Kalman/Schmidt	Weighted Least Squares	Kalman/Schmidt	Weighted Least Squares
σ_x	.018 km	.12 km	.002 km	.002 km
σ_y	.024 km	.14 km	.002 km	.002 km
σ_z	.04 km	.4 km	.003 km	.0035 km
$\sigma_{\dot{x}}$	$3.1\text{x}10^{-3}$ m/s	.02 m/sec	3.8×10^{-4} m/s	3.9×10^{-4} m/sec
$\sigma_{\dot{y}}$	$3.4\text{x}10^{-3}$ m/s	.03 m/sec	4.2×10^{-4} m/s	4.5×10^{-4} m/sec
$\sigma_{\dot{z}}$	$7.6\text{x}10^{-3}$ m/s	.1 m/sec	1.8×10^{-3} m/s	1.9×10^{-3} m/sec
σ_a	.03 km	.56 km	.007 km	.007 km
σ_i	$2.2\text{x}10^{-6}$ rad	3.8×10^{-5} rad	6.1×10^{-7} rad	6.6×10^{-7} rad
σ_Ω	$7.9\text{x}10^{-5}$ rad	1.5×10^{-3} rad	2.3×10^{-5} rad	2.2×10^{-5} rad
σ_{TA}	$10.0\text{x}10^{-7}$ rad	1.8×10^{-5} rad	3.1×10^{-7} rad	3.2×10^{-7} rad

Table III-28 Standard Deviations of Relative State Error After First TV Tracking Arc

σ	Kalman/Schmidt	Weighted Least Squares
σ_x	1.9 km	35.4 km
σ_y	.4 km	7.7 km
σ_z	.07 km	.7 km
$\sigma_{\dot{x}}$	.02 m/sec	.41 m/sec
$\sigma_{\dot{y}}$	.1 m/sec	2.1 m/sec
$\sigma_{\dot{z}}$	.006 m/sec	.12 m/sec

Table III-29 Rendezvous Dependence on Filter Type

	Kalman/Schmidt	Weighted Least Squares
ΔV_{STAT}	98.3 m/s	234.4 m/s
R99	18.0 km	656.6 km

c. Conclusions - The feasibility of this rendezvous mission depends on the use of the Kalman/Schmidt filter when only the satellite and vehicle states are solved-for. The weighted least squares filter suffices only if all the biases are solved-for. If the level of a priori satellite ephemeris error increases it will affect ΔV_{STAT} only since the filter reduces the uncertainty to a low value. The additional ΔV is expended in the LIM, MCCM, and VMM once the ephemeris has been determined. It is important therefore, that sightings on the moons be made during the Mars approach phase of the mission. The rendezvous ΔV_{STAT} is also very sensitive to the maneuver execution scale factor error. This uncertainty is manifested in burn time error. Both execution error and ephemeris error affect the rendezvous by perturbing the observation orbit timing or phasing (i.e., the satellite is not at the vehicle apoapsis after 2½ revolutions in the observation orbit). Mars gravity uncertainties should have a negligible effect on the rendezvous mission.

3. Study III: Return-to-Earth ΔV Budget - Spin vs Three-Axis

a. Assumptions and Techniques - The return-to-Earth ΔV_{STAT} budget consists of the ΔV_{STAT} requirement for trimming the satellite stationkeeping orbit prior to trans-Earth injection (TEI) and for performing trans-Earth midcourse corrections (MCCs). The out-of-orbit ΔV_{STAT} was hand computed assuming the following maneuver sequence:

1) Raise apoapsis (to 95000 km) at the appropriate place on the circular stationkeeping orbit so that the angle between the line-of-apsides and the outgoing VHE vector is the required Mars departure turning angle ($\Delta V_{APO} \backsim 746$ m/s).
2) Perform a maneuver at apoapsis which rotates the orbit plane ($\backsim 10^{\circ}$) around the line of apsides so as to contain the out-going VHE vector ($\Delta V_{PC} \backsim 35$ m/s).
3) Lower periapsis to 1500 km for a more efficient TEI maneuver by maneuvering at apoapsis ($\Delta V_{PER} \backsim 75$ m/s).
4) Perform theTEI burn at periapsis ($\Delta V_{TEI} \backsim 766$ m/s).

Only Viking system execution errors and in-orbit knowledge errors were assumed in computing the out-of-orbit ΔV_{STAT} (these are found in Table III-30). The total ΔV excursion due to 3σ execution errors and knowledge errors was defined to be the ΔV_{STAT}

The ΔV budget for the MCCs is taken to be the sum of the individual mean MCC ΔV magnitudes and the 3σ standard deviations. Three MCCs were scheduled for the return leg. Their ΔV magnitudes depend on the TEI and MCC execution errors (either spin or 3-axis) and DSN in-orbit and trans-Earth knowledge error.

Assumptions for the return to Earth midcourse ΔV analysis are summarized in Table III-30. Two vehicular systems, spin stabilized and 3-axis, were examined to determine the feasibility of each. The mission was simulated by running STEAP (Reference III-2) error analysis assuming midcourse corrections at 10, 210, and 300 days for the spin stabilized and 3-axis vehicles. Results for 2-variable and 3-variable B-plane targeting strategies were compared for the MCCs. The 2-variable B-plane policy involves calculation of B•T, B•R, and minimization of $/\Delta V/$ in order to determine the three ΔV components. With the 3-variable B-plane policy,

Table III-30 Return to Earth ΔV Budget: Spin vs 3-Axis

ASSUMPTIONS

ΔV_{STAT} Out-Of-Orbit = ΔV_{STAT} For Rendezvous to Deimos With Encounter and Execution Error Only = 82.7 m/s

All Maneuvers Modeled As Impulsive With Resolution (res), Scale Factor and Pointing Errors (α, β) In Execution

Pre-TEI In-Orbit Knowledge Position Error of 5 km (Spherical)

Transearth Leg DSN Accuracy Degraded By Station Location and Earth/Mars Gravity Uncertainties. Range-Rate Data Only

Data Processed With Kalman / Schmidt Filter. A Priori State Down Weighted Between Measurements Due to Gravity Uncertainty

MCC's @ TEI + 10 Days, TEI + 210 Days, TEI + 300 Days (Total Return = 334.2 Days)

Execution Errors (MCC / TEI)

	Spin	3-Axis
$3\sigma_{res}$	.2/3.0 m/s	.2/3.0 m/s
$3\sigma_{scale}$	1.5/1.0%	1.5/1.0%
$3\sigma_{\alpha,\beta}$	4.5/4.5°	.57/1.5°

a time condition t is specified where t is the time the vehicle intersects the B-plane. In conjunction with B·T and B·R, the solution for ΔV can be reached. A study was conducted to compare these two targeting strategies at 5, 10, and 15 days past TEI with the diagonal control covariance (100, 100, 100, 10^{-4}, 10^{-4}, 10^{-4}) to determine the optimum time of the first MCC. The results are presented below.

MCC Time (TEI + days)	Expected ΔV		σ ΔV	
	2-Var B-Plane	3-Var B-Plane	2-Var B-Plane	3-Var B-Plane
5	46.5 m/sec	68.0 m/sec	31.6 m/sec	45.1 m/sec
10	41.7 m/sec	53.6 m/sec	20.8 m/sec	21.6 m/sec
15	42.7 m/sec	55.4 m/sec	21.5 m/sec	22.6 m/sec

Since considerable savings are obtained with the 2-variable B-plane strategy, it was employed for all the MCC studies The smallest $/\Delta V/$ occurred at TEI + 10 days. Consequently, the first MCC was performed at this time.

b. Results - The out-of-orbit ΔV_{STAT} was estimated under the assumption that the 3σ scale factor execution error and DSN knowledge errors are dominant error sources. These errors can produce 3σ velocity magnitude error of 12 m/s in ΔV_{APO}. The error in ΔV_{APO} may yield a lower apoapsis altitude which in turn will increase the plane change maneuver (ΔV_{PC}) by ~2 m/s. A 3σ knowledge error (~3 m/s) at the time of the ΔV_{PER} maneuver may produce a higher than desired periapsis altitude and thereby require ΔV_{TEI} to increase by ~15 m/s. Also, the ΔV_{TEI} maneuver may have a 3σ overburn of ~12 m/s due to the 1.5% scale factor error. These ΔV errors directly add to produce a ΔV_{STAT} of ~40 m/s.

The execution errors of each vehicle for the midcourse corrections are presented in Table III-30. The initial control covariance matrix of velocity component errors was generated based on TEI execution errors (Table III-30). Three different levels of pointing angle error were assumed (Table III-31) while resolution and scale factor errors were the same. QCOMP* was employed to calculate the velocity errors presented in Table III-31. Input to this program includes ΔV_{TEI**} and the execution errors for resolution, scale factor, and pointing angles. Since the velocity dispersions are proportional to the pointing errors, the pointing angle error is the major TEI error source.

The "effective" means and variances of the ΔV magnitudes at each midcourse correction are presented in Table III-32. The ΔV components at a MCC cannot be calculated directly because the MCCs are treated in an ensemble sense by STEAP error analysis. Consequently, the "effective" mean is the expected value of $/\Delta V/$. This mean and the "effective" variance are functions of the knowledge and control covariance matrices. (For further information refer to Reference III-1.) The total ΔV is the sum of the mean $/\Delta V/$ and 3σ, which is 68.09 m/sec and 23.62 m/sec for spin stabilized and 3-axis vehicles, respectively. The factor of 3σ in ΔV arises from the original factor of 3 in the post-TEI control velocity dispersions, i.e., it takes 3 times as much fuel to remove 3 times as much control dispersion. The 1σ B-plane control dispersion, $\sigma_{B \cdot T}$ and $\sigma_{B \cdot R}$, are given before and after the MCC. After the last MCC, these quantities are comparable for both vehicle types implying the spinning vehicle affords the same quality of trajectory control.

---

* QCOMP: refer to STEAP

** trans-Earth injection

Table III-31 Control Velocity Dispersions for Various TEI Pointing Misalignments

$\sigma_{\alpha\ \beta}$	$\sigma_{\dot{x}}$	$\sigma_{\dot{y}}$	$\sigma_{\dot{z}}$
(3-Axis) .5	5.48 m/sec	6.4 m/sec	5.29 m/sec
1.0	10.5 m/sec	12.65 m/sec	10.06 m/sec
(Spin) 1.5	15.65 m/sec	18.95 m/sec	14.95 m/sec

Table III-32 Midcourse Correction ΔV_{STAT} and Control Dispersions: Spin/3-Axis

		@ 10 DAYS	@ 210 DAYS	@ 300 DAYS
"Effective" Mean $\lvert\Delta V\rvert$		23.31 / 7.96 m/s	1.92/.66 m/s	.35/.30 m/s
"Effective" Standard Deviation of $\lvert\Delta V\rvert$		12.48 / 4.18 m/s	1.45/.50 m/s	.24/.22 m/s
Mean +3 (Standard Dev)		60.75 / 20.50 m/s	6.27/2.16 m/s	1.07/.96 m/s
σ B.T	Before MCC	1.11 E06/3.91E05 km	4.03E04/1.38E04	1.31E03/1.14E03
σ B.R	Before MCC	4.09 E05/1.41E05	1.16E04/4.02E03	3.67E02/3.32E02
σ B.T	After MCC	4.03 E04/1.38E04	1.21E03/1.14E03	2.15E02/2.08E02
σ B.R	After MCC	1.16 E04/4.02E03	3.67E02/3.32E02	4.43E01/6.11E01
"Effective" ΔV Components (Ecliptic)	$\Delta V_x =$	-7.09/-2.56 m/s	.81/.28 m/s	-.06/-.035 m/s
	$\Delta V_y =$	18.20/6.18 m/s	1.41/.48 m/s	.34/.28 m/s
	$\Delta V_z =$	-12.73/-4.32 m/s	-1.02/-.36 m/s	-.07/-.092 m/s

c. Conclusions - The out-of-orbit ΔV_{STAT} is about 40 m/s whether spin or 3-axis stabilized because it is due primarily to accelerometer scale factor error and in-orbit knowledge uncertainty. The MCC budgets for the spin and 3-axis systems differ primarily because of the size of the first MCC ($\sim$61 m/s for the spin system as opposed to $\sim$21 m/s for the 3-axis). The factor of 3 difference is due to a factor of 3 larger post-TEI velocity dispersion which in turn is produced by a factor of 3 larger TEI pointing misalignment error. The two vehicular stabilization systems, however, yield about the same statistics of actual trajectory dispersions (i.e., control) after the series of MCCs.

4. Study IV: Earth Entry Deflection ΔV - Spin vs Three-Axis

a. Assumptions and Technique - As the vehicle approaches Earth it is approximately on a hyperbolic trajectory. At some point past the Earth sphere of influence, it is necessary to perform an in-plane minimum ΔV deflection maneuver that is targeted to achieve a flight path angle of -7.25° at entry interface (400,000 ft). It is assumed that the deflection errors are equal to the MCC execution errors and that a DSN update occurs immediately prior to the deflection maneuver where the update is based on coherent doppler data taken 30 days prior to the deflection time. The optimum deflection time for each vehicle type was selected by a parametric study involving candidate deflection times at .5, 1.0, 1.5, and 2.0 days past the Earth sphere of influence. To obtain the knowledge and control covariance matrices, guidance events were called for in the STEAP error analysis runs at the deflection times. The 1σ knowledge and control dispersions are presented in Table III-33. ENTRY2 (Reference III-3) was then employed to determine flight path angle (γ) and $/\Delta V/$ dispersions at the four deflection times and to determine the optimum deflection time.

Table III-33 1σ Control and Knowledge Dispersions* at Deflection Times

	SOI + .5 DAYS		SOI + 1.0 DAYS		SOI + 1.5 DAYS		SOI + 2.0 DAYS	
	Position	Velocity	Position	Velocity	Position	Velocity	Position	Velocity
Spin Control	46.6x196.2x43.6	2.4x10^{-2} x7.3x10^{-2} x1.3x10^{-2}	47.7x199.1x44.1	2.4x10^{-2} x5.96x10^{-2} x1.1x10^{-2}	48.7x201x44.4	2.6x10^{-2} x2.1x10^{-2} x7.5x10^{-3}	49.4x198.8x43.9	9.1x10^{-2} x2.1x10^{-1} x5.7x10^{-2}
3-Axis Control	18.6x178.4x82.6	1.4x10^{-2} x6.5x10^{-2} x2.4x10^{-2}	19.2x181x83.5	1.4x10^{-2} x5.3x10^{-2} x1.9x10^{-2}	19.7x182.7x84.1	1.1E^{-2}x68E^{-2} x3.9E^{-3}	19.8x180.6x82.8	3.4E^{-2} x1.9E^{-1} x9.9E^{-2}
Spin Knowledge	.87x.73x.59	7.4x10^{-4} x1.1x10^{-3} x1.9x10^{-3}	.57x.5x.5	7x10^{-4} x1.0x10^{-3} x1.9x10^{-3}	.43x.42x.46	7.4x10^{-4} x1.0x10^{-3} x1.9x10^{-3}	.27x.15x.33	8.2x10^{-4} x1.1x10^{-3} x21x10^{-3}
3-Axis Knowledge	.87x.72x.59	6.2x10^{-4} 1.1x10^{-3} x1.6x10^{-3}	.57x.5x.49	6.x10^{-4} x1.1x10^{-3} x1.6x10^{-3}	.44x.42x.46	6.4x10^{-4} 1.1x10^{-3} 1.6x10^{-3}	.26x.14x.32	7.4x10^{-4} x1.2x10^{-3} x1.7x10^{-3}

* Cartesean Ecliptic Coordinates, $\sigma_X \times \sigma_Y \times \sigma_Z$, $\sigma_{\dot{X}} \times \sigma_{\dot{Y}} \times \sigma_{\dot{Z}}$, km and m/s

a. Results - The data in Table III-34 are presented as 99.6% γ and $/\Delta V/$ dispersions which are approximately 3σ values (99.8% dispersion). Histograms representing the number of sigmas vs the number of samples for flight path angle and ΔV magnitude were calculated at each deflection time. The 99.6% dispersions were calculated by utilizing these histograms and the actual sample standard deviations. For example, take the spin stabilized vehicle at SOI + .5 days (Figures III-5 and III-6 are the required histograms). The sample standard deviations were:

$$\sigma_\gamma = .33^\circ$$

$$\sigma_{/\Delta V/} = 9.1 \text{ m/sec}$$

From the first graph (Figure III-5) 99.6% of the sample dispersions lie within ±3 and the 99.6% γ dispersion is $.99^\circ$. For $\sigma_{/\Delta V/}$, 99.6% of the samples lie within $\pm .46\sigma$ (Figure III-6). Thus the 99.6% $/\Delta V/$ dispersion is .46 (9.1) = 4.2 m/sec. Large sample standard deviations resulted from one or two outliers in the data.

As the deflection time approaches encounter, the γ dispersion decreases because the errors have a shorter time to propagate. The $/\Delta V/$ dispersion increases, however, as more ΔV is needed to change the trajectory when the velocity on the approach orbit increases towards encounter.

From Table III-34 it can be seen that SOI + 1.5 days is the optimal deflection time where the total ΔV is 14.5 m/sec and the maximum expected dispersion is $\pm .5^\circ$.

Even though the spin stabilization system has larger execution uncertainties than the 3-axis vehicle, the results of the 99.6% γ and $/\Delta V/$ dispersions are essentially equal. Data computed at SOI + 1.5 days with the pointing angle errors set equal to 0 further demonstrate that pointing angle errors are not

Table III-34 99.6 Percentile Flight Path Angle (γ) and /ΔV/ Dispersions: Spin/3-Axis

DEFLECTION TIME (S O I + DAYS)

					$\sigma_\alpha = \sigma_\beta = 0$
	.5	1.0	1.5	2.0	1.5
99.6% γ Dispersion	.99° 1.07°	.73° .74°	.50° .56°	.31° .31°	.53° .52°
99.6% |ΔV| Dispersion (m/sec)	4.2 4.13	5.6 5.5	8.5 8.3	18.1 17.8	8.5 8.3
Nominal ΔV (m/sec)	3 3	4 4	6 6	12.2 12.2	

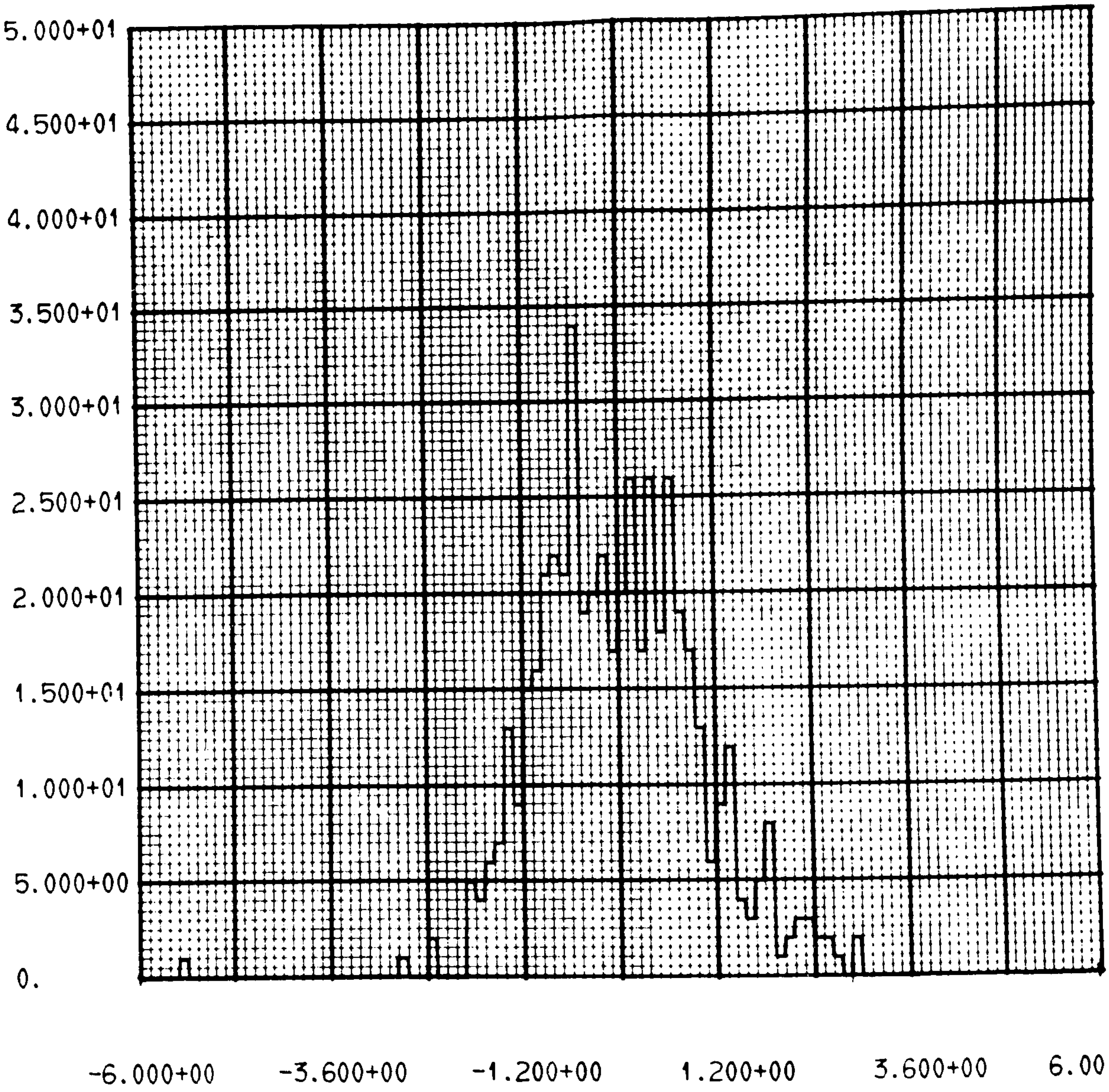

NUMBER VS SIGMA

1 FLIGHT PATH ANGLE - DEFLECTION AT 332.287

SPIN

Figure III-5 Sigma vs Sample Histogram

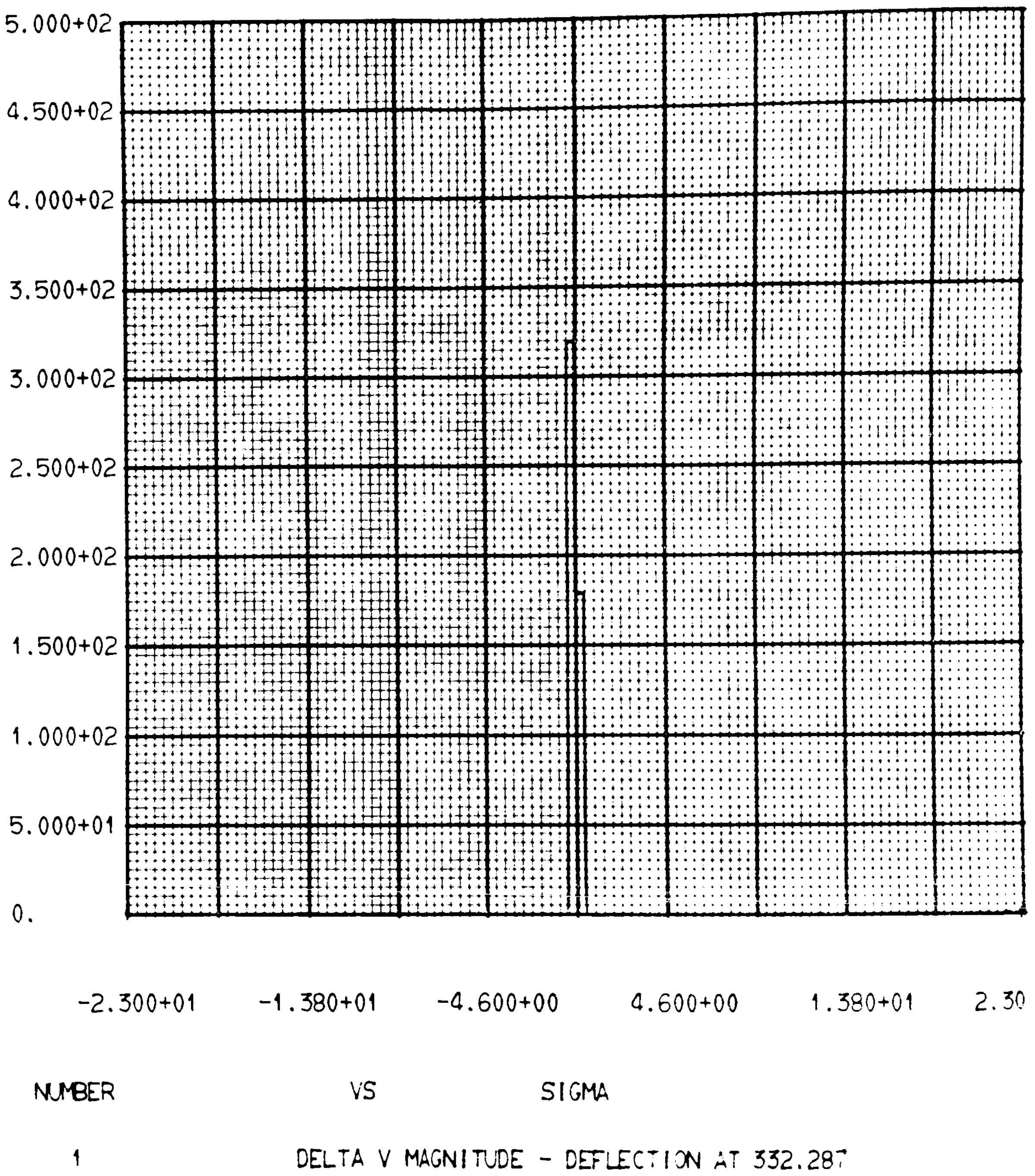

SPIN

Figure III-6 Sigma vs Sample Histogram

significant in determining $\sigma_{/\Delta V/}$ and σ_{γ}. The reason is the small ratio of deflection ΔV to vehicle velocity. The following diagram demonstrates this ratio and the effect of the angle error.

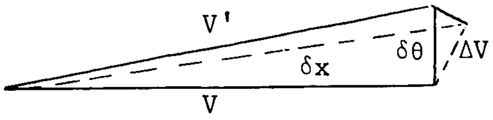

The resultant velocity angle error δx, due to a ΔV pointing error δθ, is equal to

$$\frac{\Delta V - \Delta V \cos\delta\theta}{V'} = \frac{\Delta V \ (\delta\theta)^2}{V'2}$$

The velocity magnitude is approximately 4000 m/sec and /ΔV/ is about 6 m/sec. Then the ratio

$$\frac{\Delta V}{V} = \frac{6}{4000} = 1.5 \times 10^{-3}$$

Equation 1 for 1.5° pointing angle error becomes

$$1.5 \times 10^{-3} \times \left(\frac{1.5}{57}\right)^2 \cdot \tfrac{1}{2} \approx 4.8 \times 10^{-7} \text{ rad} \approx 2.74 \times 10^{-5} \text{ deg.}$$

Consequently, the resultant angle error is small and has little effect on $\sigma_{/\Delta V/}$ and σ_{γ}.

c. Conclusions - Table III-35 gives the total return to Earth ΔV_{STAT} budget, where total ΔV equals 123 m/sec and 79 m/sec for spin stabilized and 3-axis vehicles, respectively.

Table III-35 Total Return to Earth ΔV_{STAT} Budget

- Spin Stabilization Does Not Degrade Quality of Earth Entry
- Deflection Should Occur @ SOI + 1.5 Days With Total ΔV Cost of 15.0 m/s. Max Expected γ Dispersion is ± .5°

	ΔV_{STAT} REQUIREMENT	
MANEUVER PHASE	SPIN	3-AXIS
Out-Of-Orbit	40.0 m/s	40.0 m/s
MCC's	68.0 m/s	24.0 m/s
Deflection	15.0 m/s	15.0 m/s
TOTAL ΔV	103.0 m/s	79.0 m/s

REFERENCES

III-1 Phase I Navigation Analysis

III-2 STEAP (Space Trajectories Error Analysis Programs), Version II, 3 Volumes, March 1971, Space Navigation Technology, Martin Marietta Corporation.

III-3 ENTRY2: A Program to Determine Entry Parameter Dispersions, December 31, 1970, Task Authorization 48848.

IV. Phobos/Deimos Phase II - Concept Trade Studies

IV. Phobos/Deimos Phase II
Concept Trade Studies

IV. PHOBOS/DEIMOS PHASE II - CONCEPT TRADE STUDIES

The sample return mission is unique in many dimensions, but most notable is the requirement that an **Earth** return spacecraft perform after up to two years "storage" in an interplanetary and orbital environments. The trade studies aimed at definition of candidate return vehicle concepts at compatible weights and minimum potential cost utilizing low risk technologies constituted a major proportion of the study effort during this phase.

The objective and result of this effort was to establish relative cost, performance and development risk estimates for a number of alternative mission concepts and to select a "baseline concept" for further definition. The result of the trade studies leading to mission concept rankings are reported in the following paragraphs. In concert with the scope of this study, and since numerous options exist for potential sample return missions, a simple evaluation model was employed to allow an understanding of the wide range of alternatives possible. The model (described below) utilized the dimensions of cost, performance risk and development risk on an equal weight basis to define an overall comparative score. In order to maintain high emphasis on generation of the best possible cost estimates, a space program cost model, developed for NASA by Planning Research Corporation, was employed. This model was updated by procedures used in the cost estimating organization within Martin Marietta derived from direct involvement in a number of current space programs.

A. TRADE STUDY GROUND RULES AND GUIDELINES

Groundrules and guidelines jointly established by NASA and the contractor allowed an overall comparative analysis within the scope of this study. Maximum use of Phase I launch vehicles and Phobos/Deimos orbit delivery vehicles allowed concentrated definition of return spacecraft during this phase. Potential mission elements defined in Phase I are summarized below:

Launch Systems:	Titan IIIE/Centaur Titan IIIC Titan IIIE (7) Centaur Shuttle/Centaur
Satellite Delivery Systems:	38% Stretch Viking Orbiter 60% Stretch Viking Orbiter Staged Viking Orbiter Space Storable Propellant Viking Orbiter
Satellite Landing Mode:	Landed Orbiter Separable Lander

Definition of Earth return spacecraft considered only proven or currently identified technologies in order that the lowest cost and risk candidates evolve for consideration.

The baseline launch opportunity was 1981 with considerations of 1979 and 1983 to be performed at a lesser depth.

The basic trans-Mars and Mars orbiting vehicle is the Viking Orbiter modified for the Phobos/Deimos missions.

Sample acquisition, handling, processing, and stowage equipment is defined to sufficient level to derive weight, volume, and power estimates. No detailed design trades on this subsystem were required.

Sterilization requirements were relaxed for both the satellite landing missions and Earth recovery which is direct entry with water recovery.

B. EARTH RETURN VEHICLE DEFINITION

Return vehicle definitions were accomplished drawing on technologies from current and recent space programs employing both three axis stabilized and spin stabilized spacecraft. The pacing constraint for a Phobos/Deimos sample return mission is the high energy of a round trip to Mars, in light of the payload capability of existing launch vehicles and spacecraft propulsion systems. This implies a weight allocation for a return spacecraft considerably less than that available Mariner class interplanetary spacecraft and points toward adding the required propulsion capability to the lightweight "flyby" spacecraft.

Interplanetary spacecraft were surveyed, and subsystem technologies screened for applicability to the Phobos/Deimos sample return mission. Major considerations in the return spacecraft system definition were:

a) Attitude stabilization concept:
    three axis vs spin stabilized
b) Navigation strategy:
    planar vs broken plane
    coherent doppler vs doppler, plus two-way ranging
    TV imaging for orbital corrections
c) Subsystem implementations:
    Structure, propulsion, thermal control and communication.

The survey of a subsystem technologies produced a compendium of proven candidates for a sample return spacecraft. A typical summary of guidance and control and navigation sensors is indicated in Table IV -1.

Table IV-1 Earth Return Vehicle Subsystem Trades

GUIDANCE & CONTROL COMPONENTS	Dev Status For Space Use	Reliability Considerations			
		1 mo	1 yr	3 yr	
Control Computer & Sequencer					
Viking & Mariner	Proven	Exc	**Exc**	Exc	
Surveyor	Proven	Exc	Exc	Exc	
Lunar Orbiter	Proven	Exc	Exc	Exc	
IRU					
Rate Gyros					
Teledyne	Proven	Exc	Bad	Bad	These Should Be Adequate For 3 Year Mission When Gyros Are Only Used When Needed
U. S. Time	Dev & Flown	Exc	Bad	Bad	
Mariner	Proven	Exc	Bad	Bad	
Viking	Proven	Exc	Exc	Bad	
Surveyor	Proven	Exc	Bad	Bad	
Lunar Orbiter	Proven	Exc	Bad	Bad	
Accelerometers	Proven	Exc	Exc	Exc	Not a Critical Item
Sun Sensors					
Mariner	Proven	Exc	Exc	Exc	Analog Sensors
Viking	Proven	Exc	Exc	Exc	
Surveyor	Proven	Exc	Exc	Exc	
Lunar Orbiter	Proven	Exc	Exc	Exc	
Adcole	Proven	Exc	Exc	Exc	Digital Solar Aspect Sensor
Star Sensor					
PE	Proven	Exc	Exc	Exc	Developed Technology
Mariner	Proven	Exc	Exc	Exc	
Viking	Proven	Exc	Exc	Exc	
Surveyor	Proven	Exc	Exc	Exc	Fixed FOV
Lunar Orbiter	Proven	Exc	Exc	Exc	Fixed FOV
Rendezvous Radar					
Viking	Proven	Exc	Exc	Exc	Modified Radar Altimeter
Gemini	Proven	Exc	Exc	Exc	Promising System But Will Not Be Available
Apollo		Exc	Exc	Exc	Heavy & Sophistiated RR

Interplanetary spacecraft with application to Phobos/Deimos sample return are the Pioneer, Mariner, and Planetary Explorer series (e.g., the Venus Pioneer which is planned for operation in 1977). Definition trades resulted in two candidates each for the 3-axis and spin stabilized configurations. Navigation tracking is by coherent doppler in each case with telecommunications for engineering and navigation data relay only.

Mariner type spacecraft were the only 3-axis stabilized systems functionally meeting the Earth return requirements. The Mariner, however, required significant redesign of structural, power, communications, science, and data handling subsystems to meet the weight requirements. The Mariner does provide a proven platform at a relatively heavy weight.

The Pioneer series (spin stabilized) offer lightweight vehicles but when configured to provide orbital escape, navigation and propulsion capabilities, appear very similar to the currently identified Planetary Explorer/Venus Pionner. For this reason the spin-stable spacecraft will be referred to in this study as derivations of the Planetary Explorer. The functional capability of the Planetary Explorer closely matches Phobos/Deimos sample return mission requirements. Required modifications for a minimum change version were liquid primary propulsion to replace existing solid propulsion, thermal control modified for an outer planet mission, antenna changes for Mars distances and structural changes to accommodate liquid propulsion and the entry module.

An adaptation of Mariner '71 and Planetary Explorer with minimum changes represent a current 3-axis and a spin-stable vehicle for comparative evaluation. Neither, however, are optimized for the Phobos/Deimos application but represent configuration of less potential development risk and cost. The Mariner spacecraft is about twice the weight of Pioneer for the same mission, which in some mission years generates significant impact on propulsion and launch vehicle requirements.

Another version of the Planetary Explorer was then deferred, requiring more changes than the minimum modifications listed above. This version, better optimized for this mission but still incorporating existing or planned subsystem designs, presented the lightest weight candidate for evaluation. As a competitor for this lighweight modified Planetary Explorer vehicle in the evaluation process, we also defined a new, minimum weight, 3-axis stabilized vehicle using later state of the art technology than the Mariner series. The characteristics of these candidate earth return vehicles are summarized in Table IV -2.

Table IV-2 Earth Return Vehicle Trade Results

	Weight Realm	Attitude Stabilization	Current Development State
Planetary Explorer (Minimum Changes)	633	Spin	Under Development
Mariner (Changes as Required)	1300	3-Axis	Developed
Modified Planetary Explorer (Changes as Required	410	Spin	
New 3-Axis Stable Module (Configure as Required)	450	3-Axis	

A preliminary design of an earth entry module was performed to establish weight, volume, sample accommodation properties of a module optimized for sample return. The module, described in Section V, is capable of Earth entry at up to 42,000 ft/sec. It was found that a 5 kg sample could be contained within a 40-lb module, and a 2 kg sample within a 33-lb container.

C. SAMPLE RETURN MISSION INTEGRATION

The earth return vehicle candidates required integration into a complete sample return mission. Mission operations and hardware requirements for trans-Mars through satellite landing are essentially those defined in the Phase I study. Added to the sample return mission are revised surface science operations, the earth return vehicle and the earth entry module. Space storable propellants were considered as an alternative concept since they were required to deliver some of the mission candidates. Table IV -3 summarizes the required orbiter types for each candidate earth return vehicle for the launch years of interest. The "landed orbiter" is a Viking Orbiter spacecraft modified for satellite landing in the fractional gravity environment. The separable lander is derived from landing capsule of Study Phase I modified to house the return spacecraft. The lander communicates to Earth through the return spacecraft systems.

The "round trip control module" concept indicates the potential increase in performance efficiency possible by utilizing a return spacecraft optimized for sample return and propulsion modules which are staged as their function is completed. only the lightweight three-axis stabilized module is adaptable to this configuration due to the difficulty of spin stabilizing

Table IV-3 Sample Return Configurations for Earth Return Vehicle Types

RETURN VEHICLE TYPE	LANDING CONCEPT	PROPULSION REQUIREMENT 79	 81	 83
Modified Planetary Explorer	Lander Orbiter	<38% VO	38% VO	Staged VO
	Separable Lander	38% VO	Staged VO	Space St.
New Three-Axis Stabilized	Landed Orbiter	<38% VO	38% VO	Staged VO
	Separate Lander	38% VO	Staged VO	Space St.
Planetary Explorer	Landed Orbiter	<38% VO	38% VO	Staged VO
	Separate Lander	38% VO	Staged VO	Space St.
Mariner	Landed Orbiter	60% VO	Space St.	Space St.
	Separate Lander	Staged VO	Space St.	New LV
Round Trip Control Module	Integrated Lander	<VO	VO	38% VO

the large propellant masses required for the interplanetary and Mars orbit insertion mission phases. This configuration offers the most desirable engineering solution at some deviation from initial groundrules by incorporating a completely new configuration of proven technologies.

The Titan IIIE/Centaur launch vehicle is the minimum launch vehicle for any element of the candidate matrix except the Mariner Separate Lander mission in 1983 which requires a larger launch vehicle (7 segment Titan for example).

The propulsion requirement versus sample return mission concept matrix provides initial comparative relationships with respect to the ultimate selection of a baseline mission. 1981 was specified as the baseline opportunity for the study. In this year, all separable lander configurations require staged V.O. propulsion except the Mariner which requires the use of space storable propellants. On the other hand, either of the spin-established candidates or the newly configured three-axis module can be accomplished with the 38% stretch landed orbiter configuration. From a weight and performance point of view many configurations are possible employing either a separate lander or landed orbiter in 1979 with Earth storable propellant.

Any of the candidates requiring space storable propellants can be accomplished on a larger launch vehicle utilizing Earth storable propellant. However, this would require development of a new propulsion module with a larger propellant capacity than one that could reasonably be called a modified Viking Orbiter.

D. MISSION EVALUATIONS

The evaluation model used to compare mission candidates was based on the dimensions of cost, development risk and performance risk.

Relative cost is derived from the Planning Research Corporation (PRC) model augmented by Martin Marietta data from the Viking program and other current space programs. The PRC model provides a cost indication derived from a comprehensive survey of space programs and is entered on the basis of subsystem weights.

Development and performance risk, based on qualitative judgements by experienced engineers, are assigned integral values on a scale from 1 through 4 where a one is "most desirable". A "1" on the scale for development risk indicates the least number of elements or new technology applications. A "1" on the scale for relative performance risk indicates that the least number of key mission functions must be accomplished successfully in sequence for overall mission success.

The normalized average is obtained by totaling all three dimension indicators (Relative Cost + Relative Development Risk + Relative Performance Cost) and dividing this total by the minimum total.

Summarized in Table IV -4 are the results of the overall cost and risk evaluation. The following addresses significant interrelationships within the matrix and conclusions leading to candidate rankings:

a) A 38% propellant stretch causes considerably less structural and thermal impact to the Viking Orbiter than the 60% stretch. The 38% stretch is accomplished by increasing the size of the present tank configuration whereas the 60% stretch

Table IV-4 Sample Return Configuration Evaluation

BASIC CRITERIA: Cost
Development Risk
Performance Risk

Return Vehicle Type	Landing Concept	Prop Mode on T/IIID/Centaur	Relative Cost	Relative Dev Risk	Relative Perf Risk	Normalized Average
Modified Planetary Explorer	Landed Orbiter	38%	1.0	2.0	1.0	1.0
	Sep. Lander	Staged	1.43	3.0	2.0	1.61
New 3-Axis Stabilized	Landed Orbiter	38%	1.0	3.0	1.0	1.25
	Sep. Lander	Staged	1.43	4.0	2.0	1.87
Planetary Explorer (Minimum Change)	Landed Orbiter	60%	1.05	3.0	1.0	1.26
	Sep. Lander	Staged	1.33	4.0	2.0	1.83
Mariner (Shared Orbiter Subsystems	Landed Orbiter	Space Storables	1.25	3.0	1.0	1.32
	Sep. Lander	Space Storables	2.01	4.0	2.0	2.10
Round Trip Module	Integrated Lander	Basic 75 Viking Orbiter Size	1.0	3.0	2.0	1.50

Development Risk & Performance Risk Code
1 Best

requires a new four tank configuration with supporting structure. The four tank configuration, however, lends better dynamic stability (lower c.g.) for the landed orbiter mode than the higher two tank 38% stretch orbiter.

b) A modified Planetary Explorer (new structure, power, thermal, propulsion) could be accomplished at less risk than a new three-axis stable module since such a vehicle is a completely new configuration composed of a mix of Mariner, Lunar Orbier and Planetary Explorer subsystems.

c) A space storable propellant system represents increased development and performance risk because of the early state of development of that technology. If space storables were developed by the time frame of sample return mission, cost and risk factors associated with their application could be reduced considerably. Incorporation of space storables in a Viking Orbiter causes considerable structural and thermal impact.

d) In considering a separable lander vs a landed orbiter, the relevant tradeoff is between increased complexity of integrating a lander systems and the increased risk of modifying a vehicle intended as an orbiter for a lander mission.

The overall evaluation indicates that while a Planetary Explorer with minimal change could be developed at lower cost than the P.E. optimized for the Phobos/Deimos mission, the minimim change P.E. requires a 60% propellant stretch in 1981, resulting in impact to Viking Orbiter structure and thermal control subsystems.

With respect to cost alone there is close competition among alternatives. The modified P.E., the new three-axis module, and the round trip control module on landed orbiters are all relatively equal in cost. The Mariner cost, while now handicapped by the high development cost of the space storable propulsion would also be highly cost competitive should space storables be fully developed in time for a sample return mission.

Viewing the matrix with overall assessments applied, several relationships are evident:

a) All separable lander missions present greater (less desirable) indicators than the landed orbiter missions. Lander missions, however, provide greater potential flexibility and science return since the orbiter could be used for other science or support functions.

b) The Mariner type return spacecraft would be highly competitive should space storables become fully developed.

c) The round trip module (drop-off propulsion) offers outstanding flexibility at small propulsion impact over the basic Viking Orbiter over all three opportunities (1979, 1981, and 1983) with an overall indicator less than most separable lander missions.

d) A separable lander mission involving a modified Planetary Explorer spacecraft or a new three-axis stabilized configuration offers a flexible mission at less than 50% increased cost with valuable science return even allowing an unsuccessful sample return.

Evident, then, from such an evaluation is one mission appearing definitely more desirable, with much competition and many desirable features between several alternatives. The overall matrix can be reduced to four basic categories which are summarized in Table IV -5.

The modified Planetary Explorer carried by a landed Viking Oribiter with a 38% propellant increase is the selected "most

Table IV-5 Sample Return Basic Configurations

		Relative Cost	Dev. Risk	Perform Risk
Baseline	Modified Planetary Explorer (or New Three-Axis Vehicle) Landed Orbiter - 38% Stretch	1.0	2 (3)	1
Preferred Alternate	Round Trip Control Module/Lander Propulsion Module-75 Orbiter	1.0	3	2
Alternate	Modified Planetary Explorer (or New Three-Axis Vehicle) Separable Lander-Relay Communications Orbiter - Staged	1.43	3 (4)	2
Alternate	Mariner Type Landed Orbiter - Space Storables	1.25	3	1

( ) Indicate factor if: Planetary Explorer is not developed for the Venus missions.

desirable" mission from the tradeoff evaluation. The newly configured lightweight three-axis stabilized vehicle can be substituted for the modified Planetary Explorer at a small increase in development risk.

The preferred alternate mission uses the new three-axis stabilized control module to control the spacecraft for the entire three year mission, dropping propulsion modules as they are used. This configuration offers great flexibility over all launch opportunities studied.

Alternates include a modified Planetary Explorer landed on the satellite by a separate lander capsule, and a Mariner type spacecraft utilizing space storable propellants. The lander mission provides flexibility since the orbiter can continue science studies following lander support, and the Mariner type platform offers proven subsystem technologies.

Descriptions of the study baseline follows in more detail in Chapter V.

The cost analysis performed in order to evaluate alternative configurations for the baseline sample return year of 1981 included, in addition, analyses for 1979 and 1983. In all cost studies the primary model was the Planning Research Corporation model augmented by in-house current data. A high degree of confidence is possible for relative cost indicators. Cost values are presented in a normalized fashion since a absolute value is beyond the scope of this study. Absolute cost estimates for the baseline sample return program are included in Section VII of this report. Included in Table IV -6 are the results of the cost comparison by year. These data were again normalized to the minimum of the total set. Delta costs over launch opportunities are primarily attributable to increased Mars braking

Table IV-6 Overall Relative Cost Comparison by Year

		YEAR	
	79	81	83
Modified Planetary Explorer (or New Three-Axis) Landed Orbiter	1.01	1.05	1.04
Round Trip Control Module/Lander Propulsion Module	1.0	1.0	1.05
Modified Planetary Explorer Return Separate Lander (Relay Communication) Orbiter	1.42	1.43	1.66
Mariner Type Return Landed Orbiter	1.21	1.26	1.31
Planetary Explorer Return Landed Orbiter	.98	1.06	1.01
Planetary Explorer Return Separate Lander (Relay Communication) Orbiter	1.36	1.39	1.57

propulsion and its impact on orbiter structures.

A trade study performed to establish sensitivity of cost and weight to the propulsion system options (defined in study Phase I and used for the sample return studies) is summarized in Table IV -7.

The significant increase with the 60% propellant stretch is due to the relatively great structural and thermal impact of the four tank configuration. The notable increased cost of space storables includes a high development cost which could be unnecessary by the time frame of a Phobos/Deimose sample return mission. The staged propulsion module would cause very little modification to basic Viking Orbiter structure other than to provide mounting interface for staging. Staging technology is well established resulting in a relatively low risk function. Space storable propellants and engine occupies about the same volume as the basic Viking Orbiter propulsion system and requires modified structure and thermal protection for the propellant high density and low temperature. NASA is currently funding development of space storable propellant systems.

The baseline identified for this study following the overall trade evaluations is a modified Planetary Explorer return vehicle attached to a modified Viking Orbiter with a 38% propellant increase over the 1971 Viking Orbiter. The baseline and alternate configurations are discussed in detail in Chapter V.

Trade studies showed that a newly configured three-axis stabilized vehicle of proven subsystems would be about the same weight as the modified Planetary Explorer, this return vehicle type is therefore carried as a very desirable alternate baseline with a slightly increased developmental risk.

Table IV-7 Modified Viking Orbiter Cost Trade Due to Propulsion Options

	PROPULSION OPTION			
	38% Stretch	60% Stretch	Staged	Space Storables
Orbiter & Separate Lander				
Cost	1.1	1.33	1.13	2.05
Weight	1.0	1.07	1.13	1.01
Landed Orbiter				
Cost	1.0	1.28	1.08	1.95
Weight	1.02	1.1	1.16	1.03

V. System Description

V. SYSTEM DESCRIPTION

A. SYSTEM OVERVIEW

This section presents the overview of the baseline and alternate spacecraft designs and briefly discusses the system level trades that were conducted that allowed us to select the recommended configurations. Details of the individual subsystems are presented in the remaining sections of this Chapter.

In selecting a baseline sample return mission configuration the major trade elements that were considered and analyzed are summarized below:

- Launch Systems:
  - Titan IIIC
  - Titan IIIE/Centaur
  - Titan IIIE(7)/Centaur
  - Shuttle/Centaur
- Satellite Delivery Systems:
  - 38% Stretch Viking Orbiter
  - 60% Stretch Viking Orbiter
  - Staged Viking Orbiter
  - Space Storable Propellant Viking Orbiter
  - Propulsion Module with Round Trip Control Module
- Satellite Landing:
  - Landed Orbiter
  - Separable Lander
- Earth Return Vehicles:
  - Modified Planetary Explorer
  - New Three-Axis Stabilized Vehicle
  - Mariner Derivative
  - Round Trip Control Module

The general objective was to find a baseline configuration that would require minimum cost but would also minimize development risk by using hardware and technology proven on other programs. Results of the system level trades discussed in Chapter IV allowed us to define two attractive configurations. The modified Planetary Explorer delivered to the Martian moons by a landed Viking Orbiter with a 38% propellant increase is the recommended baseline configuration. The newly configured (Phase II study effort) lightweight (197 kg) three-axis stabilized vehicle can be substituted for the modified Planetary Explorer at a small increase in development risk.

The alternate configuration employs the new three-axis stabilized control module to control the spacecraft for the entire three year mission, jettisoning the satellite delivery system propulsion module just prior to the final closure and touchdown maneuver.

Two other configurations were also carried into the conceptual design phase. These included a modified Planetary Explorer landed on the satellite by a separable lander capsule, and a Mariner-type spacecraft utilizing space storable propellants. The lander mission concept provides greater mission flexibility since the orbiter can continue science studies after deploying the lander, while the Mariner-type concept offers proven subsystem technologies.

1. Selected Baseline Configuration

The 3159 kg baseline Phobos/Deimos sample return spacecraft is shown in Figure V-1. The orbiter/launch vehicle adapter truss, which is identical to the Viking '75 adapter truss supports the Phobos/Deimos spacecraft at four symmetrical points and is attached to the modified Viking Orbiter with ordnance operated bolts and springs. This forms the Phobos/Deimos spacecraft launch

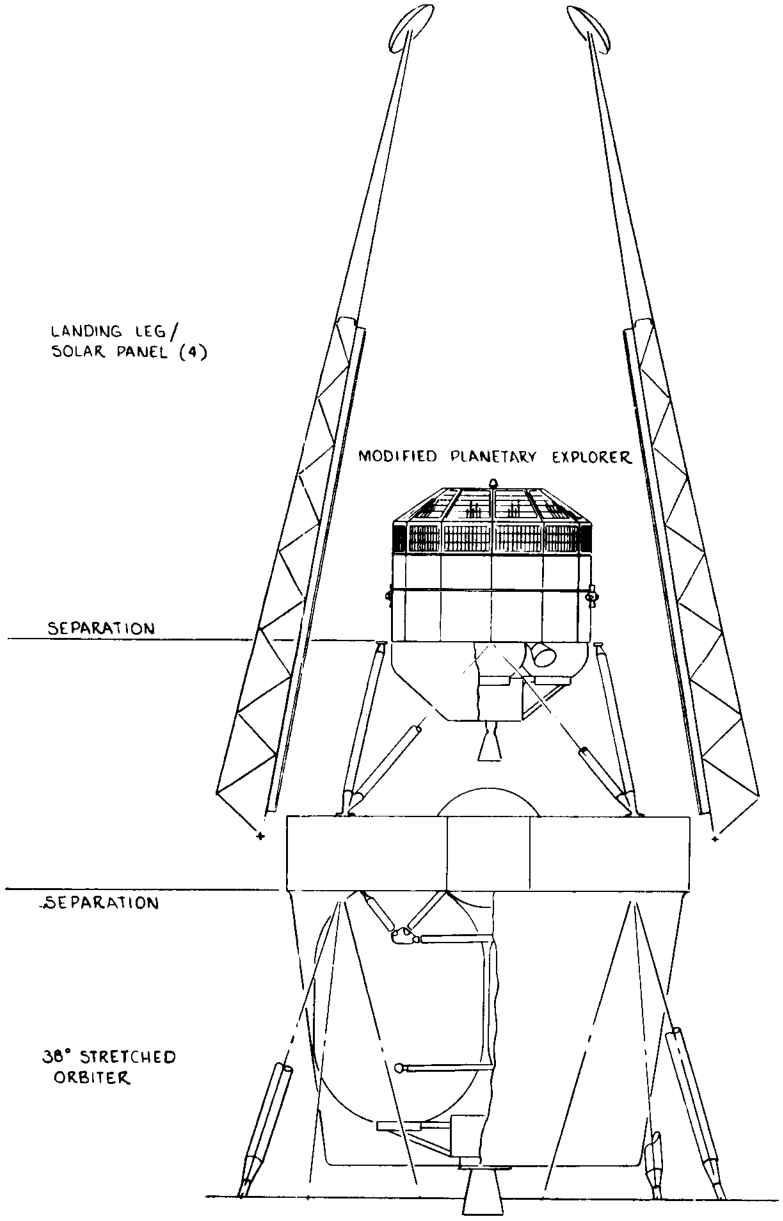
LANDING LEG/
SOLAR PANEL (4)
MODIFIED PLANETARY EXPLORER
SEPARATION
SEPARATION
38° STRETCHED
ORBITER

Figure V-1 Baseline Sample Return Configuration

vehicle separation plane. The earth return module is attached to the modified orbiter by means of a newly designed truss. The forward end of the truss attaches to the lander at four symmetrically located points. The aft end of the truss attaches to the orbiter, also at four symmetrical points, mating with the same attachments on the orbiter as is presently utilized for the baseline Viking '75 mission. Separation of the earth return vehicle from the orbiter is provided at the earth return vehicle interface by ordnance actuated bolts and springs. The truss remains with the orbiter after the earth return module is deployed on its return trip to earth. The orbiter dry weight is 972 kg (2144 pounds). Useable propellant required for the mission weighs 1928 kg (4250 pounds). Total loaded weight of the orbiter is 2900 kgs (6395 pounds). The modified Planetary Explorer earth return vehicle weighs 197 kg (435 pounds). Performance allocated weight is 259 kgs (570 pounds). Total injected payload weight at launch including mission peculiar items is 3374 kgs (7440 pounds).

a. Modified Orbiter Description - The orbiter configuration is essentially the same as the Viking '75 Orbiter with some modifications required to meet the Phobos/Deimos sample return mission and to adapt it to a lander role. Some of the most important changes are:

1) addition of four landing legs. Solar panels consisting of a gross area of 14.85 square meters (160 square feet) are integrated with the landing legs;
2) propulsion system growth (38%) to accommodate 1928 kg of propellants;
3) addition of a rendezvous radar to assist in landing operations;

4) thermal control modifications to handle the cruise and landed phases of the mission;
5) addition of an integrated sampling subsystem;
6) modification of the scan platform to handle Phobos/Deimos mission related science complement.

The landed orbiter science system provides for the acquisition and documentation of surface and subsurface samples. The basic system consists of a dust collector and small impactor-type drill on a furlable boom, a soil transfer unit, twin facsimile cameras to provide high resolution imaging, and an X-ray fluorescent-type sample analysis unit. Further relative position of the sample site is documented by noting the furlable boom gimbal angles and extension.

The modified orbiter telecommunications subsystem consists of the existing Viking '75 Orbiter S-band communications subsystem composed of the Mariner class S-band transponder with redundant 20 watt TWTAs, an articulated high gain 58 inch parabolic antenna and a low gain cavity backed cross slot antenna for command reception. The UHF relay link is deleted.

The modified orbiter power subsystem consists of the same solar panels and battery complement as used on the basic Viking '75 Orbiter. The solar panels instead of being mounted to the bus in a fan-like array are now integrated with the landed orbiter's four landing legs. Total panel gross area is the same as Viking '75, 14.85 square meters (160 square feet).

The only guidance and control subsystem hardware modification is the addition of the rendezvous radar which is identical to that used for the Phase I study.

Three axis stabilization for the modified Phobos/Deimos orbiter is provided by a dual redundant nitrogen cold gas reaction control system of the type used on the Mariner and Viking Orbiter vehicles. An increase in gas capacity of 0.3 kg is required.

The modified orbiter's primary propulsion system is identical to the Viking system except for the size of the propellant tanks and pressurant sphere. In order to handle the additional propellant (1928 kgs) the two main propellant tanks are increased 12.7 cm in length and 12.7 cm in diameter. The diameter of the pressurant tank was also increased by 7.6 cm.

The thermal control required to cope with the widely different thermal requirements during landed operations as compared to cruise was achieved by modifications to the Viking Orbiter temperature control louver system. Two sets of louvers were provided: (1) Viking Orbiter types, mounted on the sides of the equipment compartment, which are operational during cruise only, being de-activated on the surface by the use of flip covers; and (2) Sun -oriented types (covered with OSR), which function throughout the orbiter mission.

With the exception of the subsystems described in the foregoing discussion, all other Viking Orbiter subsystems can be used as they are presently conceived.

b. Modified Planetary Explorer Earth Return Vehicle - The modified planetary explorer earth return vehicle consists of a 12-sided right circular cylinder with a fixed body mounted solar array. The overall structural configuration has been changed to provide proper dynamic stability for sample return missions. The basic **Planetary Explorer's** communication and guidance and control subsystems are retained.

A liquid bipropellant main propulsion system has been substituted for the **Planetary Explorer's** solid propellant system. This system is functionally a pressure-fed multi-start, fixed thrust, storable bipropellant utilizing as propellants nitrogen tetroxide (N_2O_4) and Aerozine 50 (50% N_2H_4/50% $C_2N_2H_8$) at a weight mixture ratio of 1:60.

The attitude control system for the modified planetary explorer earth return vehicle is the monopropellant blow-down type and utilizes hydrazine propellant for precession and spin rate control.

The principal modifications to the Planetary Explorer in the thermal control area are the reduction in the required heat rejection (louver) area, as compared to the Venus missions, and the addition of a 10 watt radioisotope heater to compensate for the very minimal internal heat dissipation available during surface operations.

Body mounted solar cells (3.7 square meters) are distributed over an angular surface to provide optimum orientation for sample return. Voltage is maintained near Earth by series parallel switching logic. No batteries are required. The spacecraft will automatically maintain attitude stabilization during Sun occultations.

The earth entry module is an Apollo shaped vehicle that is stored within the modified planetary explorer just below the fixed high-gain S-band antenna. This antenna is jettisoned just prior to release of the earth entry module containing the sample. The earth entry module is designed to survive the loads imposed during Earth entry and impact. The capsule as designed can accommodate entry velocities up to 12.8 km/sec. A parachute is deployed as soon as the velocity is subsonic. Electronic tracking aids are provided to accomplish recovery of the capsule.

2. Alternate Configuration

The alternate configuration is shown in Figure V-2. The total spacecraft loaded weight is 2286 kgs. The orbiter/launch vehicle adapter truss, which is identical to the Viking '75 adapter truss supports the alternate Phobos/Deimos sample return spacecraft at four symmetrical points and is attached to an

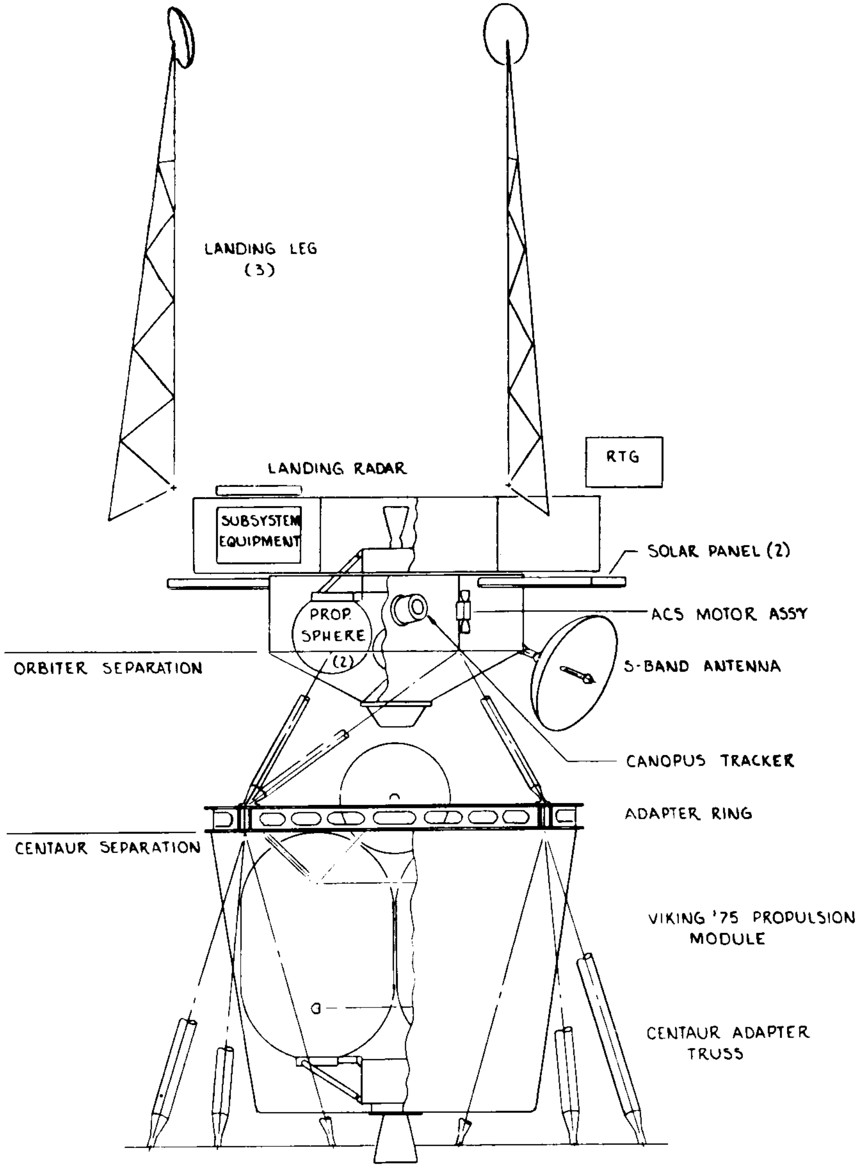
LANDING LEG
(3)
LANDING RADAR
RTG
SUBSYSTEM EQUIPMENT
SOLAR PANEL (2)
PROP. SPHERE (2)
ACS MOTOR ASSY
ORBITER SEPARATION
S-BAND ANTENNA
CANOPUS TRACKER
ADAPTER RING
CENTAUR SEPARATION
VIKING '75 PROPULSION MODULE
CENTAUR ADAPTER TRUSS

Figure V-2 Preferred Alternate Sample Return Configuration

adapter ring with ordnance operated bolts and springs. The adapter ring is substituted for the Viking Orbiter octagon bus structure since only the Viking Orbiter propulsion system is utilized for this concept.

The alternate configuration consists of an integrated three-axis stabilized control module/lander with a propulsion module which is jettisoned prior to final closure and touchdown. The subsystems contained in the earth return vehicle function throughout the mission.

The earth return vehicle (control module) is a new lightweight three-axis stabilized vehicle composed of proven or currently identified interplanetary spacecraft subsystems.

The integrated lander module which evolved from the Phase I lander/rover, houses the communications (20 watt TWTAs), tape recorders, and approach navigation TV cameras. The articulated 30 inch parabolic high-gain antenna is loacted on the earth return vehicle.

The propulsion module which is jettisoned prior to final closure and touchdown is the basic Viking '75 propulsion system. Terminal descent is provided by an added hydrazine propulsion system.

The new three-axis stabilized earth return vehicle is composed of subsystems and techniques which are currently identified or have been previously proven in space programs. Main propulsion is a bipropellant type; attitude control utilizes cold gas. Articulated solar panels maintain solar orientation. A small battery is required to energize the attitude control loop during sun occultations. Communications are extracted from Planetary Explorer employing an articulated 30 inch parabolic antenna. The guidance and control subsystem is derived from Mariner series vehicles, and Earth resources programs. Thermal control is selected for the heat retention requirements. The same earth entry module used in the baseline configuration provides for a nominal 5 kg sample payload. The module is released from the return vehicle for direct Earth entry and water recovery.

The primary propulsion system for the three-axis earth return module is essentially the same as that of the modified planetary explorer except that two propellant tanks (plus acquisition devices) and one pressurant sphere can be used instead of four and two. In addition, thrust chamber gimbaling is required for accurate thrust vector control.

The attitude control propulsion system for the three-axis earth return module is a dual redundant cold gas system of the type used on the Viking Orbiter.

The power system consists of two articulated solar arrays (0.56 square meters each), a SNAP-19 radioisotope thermoelectric generator (RTG) and nickel-cadmium batteries. The RTG and one set of batteries are left in the lander on the satellite surface. The solar cell array and a 2-AH battery provide power for the return journey to Earth. During landed operations the batteries provide the peak power needs and are replenished by the RTG during the standby periods.

Communications will be direct to Earth at S-band with the communications subsystem consisting of a hybrid of PE-type solid state modules and Mariner-type 20 watt TWTAs. The high gain antenna is an articulated 30 inch parabolic type. Landed data rate capability is 250 bps.

The principal thermal control elements include the following:

1) Lander
    a) RTG and temperature control switch
    b) Multilayer insulation

2) Earth Return Module
    a) Thermostatically controlled heaters
    b) OSR radiator

The guidance and control system consists of a CC&S unit and an IMU from the Mariner II series, a Canopus sensor and Sun sensors from the Earth resources program.

3. Competing Candidate Configurations

Two additional configurational concepts were studied at the conceptual design level for evaluation purposes during the system level trade studies. These included a modified planetary explorer that was transported to the satellite's surface by means of a separable lander, and a Mariner-type earth return vehicle that is landed on the satellite's surface by means of a landed orbiter.

The first concept consists of a modified planetary explorer earth return module, a separable lander with relay communications and a modified Viking Orbiter with staged propulsion. The orbiter delivers the lander and earth return module to final closure range, then maintains a stationkeeping position to relay communications to the lander and earth return vehicle. No earth return vehicle subsystems are shared in this configuration.

The second concept consists of a Mariner-type earth return vehicle and a modified Viking Orbiter with space storable propellants. The modified Viking Orbiter shares Mariner communications and guidance subsystems to provide for maximum subsystem commonality. Solar panels on the lander orbiter are integrated with the landing legs. Weight of the Mariner-type return vehicle requires that space storable propellants be employed in the landed orbiter. The orbiter is modified for the landing mission by incorporating landing legs, sampling subsystem, landing radar, modified scan platform, and Mariner electrical and mechanical interfaces.

B. SAMPLE RETURN GUIDANCE AND CONTROL

1. Baseline G&C Subsystem (Spin Stabilized)

a. G&C Functions - The earth return vehicle (ERV) is launched from the satellite surface using the landed orbiter as a launch platform. Before launch the vehicle attitude and position are determined using the TV imaging system and celestial sensors are used to determine the vehicle's attitude and position. The vehicle is commanded to launch with a predetermined ΔV at a predetermined time. The launching platform has no leveling capability, so the vehicle will in general not be launched vertically.

Just after liftoff and separation from the launching platform, the SRV starts to spin up to the nominal spin rate of 12 rpm. One-half of a orbital period (Phobos or Deimos) is available to track the vehicle, determine its orbit and attitude, precess over to a new attitude for the circularization insertion maneuver and to execute that maneuver. This procedure requires 13 hours nominally. If not enough time is available for tracking the vehicle and determining the orbit, as would be the case for Phobos, the orbit will have to be circularized based on the best estimate of the orbit ephemeris data. The vehicle can then be tracked and its orbit can be trimmed, if necessary, for the intermediate orbit insertion maneuver.

The initial orbital maneuver injects the vehicle into a highly elliptical orbit 9380 by 95000 km as shown in Figure V-3. This is followed by maneuvers to lower periapsis, change plane and inject to a trans-Earth trajectory.

Between maneuvers the vehicle is pointed toward the Earth so that maximum communication gain can be achieved. The beamwidth of the suggested high gain antenna is about 20 degrees so the vehicle must be pointed toward the Earth to within ± 10 degrees.

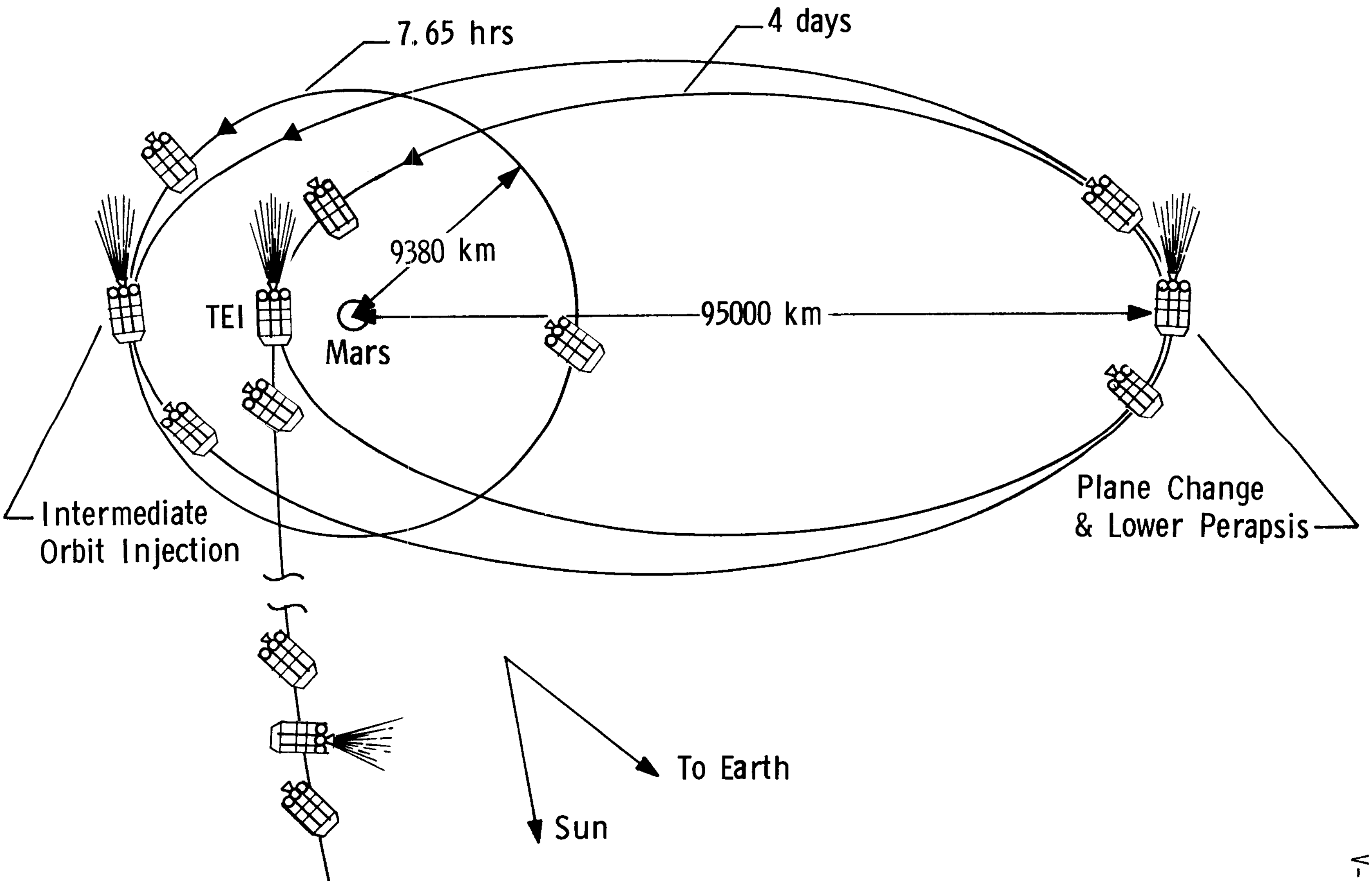
7.65 hrs
4 days
9380 km
TEI
Mars
95000 km
Intermediate
Orbit Injection
Plane Change
& Lower Perapsis
To Earth
Sun

Figure V-3 Deflection Maneuvers (Spin Stabilized)

Adequate gain is needed for two-way tracking and communication to the Earth so the vehicle's attitude and orbital parameters can be determined by the ground based computers. Downlink communications are needed to convey the sensor information to the Earth. After the information is processed on the ground to determine the vehicle's attitude and the vehicle's precessing commands, the commands are telemetered to the spacecraft via the large Earth-based antennas and received by the spacecraft omni-antenna. The spacecraft can be at any attitude, when receiving commands. Sun and star sensor information for five revolutions of the spacecraft (5 seconds per revolution) are needed for the recursive processing that determines the vehicle attitude. While only 3 seconds are required to process the sensor data and determine the vehicle attitude, about thirty minutes must be added to the attitude up-date time for the two-way communications time.

During the maneuver phases, the vehicle is precessed to the maneuver attitude about one axis at a time under an open loop control system. Estimated (3-sigma) maneuver accuracies of 4.5 percent thrust magnitude and 4.5 degree pointing angle uncertainties result from the use of only open loop control. After the thrusting phase, the vehicle is precessed back to the Earth pointing attitude by executing the precessing maneuvers in the reverse order.

All the Earth return maneuvers are executed basically in the same way, except the last two midcourse correction maneuvers are executed by the RCS engines instead of the main engine. The RCS engines are fired in synchronism with the vehicle spin rate to impart a ΔV in a prescribed direction. The maneuver phases generally take less than one-half hour to complete.

The vehicle can be placed into a sleep mode or semi-dormant mode during a large portion of the interplanetary cruise phase to reduce the power requirements. Only the command receiver needs to be on to reactivate the vehicle on a signal from the ground. This is the big advantage of the spin stabilized system over the 3-axis stabilized vehicle.

b. G&C Subsystem Description - The spin stabilized PE type vehicle uses minimum equipment to determine and control the vehicle attitude.

Figure V-4 shows the block diagram of the spin stabilized G&C subsystem. The scanning celestial attitude determination system (SCADS) consists of two star sensors, a Sun sensor, and the associated electronics. The output from the star sensor gives angle information on stars above a certain threshold--third magnitude stars or brighter. The Sun sensor senses where the Sun is relative to the spacecraft coordinates. The angular data of the Sun and the stars are fed to Earth over the telemetry link. The ground computer can then determine the inertial position of the spin axis to an accuracy of 0.1 degrees. The Sun sensor system will give the spin axis Sun angle and provide a timing pulse each time the sensor sweeps the Sun. The star sensor senses third magnitude stars or brighter. A digital output from the star sensor system will provide the angle between each star and the body axis system and where the star is relative to the Sun. The spin vector logic supplies a pulse to the propulsion system for firing the RCS engines in a specified direction. The RCS engines are fired over a 45 degree sector of the vehicle's revolution.

The digital sensor information is sent to the ground and processed by the ground computer to determine the precession commands. These precession commands are telemetered to the spacecraft command receiver via the large Earth based antennas. The programmer/data handling subsystem consists of a crystal controlled clock, telemetry encoder, A/D converter, memory, control and

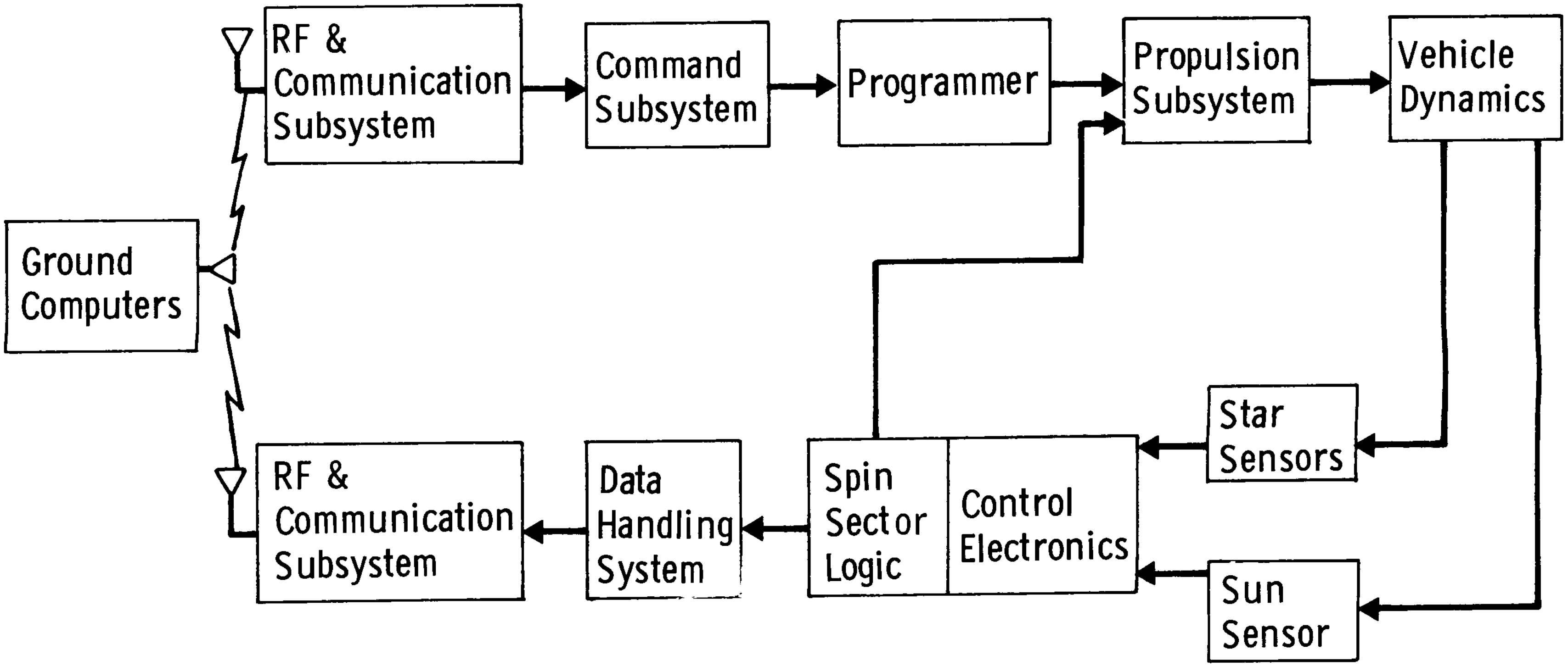
RF & Communication Subsystem
Command Subsystem
Programmer
Propulsion Subsystem
Vehicle Dynamics
Ground Computers
Star Sensors
Spin Sector Logic
Control Electronics
Sun Sensor
Data Handling System
RF & Communication Subsystem

Figure V-4 Spin Stabilized G&C Subsystem

synchronizing circuits, timer, and programmer. The precession command can be stored to be executed at a specified time or executed on command from the ground. The propulsion system is commanded via the programmer and spin sector electronics to thrust in a specified direction by firing during the appropriate sector of the revolution.

The subsystem weight and power requirements for the spin stabilized G&C subsystem are shown in Table V-1. The G&C subsystem weighs 10.5 kgms and consumes 13.7 watts of power. This power consumption is used for most of the mission when not in the sleep mode.

Figure V-5 shows how the vehicle's nutation can be damped out by the jet damping produced by the jet stream of the engine. An estimated thrust offset of 0.065 inches (3σ) can be expected during the thrusting of the main engine. This thrust offset causes the spacecraft nutation to build up and the engine jet stream dampens the nutation cone angle to a final value of 0.15 degrees. These results were produced by a digital computer program simulating a variable mass spinning vehicle with jet damping due to thrusting of the main engine. The maneuver that lowers periapsis and changes orbital plane, which takes 100 seconds to execute, was simulated as the worst case being the shortest critical maneuver phase. As can be seen by this figure, only twenty seconds are needed for the nutation to damp out. The lower curve shows the pitch angle (THETA) varies as a function of yaw angle (PSI). The upper curve shows how the absolute value of this pitch attitude angle varies during the thrusting maneuver.

Figure V-6 shows a map of stars of third magnitude or greater in the celestial sphere. A star sensor using a photo-multiplier tube with a S-20 photocathode was suggested for the baseline vehicle. Using the spectral response of this sensor, 128 stars

Table V-1 Subsystem Weight & Power Requirements (Spin Stabilized)

HARDWARE	WEIGHT (kgms)	POWER (Watts)
ATTITUDE-CONTROL ELECTRONICS	0.5	0.2
SUN SENSOR AND ELECTRONICS	1.6	2.0
SCADS STAR SENSOR (2)	3.2	2.0
SCADS ELECTRONICS	0.9	
DAMPERS (3)	2.3	------
PROGRAMMERS	2.0	9.5
TOTAL	10.5 (23.0 lb)	13.7 Watts

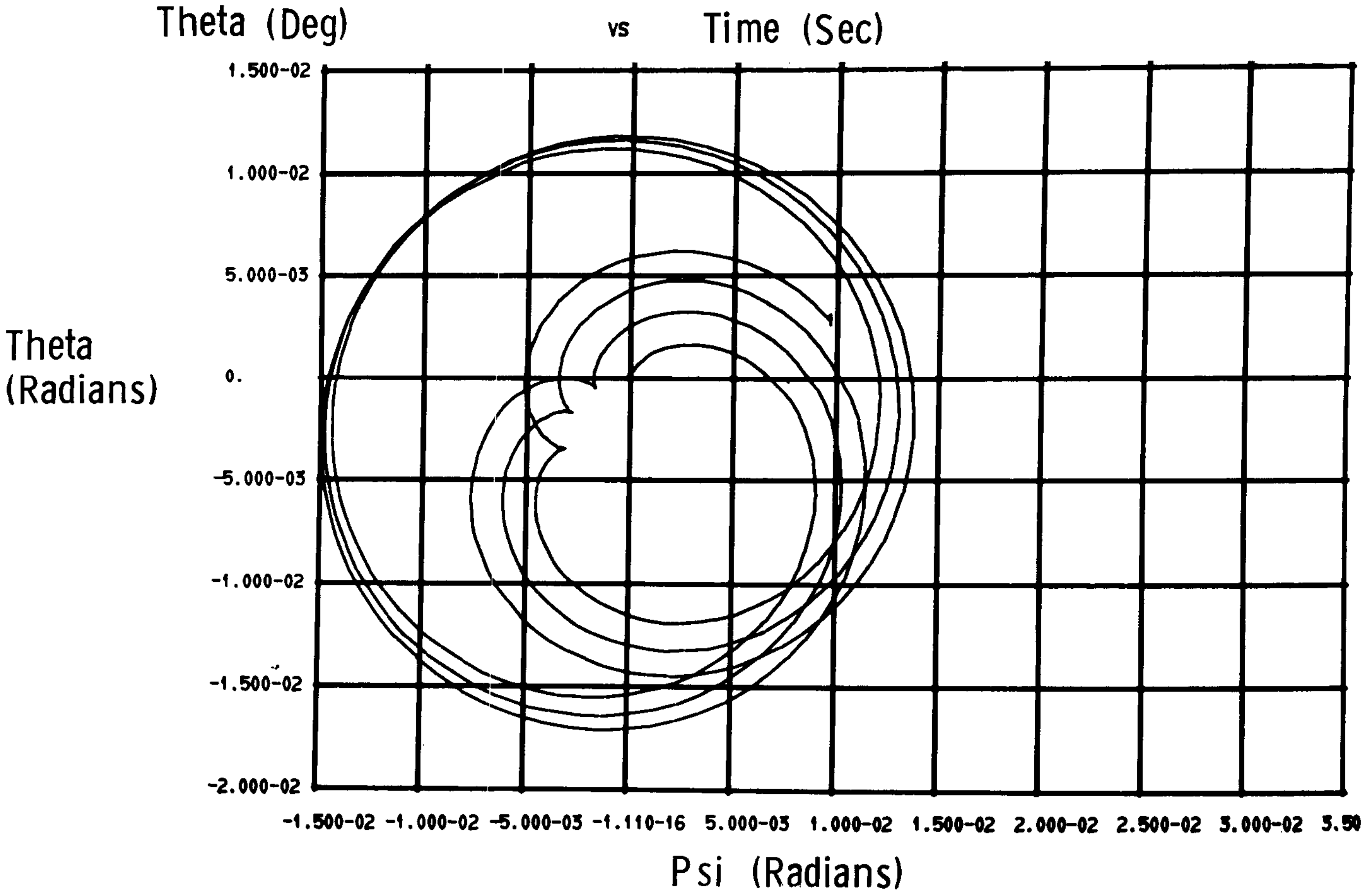

Figure V-5 Vehicle Attitudes During Orbital Deflection Maneuver

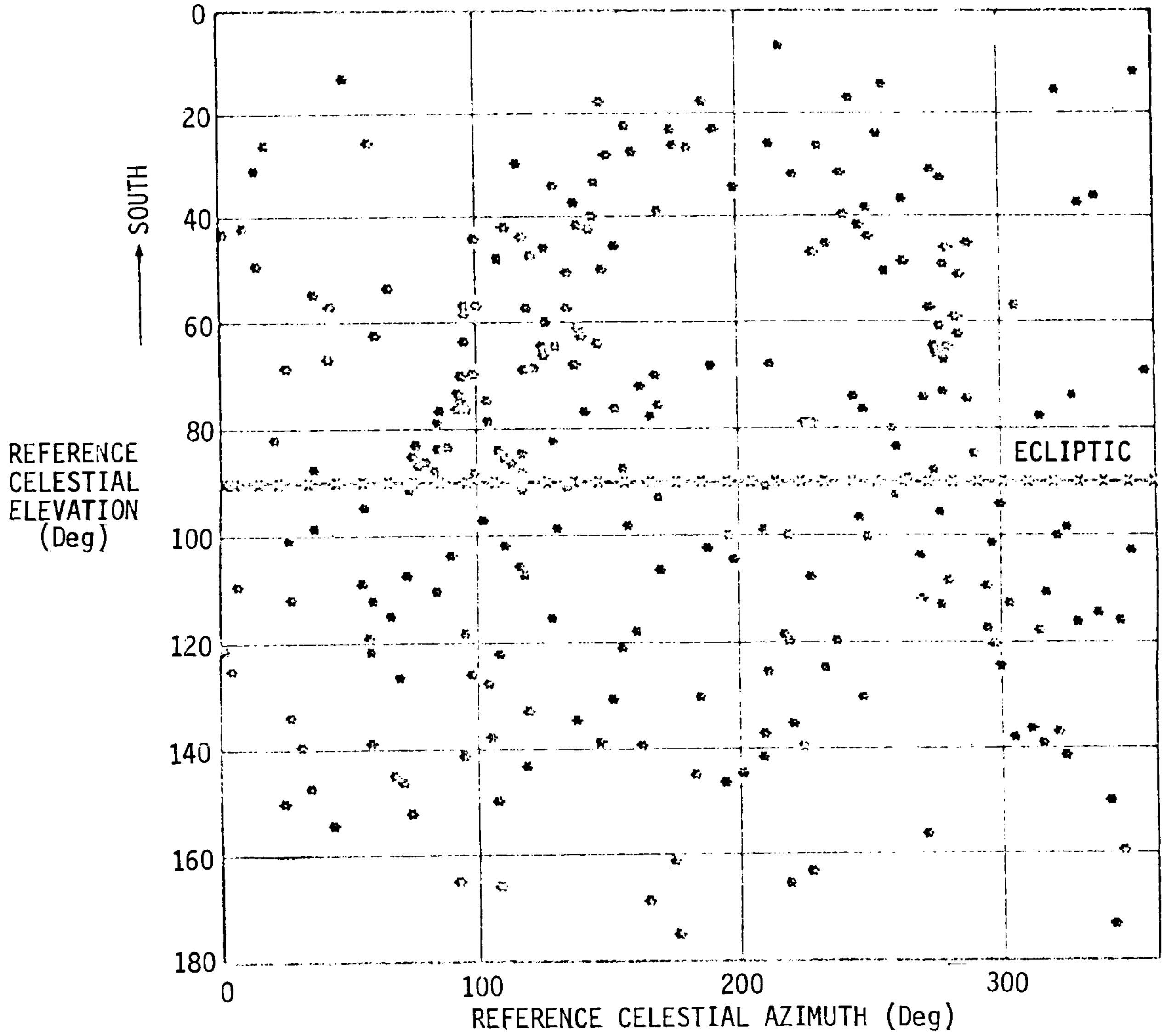

Figure V-6 Map of Stars Greater Than Third Magnitude

of third magnitude or greater can be sensed by the star sensor in the celestial sphere.

Generally the longitudinal axis of the spacecraft is aligned in the ecliptic and pointed toward the Earth for the maximum communication capability. The star sensors, which are mounted 45 degrees from the spin axis and mounted 180 degrees apart, sweep a 25 degree swath perpendicular to the ecliptic. Each star sensor has a 15 degree FOV and the sensors have a 5 degree overlap. Enough stars should be available with this FOV to determine the vehicle attitude.

3. Alternate G&C Subsystem (3-Axis Stabilized)

An attractive alternate G&C subsystem is the three-axis stabilized system. Compared with the spin-stabilized system, this G&C subsystem provides more accurate closed loop pointing control and utilizes less solar panel area to power the vehicle. The 3-axis system does however require constant active attitude control and therefore must carry more ACS consumables. Table V-2 shows the attributes of each of these systems. An important advantage of the three-axis system is that it can maintain Sun oriented solar panels and Earth pointed communication antenna at the same time.

Figure V-7 shows how all the deflection maneuvers are executed with the 3-axis stabilized system. The Sun and Canopus acquisitions are executed similar to the Viking or the Mariner missions. An Adcole digital solar aspect sensor system having complete spherical coverage is used to provide the Sun angle in spacecraft coordinates. This sensor system utilizes five sensors of the type 14135 or equivalent where each sensor has a field of view of 128 by 128 degrees with an accuracy of ± 1/4 degree accuracy. This digital solar aspect sensor is a flight proven piece of hardware as it is flown on many space vehicles, such as ATS, GGTS, OAO, SAE and others.

Table V-2 Attributes of Three-Axis vs Spin Attitude Stabilized Spacecraft

Three-Axis Stabilized	Spin Stabilized
Attitude must be maintained by relatively heavy subsystems which continually consume power	Attitude maintained automatically at no expense of power or weight for auxiliary subsystems
More efficient to slew attitude, therefore	Less efficient to change attitude, therefore
More efficient for missions requiring "many" attitude re-orientations	More efficient for long mission requiring "few" attitude re-orientations
Less sensitive to dynamic imbalance	More sensitive to dynamic imbalance
Higher power requirements	Probably lower overall power requirements
Heavier attitude references required, i. e., gyros, gimballed or electronically scanned star trackers, etc.	Very light-weight attitude references available (i. e., SCADS, etc.) since vehicle spin is accomplishing the scan
Less complex computations required to determine inertial attitude	Complex calculations required for interface attitude determination
Requires more complex thermal protection	Good thermal characteristics
Articulated antennas probably required to maintain Earth communications	Can use spin to advantage when orienting antennas to Earth, i. e., provide functional commonality of rf subsystem with navigational system without using articulated antenna
	Interplanetary spacecraft of lightest weight to date have been spin stabilized

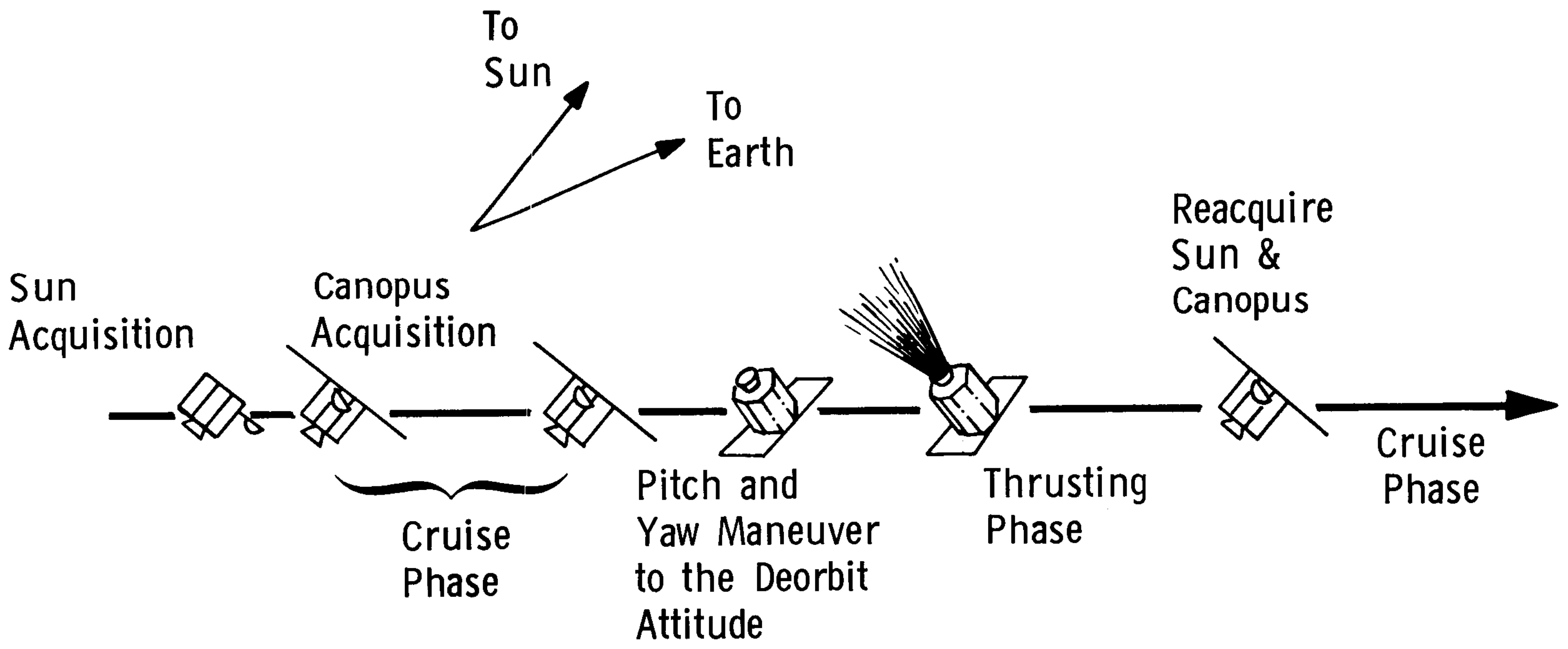
To
Sun
To
Earth
Sun
Acquisition
Canopus
Acquisition
Cruise
Phase
Pitch and
Yaw Maneuver
to the Deorbit
Attitude
Thrusting
Phase
Reacquire
Sun &
Canopus
Cruise
Phase

Figure V-7 Time Profile of Deflection Maneuver (Three-Axis)

The recommended 3-axis system uses a new scheme to execute attitude changes. Using the Sun sensor as an inertial reference the vehicle is precessed about both the pitch and yaw axes simultaneously while the roll channel uses a roll rate gyro to lock the roll axis. The solar aspect sensor (SAS) measures two angles which define the position of the Sun line with respect to the vehicle. The SAS system provides separate pitch and yaw error signals to the control system. The advantages of this control scheme are:

1) simultaneous pitch and yaw maneuvers save time;
2) no gyro warmup is needed since dry gyros can be used;
3) cheap and inaccurate gyros can be used.

The pitch and yaw rate gyros are used only during Sun occultations to hold the vehicle attitude. The rate gyros can be lightweight, cheap, and inaccurate gyros. The three-axis rate sensor system produced by U. S. Time Inc. was selected for the baseline vehicle because this component was lightweight and consumed little power. This gyro system has a non-random and random bias drift of less than 10 degrees per hour.

After the pitch and yaw maneuvers are performed and the vehicle attitude is trimmed to ± 1/4 degree of the required attitude, the vehicle main engine is fired to impart a specified ΔV to the vehicle. When this velocity is reached as indicated by an axial accelerometer, the main engine is shut down. The vehicle is then commanded to reacquire the Sun and Canopus by setting the pitch and yaw commands to zero. All the maneuvers are executed this way. No gyro warmup is needed and only one-half hour is needed to execute these maneuvers. Considerably less power is consumed from the Sun oriented solar panels and the batteries by this technique.

Figure V-8 shows a block diagram of the suggested mechanization of the 3-axis flight control system. The Sun and Canopus sensors sense the pitch, yaw and roll attitude errors for vehicle control. The Sun occultation sensor feeds a discrete to the CC&S during Sun occultation so the pitch and yaw rate gyros can be activated for vehicle control. The stray light sensor issues a discrete to the CC&S and activates the Canopus sensor shutter when stray light could effect the operation of the Canopus sensor. This discrete commands activation of the roll rate gyro so the vehicle roll attitude can be controlled. The accelerometer is used to determine when a specified axial velocity is reached during the thrusting phases. The attitude control logic, which is mechanized in the CC&S, is similar to that used in the Viking Lander. The attitude control electronics provide thrust activating signals to the ACS gas jet activators and to the main engine gimbal servo motors. This mechanization has the capability of using commands from the command system or stored commands executed at a specified time from the CC&S.

Table V-3 shows the estimated weight and power requirements. This figure also shows which components were selected for the baseline vehicle.

4. Round Trip Control Module - G&C Subsystem

This configuration uses the same G&C subsystem components on both the Earth to Mars and Mars to Earth legs of the sample return mission. A rendezvous radar was added to the otpimized three-axis system to perform the satellite rendezvous. The weight and power requirements are shown in Table V-4. The power requirements for the rendezvous phase size the battery requirement.

5. Method of Minimizing Landing Site Alteration

One potential problem identified in the Phase 1 study was the possibility that the landing on the satellite might disturb or

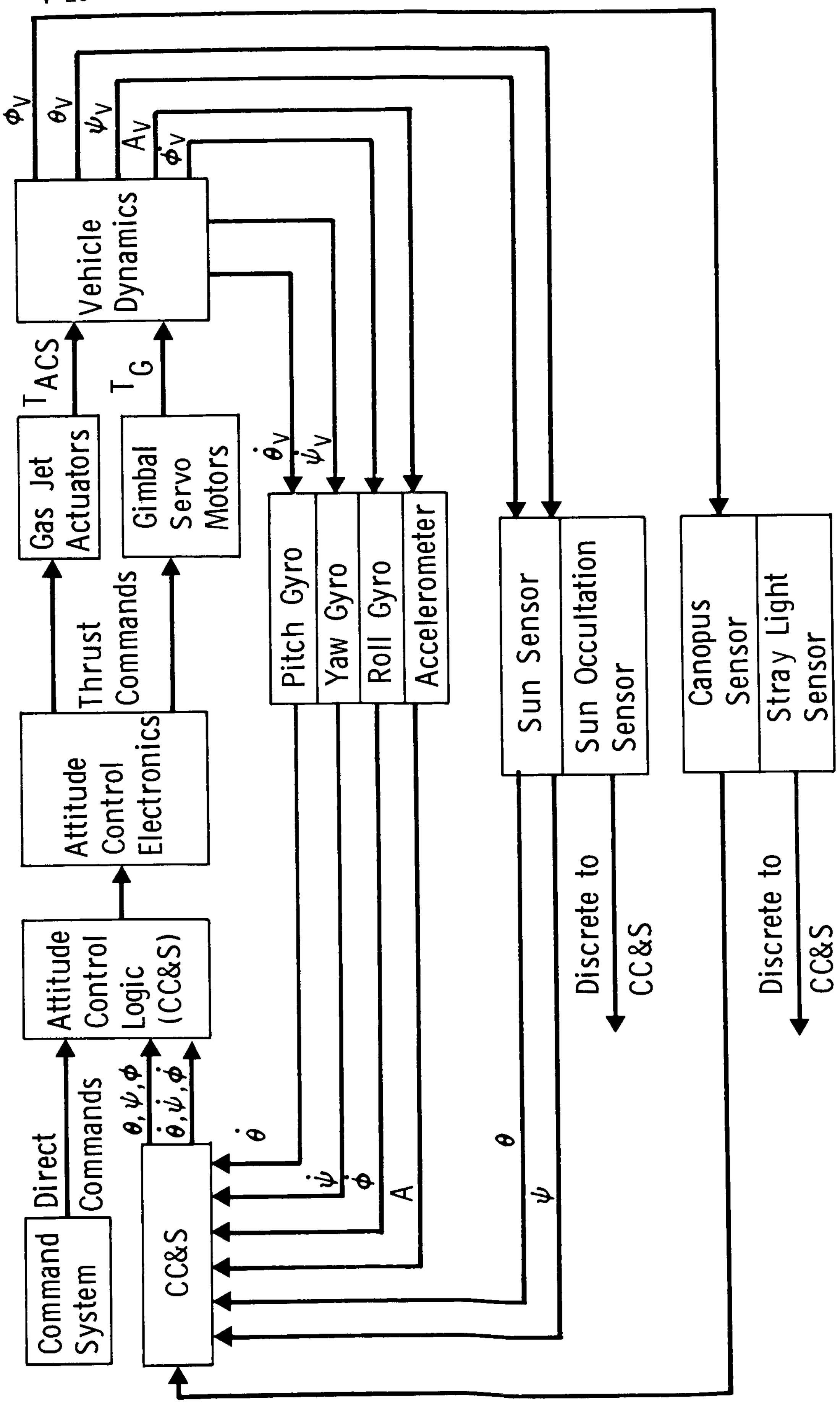
Command System
Direct Commands
Attitude Control Logic (CC&S)
Attitude Control Electronics
Thrust Commands
Gas Jet Actuators
Gimbal Servo Motors
T_{ACS}
T_G
Vehicle Dynamics
ϕ_V
θ_V
ψ_V
A_V
$\dot{\phi}_V$
$\dot{\theta}_V$
$\dot{\psi}_V$
Pitch Gyro
Yaw Gyro
Roll Gyro
Accelerometer
Sun Sensor
Sun Occultation Sensor
Canopus Sensor
Stray Light Sensor
Discrete to CC&S
Discrete to CC&S
CC&S
θ, ψ, ϕ
$\dot{\theta}, \dot{\psi}, \dot{\phi}$
$\dot{\theta}$
$\dot{\psi}$
$\dot{\phi}$
A
θ
ψ

Figure V-8 Flight Control Subsystem Block Diagram (Three-Axis)

Table V-3 Subsystem Weight and Power Requirements (Three-Axis)

HARDWARE	WEIGHT (kgms)	POWER (WATTS)	
		During Maneuvers (1/2 hr)	Cruise
CC&S*	5.0 kgms	15.0 Watts	15.0 Watts
IMU**	0.5 kgms	9.0 Watts	----------
CANOPUS SENSOR*	2.3 kgms	----------	5.0 Watts
SUN SENSORS***	1.1 kgms	----------	0.2 Watts
TOTAL	8.9 kgms (19.5 lb)	24.0 Watts	20.2 Watts

* Mariner II
** U.S. Time
*** Adcole Digital Solar Aspect Sensor

Table V-4 Round Trip Control Module/Lander Configuration Weights

Hardware	Weight (kgms)	POWER (WATTS)		
		During Maneuvers (1/2 hrs)	Cruise	Rendezvous (2 hrs)
CC&S	5.0 kgms	15.0	15.0	15.0
IMU	0.5	9.0	-----	9.0
Canopus Sensor	2.3	-----	5.0	-----
Sun Sensors	1.1	-----	0.2	-----
Rendezvous Radar	10.5	-----	-----	60.0
Total	19.4 kgms	24.0 Watts	20.2 Watts	84.0 Watts

contaminate the surface such that samples taken for scientific analysis might not represent true in-situ conditions.

It was also felt that landings on these small bodies might take advantage of the low gravity conditions to employ some unique deceleration schemes. This section describes several alternative landing techniques as depicted in Figure V-9. All of these methods are used during or after the constant velocity phase of the terminal descent.

One way to reduce landing site contamination is to hop to a new landing site by means of a ballistic trajectory after a conventional landing. The RCS engines facing downward are fired initially to initiate the hopping trajectory. Attitude control would be required during most of the maneuvers but this could be expected to cause only small site alteration effects. The RCS engines could be fired downward during the last few seconds of the hopping maneuver to give the vehicle some damping during landing to reduce vehicle bounce.

Another approach to controlling site alteration would be to employ roll thrusters canted slightly downward instead of the RCS engines facing downward during the final few meters of descent. The canted roll engines would not effect the efficiency of terminal rendezvous and landing phases, as it would slow down the vehicle slightly when roll control is needed.

A free fall phase after the constant velocity phase can eliminate site alternation if the higher landing velocity can be tolerated. The free fall phase can start at any altitude that will minimize landing site alteration and landing velocity. This latter figure shows how the landing velocity varies as a function of initial altitude. The comparison between the final velocity for a conventional landing and a 30 m free fall landing is also shown.

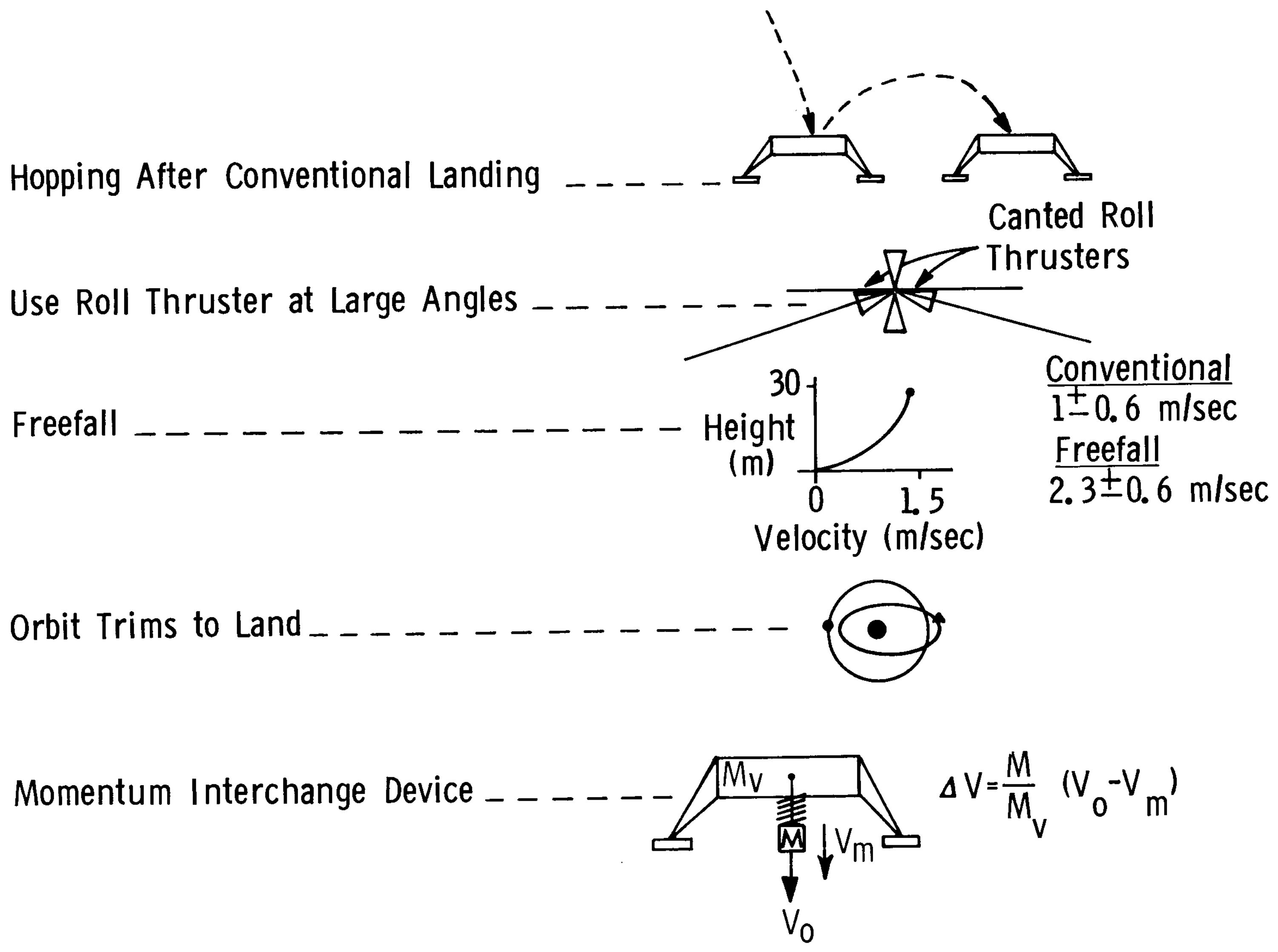
Hopping After Conventional Landing
Canted Roll Thrusters
Use Roll Thruster at Large Angles
Conventional
1±0.6 m/sec
Freefall
2.3±0.6 m/sec
Freefall
30
Height (m)
0
1.5
Velocity (m/sec)
Orbit Trims to Land
Momentum Interchange Device
M_V
M
V_m
V_0
$\Delta V = \frac{M}{M_V} (V_o - V_m)$

Figure V-9 Methods of Minimizing Landing Site Alteration

Orbital trims can be used to cause the vehicle and the satellite to gently collide at the intersection of their orbits thus effecting a non-propulsive soft landing. The rendezvous radar can be used to gather data to update the orbit ephemeris data. Orbital trim maneuvers can then be used to match the orbits. This method of minimizing site alteration is used after the terminal rendezvous phase and when the vehicle is co-orbiting the satellite. The satellite will probably be within rendezvous radar acquisition range during most of the time, so the relative orbits should be determined very accurately.

A momentum interchange device could also be considered as a decelerating technique in the low gravity fields of Phobos and Deimos. This involves ejecting part of the lander forward along the velocity vector to kill some of the lander's velocity. The equation in the Figure V-9 shows the ΔV capability of this method. Large ejection velocities or ejected masses are needed to make this an efficient system. For example, a 480 kg separable lander descending at 1.5 mps would be decelerated to 1.34 mps by ejecting a 2 kg mass at 40 mps.

C. STRUCTURAL DESIGN

1. Design Approach

Structural design and systems installation of the major components of the spacecraft were examined in detail to ensure the structural integrity of the spacecraft.

The structural configuration selected for the baseline Phobos/Deimos spacecraft is a modified Viking '75 Orbiter and a modified planetary explorer earth return vehicle. The structural design philosophy is the same as that used during the Phase I study effort, that is, all structural components use state-of-the-art processes and materials to minimize costs and to give high reliability.

The loaded Phase II baseline sample return spacecraft as shown in Figure V-10 weighs 3159 kg , including an allocated weight of 259 kg for a modified planetary explorer earth return vehicle. Detailed subsystems implementation studies indicated that the earth return vehicle could be built for 197 kg which is about 62 kg less than the allocated (based on performance capability) weight. This excess capability could be converted to additional landed science or to vehicle contingency weight.

The composite CG of the loaded sample return configuration is approximately 63.5 cm (25 inches) closer to the spacecraft-Centaur interface (Sta 0) than the Mars Viking '75 spacecraft, resulting in lower design loading in the various spacecraft structural elements. As in Phase I, all structural members were sized to accommodate Titan IIIE/Centaur launch and mission induced loading and dynamic response requirements.

Using the structural design discussion of Phase I as a basis, this section describes the major differences that exist between the Phase II spacecraft and the vehicle developed during the Phase I study effort.

The baseline configuration weight summary is presented in Table V-5.

a. Modified Orbiter - The orbiter structure, both the octagonally shaped bus and the truss which attaches the orbiter to the Centaur-spacecraft adapter were evaluated for their capability to accommodate the loads and moments induced by increased propellant loading and by the modified planetary explorer earth return vehicle.

The basic orbiter bus is designed by loads encountered during the launch phase. The loaded weight of the Phase II spacecraft is 3159 kg compared to the Phase I spacecraft weight of 3393 kg .

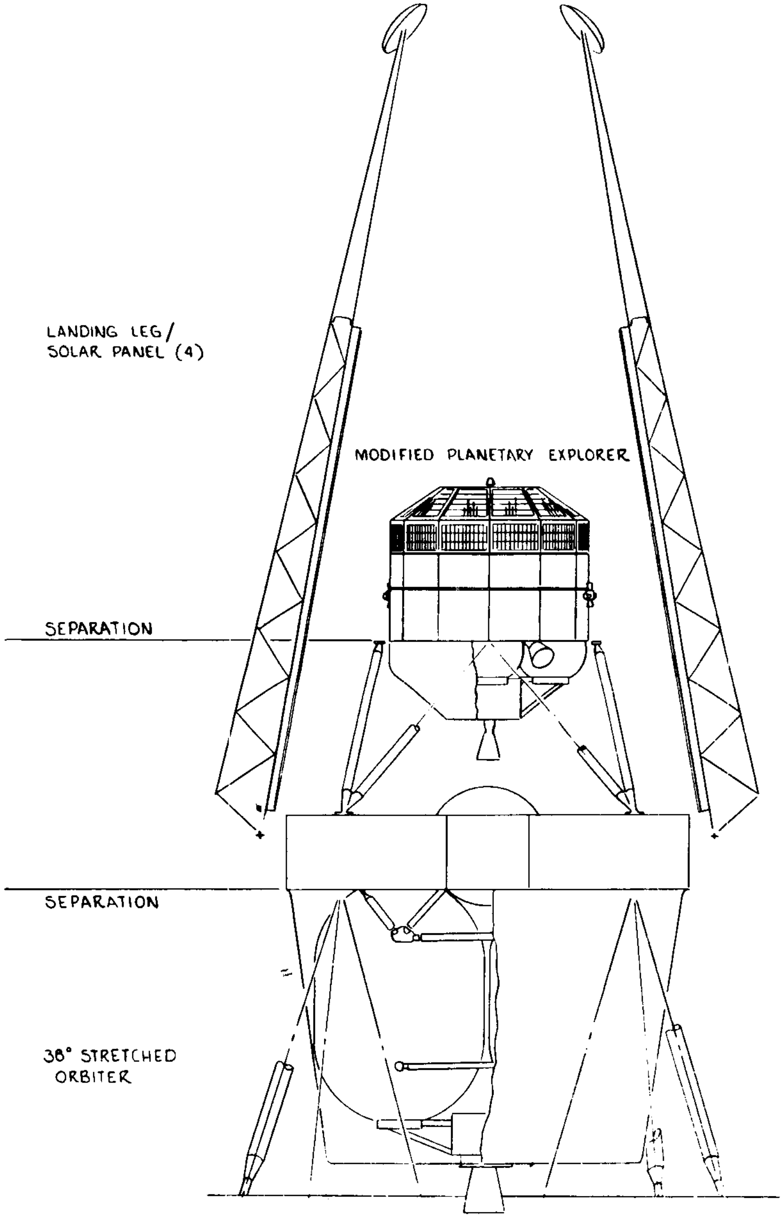
LANDING LEG/
SOLAR PANEL (4)
MODIFIED PLANETARY EXPLORER
SEPARATION
SEPARATION
38° STRETCHED
ORBITER

Figure V-10 Baseline Sample Return Configuration

Table V-5 Baseline Configuration Weight Summary, KGS

ORBITER		
Structures & Mech Devices	252.7	
Communications	45.7	
Power	129.2	
Guidance & Control	67.9	
Data Handling	36.2	
Cabling	54.0	
Pyrotechnics	5.0	
Propulsion-Inerts	304.1	
Imaging	18.1	
Sampling Subsystem	27.2	
P/L-Orbiter Adapter	6.8	
Contingency (4%)	25.4	
ORBITER DRY WEIGHT		972.3 (2143.9 lb)
Expendable Propellant	1927.8 (4250.0 lb)	
ORBITER LOADED WEIGHT		2900.1 (6394.7 lb)
MODIFIED PE EARTH RETURN VEHICLE ALLOCATION		258.6 (570.0 lb)
SPACECRAFT LOADED WEIGHT		3158.7 (6964.9 lb)
Orbiter / Launch Vehicle Adapter	68.0	
Project Reserve	56.7	
LVMP	90.7	
INJECTED PAYLOAD WEIGHT		3374.1 (7439.9 lb)

Composite CG location of the Phase II spacecraft is some 23 cm closer to the spacecraft-Centaur interface than the Phase I vehicle. The combination of these two factors, lower weight (234 kg less) and shorter moment arm combine to result in significantly lower loadings and bending moments for the Phase II spacecraft. Thus, no structural modifications will be required to be made to the basic bus structure with the exception of some local "beef-up" of the orbiter lower ring structure to handle the increased weight of the propulsion system module.

Four landing legs approximately 5.5 m (18 feet) in length are provided. These four landing legs pick up the same "hard" points on the orbiter bus that formerly served to support the four outriggers that attached the fan-like array of four solar panels to the Viking Orbiter bus. Since the landing dynamics program indicated that the total leg load is somewhat less than 68 kg at impact, no structural modifications are required to be made to the basic bus structure to handle this load introduction. The solar panels have been integrated into the landing leg design, with the structure of the landing legs serving as backup structure for the solar array. The solar panel/leg assembly is stowed at launch similar to the Viking '75 concept. After payload shroud separation, the panels are extended in a plane normal to the roll axis of the spacecraft. Just prior to final descent, the legs are prepared for landing by pulling an explosive pin which allows the legs to be driven (spring) to the landing position.

The spacecraft is attached to the orbiter turss at the four longerons in the middle of the long bays. The attachment is made to the truss through pyrotechnically separable bolt and spring assemblies . The orbiter truss is fabricated of aluminum alloy with each member being approximately 8.0 cm in diameter.

This truss structure spans from the launch vehicle's 12-point truss adapter (Centaur-spacecraft adapter) to four separation points on the lower ring of the orbiter bus.

The propulsion module for the Phase II spacecraft is identical to that described for the Phase I study.

An integrated sampling subsystem has been mounted on the upper surface of the orbiter bus structure. The basic system consists of a drill, sample boom and dust collector head, soil transfer and loading unit, two facsimile camers to provide high resolution imaging, and an X-ray fluorescent-type sample analysis unit. The sampling unit weighs 27.2 kg. A truss member-type structure is provided to introduce this load into the side longerons of the orbiter bus.

The scan platform has been modified to contain only the two TV cameras, a wide angle camera and a narrow angle camera. The wide angle camera serves a dual purpose, providing rendezvous navigation support as well as surface sampling support. The two experiments used on the Viking Orbiter, the IR thermal mapper and the Mars water detector have been deleted.

The rendezvous radar is mounted on the lower portion of the propulsion module.

b. Centaur-Spacecraft Adapter - As discussed in Phase I the Centaur-spacecraft adapter truss which is supplied by General Dynamics Corporation is designed to accommodate a wide range of different spacecraft payloads.

A preliminary stress analysis was conducted to evaluate the capability of the Mars Viking Centaur-spacecraft adapter to handle the Phobos/Deimos sample return loading conditions. The results of this analysis indicated that the present adapter was adequate to sustain the loadings imposed by the sample return mission.

c. Earth Return Vehicle/Orbiter Adapter - The adapter truss consists of 2024 aluminum alloy tubular members that attach at four points to the orbiter and at four points to the earth return vehicle. Separation bolts and springs are installed on the upper end fitting of each of the four attachment points. The juncture of the adapter truss with the earth return vehicle provides the separation plane of the adapter truss and the earth return vehicle when the earth return vehicle is separated from the orbiter. The adapter truss remains with the orbiter. Since the payload weight supported by the truss is 259 kg compared to 482 kg for Phase I, the load in the individual truss members are lower resulting in a lighter overall truss (6.8 kg compared to 13.6 kg for Phase I).

d. Modified Planetary Explorer Earth Return Vehicle - The modified planetary explorer vehicle which is used as the earth return vehicle is shown in Figure V-11. The bus configuration as shown consists of a 12-sided right cylindrical body with a fixed upper body mounted solar array of approximately 3.7 square meters. The bus is approximately 126 cm (48 inches) across the flats and 79 cm (30 inches) in height. This design was based on the following structural guidelines:

a) Use design concepts, materials, devices, and other technology proved acceptable through testing and ub-flight use;

b) Incorporate modular components which can be designed, fabricated, and tested independently of the rest of the spacecraft;

c) Minimize weight and complexity of integration;

d) Utilize a center structure which will transmit the loads to the earth return vehicle/orbiter adapter truss during launch and will support all major loads during flight.

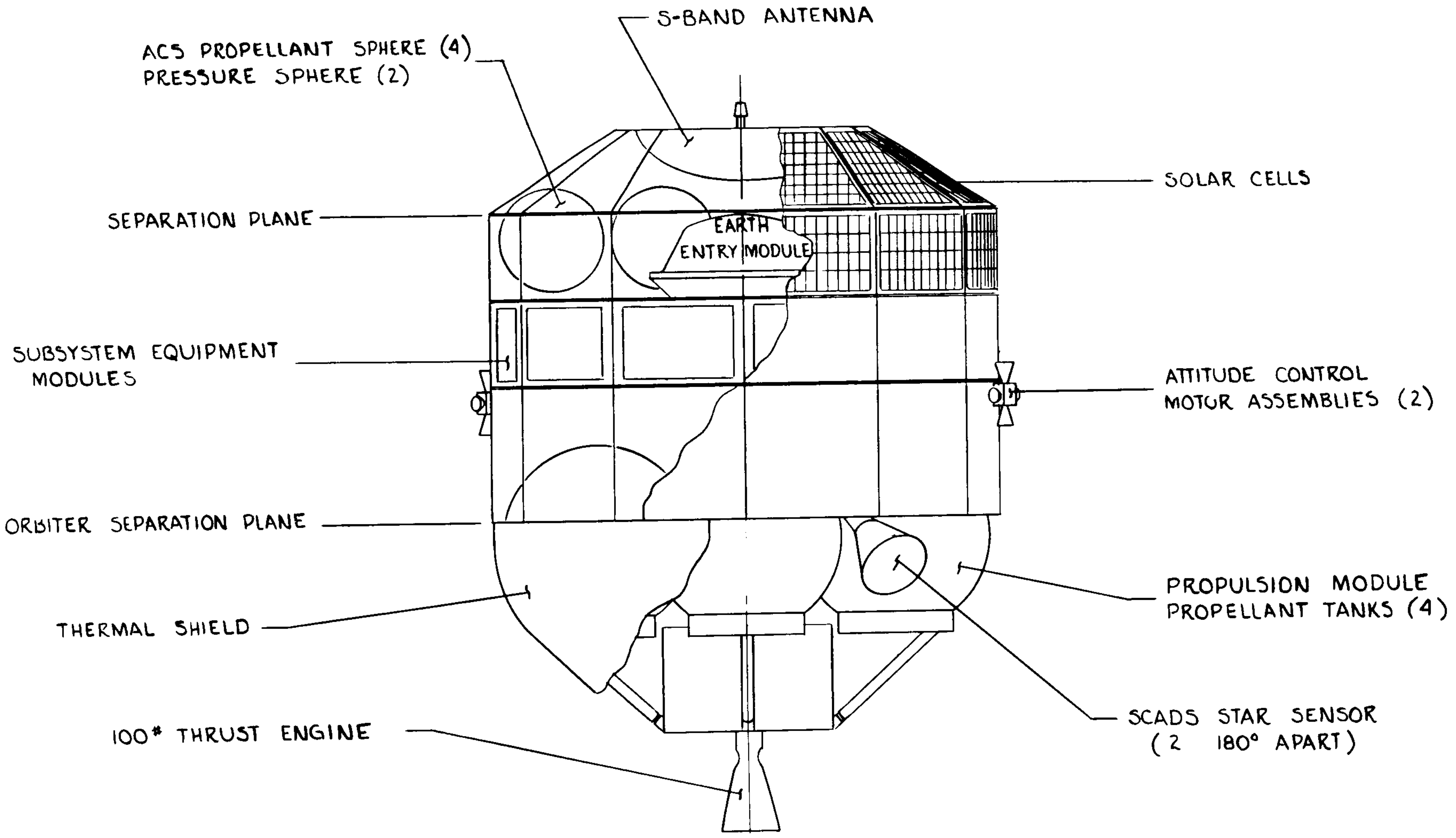
S-BAND ANTENNA
ACS PROPELLANT SPHERE (4)
PRESSURE SPHERE (2)
SOLAR CELLS
SEPARATION PLANE
EARTH ENTRY MODULE
SUBSYSTEM EQUIPMENT MODULES
ATTITUDE CONTROL MOTOR ASSEMBLIES (2)
ORBITER SEPARATION PLANE
PROPULSION MODULE PROPELLANT TANKS (4)
THERMAL SHIELD
SCADS STAR SENSOR (2 180° APART)
100* THRUST ENGINE

Figure V-11 Modified Planetary Explorer Earth Return Vehicle

Module frames serve to support electronic components and other supporting subsystems. Stacked vertically, these frames create a compact modular compartment. On the platform the frames support vertical loads and slide into their support structure, thus insuring repeatable alignment, electrical connection, and mechanical attachment. The support structure is designed as a unit to increase rigidity and to ensure proper alignment.

Eight hydrazine engines each have a 2.26 kg (5 pound) thrust level. These engines are arranged symmetrically around the bus in two clusters of four engines each to provide translational forces, spin axis precession torques, and spin torques as requireed by the spacecraft. Propellant is housed in four spheres, 25.4 cm in diameter and located in the upper portion of the spacecraft. Pressurization spheres for the main propulsion system are also located in the attitude control propellant tank bay.

The primary propulsion system is located in the lower bay of the spacecraft and consists of four equal volume propellant tanks, 45.5 cm in diameter. These are located in a single row around the periphery of the spacecraft.

Subsystem weights are summarized in Table V-6.

e. Earth Entry Module - Two earth entry modules were configured as shown in Figures V-12 and V-13. The basic design characteristics of the entry module are presented in Table V-7. The Apollo shaped capsule is fabricated basically of 6Al-4V titanium alloy. Heatshield material is ESA 5300-M3 approximately 1.9 cm in thickness. The sample is housed in a hermetically sealed container, which is stowed in the center of the earth entry module. Thermal insulation is provided around the periphery of the capsule. Prior to launch the capsule is filled with an inert gas and hermetically sealed.

The mechanism which transfers the surface sample into the

Table V-6 Modified Planetary Explorer Earth Return Vehicle Weight Summary, KGS

Structures	11.3	
Power	10.2	
Cabling	3.2	
Communications	10.5	
Guidance & Control	10.5	
Thermal Control	2.3	
Mechanical Devices	2.3	
Earth Entry Module	13.6	
Attitude Control	18.1	
Propulsion Inerts	18.1	
Reserve	6.4	
Dry Weight		106.5 (234.6 lb)
Propellant		90.9
Loaded Weight		197.4 (435.0 lb)
Growth Contingency		61.2 (135.0 lb)
Allocated Weight		258.6 (570.0 lb)

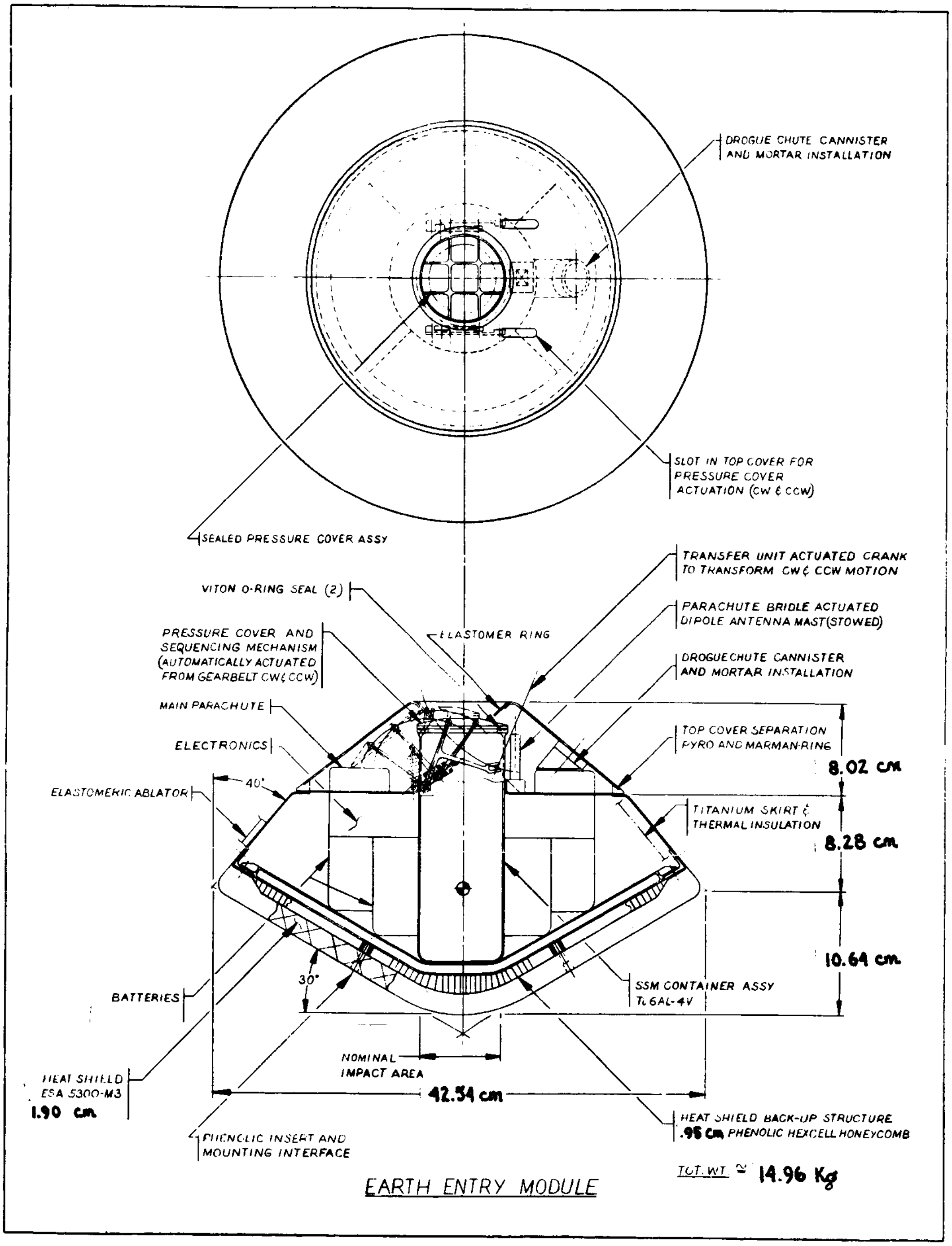
DROGUE CHUTE CANNISTER AND MORTAR INSTALLATION
SLOT IN TOP COVER FOR PRESSURE COVER ACTUATION (CW & CCW)
SEALED PRESSURE COVER ASSY
TRANSFER UNIT ACTUATED CRANK TO TRANSFORM CW & CCW MOTION
VITON O-RING SEAL (2)
PARACHUTE BRIDLE ACTUATED DIPOLE ANTENNA MAST(STOWED)
PRESSURE COVER AND SEQUENCING MECHANISM (AUTOMATICALLY ACTUATED FROM GEARBELT CW & CCW)
ELASTOMER RING
DROGUECHUTE CANNISTER AND MORTAR INSTALLATION
MAIN PARACHUTE
ELECTRONICS
TOP COVER SEPARATION PYRO AND MARMAN-RING
8.02 cm
40°
ELASTOMERIC ABLATOR
TITANIUM SKIRT & THERMAL INSULATION
8.28 cm
10.64 cm
30°
BATTERIES
SSM CONTAINER ASSY Ti 6AL-4V
NOMINAL IMPACT AREA
HEAT SHIELD ESA 5300-M3 1.90 cm
42.54 cm
HEAT SHIELD BACK-UP STRUCTURE .95 cm PHENOLIC HEXCELL HONEYCOMB
PHENOLIC INSERT AND MOUNTING INTERFACE
EARTH ENTRY MODULE
TOT. WT. ≅ 14.96 Kg

Figure V-12 Earth Entry Module

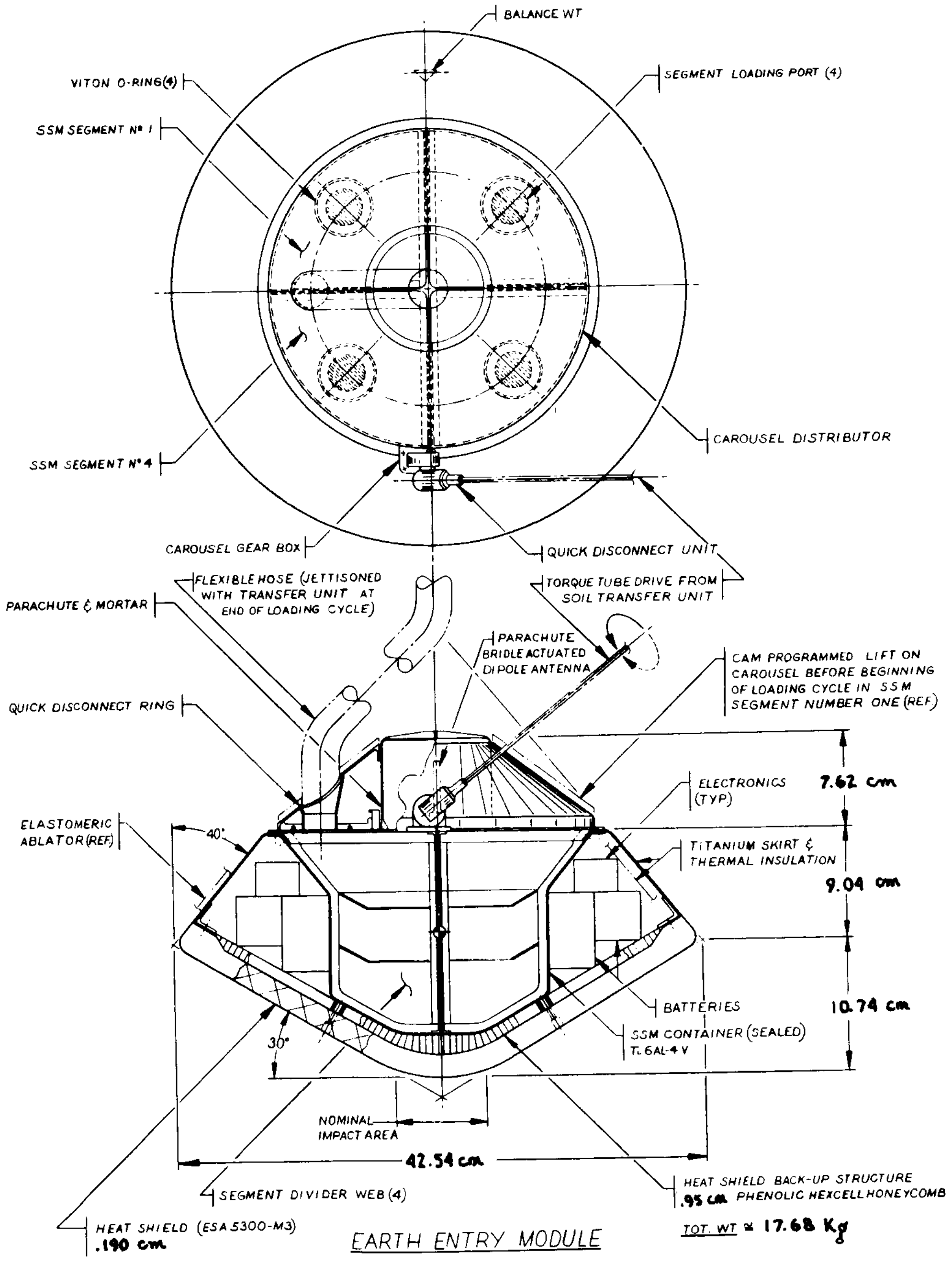
BALANCE WT
VITON O-RING(4)
SEGMENT LOADING PORT (4)
SSM SEGMENT Nº 1
CAROUSEL DISTRIBUTOR
SSM SEGMENT Nº 4
CAROUSEL GEAR BOX
QUICK DISCONNECT UNIT
FLEXIBLE HOSE (JETTISONED WITH TRANSFER UNIT AT END OF LOADING CYCLE)
TORQUE TUBE DRIVE FROM SOIL TRANSFER UNIT
PARACHUTE & MORTAR
PARACHUTE BRIDLE ACTUATED DIPOLE ANTENNA
CAM PROGRAMMED LIFT ON CAROUSEL BEFORE BEGINNING OF LOADING CYCLE IN SSM SEGMENT NUMBER ONE (REF)
QUICK DISCONNECT RING
ELECTRONICS (TYP)
7.62 cm
ELASTOMERIC ABLATOR (REF)
40°
TITANIUM SKIRT & THERMAL INSULATION
9.04 cm
BATTERIES
10.74 cm
SSM CONTAINER (SEALED) Ti 6AL-4 V
30°
NOMINAL IMPACT AREA
42.54 cm
HEAT SHIELD BACK-UP STRUCTURE .95 cm PHENOLIC HEXCELL HONEYCOMB
SEGMENT DIVIDER WEB (4)
HEAT SHIELD (ESA 5300-M3) .190 cm
EARTH ENTRY MODULE
TOT. WT ≅ 17.68 Kg

Figure V-13 Earth Entry Module

Table V-7 Earth Entry Module Design Characteristics

Entry Velocity Capability	Up to 12.8 km/sec (42,000 ft/sec)
Sample Capacity (Nominal)	5 kg and 2 kg
Ballistic Coefficient $\frac{W}{C_DA}$	94 kg/m^2 (19.3 lb/ft^2)
Subsonic Parachute Deployment	
Water Recovery	
Electronic Tracking Aids	Transponder, 30 day life
Power Source	Battery self-activated sliver-zinc during entry sea water activated magnesium-iron- 30 day life

return canister is shown in Figures V-14 and V-15. The sample canister lid is actuated before and after sample loading from the transfer unit by use of gearbelt actuated torque tube drive and cam sequenced carousel programming. The entire soil transfer unit is jettisoned after completion of the loading cycle and lid closing. Recovery of the capsule at Earth is facilitated by electronic tracking aids that provide signals for a minimum of 30 days using a sea water actuated battery.

2. Alternate Configuration

The alternate configuration is shown in Figure V-16. The delivery system is the Viking Orbiter propulsion module with an adapter ring at the forward end which replaces the orbiter octagon bus structure. This adapter ring serves to attach the propulsion module to the sample return vehicle. The sample return vehicle is composed of a lander which is an evolutionary development from the Phase I lander/rover design and an entirely new three-axis stabilized earth return vehicle as shown in Figure V-17. The thermally enclosed aluminum box structure which houses the supporting subsystem equipment is patterned after the Mariner series spacecraft. Two articulated solar panels are located symmetrically around the bus structure. The same earth entry module described earlier which provides for a nominal 5 kg sample return is stowed in the upper portion of the vehicle. Weight summary of the three-axis stabilized earth return vehicle is presented in Tavle V-8.

System level weights for the alternate configuration are given in Table V-9.

3. Competitive Alternative Configurations

Two other alternative configurations which were studied during Phase II and described earlier are shown in Figures V-18 and V-19. System weights for these concepts are summarized in Tables V-10 and V-11 respectively.

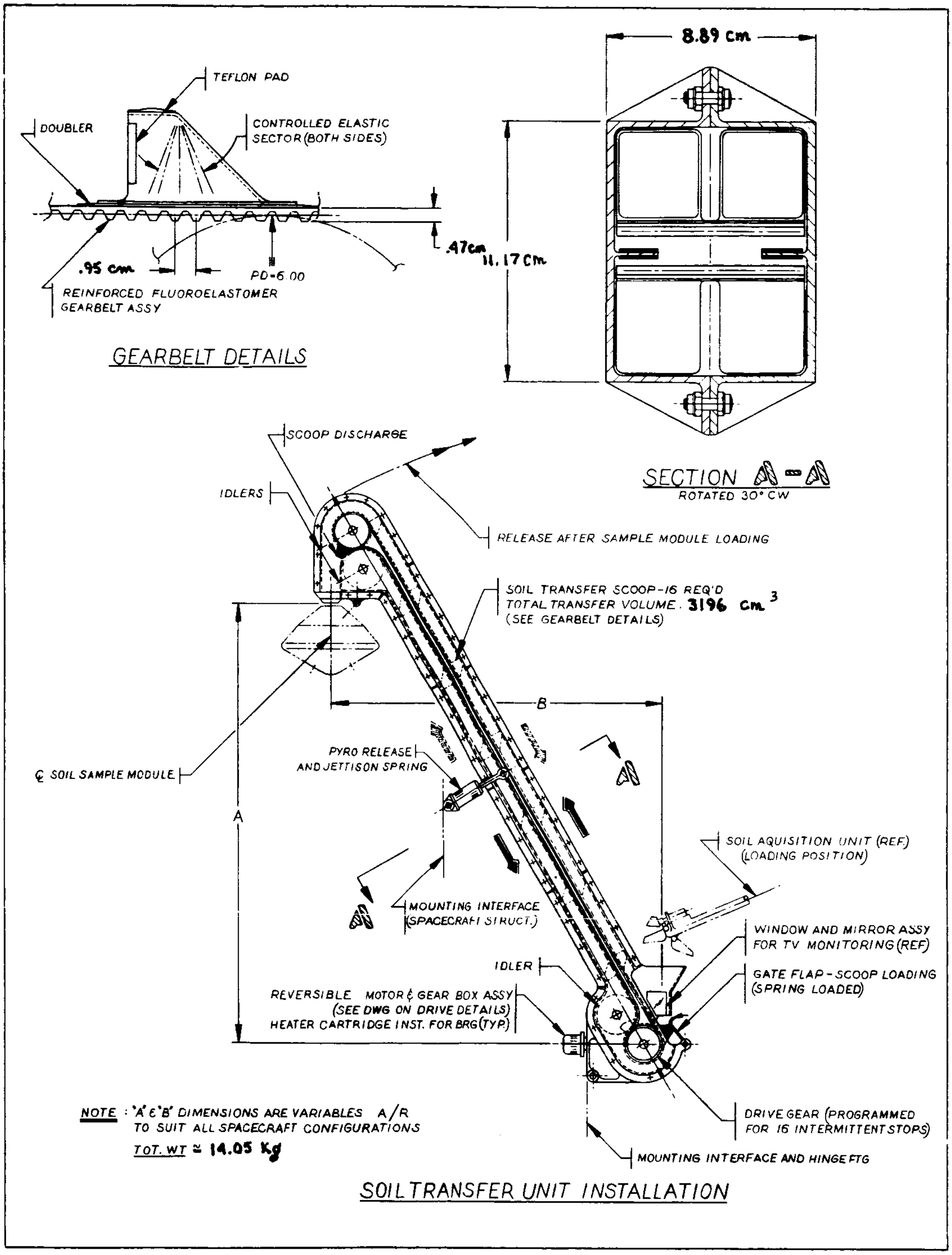
TEFLON PAD
DOUBLER
CONTROLLED ELASTIC SECTOR (BOTH SIDES)
.95 cm
PD-6.00
.47cm
REINFORCED FLUOROELASTOMER GEARBELT ASSY
GEARBELT DETAILS
8.89 cm
11.17 cm
SECTION A-A
ROTATED 30° CW
SCOOP DISCHARGE
IDLERS
RELEASE AFTER SAMPLE MODULE LOADING
SOIL TRANSFER SCOOP-16 REQ'D
TOTAL TRANSFER VOLUME. 3196 cm³
(SEE GEARBELT DETAILS)
B
℄ SOIL SAMPLE MODULE
PYRO RELEASE AND JETTISON SPRING
A
A
A
SOIL AQUISITION UNIT (REF) (LOADING POSITION)
MOUNTING INTERFACE (SPACECRAFT STRUCT.)
WINDOW AND MIRROR ASSY FOR TV MONITORING (REF)
IDLER
GATE FLAP-SCOOP LOADING (SPRING LOADED)
REVERSIBLE MOTOR & GEAR BOX ASSY (SEE DWG ON DRIVE DETAILS)
HEATER CARTRIDGE INST. FOR BRG (TYP)
DRIVE GEAR (PROGRAMMED FOR 16 INTERMITTENT STOPS)
NOTE: 'A' & 'B' DIMENSIONS ARE VARIABLES A/R TO SUIT ALL SPACECRAFT CONFIGURATIONS
TOT. WT ≈ 14.05 Kg
MOUNTING INTERFACE AND HINGE FTG
SOIL TRANSFER UNIT INSTALLATION

Figure V-14 Soil Transfer Unit Installation

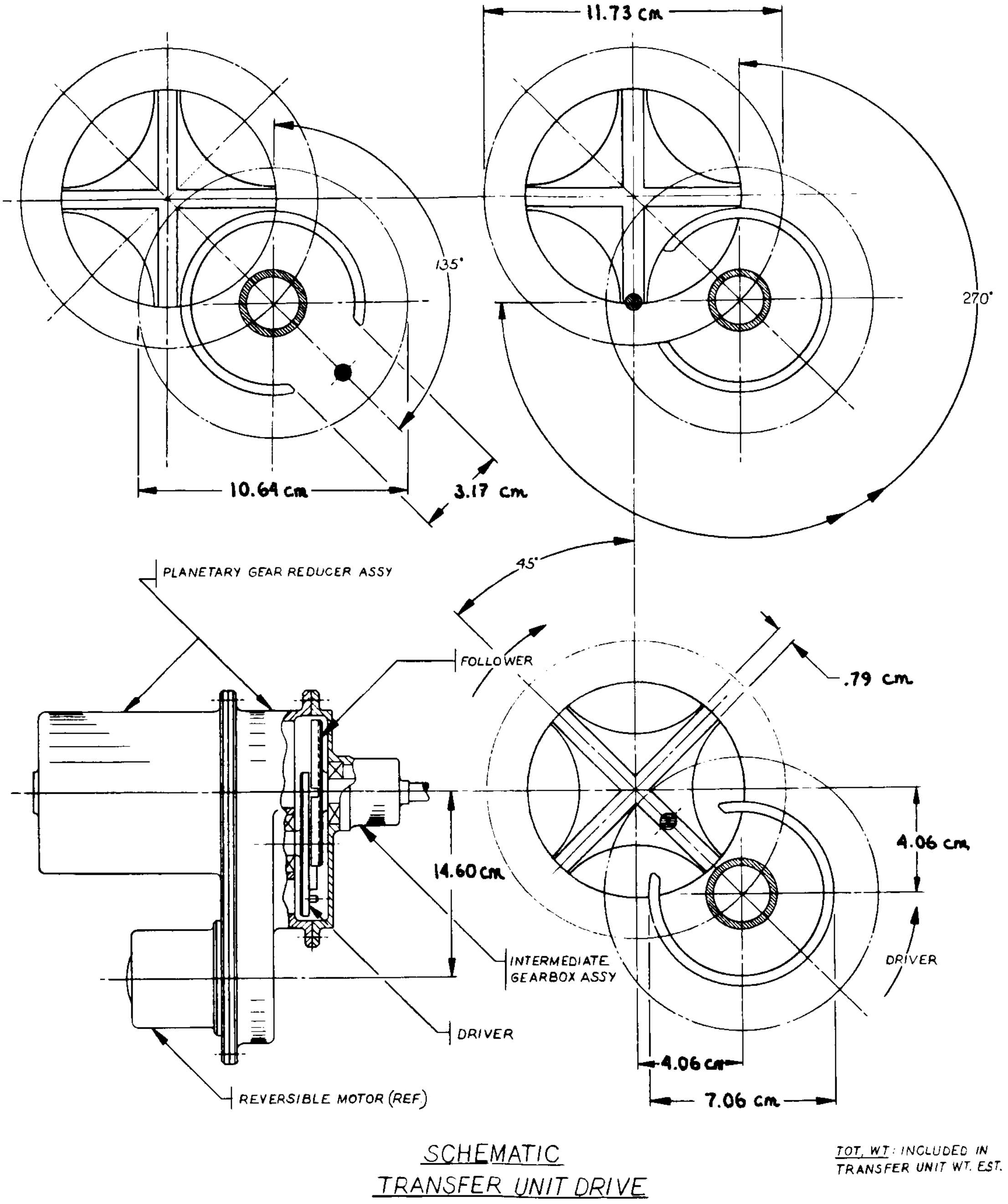
11.73 cm
135°
270°
10.64 cm
3.17 cm
45°
PLANETARY GEAR REDUCER ASSY
FOLLOWER
.79 cm
14.60 cm
4.06 cm
INTERMEDIATE GEARBOX ASSY
DRIVER
DRIVER
4.06 cm
7.06 cm
REVERSIBLE MOTOR (REF)
SCHEMATIC
TRANSFER UNIT DRIVE
TOT. WT: INCLUDED IN TRANSFER UNIT WT. EST.

Figure V-15 Schematic Transfer Unit Drive

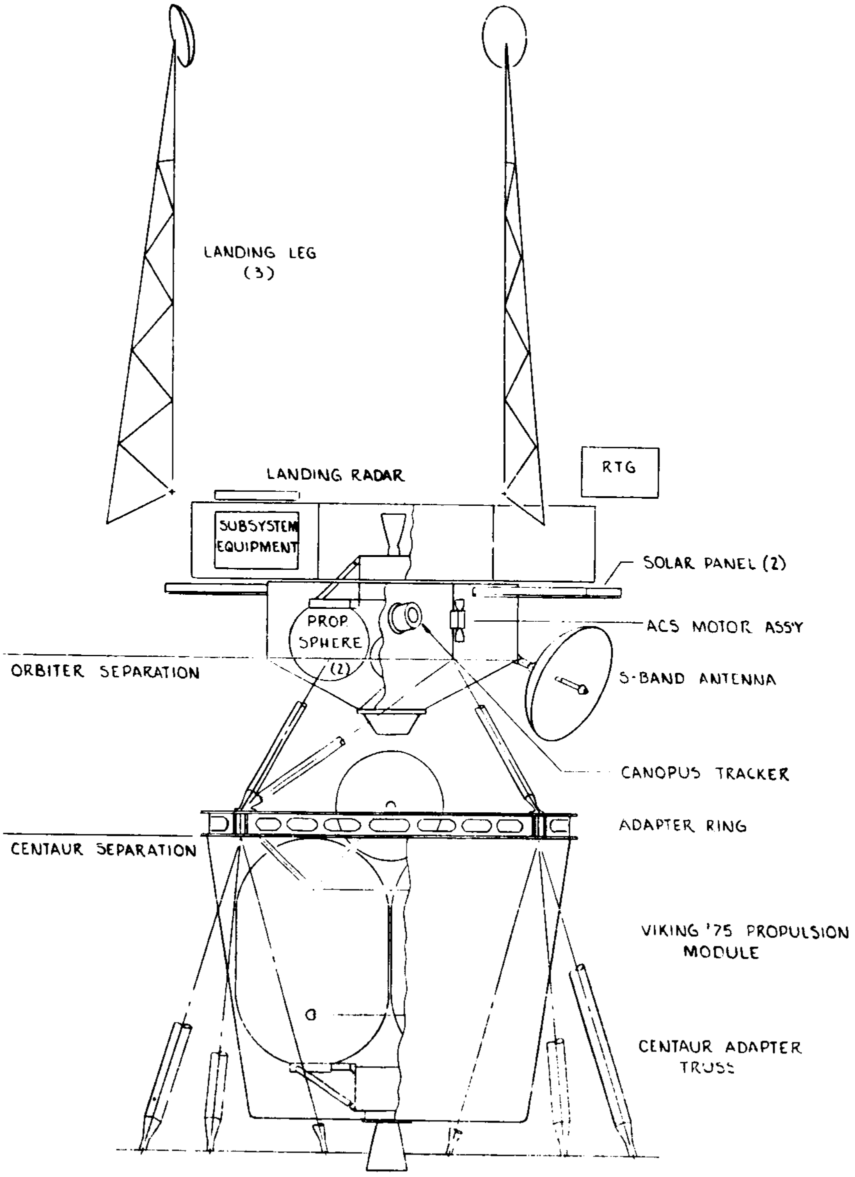
LANDING LEG
(3)
LANDING RADAR
RTG
SUBSYSTEM EQUIPMENT
SOLAR PANEL (2)
PROP SPHERE (2)
ACS MOTOR ASS'Y
ORBITER SEPARATION
S-BAND ANTENNA
CANOPUS TRACKER
ADAPTER RING
CENTAUR SEPARATION
VIKING '75 PROPULSION MODULE
CENTAUR ADAPTER TRUSS

Figure V-16 Preferred Alternate Sample Return Configuration

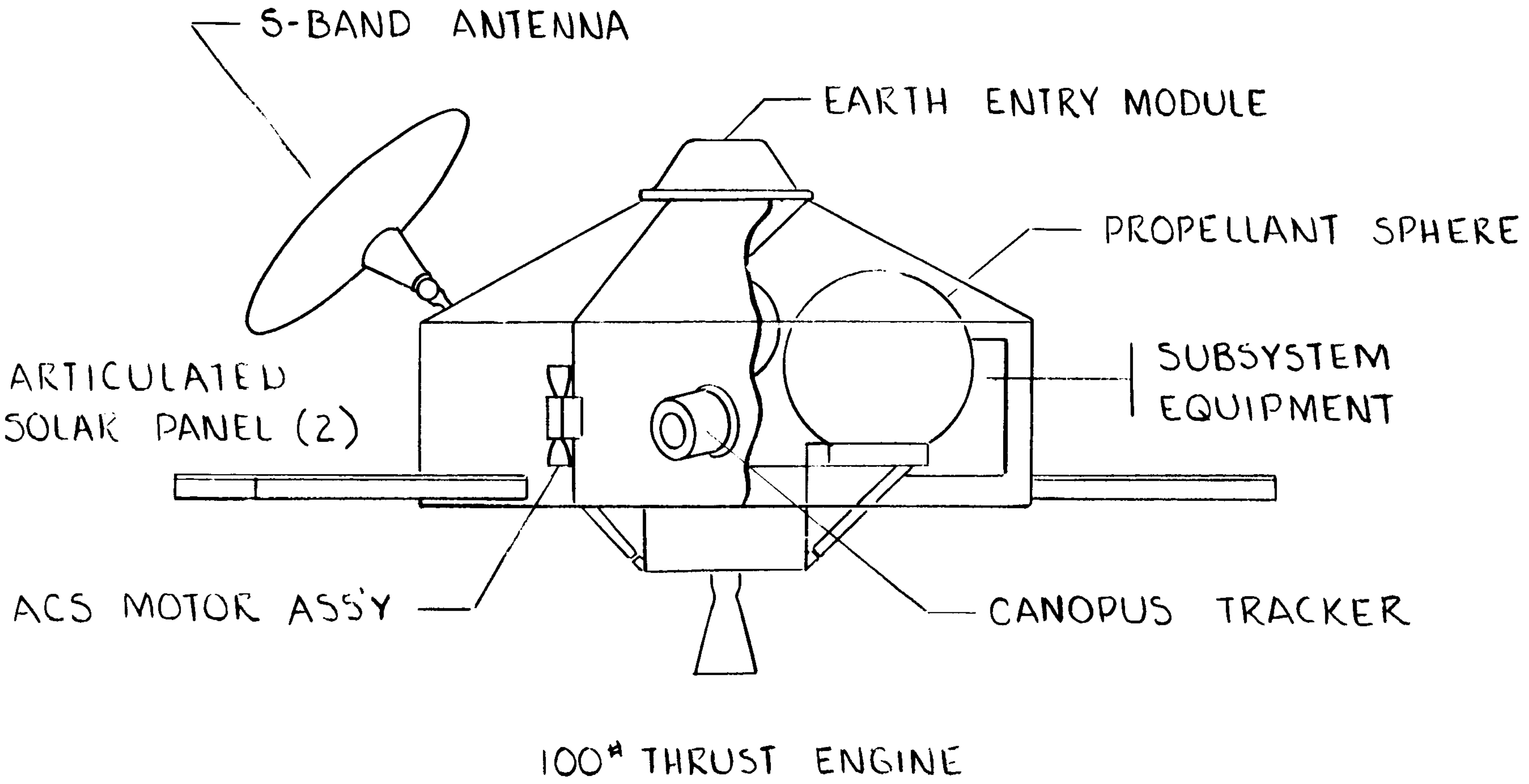
S-BAND ANTENNA
EARTH ENTRY MODULE
PROPELLANT SPHERE
ARTICULATED SOLAR PANEL (2)
SUBSYSTEM EQUIPMENT
ACS MOTOR ASS'Y
CANOPUS TRACKER
100# THRUST ENGINE

Figure V-17 Earth Return Vehicle (Three-Axis)

Table V-8 Three-Axis Stabilized Earth Return Vehicle Weight Summary, KGS

Structures	10.7	
Power	9.8	
Cabling	3.0	
Communications	10.6	
Guidance & Control	8.9	
Thermal Control	4.5	
Mech Devices	2.0	
Earth Entry Module	13.6	
Attitude Control	13.6	
Propulsion Inerts	22.7	
Reserve	6.4	
Dry Weight		105.8 (233.7 lb)
Propellant	91.6	
Loaded Weight		197.4 (435.0 lb)
Growth Contingency		61.2 (135.0 lb)
Allocated Weight		258.6 (570.0 lb)

Table V-9 Preferred Alternate Weight Summary, KGS
(Round Trip Control Module/Lander)

Orbiter		
Bus Structure Assy	89.8	
Propulsion - Inerts	230.0	
P/L - Orbiter Adapter	15.9	
Contingency (4%)	13.6	
Orbiter Dry Weight		349.3 (770.0 lb)
Expendable Propellant	1397.1	
Orbiter Loaded Weight		1746.4 (3850.0 lb)
Modified PE Earth Return Vehicle		197.3 (435.0 lb)
Round Trip Control Module Lander		
Structures	95.3	
Power	59.1	
Cabling	26.9	
Communications	8.9	
Guidance & Control	10.4	
Data Handling	23.1	
Thermal Control	11.7	
Pyrotechnics	7.4	
Propulsion (inerts + usable propellant)	56.1	
Sampling Subsystem	27.2	
Contingency	15.8	
Spacecraft Loaded Weight		2285.6 (5038.8 lb)
Orbiter/Launch Vehicle Adapter	68.0	
Project Reserve	56.7	
LVMP	90.7	
Injected Payload Weight		2501.1 (5513.8 lb)

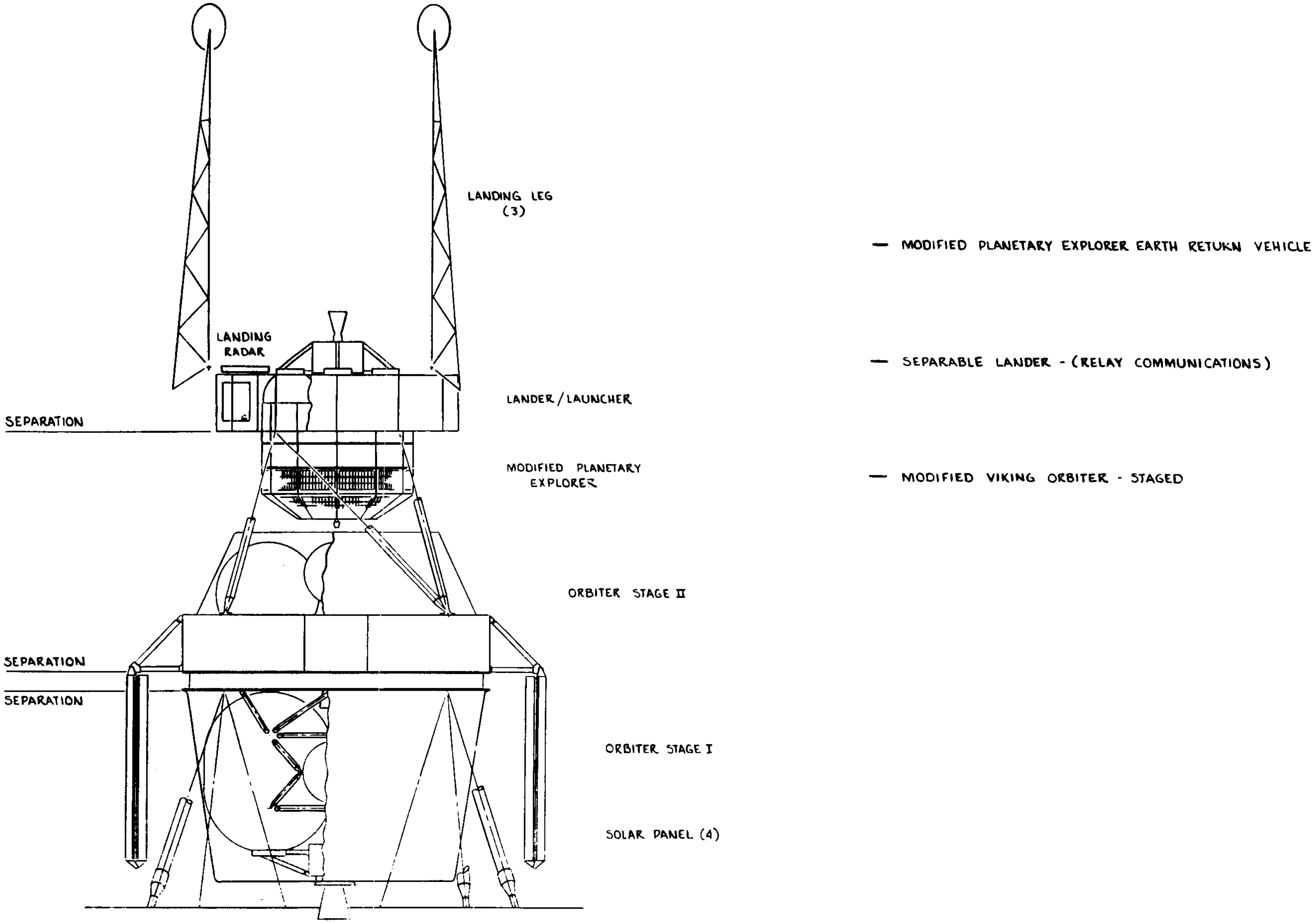
LANDING LEG (3)
LANDING RADAR
SEPARATION
LANDER/LAUNCHER
MODIFIED PLANETARY EXPLORER
ORBITER STAGE II
SEPARATION
SEPARATION
ORBITER STAGE I
SOLAR PANEL (4)
— MODIFIED PLANETARY EXPLORER EARTH RETURN VEHICLE
— SEPARABLE LANDER - (RELAY COMMUNICATIONS)
— MODIFIED VIKING ORBITER - STAGED

Figure V-18 Alternate Sample Return Configuration

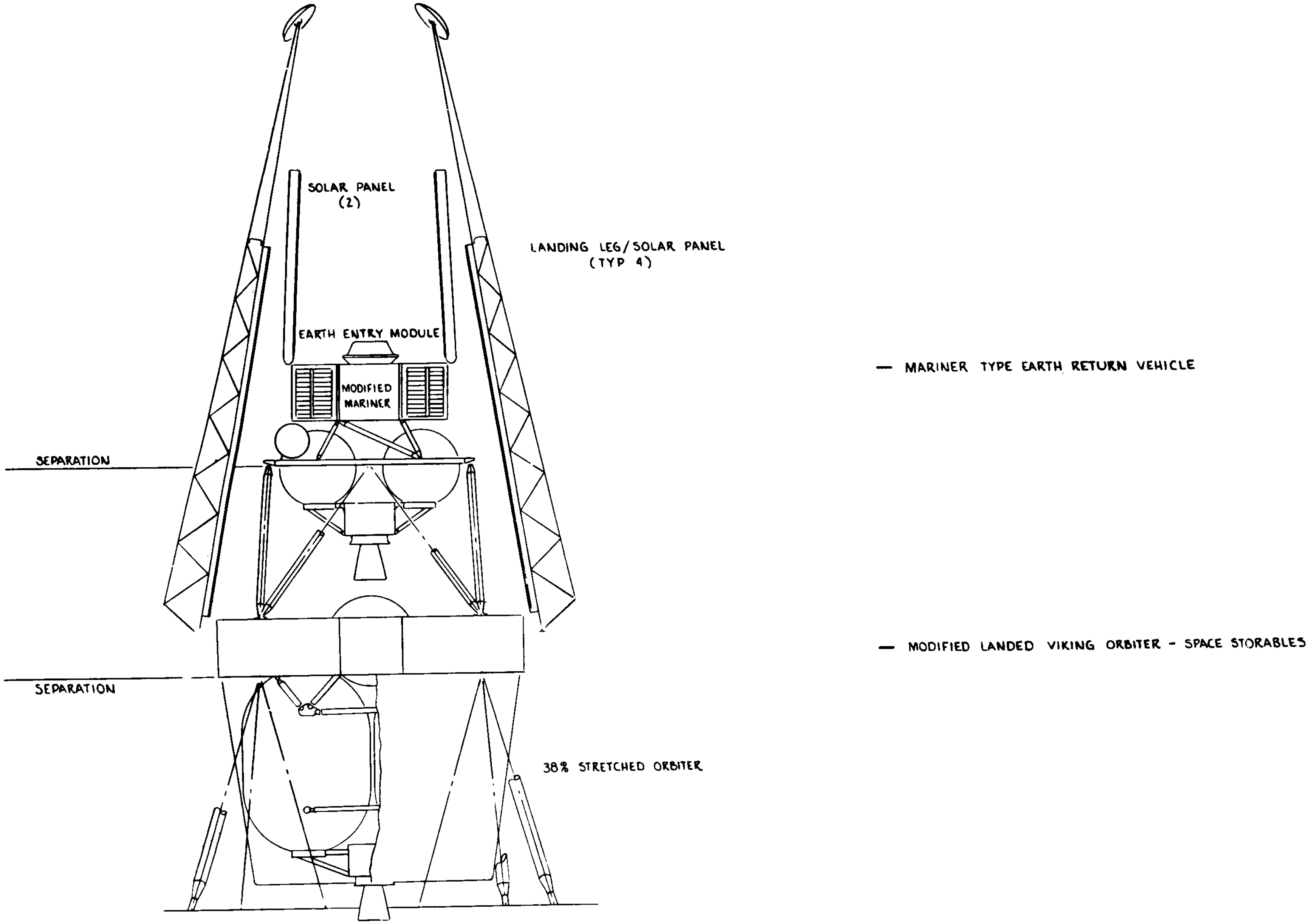
SOLAR PANEL
(2)
LANDING LEG/SOLAR PANEL
(TYP 4)
EARTH ENTRY MODULE
MODIFIED
MARINER
— MARINER TYPE EARTH RETURN VEHICLE
SEPARATION
— MODIFIED LANDED VIKING ORBITER - SPACE STORABLES
SEPARATION
38% STRETCHED ORBITER

Figure V-19 Alternate Sample Return Configuration

Table V-10 Alternate Configuration Weight Summary, KGS

Orbiter Dry Weight		1102.2 (2430 lb)
Expendable Propellant	2301.1 (5073 lb)	
Orbiter Loaded Weight		3403.3 (7503 lb)
Modified PE Earth Return Vehicle		197.3 (435.0 lb)
Separable Lander		322.1 (710.0 lb)
Spacecraft Loaded Weight		3922.7 (8648 lb)
Orbiter/Launch Vehicle Adapter	68.0	
Project Reserve	56.7	
LVMP	90.7	
Injected Payload Weight		4138.1 (9123 lb)

Table V-11 Alternate Configuration Weight Summary, KGS

Orbiter Dry Weight		952.6 (2100 lb)
Expendable Propellant (Space Storable)	1546.8 (3410 lb)	
Orbiter Loaded Weight		2499.0 (5510 lb)
Mariner Type Earth Return Vehicle		561.1 (1237 lb)
Spacecraft Loaded Weight		3060.1 (6747 lb)
Orbiter/Launch Vehicle Adapter	68.0	
Project Reserve	56.7	
LVMP	90.7	
Injected Payload Weight		3275.9 (7222 lb)

4. Landing Stability

The computer program which was used to determine the stability boundaries for our Phase II studies is a modified version of the program being utilized for all landing dynamic analyses for the Viking '75 program. The inputs to that program that are necessary to compute the landing stability of the baseline configuration are shown in Table V-12. Results of that analyses are also presented in Table V-12.

5. Dynamic Environment

The acoustic environment to which the Phase II Phobos/Deimos sample return configurations are subjected during launch is identical to the Phase I study.

Load factors including landing shock levels were also identical to those encountered during the Phase I study.

D. THERMAL CONTROL

The Phase II thermal studies were directed towards establishing conceptual thermal designs for the baseline and preferred alternate sample return configurations. Environmental predictions for the interplanetary and landed phases of the mission were adapted from the results of the Phase I studies; the basic concepts of vehicle configurations were evolved by the other study tasks of the program, with thermal support as required to demonstrate mission feasibility, but without an attempt at thermal design optimization.

The concerns and resolutions of the sample return thermal studies can be best summarized by outlining the principal thermal constraints of the mission and their impact on design. The thermal constraints stem from four general sources: (a) variable solar intensities, (b) variable internal heat dissipation,

Table V-12 Landing Dynamics Analysis

Study Guidelines

Max $V_V = V_H = .36$ km/sec (1.5 fps)

Coefficient of friction $\mu = 1.0$

Worst case stability landing
2 legs leading downhill

Vehicle Weights
1150 kg (2530 lb) Landed Orbiter
567 kg (1250 lb) Separable Lander

CG height above ground line
2.12 m (85 in.) Landed Orbiter
1.75 m (70 in.) Separable Lander

Initial ground clearance
.45m (18 in.) Landed Orbiter
.83m (33 in.) Separable Lander

Assumed net thrust toward surface = 7 lb_F

Study Results

Stability - 100% on 25° ground slopes

Ground clearance (after stroking)
Landed Orbiter - exceeds .3m (12 in.)
Separable Lander - exceeds .6m (24 in.)

Loads
< 68 kg (150 lb) per leg

Recommendations
Max V_V, V_H not to exceed ~ 1.5 fps

Active attitude rate damping

Provide net thrust toward surface

(c) thermal blockage due to staging, and (d) unfavorable coupling between external and internal heat loads. These will be discussed below.

The solar intensity may vary during a Mars mission from 1353 w/m^2 near Earth, to 709 W/m^2 near Mars at perihelion, or 487.4 w/m^2 at aphelion. Superimposed on these long-range variations is the diurnal cycling on the surface, with zero solar flux during the "night" hours. In the case of the landed quipment, the effect is magnified by the presence of the ground, which reflects and/or emits radiation in concert with the solar flux. The standard thermal control approach to minimizing these effects is either shielding (by the use of insulation or reflective finishes) or compensation (by the use of controlled heat flow into or out of the vehicle). Both of these methods have been employed in the conceptual thermal designs of the baseline and preferred alternate configurations.

An area of concern in the thermal design of the landed orbiter is the relatively large difference in heat dissipation requirements between the cruise and landed phases of the mission. The average internal power dissipation during cruise is 415 watts (with 796 w peak), as compared to 90 watts average during landed operations. A further complication is afforded by the absence of a convenient radiation heat sink on the surfaces of the satellites. This compares with the use of outer space as a heat sink with an effective temperature of 4°K during the interplanetary phases of the mission. It will be shown that the landed orbiter concept hinges on significant modifications of the Viking Orbiter heat rejection system.

The dissipation of equipment (or environmental) heat during landed operations may be accomplished by either a combination of two basic modes of heat rejection: (1) the "night mode," whereby the equipment heat generated during the day is stored by the thermal mass of the system, followed by controlled dissipation to the environment during the night, when the ground as well as the sky can be used as effective heat sinks; and (2) the "day mode," accomplished during the day (or night) by the use of solar-reflector radiators with high view factors to the sky, and negligible view factors to the ground or external surfaces of the vehicle. The selection among these modes, and, consequently, the overall thermal design of the landed configurations, depend critically on the availability of potential sky-oriented radiator surfaces; or the absence of radiation blockage by other equipment, such as upper stages of a complex landed configuration. The landed configurations of both the baseline and alternate configurations are two-stage vehicles; however, blockage by the upper stage in the former case is less severe than in the preferred alternate configuration.

Finally, a fourth major concern is the apparent simultaneity of maximum internal and external heat loads during typical landed operations. Imagery and soil sample temperature constraints establish a day-time preference for scientific investigations, and solar-powered vehicles depend on the availability of solar energy during their peak power operation. It is also during the day time that external heating due to solar and ground radiation are at a maximum. Conversely, internal heat dissipation is at a minimum or zero during the night, and the vehicle is subjected to maximum cooling in the absence of appreciable external heat sources. Because of this unfavorable coupling between external and internal heating (and cooling), active thermal control techniques will be required, as a general rule, in the design of Phobos/Deimos landers.

In the following paragraphs, the thermal design of the baseline and preferred alternate configurations are described in more detail.

1. Thermal Design - Baseline Sample Return Configuration

The baseline sample return configuration consists of a modified landed Viking Orbiter and a modified planetary explorer earth return vehicle.

a. Modified Orbiter Thermal Control - The thermal control subsystem of the Viking Orbiter is modified to accommodate the widely different thermal requirements during landed operations as compared to the interplanetary phases of the mission. The modifications consist in a redesign of the heat rejection system, and the addition of Phase Change Material (PCM) to minimize internal equipment temperature fluctuations due to diurnal cycle effects on the satellite surface. The modifications to the heat rejection system consist in providing two sets of louvers: (1) Viking Orbiter types, mounted on the sides of the equipment compartment, which are operational during cruise only, and are de-activated on the satellite surface by the use of insulated flip covers; and (2) Sun-oriented types (covered with OSR) which function throughout the orbiter mission. Heat rejection during the landed operations is by the "day mode," as described in the previous paragraph; the OSR-covered louver system is actuated by the variations of internal temperatures, and are closed during the night.

b. Modified Planetary Explorer Thermal Control - The principal modifications to the **Planetary Explorer** thermal control system are the considerable reduction of the heat rejection (louver) area (as compared to the Venus mission configuration), and the addition of a 10 watt radioisotope heater to compensate for the very minimal internal heat dissipation available during the surface operations. The total heat budget of the **Planetary Explorer** during the interplanetary phases of the mission (Earth-Mars cruise and Mars-Earth curise) is in the order of 20 watts.

Internal heat dissipation is through heat leaks through the propulsion nozzle, supports, insulation penetrations, and insulation; supplemented by controlled heat rejection through two OSR-covered specular louver panels.

The baseline thermal control approach is summarized on Table V-13, a thermal schematic of the landed configuration is depicted on Figure V-20.

2. Thermal Design - Preferred Alternate Configuration

The preferred alternate sample return configuration consists of a three-axis control module, a lander, and a propulsion module which is jettisoned prior to final closure and touchdown.

The propulsion module is Sun-oriented during cruise, and it is insulated and covered with solar-reflective external coatings. Thermal control is achieved by the use of thermostatically controlled heaters.

The lander thermal control concept is similar to that of the Viking lander, consisting of an insulated equipment compartment, with RTG waste heat input to the compartment controlled by a thermal switch. Heat rejection is through uncontrolled heat leaks through the insulation and insulation penetrations.
During the landed phases of the mission, heat rejection is by the "night mode" as defined in paragraph 1 above.

The 3-axis sample return vehicle is completely insulated, with the exception of louver-controlled OSR radiators, which provide heat rejection during all phases of the mission. Thermostatically-controlled heaters compensate for duty-cycle variations. Heat rejection on the surface is by the "day mode" as defined above. Return configuration is depicted on Figure V-21.

3. Thermal Control Summary

A summary of thermal considerations for the sample return mission is shown on Table V-14.

Table V-13 Baseline Thermal Control Approach

Modified Orbiter:	-415 Watts Avg Equipment Heat During Cruise - 90 Watts Avg Heat From Equipment and Heaters on Surface - 20 lbs Phase Change Material (PCM) to Equalize Diurnal Variations -Modified Heat Rejection System: -10 ft^2 VO-Type Louvers + Insulated Flip Cover (to Deactivate During Surface Operations) -6 ft^2 Sun-Oriented Louvers Covered With OSR Radiator
Modified Planetary Explorer:	-Vehicle Completely Insulated With MLI, Except 2 ft^2 Louver Controlled OSR Radiator -10 Watt Radio Isotope Heater Unit to Augment Equipment Heat -Thermostically Controlled Heaters Compensate for Duty Cycle Variations -High Temperature Insulation on Plume Exposed Surfaces

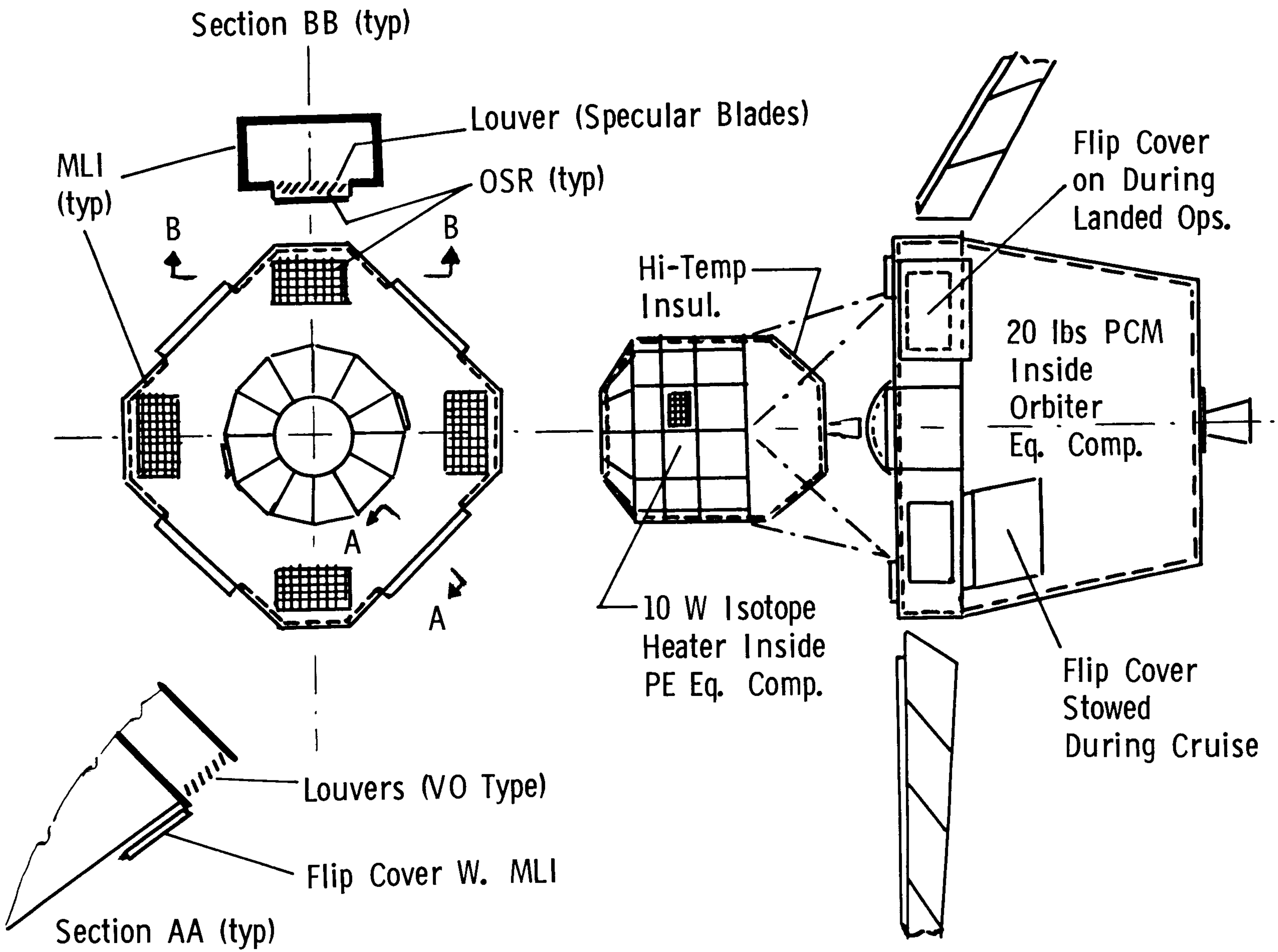
Section BB (typ)
Louver (Specular Blades)
MLI (typ)
OSR (typ)
B
B
A
A
Louvers (VO Type)
Flip Cover W. MLI
Section AA (typ)
Hi-Temp Insul.
10 W Isotope Heater Inside PE Eq. Comp.
Flip Cover on During Landed Ops.
20 lbs PCM Inside Orbiter Eq. Comp.
Flip Cover Stowed During Cruise

Figure V-20 Baseline Thermal Schematic

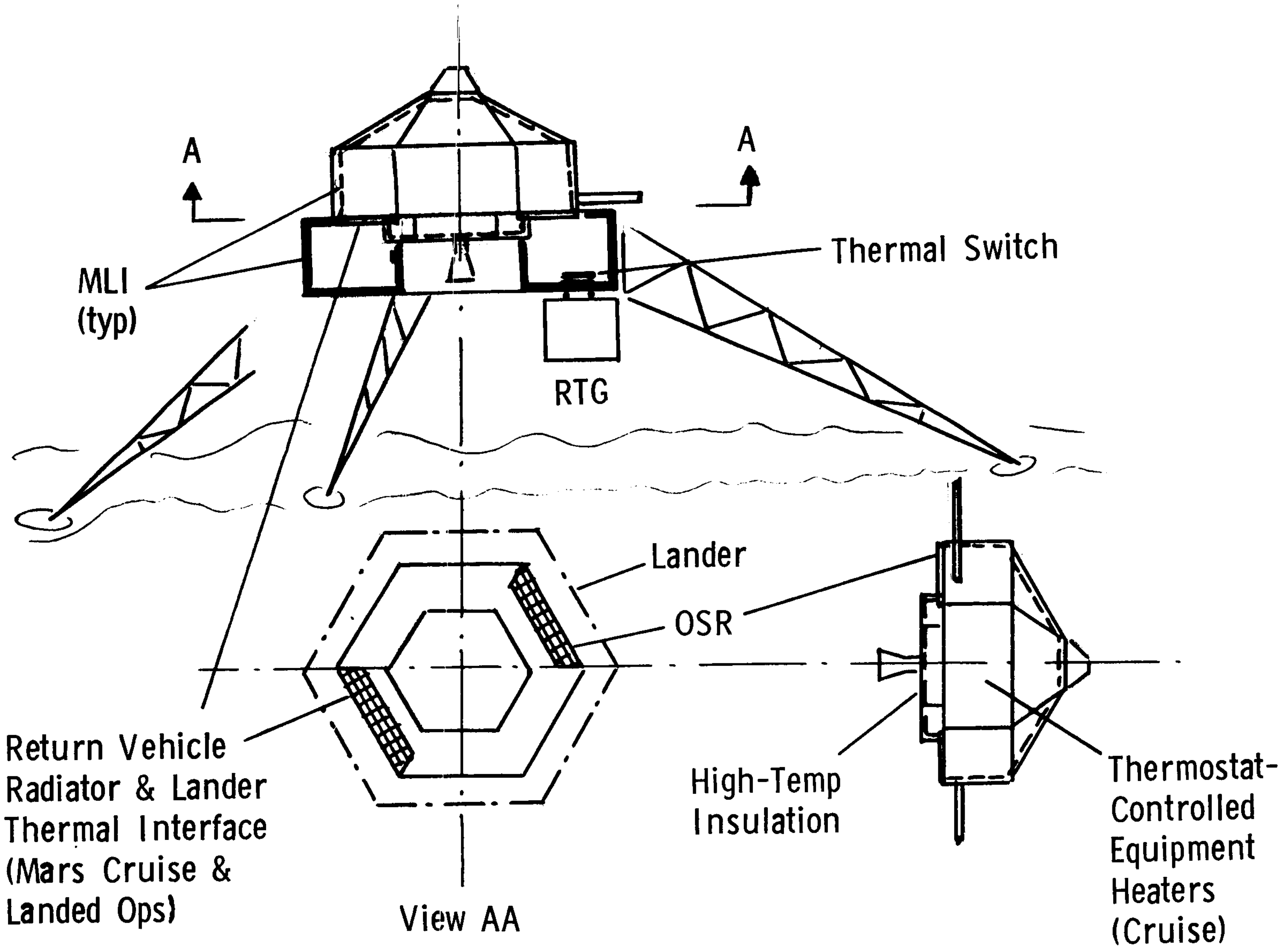
A
A
MLI
(typ)
Thermal Switch
RTG
Lander
OSR
Return Vehicle
Radiator & Lander
Thermal Interface
(Mars Cruise &
Landed Ops)
View AA
High-Temp
Insulation
Thermostat-
Controlled
Equipment
Heaters
(Cruise)

Figure V-21 Preferred Alternate Thermal Schematic

Table V-14 Sample Return Mission Thermal Control Summary

Principal Thermal Constraints:	- Large Variations In Solar Constant 188 Per Cent Throughout the Mission 46 Per Cent On the Surface - Large Variations in Internal Heat Dissipation 796 w Peak Cruise Load vs 0 w During Night on Phobos - Available "View" of Natural Heat Sinks and Sources Constrained by the Necessity of "Staging" both During Cruise and On the Surface - Uncertainties of Satellite Surface Effects (Dust, Craters, Etc.)
Baseline Thermal Control:	- Landed Orbiter Feasibility Established Via Extensive Modifications to the VO Heat Rejection System - Both Orbiter and Planetary Explorer Thermal Control Can Be Achieved By the Use of State-Of-The-Art Hardware - Extended Surface Operations are Limited to Equatorial Landing Sites; Thermal System Becomes Marginal for Diurnal Cycles Longer Than 7 hrs
Preferred Alternate Thermal Control:	- The Use of RTG Waste Heat for Thermal Control Provides Flexibility in Design, Landing Site Selection, and Surface Operations

E. PROPULSION

The primary objective of the Phase II propulsion studies was to define appropriate primary and attitude control propulsion subsystems for the earth return vehicles used in the satellite sample return mission. The primary propulsion system for the earth return vehicle must provide sufficient thrust to accomplish the following mission events:

a) liftoff from Phobos,
b) raise apoapsis,
c) lower periapsis and change orbital plane,
d) trans-Earth injection,
e) midcourse corrections (3),
f) Earth entry deflection maneuver.

For a Phobos baseline mission launch date of November 19, 1983, the total velocity increment required of the earth return vehicle is 1786 meters/second.

Spacecraft attitude control propulsion systems were defined during this phase to support both the 3-axis stabilized and the spin stabilized earth return vehicle concepts.

1. Baseline Propulsion Subsystem (Spin Stabilized)

The baseline earth return vehicle for the Phobos sample return mission generated during Phase II is a modification of the Planetary Explorer or Venus Pioneer spin stabilized interplanetary cruise spacecraft. The vehicle requires an ACS for spin rate control and spin axis orientation and a primary propulsion system for velocity changes.

a. Modified P.E. Primary Propulsion - The modified planetary explorer vehicle propulsion system was sized for the following total velocity requirement and spacecraft and sample capsule weights:

Total ΔV Requirements	1786 meters/second
Spacecraft Weight (excluding propulsion)	68 kg
Capsule Weight	16 kg

A requirement of the propulsion system is that it must be capable of performing the aforementioned orbital maneuvers, after being space stored for approximately 700 days. Its operational period following storage will be 320 days.

Since propulsion system weight for the earth return vehicle is critical, a lower weight engine than that used on the Viking Orbiter was required. The **Planetary Explorer** solid motor propulsion system did not qualify for the Phobos mission because it could not perform the multiple velocity adjustment requirements.

Several high performance storable bi-propellant engines with thrust levels compatible with modified planetary explorer spacecraft and structural design were reviewed. Three engines of the 100 lb thrust class were selected for further study:

a) Marquardt - Model R-4D
b) Thiokol, RMD - Model C-1
c) TRW Systems - Model MIRA-150R

The Marquardt engine was selected over that of the Thiokol and TRW engines. The RMD C-1 engine does have equivalent design features, however, it lacks the test and development experience. The TRW engine is throttable and therefore is heavier and requires a higher pressure propellant supply. The Marquardt R-4D engine has been successfully demonstrated on the **Lunar Orbiter** as a velocity control engine and as a secondary velocity control engine on the Agena launch vehicle. It is also used on the Apollo Service Module and Lunar Module for attitude control. A schematic and engine characteristics for the Marquardt engine are presented in Figure V-22. The engine performance values given in this figure are for the propellants N_2O_4 and MMH

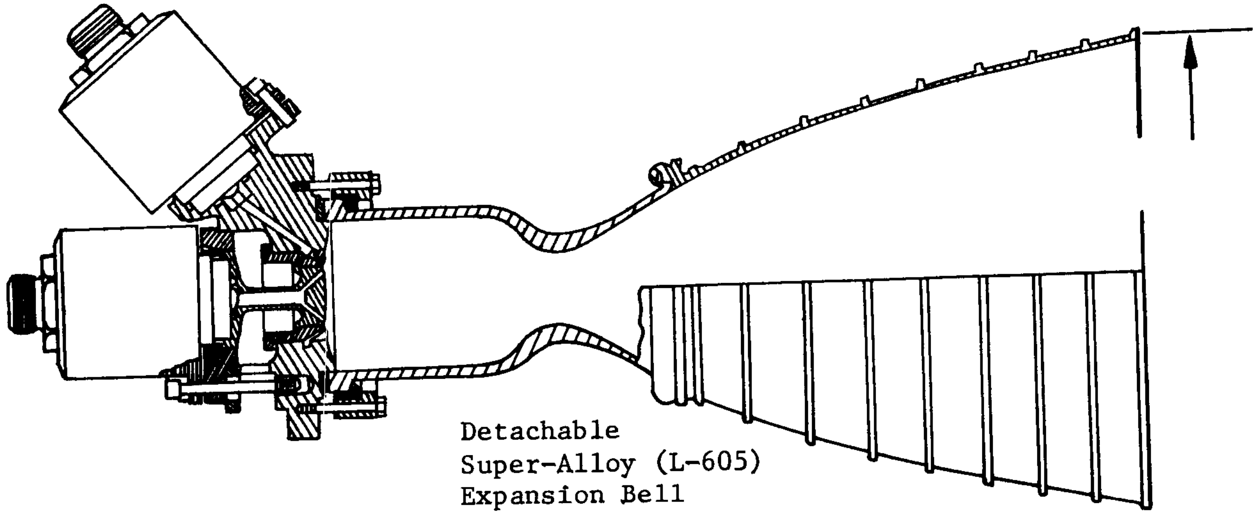

Vacuum Thrust (lb_f)	100
Specific Impulse (sec) (vacuum nominal)	295
Characteristic Velocity (fps) [nominal (C*)]	5350
Thrust Coefficient (vacuum nominal)	1.70
Operating Life (sec) (demonstrated)	12,960
Maximum Steady-State Duration with NTO/MMH (sec)	1020
Chamber Pressure (psia) (nominal)	97
Oxidizer, N_2O_4 to Fuel, MMH	1.6
Mixture Ratio (nominal)	40:1

Fuel
Valve

Oxidizer
Valve

Straight Wall
Columbium Combustor

$L^* = 11.5$

$A_t = 3.74\ cm^2$

$D_e = 17.6\ cm$
$\varepsilon = 65$

Figure V-22 Model R-4B Bipropellant Rocket Engine

(CH_3NHNH_2). The propellant combination of N_2O_4 and Aerozine 50 will theoretically yield equivalent performance values. Aerozine 50 (50/50 blend of hydrazine and unsymmetricaldimethlhydrazine) when compared to MMH, has more desirable handling characteristics such as improved stability. In addition, aerozine 50 is less expensieve to produce than MMH. Subsequent vendor contact indicated that performance degradation with the use of A-50 instead of MMH would be negligible and that deliverable specific impulse values of 295 seconds were obtainable. Because of the criticality of propellant storability and handling to the return phase of the mission, the propellants N_2O_4 and Aerozine 50 were selected for use for the earth return vehicle.

A schematic of the modified planetary explorer propulsion system is illustrated in Figure V-23. The weight statement for this propulsion system is presented in parametric form in Tavle V-15. The principal subsystem components consist of two high pressure titanium helium spheres, a pneumatic pressure regulator, four equal volume titanium propellant tanks, ordnance and latching solenoid acquisition valves, check valves, filters, and engine assembly. Ambient helium was chosen as a pressurant over that of nitrogen because of its weight savings. It was felt that with the proper selection of pressurization hardware, helium loss due to leakage and diffusion could be kept at an insignificant level. The 21 cm diameter helium pressurization spheres are located in the attitude control propellant tank bay, immediately in front of the main subsystem equipment bay. Since the pressurization system will be space-stored for a long duration (approximately 700 days) a normally closed explosive valve is installed immediately downstream of the tank outage port to eliminate leakage. Prior to launch from Phobos, the ordnance valve is opened and a solenoid valve is used to isolate propellant

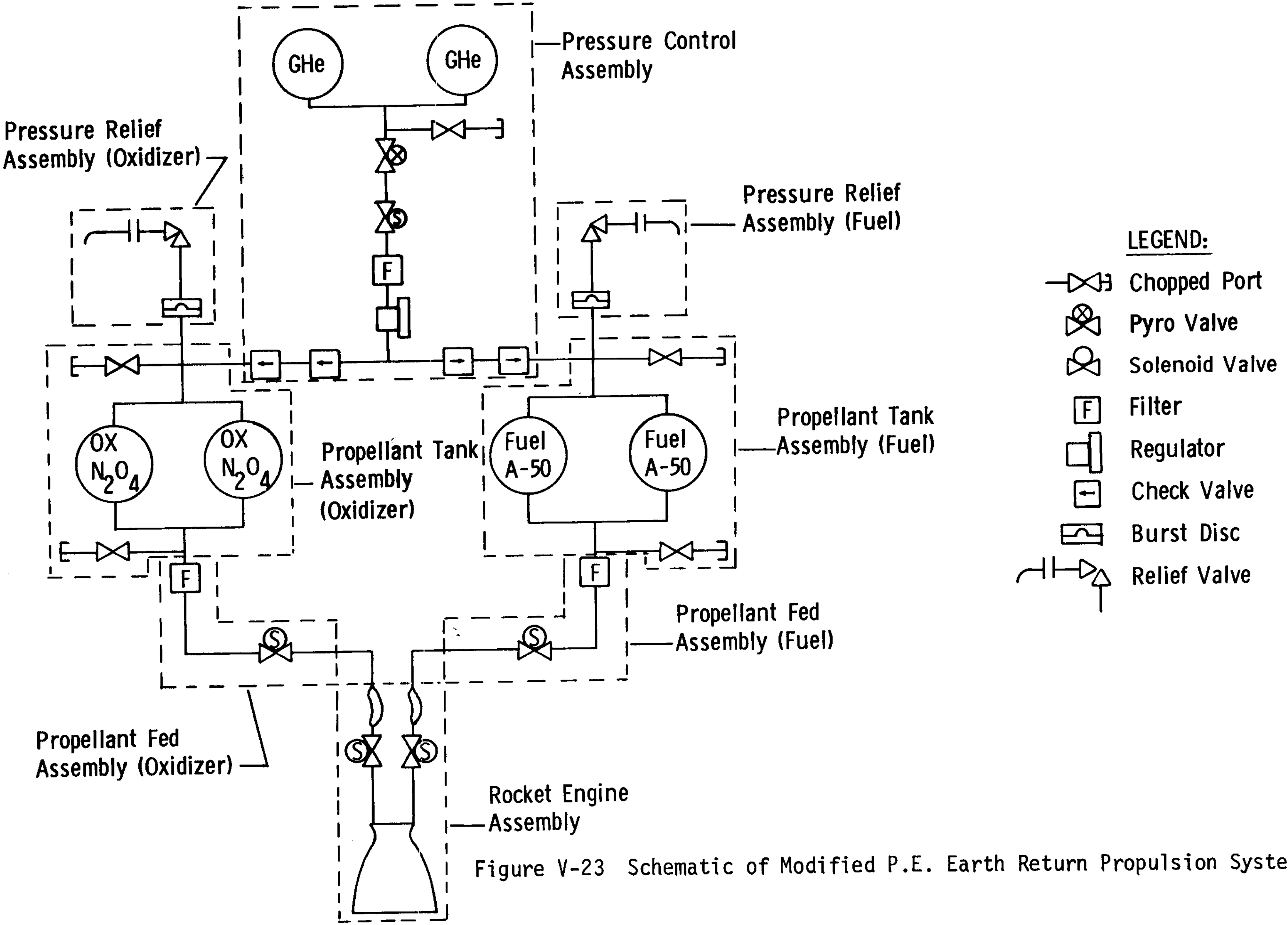
Pressure Control Assembly
GHe
GHe
Pressure Relief Assembly (Oxidizer)
Pressure Relief Assembly (Fuel)
F
OX N_2O_4
OX N_2O_4
Propellant Tank Assembly (Oxidizer)
Fuel A-50
Fuel A-50
Propellant Tank Assembly (Fuel)
F
F
S
S
Propellant Fed Assembly (Fuel)
Propellant Fed Assembly (Oxidizer)
S
S
Rocket Engine Assembly
LEGEND:
Chopped Port
Pyro Valve
Solenoid Valve
F
Filter
Regulator
Check Valve
Burst Disc
Relief Valve

Figure V-23 Schematic of Modified P.E. Earth Return Propulsion System

Table V-15 Modified P.E. Return Vehicle Propulsion System Weight Statement

Item	Modified P.E. Weight		New 3-Axis Weight	
	Kgs	(lbs)	Kgs	(lbs)
Engine assembly (includes lines and fittings)	4.50	(9.8)	5.81	(12.8)
Propellant Supply Assembly				
Oxidizer Side	0.68	(1.5)	0.68	(1.5)
Fuel Side	0.68	(1.5)	0.68	(1.5)
Propellant Tank Assembly				
Oxidizer Side	2.54	(5.6)	2.09	(4.6)
Fuel Side	2.54	(5.6)	2.09	(4.6)
Pressure Relief Assembly				
Oxidizer Side	0.41	(0.9)	0.41	(0.9)
Fuel Side	0.41	(0.9)	0.41	(0.9)
Pressure Assembly	6.18	(13.6)	6.18	(13.6)
Propellant	91.09	(200.4)	91.50	(201.3)
Residual Propellant	2.73	(6.0)	2.73	(6.0)
Pressurant	0.32	(0.7)	0.32	(0.7)
Total Propulsion System Weight	112.05	(246.5)	112.91	(248.4)

and pressurization tanks for the duration of the mission. A pneumatic regulator is used to regulate the 4000 psia helium down to 200 psia propellant tank service pressure. The propellant tank pressure requirement was established to meet the minimum operating supply pressure of the Marquardt R-4D engine. The Marquardt and Thiokol engine nominal engine supply pressures are 180 psia and were used as a basis for the selected system propellant tank operating pressure of 200 psia. Check valves are used for propellant separators. In order to preclude the possibility of a check valve failing closed, a quad-redundant check valve assembly has been installed in each branch of the propellant tank pressurization circuits. The pressurant fill and propellant fill and drain valve assemblies are manually operated with metal seals and caps for positive sealing against leakage. Relief valves are installed on each pressurization line with a burst disc upstream. This arrangement will prevent overpressurization of the propellant tanks in event of regulator failure or tank overpressure for any other reason. The burst disc in series with the relief valve eliminates helium leakage during the Earth return phase of the mission. The four equal volume 36 cm diameter propellant tanks divide the fuel and oxidizer to minimize spacecraft center of gravity migration as propellants are consumed. The tanks are located in a single row at the rear of the spacecraft bus, behind the main subsystem equipment bay. The nominal spin rate for the vehicle is 12 rpm which is sufficient to force the propellant over the tank outage ports and as a result eliminate the requirements for propellant tank acquisition devices. Prior to initiation of the engine start sequence, during the launch phase from Phobos, the vehicle will be spun up with the use of the attitude control thrusters. This will ensure engine propellant supply line filling and proper tank ullaging.

b. Modified P.E. Attitude Control Propulsion - The modified P.E. earth return vehicle attitude control propulsion system design permits two functions:

a) spin rate control,
b) spin vector precession control.

Aside from these functions, available impulse has been allocated for midcourse correction maneuvers in lieu of the primary propulsion system. The attitude control propulsion subsystem is similar to that used on the Planetary Explorer spacecraft. It consists of a unified attitude and spin control monopropellant hydrazine blowdown propulsion system.

The major components of the attitude control propulsion system are: 4 titanium hydrazine propellant tanks, 3 propellant isolation valves, a filter and 2 quad-thruster assemblies. A schematic of the attitude control propulsion subsystem and sketch illustrating propellant tank location are described in Figure V-24. The 4.21 cm diameter titanium propellant tanks are located ahead of the main equipment bay in one row and spaced at equal angles in conjunction with the two primary propulsion pressurant spheres. These tanks are located at the maximum outboard position. This arrangement tends to increase the spacecraft roll-to-pitch moment of inertia ratio while maximizing the centrifugal loading of the propellant. The vehicle spin rate is 12 rpm and is sufficient to force the propellants over the attitude control tank outage ports and as a result, eliminate the requirements for propellant acquisition devices. The two quad-thruster assemblies are mounted on the outside of the spacecraft bus and are diametrically opposed. The dual quad-thruster arrangement differs from that of the P.E. but it is felt that this design will be more flexible and less sensitive on a performance basis, to spacecraft center of gravity offsets. The thrusters apply

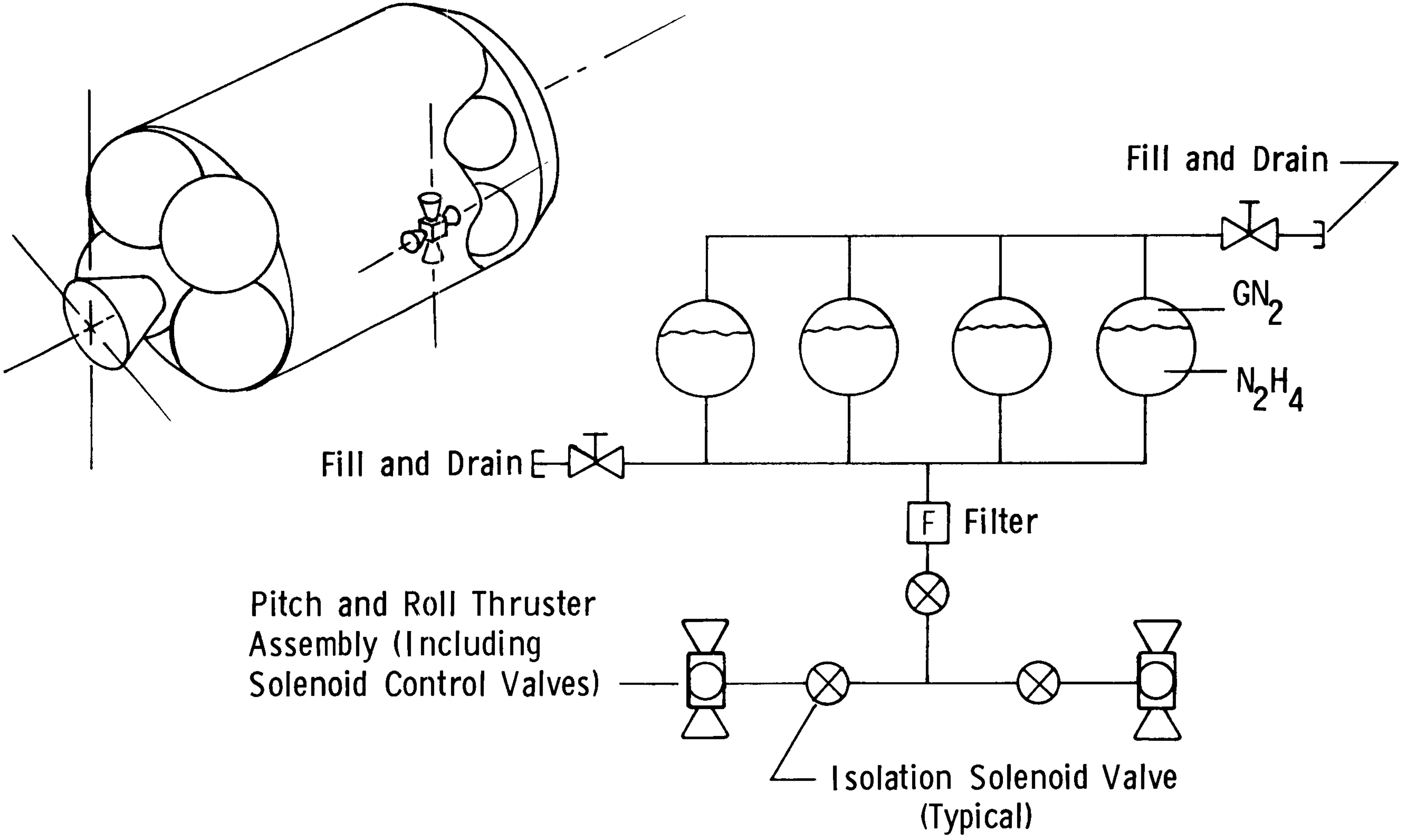
Fill and Drain
GN_2
N_2H_4
Fill and Drain
Filter
F
Pitch and Roll Thruster Assembly (Including Solenoid Control Valves)
Isolation Solenoid Valve (Typical)

Figure V-24 Attitude Control Schematic for Modified P.E. Earth Return Vehicle

spacecraft torques as couples and provide redundant operational modes. A thruster chamber assembly contains Shell 405 Catalyst which is used to initiate decomposition of the hydrazine fuel. Normal engine steady state thrust decays from 5 pounds to 2 pounds as the propellant tank pressure is reduced from an initial pressure of 250 psia through a 3:5 to 1 blowdown operation. (As is on the P.E. design, the blowdown type system is preferred because at little or no weight penalty it minimizes the functional hardware requirements). A pressure transducer which measures thruster nozzle inlet pressure is mounted on each engine assembly to monitor engine performance during flight operation. Maneuvers may be divided into several steps to allow for periodic update of the spacecraft spin-axis attitude. A schematic and associated characteristic of the 5 pound thruster of the type to be used is presented in Figure V-25. A maneuver budget and weight profile for the modified planetary explorer earth return vehicle is presented in Table V-16.

During maneuvers, the precession control thrusters operate in the pulse mode and fire over a 45 degree angle of each spacecraft revolution. The nominal spin rate is 12 rpm resulting in a pulse firing time of 0.625 seconds. A single 90 degree precession maneuver will require 10 pulses per thruster. The precession thrusters may be used for small spacecraft midcourse velocity changes in event of main engine failure.

Listed in Table V-17 is the attitude control system weight statement for the modified P.E. earth return vehicle. The subsystem component weights are based on Planetary Explorer technologies. The propulsion subsystem provides a total impulse of 3380 lb-sec to:

a) precess the vehicle spin vector a total of 1500°;
b) provide a spin capability of 40 rpm;
c) provide for 3 midcourse velocity corrections and an Earth entry deflection maneuver resulting in a ΔV of 25.4 mps.

Parameter	Engine Characteristics
Weight	0.393 kg
Operating Pressure (inlet)	250 to 73.5 psia
Thrust Rating (250 psia)	5.0 lb_f ± 4%
Qualification Life	20,000 cycles
Demonstrated Life	100,000 cycles
Pulse Impulse Bit (250 psia)	0.410 lb-sec
Pulse Impulse Bit (73.5 psia)	0.180 lb-sec
Specific Impulse (250 psia)	220 sec (hot) 145 sec (cold)
Specific Impulse (73.5 psia)	210 sec (hot) 110 sec (cold)

5 lb_f Thrust Monopropellant Hydrazine Rocket Engine Schematic

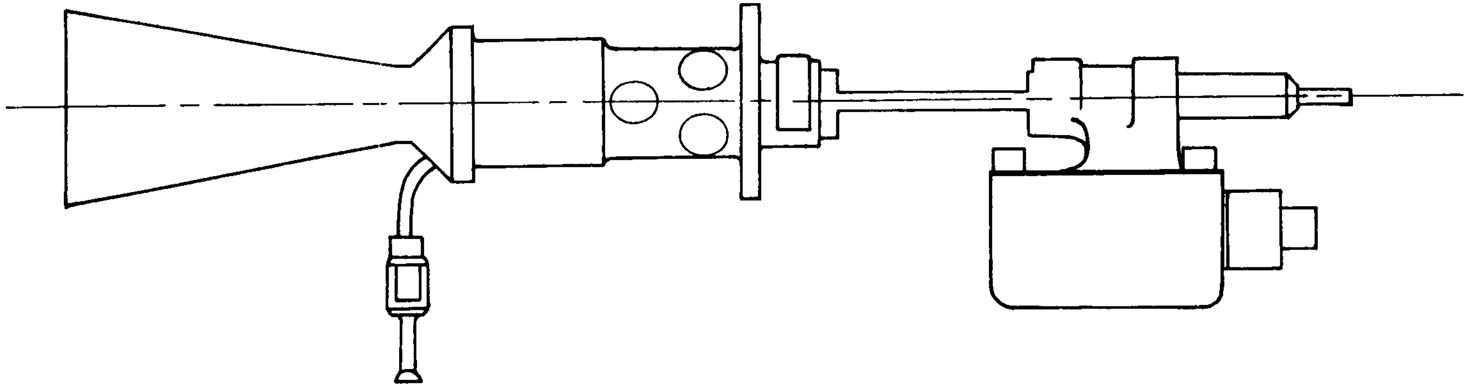

Figure V-25 Modified Planetary Explorer Attitude Control Thruster

Table V-16 Maneuver Budget and Required Propellant Expenditure Weight for Modified Planetary Explorer Earth Return Vehicle

	Primary Propulsion System		Attitude Control Propulsion System		
Maneuver	Velocity Change (m/sec)	Propellant Used (kg)	Spin Vector⁽¹⁾ Precession (deg)	Propellant Used (lb)	Spin Rate (RPM)⁽³⁾
1. Launch from Phobos to loose elliptic orbit about Mars	746	47.3	300	0.48	12
2. Lower periapsis and orbital plane change	110	5.6	300	0.48	
3. Trans-Earth Injection	710	34.5	300	0.48	
4. Midcourse trajectory corrections (2) a. 1st at 10 days b. 2nd at 210 days c. 3rd at 273 days d. deflection maneuver	 60.8 6.3 1.1 15.0	 3.2 5.0⁽²⁾	 180 90 90 90	.57	
5. Trans-Earth vehicle attitude maintenance			40	0.30	
6. Gravity and steering losses plus navigational uncertainties	200	12.7			

(1) Spin vector precession for complete maneuver; from and back to Earth pointing position.

(2) Midcourse trajectory corrections performed with precession attitude control thrusters.

(3) Spin rate capability of 40 rpm alloted for spin maintenance (propellant required = 0.30 lb).

Table V-17 Modified P.E. Attitude Control System Weight

Component	KGS	LBS
Tanks (4)	2.73	6.00
Engines (8)	3.19	7.04
Fill and Drain Valve (2 Assemblies)	0.25	0.56
Isolation Valves (3)	1.35	3.00
Filter	0.19	0.42
Fittings and Tubing	1.15	2.50
Tank and Engine Mounting Structure	3.42	7.30
Instrumentation and Cabling	1.09	2.39
Pressurant	0.19	0.41
Residual Propellant (5%)	0.34	0.74
TOTAL	13.90	30.36
Useable Propellant	6.86	15.1
TOTAL	20.66	45.46

2. Alternate Propulsion Subsystem (3-Axis Stabilized)

The preferred alternate to the baseline earth return spacecraft configuration is a 3-axis stabilized vehicle as described in Section V. The primary propulsion system for this vehicle was similar to that of the baseline spacecraft configuration since the total velocity change requirements, weights and space storability requirements were nearly the same. Maintenance of vehicle 3-axis stabilization is required throughout the return leg of the mission.

a. New 3-Axis Primary Propulsion - The primary propulsion system for the new 3-axis earth return vehicle is essentially the same as that of the modified P.E. with the following exceptions. The new 3-axis vehicle requires two propellant tanks and one pressurant sphere. In addition, thrust chamber gimballing will be required for accurate thrust vector control. A schematic of the propulsion system is given in Figure V-26.

The two equal volume propellant tanks and pressurant sphere are nested with the subsystem equipment in the hexagon "wrap around" spacecraft bus. The titanium propellant and pressurant tanks are 43.5 inch and 24.4 inch in diameter respectively. The two tank configuration will create a small c.g. migration during propellant outflow which is within the engine gimbal capability. Since there are problems associated with propellant orientation and control during zero g a propellant tank acquisition device is required. A Fruhof low gravity type surface tension device is preferred for the mission. The inherent lightweight, reliability and temperature insensitivity characteristics make this system preferable to acquisition devices such as polymeric and metallic bladders and diaphragms, bellows, dielectrophoretic systems, main engine start tanks and external propellant settling systems.

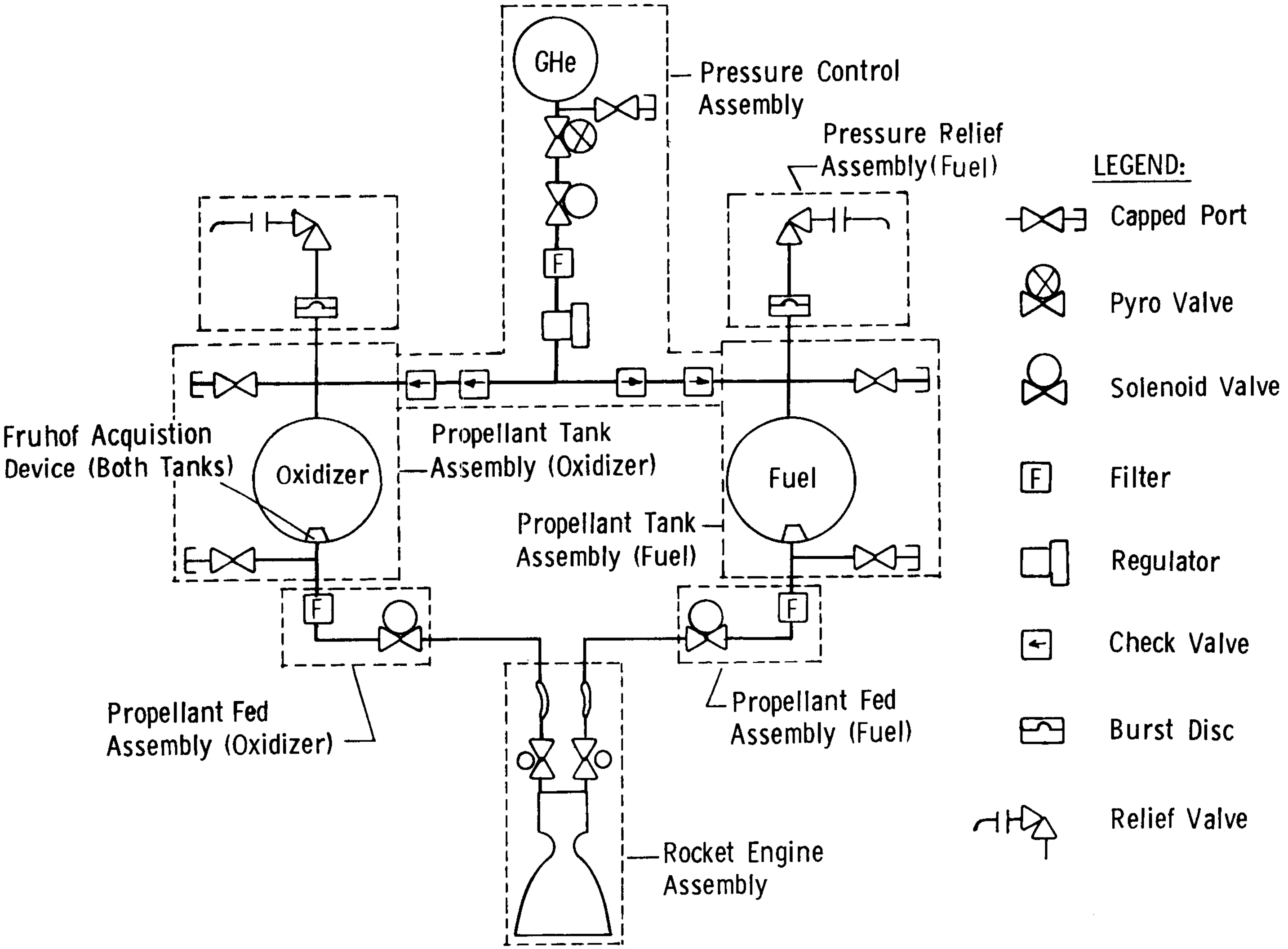
GHe
Pressure Control Assembly
Pressure Relief Assembly(Fuel)
LEGEND:
Capped Port
Pyro Valve
Solenoid Valve
F
Filter
Regulator
Check Valve
Burst Disc
Relief Valve
Fruhof Acquistion Device (Both Tanks)
Oxidizer
Propellant Tank Assembly (Oxidizer)
Propellant Tank Assembly (Fuel)
Fuel
Propellant Fed Assembly (Oxidizer)
Propellant Fed Assembly (Fuel)
Rocket Engine Assembly

Figure V-26 Schematic of New Three-Axis Vehicle Propulsion System

During firings, three-axis attitude control is accomplished by two-axis gimballing of the engine with third axis (roll) provided by the roll attitude control thruster. The gimbal control system positions the engine through the use of two torque actuators aligned with the pitch and yaw directions. The recommended gimballing arrangement is similar to that on the Phobos orbiter engine and is presented in Figure V-27. This engine rotation allows the thrust vector control system to point the thrust vector through the spacecraft center of mass. A weight statement for the primary propulsion system for the new 3-axis earth return vehicle is presented in Table V-15. A total of 91.4 kilograms of propellant has been allocated for expenditure and an additional 3% for residuals. This appropriation of residual propellant will be sufficient to insure complete wetting of the tank exit ports for the entire mission.

b. New 3-Axis Attitude Control Propulsion -The attitude control propulsion system for the new 3-axis earth return vehicle is a dual redundant cold gas system of the type used on the Viking Orbiter. The gas-jet attitude control system will provide torques required to stabilize the spacecraft during the return transit phase of the mission from liftoff from Phobos to injection of the surface sample canister into the Earth's atmosphere. The basic requirements of the attitude control propulsion system are:

a) maintain spacecraft orientation with respect to the Sun and the star Canopus during the entire transit;

b) orient the spacecraft to the desired thrust attitudes for trajectory corrections;

c) orient the spacecraft to provide proper attitude of sample canister prior to Earth atmospheric injection.

The gas-jet attitude control system is a cold gas system using nitrogen as a propellant. A schematic of the assembly is presented in Figure V-28. The system consists of a pair of nitrogen

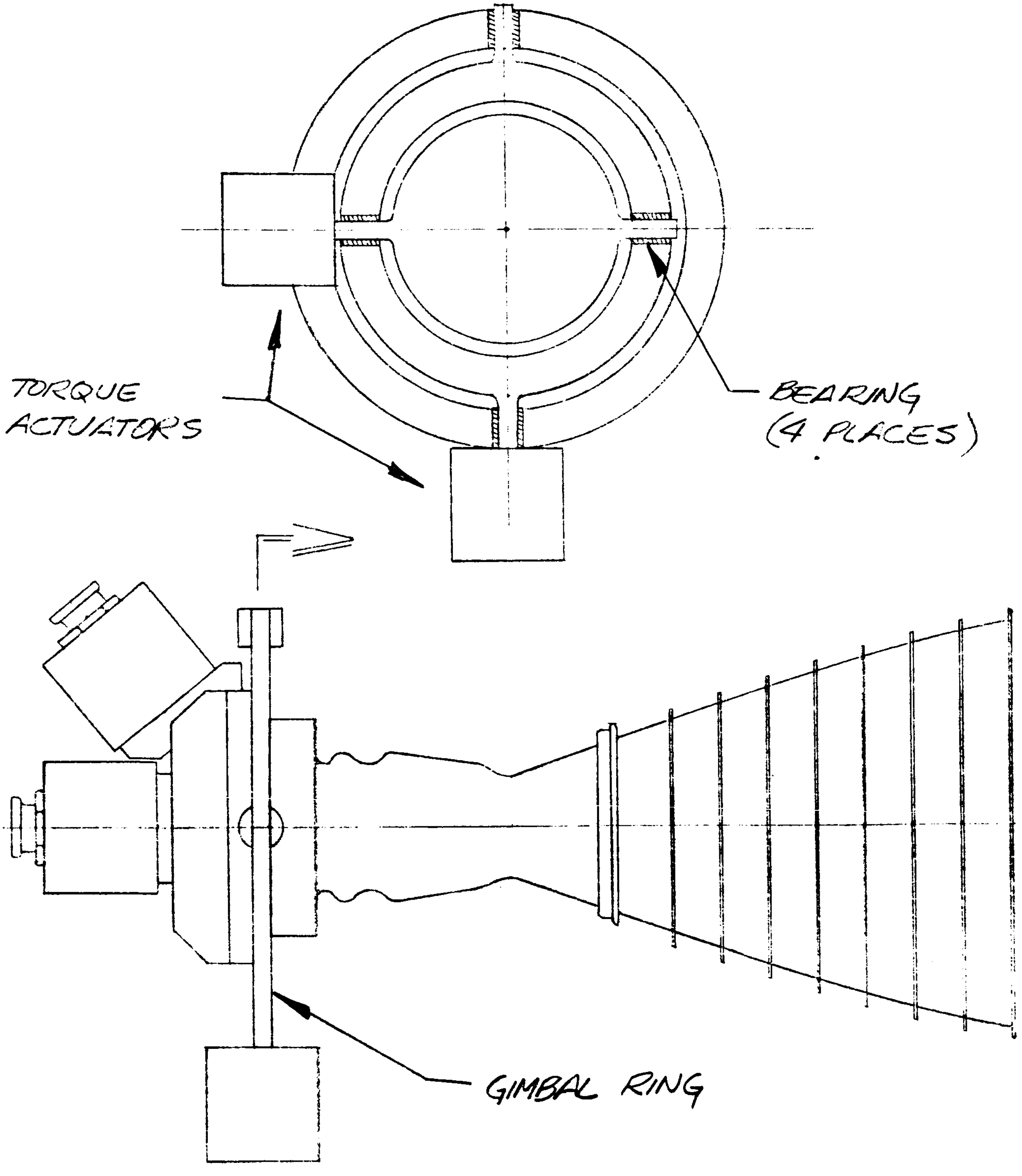
TORQUE
ACTUATORS
BEARING
(4 PLACES)
GIMBAL RING

Figure V-27 Engine and Gimbal Mounting Arrangement

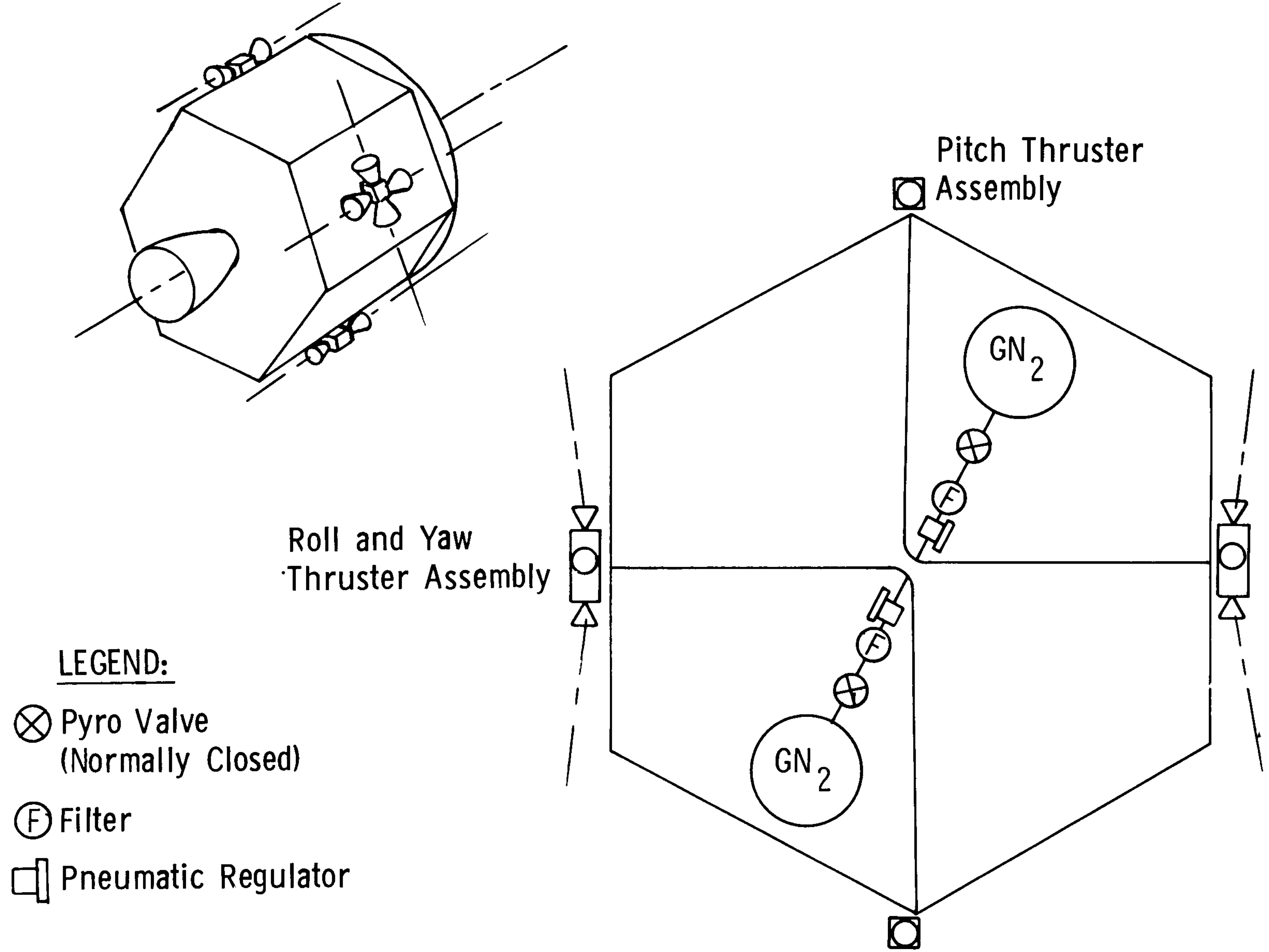
Pitch Thruster Assembly
GN$_2$
GN$_2$
F
F
Roll and Yaw Thruster Assembly
LEGEND:
⊗ Pyro Valve (Normally Closed)
Ⓕ Filter
Pneumatic Regulator

Figure V-28 New Three-Axis Attitude Control Propulsion Schematic

supply assemblies, and twelve solenoid valve operated gas jets interconnected with tubing. A supply assembly consists of a spherical nitrogen tank with an integral fill valve, pyro-valve, pressure regulator and pressure and temperature transducer instrumentation. Since the propulsion subsystem is inactive until the return leg of the mission, a normally closed explosive valve is provided immediately downstream of the nitrogen tank outage port to eliminate leakage until the system is activated. This is opened and the system activated just prior to launch from Phobos. The nitrogen supply tanks are initially charged to a nominal pressure of 4000 psia. Pressure to the gas jets is controlled to 15 psia by a pneumatic regulator. The quad-roll/yaw and pitch thruster assemblies are mounted on the outside of the spacecraft bus as illustrated in Figure V-28. Each of the body mounted .07 pound thrust jets are canted 7-1/2 degrees to avoid interference effects with the spacecraft bus. Listed in Table V-18 is the attitude control system weight statement for the new 3-axis earth return vehicle. The attitude control and corresponding nitrogen requirements for the new 3-axis vehicle are tabulated in Table V-19. The nitrogen attitude control gas tank will carry 3.09 kilograms of gas (total) of which 1.61 kilograms will be required for normal dual mode operation.

F. TELECOMMUNICATIONS

The communications links required between the spacecraft and Earth for the sample return mission will vary depending upon the mission phase. The phases are: interplanetary cruise, "landed" operation from the satellite, and the Earth return phase. For all of the phases, the vehicle must receive and decode uplink commands from Earth. These requirements are summarized in Table V-20.

Table V-18 New Three-Axis Earth Return Attitude Control System Weight

ITEM (Quantity)	KGS	LBS
Tank (2) Ti6A14V	4.91	10.80
Nitrogen	3.08	6.79
Regulator (2)	1.09	2.40
Squib Valves (2)	0.18	0.40
Filter (2)	0.91	2.00
Fill Valve (2)	0.18	0.40
Thrusters (12)	1.64	3.60
Lines, Brackets, Clamps, & Fittings	2.04	4.50
TOTAL	14.04	30.89

Table V-19 New Three-Axis Attitude Control Gas Requirements

	FULL GAS SYSTEM	
DISCRETE EVENTS	KGS	LBS
Acquisitions	0.061	0.135
Roll Searches	0.025	0.056
Roll Override	0.041	0.090
Commanded Turns	0.566	1.245
Motor Burns	0.165	0.364
CRUISE		
Limit Cycling		
Transit (307 Days)	0.178	0.392
Orbital (10 Days)	0.005	0.010
Sun Occultations	0.014	0.030
Leakage	0.548	1.205
TOTAL	1.603	3.527

RCS Sized for Three Times Half Gas System Requirements
6.790 Lb (3.086 KGS) GN_2

Table V-20 Required Communication Links

Interplanetary Cruise	Uplink Commands From Earth
	Low Data Rate Telemetry and Command Verification to Earth & Doppler Tracking
	Two Way Turn Around Ranging From Earth
"Landed" From Satellite	Uplink Commands From Earth
	Medium Data Rate Telemetry and Command Verification Direct to Earth (Baseline Landed Orbiter Configuration)
	Low Data Rate Telemetry Direct to Earth (Alternate Round Trip Control Module / Lander)
Earth Return	Uplink Commands From Earth
	Minimum Signal to Earth to Provide Doppler Tracking and Low Data Rate Telemetry

During interplanetary cruise, a signal must be transmitted back to Earth which is phase coherent with the received signal to provide two-way doppler tracking information. Low data rate housekeeping telemetry information and two-way pseudo-noise modulated ranging information is also transmitted during this phase.

For "landed" operation from the satellite, telemetry information is transmitted to Earth at 4 kbps for the baseline landed orbiter configuration or at a nominal 250 bps for the alternate round trip control module/lander configuration. The data rate for the separable lander can be increased to a maximum of 500 bps by combining engineering and science data on a single subcarrier instead of dividing these data into two subcarriers as is done on the Viking '75 Lander. The difference in data rate capability between the two configurations is due primarily to the smaller antenna aperture used for the round trip control module/lander configuration. For both configurations, transmission will be direct to Earth at S-band. There will not be a relay link since there will not be an additional orbiter. The baseline landed orbiter communications subsystem will consist of the Mariner class S-band transponder with redundant 20 watt output travelling wave tube amplifiers (TWTAs), an articulated high gain 58 inch diameter parabolic antenna and a low gain cavity backed cross slot antenna for command reception. Transmission time will be two hours per twenty four hours. Nominal ground acquisition time is considered to be approximately 15 minutes, leaving 1.75 hours per 24 hours for actual data transmission of 4 kbps. This amounts to a total data volume of 25.2 megabits transmitted to Earth per 24 hour period.

Video transmission to Earth is required to aid the navigation process prior to and during rendezvous.

The required data volume per picture is shown in Table V-21 for the Viking Orbiter type television system. The data volume per picture is seen to be over 5 megabits. In the alternate mission mode in which the round trip control module is used, providing a maximum data transmission capability to Earth of 500 bps, a period of 2.9 hours would be required for the transmission of one picture. It therefore becomes necessary to consider a form of pre-modulation data compression to reduce the data volume prior to transmission.

By the use of a modified delta modulation technique the total data volume is reduced considerably by the removal of a large amount of redundant data prior to encoding. A compression ratio of about 3 is shown in Table V-22, resulting in a total data volume of 1.75 megabits per picture. At the 500 bps transmission rate, slightly less than one hour would be required to transmit one picture. This period of time is acceptable to the navigation determination process.

The following will discuss the requirements and the implementation of communications subsystem for the baseline sample return vehicle. Link analyses show that the required minimum effective radiated power (ERP) to provide doppler tracking of the vehicle from the ground is 25.3 dbw. This amount or ERP provides sufficient signal power at the ground DSN receiver to allow locking of the receiver phase lock loop and to provide the required system margin. The effective radiated power is the product of the transmitted power and the antenna gain or the sum of these two quantities when expressed in dB (ERP = P_T(db) + G_T(db). There are a number of combinations of transmitter power output and antenna gain meeting the requirement of 25.3 dbw. Some possible combinations are shown in Table V-23. Telemetry design control tables for two of the possible combinations are

Table V-21 Video Transmission Capability

Picture - 700 lines, 832 pixels/line, 9 bits/pixel = 5.25×10^6 bits/picture

Readout rate - 126 KBPS

Readout time - $5.25 \times 10^6 / 126 \times 10^3$ = 42 sec/picture

Recording capability - VLC type recorder - 40×10^6 bits storage capacity
- 8 picture storage capacity

Maximum data transmission rate to Earth - 500 BPS (20 W transmitter, 30" dish)

Time for picture transmission (without data compression) -
5.25×10^6 bits/picture/500 BPS = 2.9 hours

Table V-22 Video Transmission Capability.

Use Data Compression to Reduce Data Volume Per Picture Prior to Transmission

Use 3 Bit Delta Modulation to Reduce Redundancy in Transmitted Data

Data Volume/Picture (3 bits/pixel) - 1. 75 x 10^6 bits

Time for Picture Transmission - 1. 75 x 10^6 bits/picture/500 BPS = 0. 97 hrs

Table V-23 Antenna/Transmitter Power Trade-Offs

Required Minimum ERP For Doppler Tracking = 25.3 dBW (Max Range)

COMBINATIONS MEETING ERP REQUIREMENTS

Transmitter Power Output (Watts)	DBW	Antenna Gain (DB)	Antenna HPBW
1	0	25.3	9°
2	3	22.3	12.5°
3	4.78	20.5	15.5°
* 4	6	19.3	18°
5	7	18.3	20°
6	7.78	17.5	22°
7	8.45	16.9	24°
8	9	16.3	25°
9	9.54	15.8	27°
10	10	15.3	29.5°
15	11.76	13.54	36°
20	13	12.3	44°

* Baseline Return Vehicle Design

shown in Table V-24 and V-25. The combination shown with the asterisk, transmitter power output of 4 watts (6dbw) and an antenna gain of 19.3 db was chosen for the baseline return vehicle communication subsystem point design. The reasons for choosing this combination are the following: the antenna gain of 19.3 db is obtainable from a parabolic reflector 20 inches in diameter which is compatible with the vehicle size and shape, for the de-spun antenna option. This gain represents a practical maximum for the size and weight constraints considered here, the resulting antenna half power beamwidth of 18 degrees is as narrow as desired for look angle considerations, and the transmitter power output of 4 watts is consistent with the return vehicle primary power capability.

A plot of required transmitter power output as a function of antenna half power beamwidth is shown in Figure V-29.

In addition to providing a signal to Earth for doppler tracking, downlink telemetry from the return vehicle to Earth can be sent at a data rate of 40 bits per second. The telemetry design control table for this link is shown in Table V-26.

The return vehicle S-band communications subsystem will be a small, lightweight, all solid state package. The block diagram of this configuration is shown in Figure V-30. There will not be any new development required for this configuration as it is well within the present state-of-the-art. The subsystem is similar to that proposed for the Venus Pioneer program (formerly Planetary Explorer.)

A weight and power breakdown for the P.E. type return vehicle communications subsystem elements is given in Table V-27. Redundant elements include the S-band receiver command detector, mod exciter and S-band power amplifier. The total communications subsystem weight is slightly over 23 pounds and the required primary

Table V-24 Telemetry Design Control

NO.	PARAMETER	NOMINAL VALUE	TOLERANCE		
			FAVORABLE	ADVERSE	
1	TOTAL TRANSMITTER POWER (DBM)	+36 dBM	0.75	0.8	4 Watts
2	TRANSMITTING CIRCUIT LOSS (DB)	-0.4 dB	0.05	0.05	
3	TRANSMITTING ANTENNA GAIN (DB)	+22.3 dB	0.32	0.32	30" Dish
4	TRANSMITTING ANTENNA POINTING LOSS (DB)	-3.0 dB	+3.0	0.0	
5	SPACE LOSS (DB) F = 2297 MHz, R = 350×10^6 KM	-270.5 dB	0.00	0.00	
6	POLARIZATION LOSS (DB)	-0.05 dB	0.02	0.02	
7	RECEIVING ANTENNA GAIN (DB)	+61.4 dB	0.4	0.4	
8	RECEIVING ANTENNA POINTING LOSS (DB)	0.00	0.00	0.00	
9	RECEIVING CIRCUIT LOSS (DB)	0.00	0.00	0.00	
10	NET CIRCUIT LOSS (DB) (2+3+4+5+6+7+8+9)	-190.23dB	3.79	0.79	
11	TOTAL RECEIVED POWER P(T) (DBM) (1+10)	-154.23dBM	4.54	1.59	
12	RECEIVER NOISE SPECTRAL DENSITY (DBM/HZ) ELEV = 25 DEG. ZENITH NOISE TEMP (DEG K) 28° ZENITH NOISE SPEC DEN (DBM/HZ)	-183.2dBM	0.15	0.42	
13	CARRIER POWER/TOTAL POWER (DB)	-3.14 dB	1.0	1.0	$\theta = 0.8$ R
14	RECEIVED CARRIER POWER (DBM) (11+13) $2BL_O$.	-157.34dBM	5.54	2.99	45.8°
15	CARRIER THRESHOLD NOISE BW (DB.HZ) = 12 HZ	+10.8	0.96	0.00	±10%
	CARRIER TRACKING (ONE-WAY)				
16	THRESHOLD SNR IN $2B_{LO}$ (DB)	+ 8 dB	----	----	
17	THRESHOLD CARRIER POWER (DBM) (12+15+16)	-164.4dBM	1.11	0.42	
18	PERFORMANCE MARGIN (DB) (14-17)	+7.0 dB	6.65	-3.0	
	DATA CHANNEL				
19	DATA POWER/TOTAL POWER (DB)	-2.89 dB	0.3	0.3	
20	WAVEFORM DISTORTION LOSS (DB)	-0.1 dB	0.1	0.1	
21	LOSS THROUGH RADIO SYSTEM (DB) UPLINK SNR IN $2B_{LO}$ (DB) 1-WAY DOWNLINK SNR IN $2B_{LO}$ (DB)	-0.1 dB	0.1	0.1	
22	SUBCARRIER DEMOD LOSS (DB)	-0.1 dB	0.1	0.1	
23	BIT SYNC/DETECTION LOSS (DB)	-0.1 dB	0.1	0.1	
24	RECEIVED DATA POWER (DBM) (11+19+20+21+22+23)	-157.5dBM	5.24	2.29	
25	THRESHOLD DATA POWER (DBM) (12+25a+25b)	-161.75dBM	0.15	0.42	
a	THRESHOLD PT/N (DB) (WER = 10^{-2})	+3.0 dB	0.0	0.00	Block Coded
b	BIT RATE (DB.BPS) 70 BPS	+18.45 dB	0.0	0.00	
26	PERFORMANCE MARGIN (DB) (24-25)	+4.25 dB	5.39	-2.71	
	DATA CHANNEL				
27	DATA POWER/TOTAL POWER (DB)				
28	WAVEFORM DISTORTION LOSS (DB)				
29	LOSS THROUGH RADIO SYSTEM (DB) UPLINK SNR IN $2B_{LO}$ (DB) 1-WAY DOWNLINK SNR IN $2B_{LO}$ (DB)				
30	SUBCARRIER DEMODULATION LOSS (DB)				
31	BIT SYNC/DETECTION LOSS (DB)				
32	RECEIVED DATA POWER (DBM) (11+27+28+29+30+31)				
33	THRESHOLD DATA POWER (DBM) (12+33a+33b)				
a	THRESHOLD PT/N (DB) (BER =				
b	BIT RATE (DB.BPS)				
34	PERFORMANCE MARGIN (DB) (32-33)				

Table V-25 Telemetry Design Control

NO.	PARAMETER	NOMINAL VALUE	TOLERANCE		NOTES
			FAVORABLE	ADVERSE	
1	TOTAL TRANSMITTER POWER (DBM)	+40 dBM	0.75	0.8	10 Watts
2	TRANSMITTING CIRCUIT LOSS (DB)	-0.4 dB	0.05	0.05	
3	TRANSMITTING ANTENNA GAIN (DB)	+15.3 dB	0.32	0.32	30° HPBW
4	TRANSMITTING ANTENNA POINTING LOSS (DB)	-3.0 dB	3.0	0.0	13" Diameter Parabola
5	SPACE LOSS (DB) F = 2297 MHz, R = 350 x 10^6 KM	-270.5 dB	0.0	0.0	
6	POLARIZATION LOSS (DB)	-0.3 dB	0.02	0.02	
7	RECEIVING ANTENNA GAIN (DB)	+61.4 dB	0.4	0.4	
8	RECEIVING ANTENNA POINTING LOSS (DB)	0.00	0.00	0.00	
9	RECEIVING CIRCUIT LOSS (DB)	0.00	0.00	0.00	
10	NET CIRCUIT LOSS (DB) (2+3+4+5+6+7+8+9)	-197.5dB	3.79	0.79	
11	TOTAL RECEIVED POWER P(T) (DBM) (1+10)	-157.5dBM	4.54	1.59	
12	RECEIVER NOISE SPECTRAL DENSITY (DBM/HZ) ELEV = 25 DEG 28°K $\pm^{4°}_{3°}$ ZENITH NOISE TEMP (DEG K) ZENITH NOISE SPEC DEN (DBM/HZ)	-183.2dBM	0.15	0.42	
13	CARRIER POWER/TOTAL POWER (DB)	-3.14 dB	1.0	1.0	θ = 0.8 R (45.8°)
14	RECEIVED CARRIER POWER (DBM) (11+13) 2 BL_O	-160.6dBM	5.54	2.99	
15	CARRIER THRESHOLD NOISE BW (DB.HZ) 12 HZ	+10.8 dB	0.96	0.00	±10%
	CARRIER TRACKING (ONE-WAY)				
16	THRESHOLD SNR IN $2B_{LO}$ (DB)	+ 8 dB	----	----	
17	THRESHOLD CARRIER POWER (DBM) (12+15+16)	-164.4dBM	1.11	0.42	
18	PERFORMANCE MARGIN (DB) (14-17)	+3.8 dB	6.65	-3.0	
	DATA CHANNEL				
19	DATA POWER/TOTAL POWER (DB)	-2.89 dB	0.3	0.3	
20	WAVEFORM DISTORTION LOSS (DB)	-0.1 dB	0.1	0.1	
21	LOSS THROUGH RADIO SYSTEM (DB) UPLINK SNR IN $2B_{LO}$ (DB) 1-WAY DOWNLINK SNR IN $2B_{LO}$ (DB)	-0.1 dB	0.1	0.1	
22	SUBCARRIER DEMOD LOSS (DB)	-0.1 dB	0.1	0.1	
23	BIT SYNC/DETECTION LOSS (DB)	-0.1 dB	0.1	0.1	
24	RECEIVED DATA POWER (DBM) (11+19+20+21+22+23)	-160.8dBM	5.24	2.29	
25	THRESHOLD DATA POWER (DBM) (12+25a+25b)	-164.2dBM	0.15	0.42	
a	THRESHOLD PT/N (DB) ((WER = 10^{-2})	+3.0 dB	0.0	0.00	Block Coded
b	BIT RATE (DB.BPS) 40 BPS	+16 dB	0.0	0.00	
26	PERFORMANCE MARGIN (DB) (24-25)	+3.4 dB	5.39	-2.71	
	DATA CHANNEL				
27	DATA POWER/TOTAL POWER (DB)				
28	WAVEFORM DISTORTION LOSS (DB)				
29	LOSS THROUGH RADIO SYSTEM (DB) UPLINK SNR IN $2B_{LO}$ (DB) 1-WAY DOWNLINK SNR IN $2B_{LO}$ (DB)				
30	SUBCARRIER DEMODULATION LOSS (DB)				
31	BIT SYNC/DETECTION LOSS (DB)				
32	RECEIVED DATA POWER (DBM) (11+27+28+29+30+31)				
33	THRESHOLD DATA POWER (DBM) (12+33a+33b)				
a	THRESHOLD PT/N (DB) (BER =				
b	BIT RATE (DB.BPS)				
34	PERFORMANCE MARGIN (DB) (32-33)				

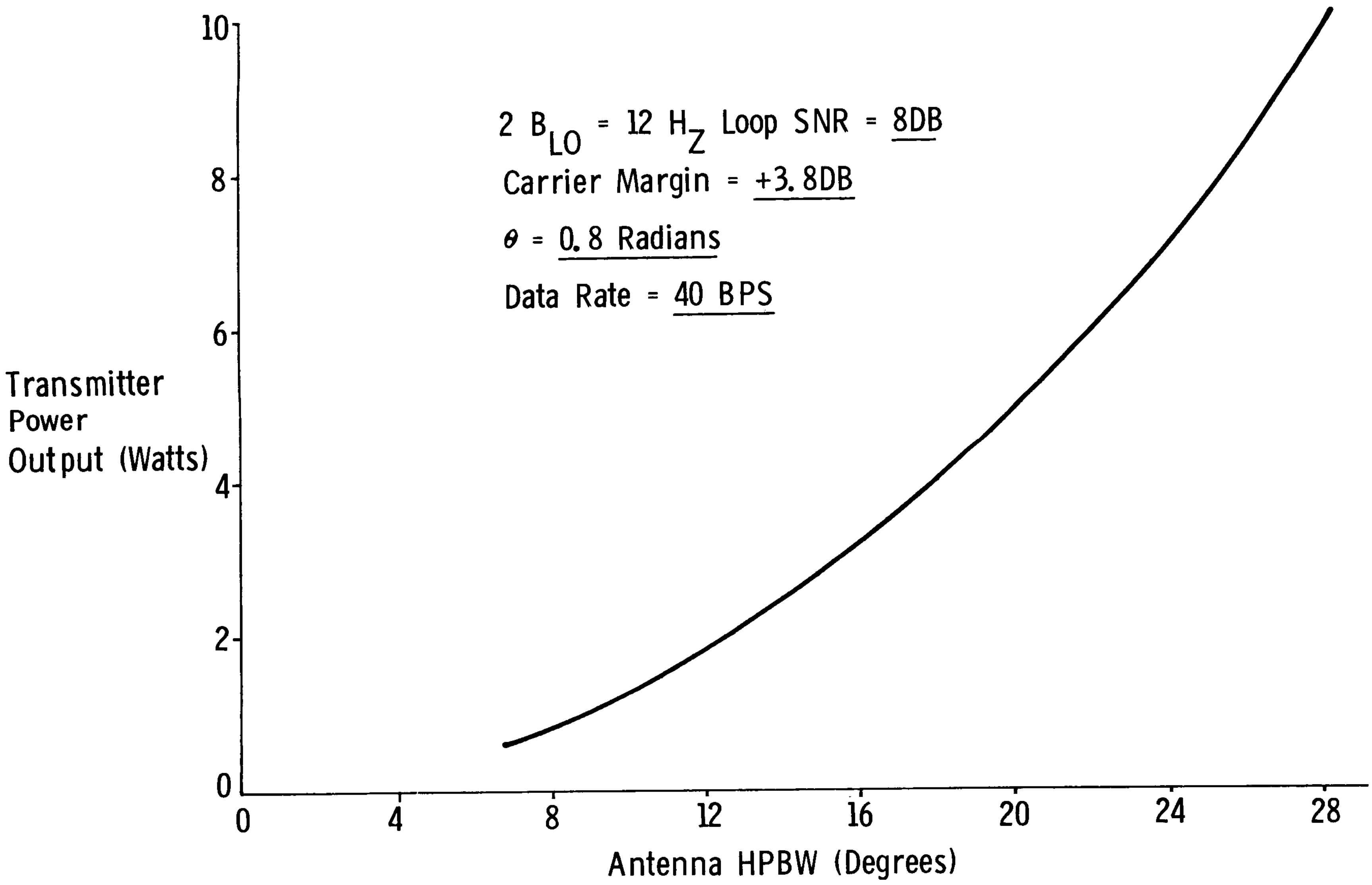

Figure V-29 Return Vehicle Required Transmitter Power Output vs Antenna Half Power Beamwidth

Table V-26 Telemetry Design Control

NO.	PARAMETER	NOMINAL VALUE	TOLERANCE		
			FAVORABLE	ADVERSE	
1	TOTAL TRANSMITTER POWER (DBM)	+36 dBM	0.75	0.8	4 Watts
2	TRANSMITTING CIRCUIT LOSS (DB)	-0.4 dB	0.05	0.05	
3	TRANSMITTING ANTENNA GAIN (DB)	+19.3 dB	0.32	0.32	18° HPBW
4	TRANSMITTING ANTENNA POINTING LOSS (DB)	-3.0 dB	3.0	0.0	20" Dish
5	SPACE LOSS (DB) F = 2297 MHz, R = 350 x 10^6 KM	-270.5 dB	0.00	0.00	
6	POLARIZATION LOSS (DB)	-0.3 dB	0.02	0.02	
7	RECEIVING ANTENNA GAIN (DB)	+61.4 dB	0.4	0.4	
8	RECEIVING ANTENNA POINTING LOSS (DB)	0.00	0.00	0.00	
9	RECEIVING CIRCUIT LOSS (DB)	0.00	0.00	0.00	
10	NET CIRCUIT LOSS (DB) (2+3+4+5+6+7+8+9)	-193.5 dB	3.79	0.79	
11	TOTAL RECEIVED POWER P(T) (DBM) (1+10)	-157.5dBM	4.54	1.59	
12	RECEIVER NOISE SPECTRAL DENSITY (DBM/HZ) ELEV = 25 DEG ZENITH NOISE TEMP (DEG K) ZENITH NOISE SPEC DEN (DBM/HZ)	-183.2dBM	0.15	0.42	
13	CARRIER POWER/TOTAL POWER (DB)	-3.14 dB	1.0	1.0	Θ = 0.8 R
14	RECEIVED CARRIER POWER (DBM) (11+13) $2BL_O$ =	-160.6dBM	5.54	2.99	(45.8°)
15	CARRIER THRESHOLD NOISE BW (DB.HZ) 12 HZ	+10.8 dB	0.96	0.00	
	CARRIER TRACKING (ONE-WAY)				
16	THRESHOLD SNR IN $2B_{LO}$ (DB)	+ 8 dB	----	----	
17	THRESHOLD CARRIER POWER (DBM) (12+15+16)	-164.4dBM	1.11	0.42	
18	PERFORMANCE MARGIN (DB) (14-17)	+3.8 dB	6.65	-3.0	
	DATA CHANNEL				
19	DATA POWER/TOTAL POWER (DB)	-2.89 dB	0.3	0.3	
20	WAVEFORM DISTORTION LOSS (DB)	-0.1 dB	0.1	0.1	
21	LOSS THROUGH RADIO SYSTEM (DB) UPLINK SNR IN $2B_{LO}$ (DB) 1-WAY DOWNLINK SNR IN $2B_{LO}$ (DB)	-0.1 dB	0.1	0.1	
22	SUBCARRIER DEMOD LOSS (DB)	-0.1 dB	0.1	0.1	
23	BIT SYNC/DETECTION LOSS (DB)	-0.1 dB	0.1	0.1	
24	RECEIVED DATA POWER (DBM) (11+19+20+21+22+23)	-160.8dBM	5.24	2.29	
25	THRESHOLD DATA POWER (DBM) (12+25a+25b)	-164.2dBM	0.15	0.42	
a	THRESHOLD PT/N (DB) (WER = 10^{-2})	+3.0 dB	0.0	0.00	Block Coded
b	BIT RATE (DB.BPS) 40 BPS	+16 dB	0.0	0.00	
26	PERFORMANCE MARGIN (DB) (24-25)	+3.4 dB	5.39	-2.71	
	DATA CHANNEL				
27	DATA POWER/TOTAL POWER (DB)				
28	WAVEFORM DISTORTION LOSS (DB)				
29	LOSS THROUGH RADIO SYSTEM (DB) UPLINK SNR IN $2B_{LO}$ (DB) 1-WAY DOWNLINK SNR IN $2B_{LO}$ (DB)				
30	SUBCARRIER DEMODULATION LOSS (DB)				
31	BIT SYNC/DETECTION LOSS (DB)				
32	RECEIVED DATA POWER (DBM) (11+27+28+29+30+31)				
33	THRESHOLD DATA POWER (DBM) (12+33a+33b)				
a	THRESHOLD PT/N (DB) (BER =				
b	BIT RATE (DB.BPS)				
34	PERFORMANCE MARGIN (DB) (32-33)				

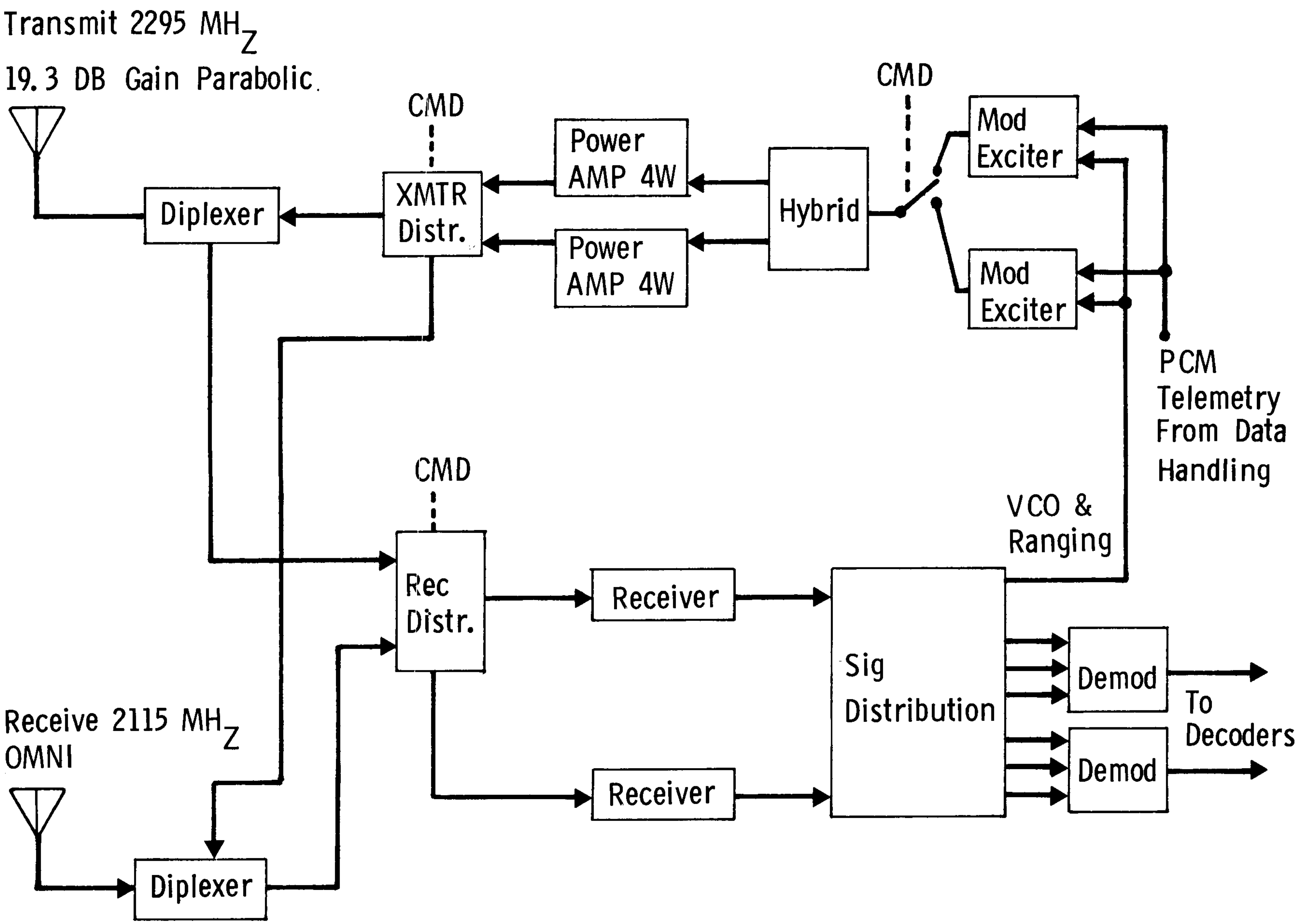
Transmit 2295 MHZ
19.3 DB Gain Parabolic
CMD
Diplexer
XMTR Distr.
Power AMP 4W
Power AMP 4W
Hybrid
CMD
Mod Exciter
Mod Exciter
PCM Telemetry From Data Handling
VCO & Ranging
CMD
Rec Distr.
Receiver
Receiver
Sig Distribution
Demod
Demod
To Decoders
Receive 2115 MHZ
OMNI
Diplexer

Figure V-30 Return Vehicle S-Band Communication Subsystem

Table V-27 P.E. Type Return Vehicle Communications Subsystem

ELEMENT	NO.	WT (lbs)	TOTAL WT (lbs)	PRIMARY POWER (Watts)
S-Band Receiver	2	2 (ea)	4	2
Command Detector	2	2 (ea)	2	1.7
MOD / Exciter	2	1.6 (ea)	3.2	2.3
S-Band Power AMP & Filter Assy (4 W Output)	2	2 (ea)	4	13
* S-Band Parabolic Antenna	1	5	5	
Diplexers	3	0.5 (ea)	1.5	0.2
Switches SPDT	1	0.2	0.2	
Transfer Switches	4	0.225	0.9	
S-Band Low Gain Antenna	1	0.6	0.6	
Telemetry	1	2	2	2.0
			23.4 lbs	21.2 Watts

* Electronically Despun Antenna Weight = 7 lbs

power slightly over 21 watts. If the electronically despun antenna option is employed, the total subsystem wieght increases to 25 pounds since the despun antenna will weigh 7 pounds vs 5 pounds for the parabolic dish.

A conceptual drawing of the electronically despun antenna is shown in Figure V-31. Operation with a despun antenna would be required if the spin axis of the vehicle were perpendicular to the plane of the ecliptic.

The electronically despun antenna will consist of 24 bifilar helical elements located 15 degrees apart on a 14 inch diameter cylinder 6 inches high. Each bifilar helix is approximately 15 inches long by 1.7 inches in diameter and oriented normal to the cylinder (normal to vehicle spin axis). The despun beam will be normal to the spin axis and directed toward Earth using the sun pulse to give directional information. The antenna will have the following characteristics:

Gain	+19 dbi
Gain Ripple	2.5 db
HPBW	17° x 17°
Element Length	15 inches (bifilar helices)
Total Array Diameter	44 inches
Height	6 inches
Weight	7 lbs
Phase Jitter	± 5°
De-spin Rate	0 to 100 rpm
Efficiency	43%

The communications subsystem configuration and capability for the alternate round trip control module/lander configuration is shown in Figure V-32. For "landed" operation, a hybrid S-band subsystem will be employed. This will consist of a combination of solid state low power P.E. type modules in conjunction with Mariner type TWTAs for a power output of 20 watts. An

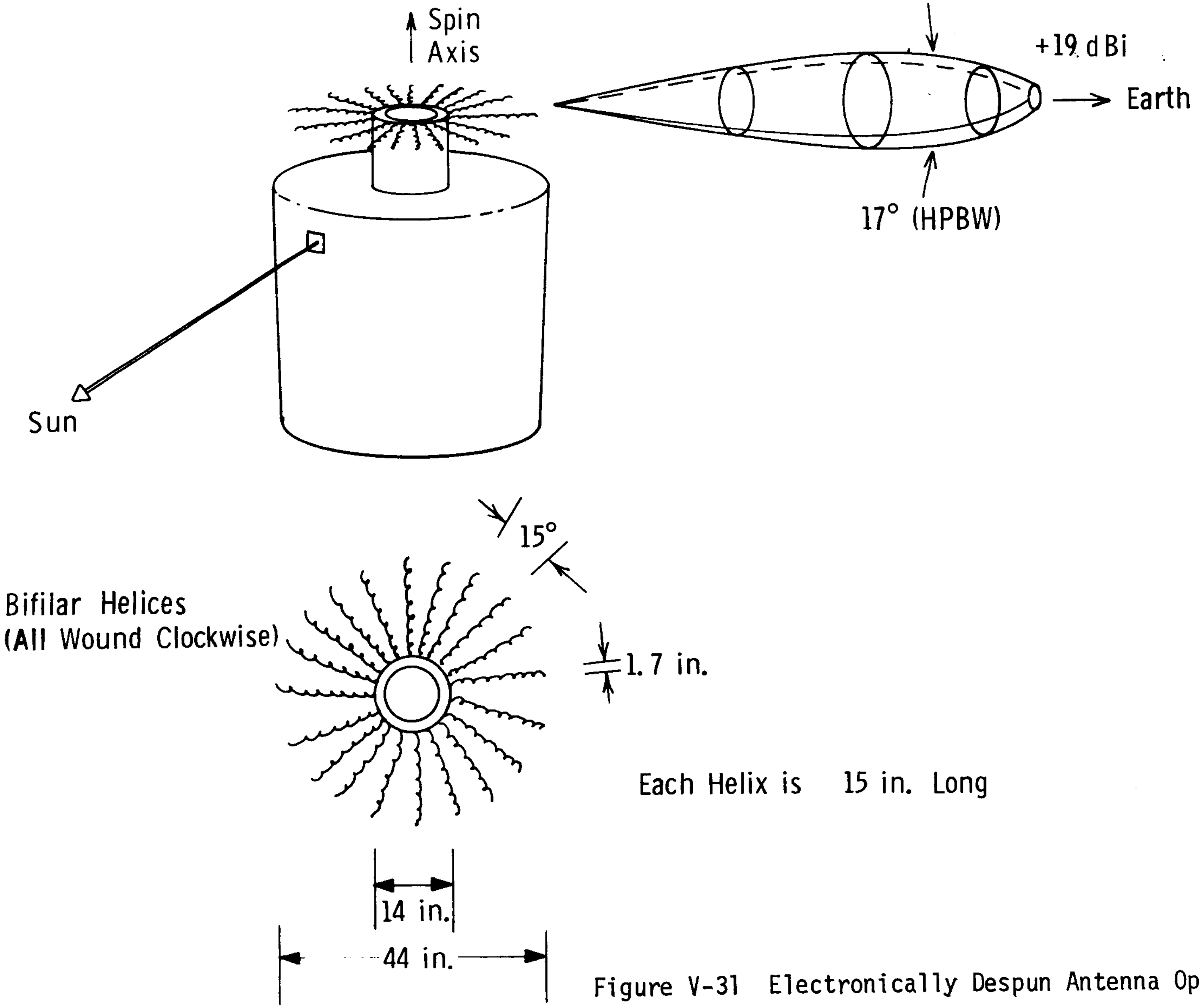
Spin
Axis
+19 dBi
Earth
17° (HPBW)
Sun
15°
Bifilar Helices
(All Wound Clockwise)
1.7 in.
Each Helix is 15 in. Long
14 in.
44 in.

Figure V-31 Electronically Despun Antenna Option

LANDED OPERATION

S-Band Direct To Earth

Hybrid S-Band Subsystem -- PE Modules & Mariner Type TWTA's - 20 Watt Output

Articulated 30" Diam High Gain Antenna
Low Gain Command Antenna
VLC Type Recorder -- 40 Megabit Storage Capacity

Data Transmission Rate -- 500 BPS

RETURN OPERATION

PE Type S-Band Subsystem -- 4 Watts Output

Articulated 30" Diam Antenna

Figure V-32 Round Trip Control Module/Lander Configuration

articulated 30 inch diameter high gain antenna and low gain command antenna (both VL '75 type) and a VL '75 type recorder with 40 megabit storage capacity will be used. The data transmission capability to Earth will be 500 bits per second.

For the return vehicle, the heavy high power TWTAs and associated components will be "left behind" and the return vehicle communications subsystem will consist of the P.E. type modules with 4 watts output at S-band and the articulated 30 inch diameter high gain S-band antenna.

G. POWER

The baseline configuration utilizes the Viking Orbiter for the journey from Earth to Mars. It carries with it the scientific package together with a spin stabilized sample return vehicle. Its power system is the original solar panel/battery system. The return vehicle is provided with body mounted solar cells. Table IV-28 lists the main elements for this configuration.

The Viking Orbiter is provided with 160 sq ft of solar panels. The output of the solar cells decreases as the spacecraft travels from Earth to Mars due to variation of light intensity according to the inverse square ratio. However, the output power from a silicon solar cell increases with decreasing temperature partially compensating for the variation in radiant solar intensity. Examination of flight data from Mariner VII shows that the relationship of output to distance from the Sun can be modeled by the expression:

$$\underset{\text{(in space)}}{\text{Specific output}} = \frac{10.42}{\text{AU}^{1.59}}\ \text{W/ft}^2$$

Table V-28 Baseline Configuration

Earth to Mars	Mars to Earth
Viking Orbiter 160 sq ft solar panel, and battery power system is used. After landing the solar panels will provide power for imaging, sampling and data transmission. The two 30-AH nickel cadmium batteries, a part of the system, will be used to supplement the solar panels if operations become necessary during non-sun periods.	The spin stabilized type return vehicle possesses an area of 40 sq ft of body mounted solar cells. At launch the A U distance from the sun is 1.67. With an angle of 38° between the spin axis and the sun line an effective area of 13 sq ft is presented to the sun. This can provide an output of 60 watts from the solar cells. Weight: Body mounted solar cells 9.1 kg Control logic .5 Shunt regulator & load bank 1.3 10.9 kg (24 lb)

where AU is the distance of the spacecraft from the Sun in astronautical units. When the orbiter is landed on Phobos the back surfaces of the solar panels can no longer radiate to space, causing the temperature of the panels to be higher. For purposes of establishing a modeling relationship the panels are assumed to perform as if their back surfaces were thermally insulated. For the purposes of computing specific output this is a conservative assumption. The resulting expresion for specific output of the panels when the vehicle is in the landed condition is then:

$$\underset{\text{(landed)}}{\text{Specific output}} = \frac{7.62}{\text{AU}^{1.59}} \ \text{W/ft}^2$$

The total output of the panels is the product of the specific output and the area intercepting the Sun's rays, which varies with the time of day. Figure V-33 shows panel output as a function of Sun angle from the zenith at an AU distance from the Sun of 1.666 which corresponds to the time of liftoff from the surface of Phobos on November 19, 1983. At this time Mars is near its aphelion distance. As seen from Figure V-33, the output of the solar panels is sufficient to supply the electrical loads totaling 298 watts incurred during transmission.

As stated, the worst case from the standpoint of power output system occurs near the end of the landed period. Shown below are the power margins for various dates starting with the landing on Phobos on October 13, 1982. The spacecraft is assumed to be landed and the solar panels positioned so that they droop 32 degrees below the horizontal. It is also assumed that 2 hours per orbit of transmission are needed which requires a remaining margin of power at a Sun angle of 47.5 degrees from the zenith. Values shown are for this angle with a corresponding solar panel area intercept of 91.6 sq ft.

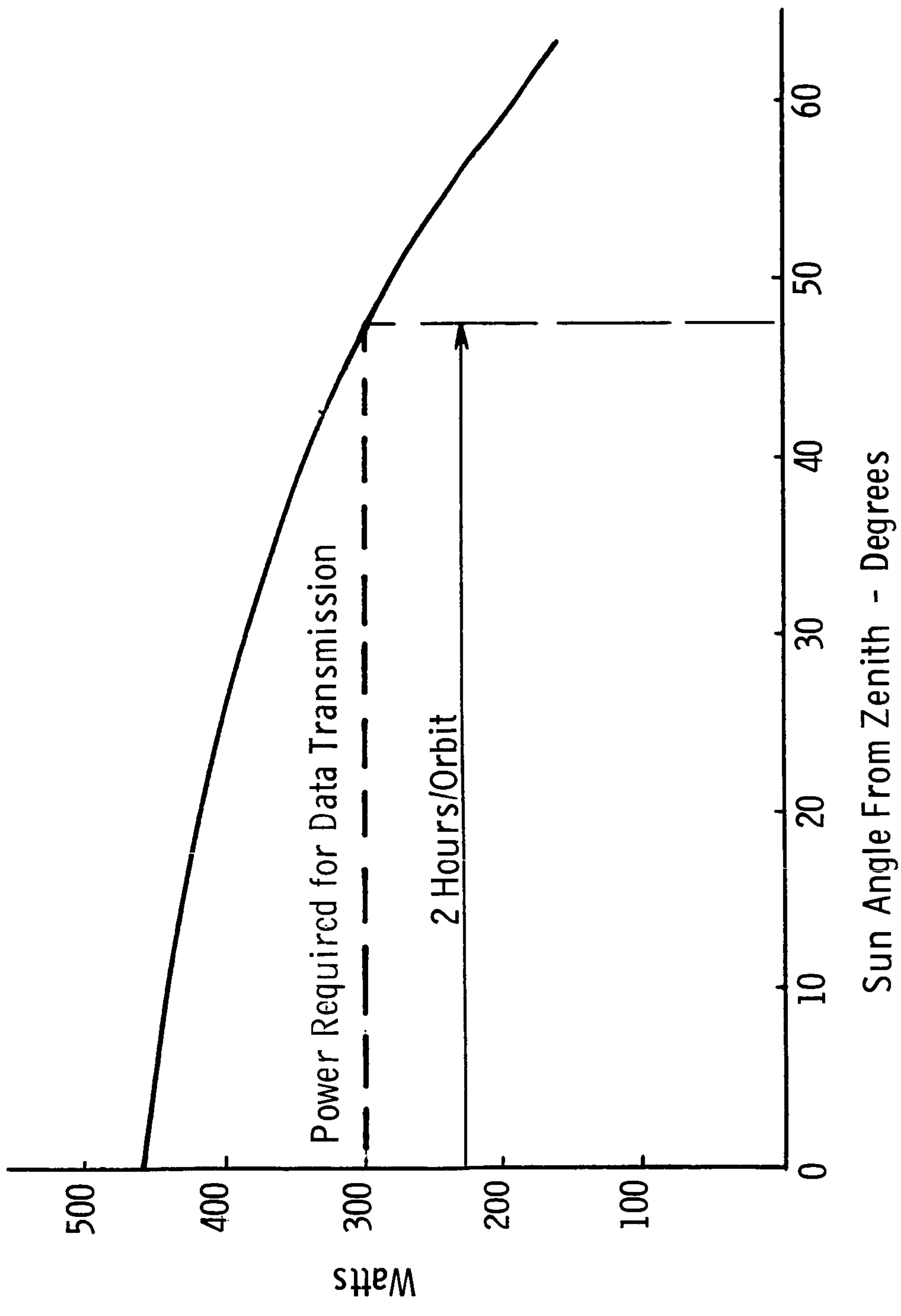

Figure V-33 Solar Panel Output Landed Orbiter

Date	AU Distance	Panel Output (W)	Margin (W)
Oct. 13, 1982 (Arrival)	1.415	402	104
Dec. 20, 1982	1.380	418	120
Mar. 10, 1983	1.423	398	100
Jun. 8, 1983	1.532	354	56
Aug. 7, 1983	1.610	327	29
Nov. 19, 1983 (Departure)	1.666	310	12

Shown in Table V-29 are the power needs for the various phases of operation employed in the return of the science sample to Earth. The maximum power required is 38.4 watts. The spin stabilized type return vehicle possesses an area of 40 sq ft of body mounted solar cells. In the interests of holding the weight of the return vehicle to a minimum, no energy storage is provided, it being assumed that the spin stabilized vehicle will be able to maintain solar orientation through maneuvers. Voltage control during light load periods is obtained through use of a shunt regulator and dump load bank.

The area available upon the vehicle for body mounted solar cells consists of two areas, one in the form of a cone and the other in the form of a cylinder. At the start of the return journey, the angle of the spin axis to the sunline is 38 degrees. This gradually increases to 90 degrees as the spacecraft approaches Earth. However, the combination of distance from the Sun and intercept area is such that the minimum power condition occurs just after launch.

The return vehicle is equipped with solar cells on the forward cone portion having a lateral area of 14.65 sq ft and on the cylindrical portion having an area of 25.16 sq ft. As stated,

Table V-29 Baseline (Spin-Stabilized) Configuration Power Summary (Watts) Mars to Earth

Equipment Name	Launch	Earth Acquisition	Orbital Tracking Maneuver	Cruise	Midcourse Maneuver	Post Midcourse Maneuver	Cruise	Pre-Entry	Sleep-Mode
	1	2	3	4	5	6	7	8	9
Communications									
S-Band Transmitter (4 Watt)			19	19*		19	19*	19	
Command Receiver		3.7	3.7	3.7	3.7	3.7	3.7	3.7	3.7
Data Management									
Telemetry			2	2*		2	2*	2	
Guidance, Navigation & Control									
Attitude Control Electronics	0.2	0.2	0.2	0.2	0.2	0.2	0.2	0.2	
Sun Sensor	2.0	2.0	2.0	2.0	2.0	2.0	2.0	2.0	
SCADS Star Sensor (2)	2.0	2.0	2.0	2.0	2.0	2.0	2.0	2.0	
Programmers	9.5	9.5	9.5	9.5	9.5	9.5	9.5	9.5	
TOTAL	13.4	17.4	38.4	38.4	17.4	38.4	38.4	38.4	3.7

* Transmit 2 hours per 24 hours

initially on return the spin axis is at an angle of 38 degrees to the sunline. Aspect ratios useful in determining the solar intercept for different body shapes have been developed in reference 1. These ratios may be used in obtaining an estimate of available power as follows:

Item	Installed Area (sq ft)	Aspect Ratio	Intercept (sq ft)
Cone	14.65	0.55	8.05
Cylinder	25.16	0.195	4.90
			12.95

The specific output at 1.66 AU, the distance to the Sun at the beginning of the return journey, for a solar panel, is 4.63 w/ft^2. This, when applied to the area, gives an available output of 60.1 watts.

The alternate configuration consists of a 3-axis stabilized vehicle which is used both for the journey to and the return from Mars. The power system consists of oriented solar cells, a SNAP-19 radioisotope thermoelectric generator (RTG), and nickel-cadmium batteries. The RTG and one set of batteries are left on the satellite. Details of the power system are given in Table V-30. A block diagram of the RTG together with battery charging provisions is shown in Figure V-34. Table V-31 gives a listing by mission phases of the power requirements for the preferred alternate configuration in travel from Earth to Mars. During cruise the power sources are sufficient to supply needs but during operation of imagery science and during lander descent the batteries operate in a load share mode. Power requirements during landed operations are given in Table V-32. During standby the 35-watt RTG recharges the batteries so that the peak demands of imaging, sampling and data transmission can be carried out. Table V-33 shows power requirements for the preferred alternate configuration in its return to Earth. The solar panel system is adequate to supply power needs except during Sun loss due to maneuvers or Sun occultations when the battery is used.

Table V-30 Alternate Configuration

Earth to Mars

Gross Capacity:

At Earth	165 watts
At Mars	95 watts

Battery provides peak power requirements during landed operations

Weight:

Solar panel	5.9 kg
RTG	16.0
Converter	1.0
Control logic	1.4
Shunt regulator & load bank	2.3
Batteries (3-8 AH)	33.0
Chargers	2.0
Orientation drive & support	1.3
	62.9 kg (134 lb)

Mars to Earth

Gross Capacity:

At Mars	60 watts
At Earth	130 watts

Solar orientation required for 13 sq ft panel

Weight:

Solar panel	5.9 kg
Control logic	.5
Shunt regulator & load bank	.5
Orientation drive & support	1.3
Battery (2 AH)	2.7
Charger	0.5
	11.4 kg (16 lb)

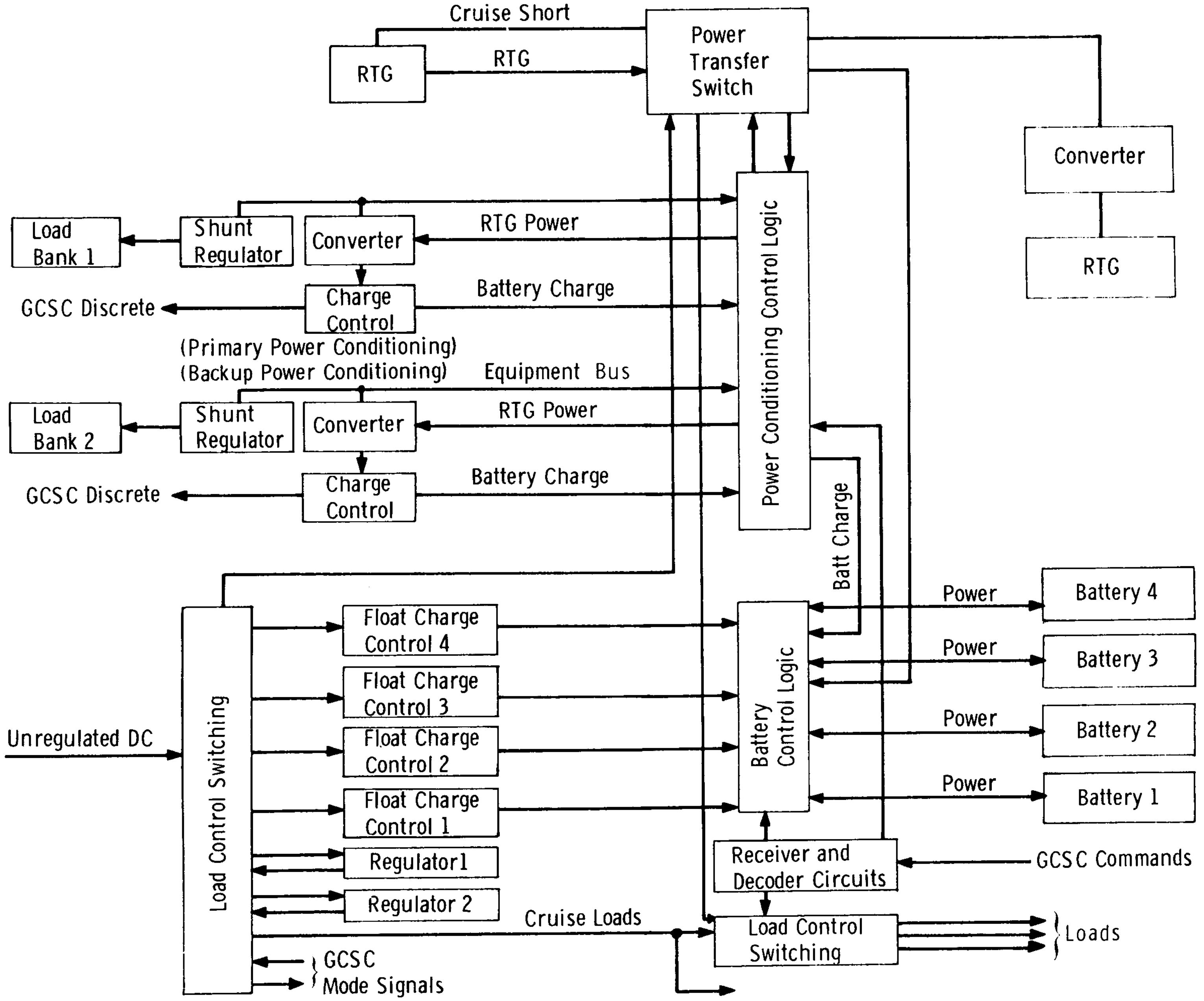
Cruise Short
RTG
RTG
Power Transfer Switch
Converter
RTG
Load Bank 1
Shunt Regulator
Converter
RTG Power
Charge Control
Battery Charge
GCSC Discrete
(Primary Power Conditioning)
(Backup Power Conditioning)
Equipment Bus
Load Bank 2
Shunt Regulator
Converter
RTG Power
Charge Control
Battery Charge
GCSC Discrete
Power Conditioning Control Logic
Batt Charge
Power
Battery 4
Power
Battery 3
Power
Battery 2
Power
Battery 1
Battery Control Logic
Float Charge Control 4
Float Charge Control 3
Float Charge Control 2
Float Charge Control 1
Regulator1
Regulator 2
Unregulated DC
Load Control Switching
Receiver and Decoder Circuits
GCSC Commands
Cruise Loads
Load Control Switching
Loads
GCSC Mode Signals

Figure V-34 RTG Power System

Table V-31 Preferred Alternate Configuration Power Summary (Watts) Earth to Mars

Equipment Name	Launch	Canopus Acquisition	Cruise	Midcourse Maneuver	Orbit Insertion	Captive Orbit Trims	Phasing Orbit Insertion	Observation Orbit Insertion	Transfer to Satellite Orbit	Satellite Station Keeping	Propulsion Module Jettison	Lander Descent	Sun Occultation
	1	2	3	4	5	6	7	8	9	10	11	12	13
Communications													
S-Band Transmitter (4/20 watt)		19	19	19	19	19	19	91	19	91	0	0	
Command Detector/Receivers		3.7	3.7	3.7	3.7	3.7	3.7	3.7	3.7	3.7	3.7	3.7	3.7
Antenna Drive		0.1	0.1	0.1	0.1	0.1	0.1	0.1	0.1	0.1	0.1	0.1	
Data Management													
Telemetry	2	2	2*	2	2	2	2	2	2	2	2	2	
Recorder	10	10		10	10	10	10	10	10	10	10	10	
Guidance, Navigation & Control													
Guid., Control & Seq. Computer	15	15	15	15	15	15	15	15	15	15	15	15	15
IMU				3	3	3	3	3	3			15	15
Canopus Sensor		5	5										
Sun Sensors		0.2	0.2		0.2	0.2	0.2	0.2	0.2	0.2			
Rendezvous Radar												60	
Science													
Orbiter Imagery (1 Camera)								20		20			
TOTAL	27	55.0	45.0	52.8	53.0	53.0	53.0	145.0	53.0	142.0	30.8	105.8	30.7

* Transmit 2 hours per 24 hours

Table V-32 Preferred Alternate Configuration Landed Operations Power Summary (Watts)

Equipment Name	Imaging	Sampling			Transmission (2 hours)	Standby
		Boom Oper.	Drilling	Stowage		
Communications						
S-Band Transmitter (20 Watt)					91	
Command Receiver		3.7	3.7	3.7	3.7	3.7
Data Management						
Telemetry					2	
Recorder	10	10	10	10	10	
Guidance, Navigation & Control						
Guid., Control & Seq. Computer	15	15	15	15		
Science						
Facsimile Camera (2)	18 (22 peak)					
Sampling		1 (50 peak)	2 (50 peak)	10 (50 peak)		
Sample Analysis				3		
TOTAL	43	29.7	30.7	41.7	106.7	3.7

Table V-33 Preferred Alternate Configuration (Three-Axis Stabilized) Power Summary (Watts) Mars to Earth

Equipment Name	Launch	Canopus Acquisition	Cruise	Orbital Tracking	Maneuver	Cruise	Pre-Entry	Sun Occultations
	1	2	3	4	5	6	7	8
Communications								
S-Band Transmitter (4 watt)			19*	19	19	19*	19	
Command Receiver & Detector		3.7	3.7	3.7	3.7	3.7	3.7	3.7
Data Management								
Telemetry			2*	2	2	2*	2	
Guidance, Navigation & Control								
Guid., Control & Seq. Computer	15	15	15	15	15	15	15	15
Inertial Measurement Unit					3			9
Canopus Sensor		5	5	5		5		
Sun Sensor		0.2	0.2	0.2		0.2		
TOTAL	15	23.9	44.9	44.9	42.7	44.9	39.7	27.7

* Transmit 2 hours per 24 hours

Figure V-35 describes the recovery package power supply. In order to avoid the weight and complexity of conditioning equipment to maintain a wet battery for two years, a self-activated dry charged silver zinc battery is used to power the transponder during the parachute descent phase. But since this type of battery has a short life, once activated, a sea water battery is used once the package is afloat. Considerable development and testing (reference 2) has been carried out by the U. S. Navy on sea water activated batteries. The design envisioned for this application would employ a magnesium anode and an iron screen cathode.

Two energy sources are used in the entry and recovery of the sample package. One is a silver zinc battery of the self-activated type which functions during entry. The other is a magnesium-iron battery activated by immersion in sea water. It functions until the package is recovered. Both supply a transponder having a one-watt requirement for one second at four-second intervals. Quiescent power needs are 200 milliwatts. The two batteries are described below.

Item	Primary Silver Zinc Battery	Sea Water Battery
Time of operation	1/2 hour	30 days
Average power	0. 4 watt	0. 2 watt
Peak power	1. 0 watt	1. 0 watt
Energy density	40 Wh/lb	75 Wh/lb
Weight	2 lb	3 lb

Figure V-35 Recovery Package Power Supply

REFERENCES

1. Bernard J. Saint-Jean: *Theoretical Considerations for a Preliminary Design of a Solar Cell Generator on a Satellite*. NASA/GSFC Technical Note D-1904, September 1963

2. Telecon with B. J. Wilson, Naval Research Laboratory, Washington, D. C., 16 November 1971.

VI. Phobos/Deimos Rover Studies

VI. PHOBOS/DEIMOS ROVER CONCEPTS

Phase I analyses indicated that wheeled, flying, and deployable boom science mobility modes should be examined in greater detail in Phase II to determine their capability to be tailored to, operate in, and take advantage of the unique low gravity environments of Phobos and Deimos (see Table VI-1) and to evaluate their relative operational and weight characteristics. Phase II mobility analyses utilized the baseline separable lander concept developed in Phase I as illustrated in Figure VI-1. Benefits that can be realized through addition of mobility to this, or any other, Phobos/Deimos Lander include the following:

1) Access to surface variations
    - "Best" landing sites (smooth) "Best" science sites (irregular)
    - Best science sites cannot be determined until after landing
2) Increased data return
    - Remove lander from depression
    - Maintain favorable communication windows
3) Removal from landing site contamination
4) Separation from lander interferences (requires separable science)
    - RTG radiation
    - Outgassing
    - Noise (electrical, magnetic, mechanical)

With wheeled systems, the low gravity permits the use of large diameter, light-weight wheels which give the rover high obstacle performance capability with a mobility subsystem weight (approximately 12 kg) well below that required for similar performance on a Lunar or Mars rover.

Table VI-1 Rover Operating Environment

Gravitational Acceleration at Surface:
Phobos: 0.4 to 3 cm/sec^2
Deimos: 0.2 to 1 cm/sec^2

Craters (Minimum):

Diameter	Number of Craters with Larger Diameter	
(KM)	Phobos	Deimos
0.1	68	14
1	3	0.8
10	0.2	0.05

Major Deformities Preserved
- Craters
- Low Velocity Ejecta

Terrain Could Be Jagged and Irregular With Steep Slopes On All Scales of Observation

Dust (Baseline Assumption): Thin Layer, Loosely Compacted

Surface Coefficient of Friction: $\mu = 0.5$

Interplanetary Vacuum

Temperature Range: -150°C to +40°C

Synchronous Rotation (Same Side Always Faces Mars)

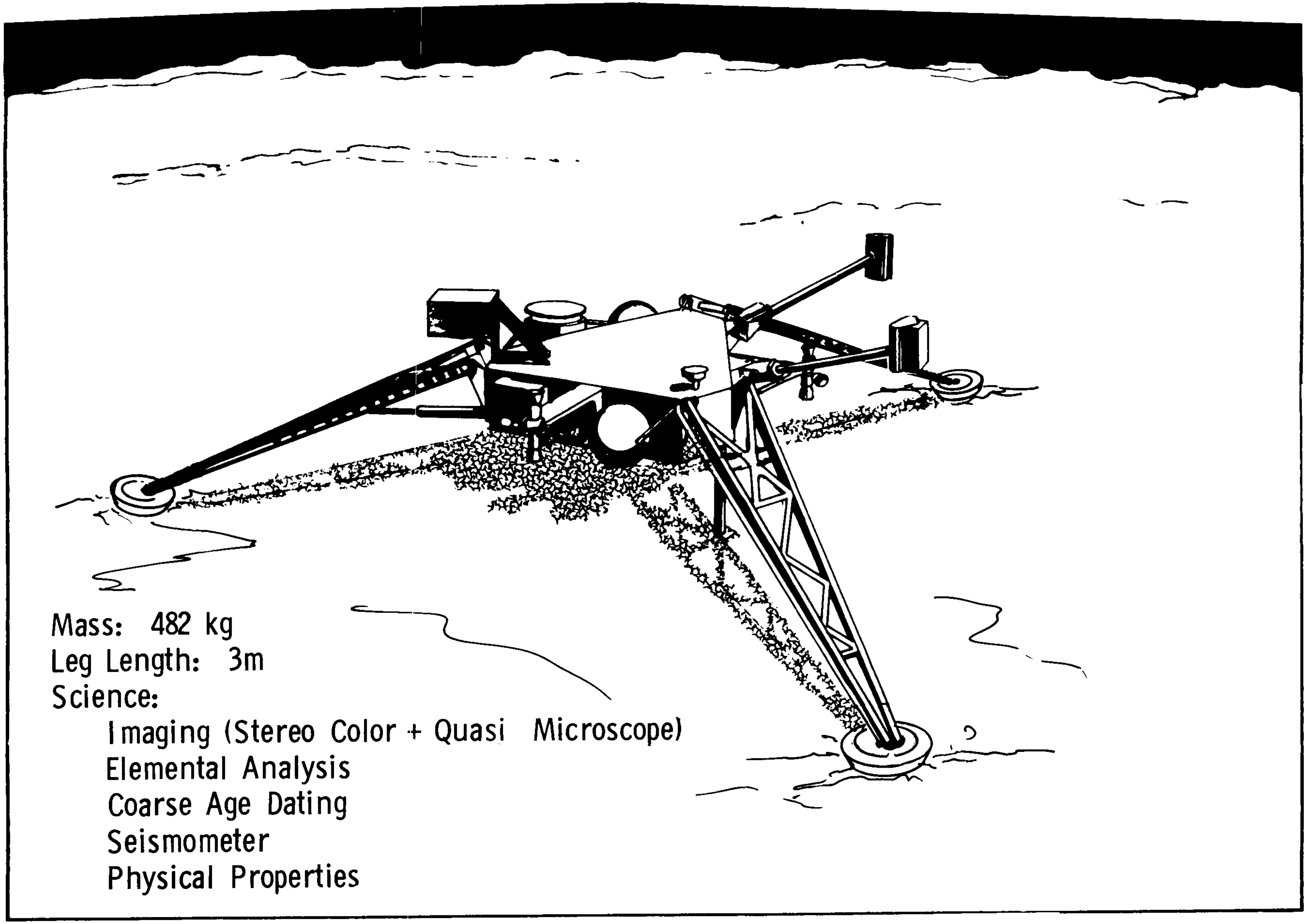

Mass: 482 kg
Leg Length: 3m
Science:
  Imaging (Stereo Color + Quasi Microscope)
  Elemental Analysis
  Coarse Age Dating
  Seismometer
  Physical Properties

Figure VI-1 Baseline Lander for Phase II Mobility Studies

A flying rover is attractive since low ΔVs are required for ballistic hops in the low-g environment and no totally new subsystems must be added to achieve post-landed mobility. Weight charged to flying mobility would include larger tanks and fuel loads and reusable shock absorbers in the landing legs.

Furlable booms are the third concept considered, such systems having significantly greater range per unit weight than booms used in higher-g environments. Although booms only provide access to the lander's immediate surroundings, such science mobility may be desirable on a simple first mission or in the event extreme surface irregularities prevent lander mobility.

The following sections describe these mobility modes in greater detail and present the results of analyses of mobility dynamics, navigation, and communications for Phobos/Deimose rover missions.

A. PHOBOS/DEIMOS WHEELED ROVER

1. Overall Configuration

Traveling on three 2.0 m diameter "umbrella-frame" wheels, the Phobos/Deimos rover shown in Figure VI-2 displays the lightweight wheels that can be used in the low-g environment. With a nominal vertical static load of less than one pound per wheel, only one square inch of surface contact area is required per wheel to keep the contact load in the desirable range below one psi.

Due to the low loads (including drivemotor torque) on the wheels, each spoke can carry the entire static and dynamic load without support from adjacent spokes.

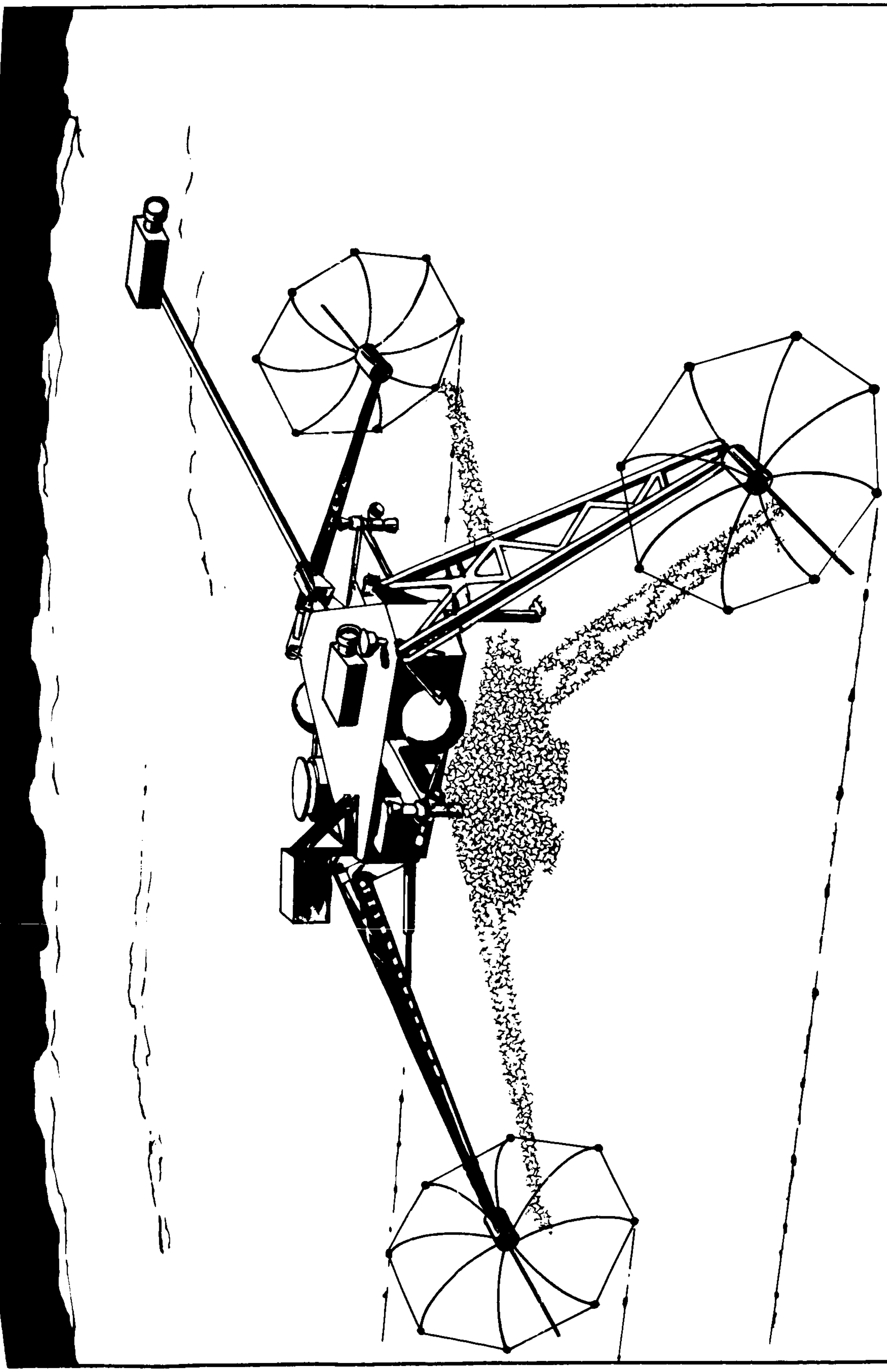

Figure VI-2 Phobos/Deimos Wheeled Roving Lander

As shown in Figure VI-3, the wheels used on the rover are folded for stowage similar to an umbrella. This permits stowage of each wheel and its one-watt drivemotor within a 12 cm diameter by 1.3 m long envelope. Opening each wheel would be accomplished, on command, using a spring-loaded slide on the axle, the wheels opening fully during the first full revolution of the drives. The wheels' treads consist of 3 cm diameter balls on the ends of the spokes.

2. Wheeled Mobility Performance

Of the three candidate mobility techniques, the wheeled concept is the most conventional. Three configurations have been conceived for a three-wheeled, Phobos/Deimos rover, all adding a wheel on each of the three landing legs. Since the payload is assumed identical for each configuration, the mobility performance afforded by each will be dependent upon the relationships between Center of Mass (CM) and wheel location. Figure VI-4 shows the three configurations considered in this study.

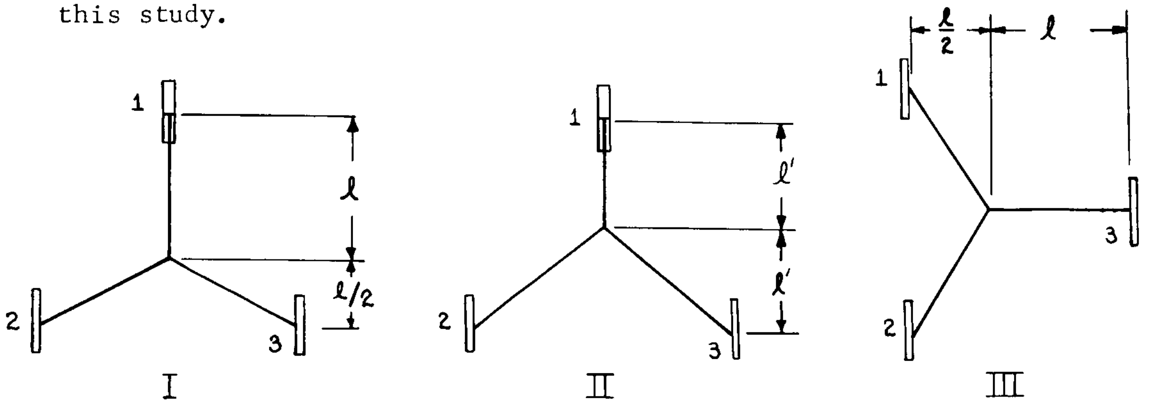

Figure VI-4 Mobility Configurations

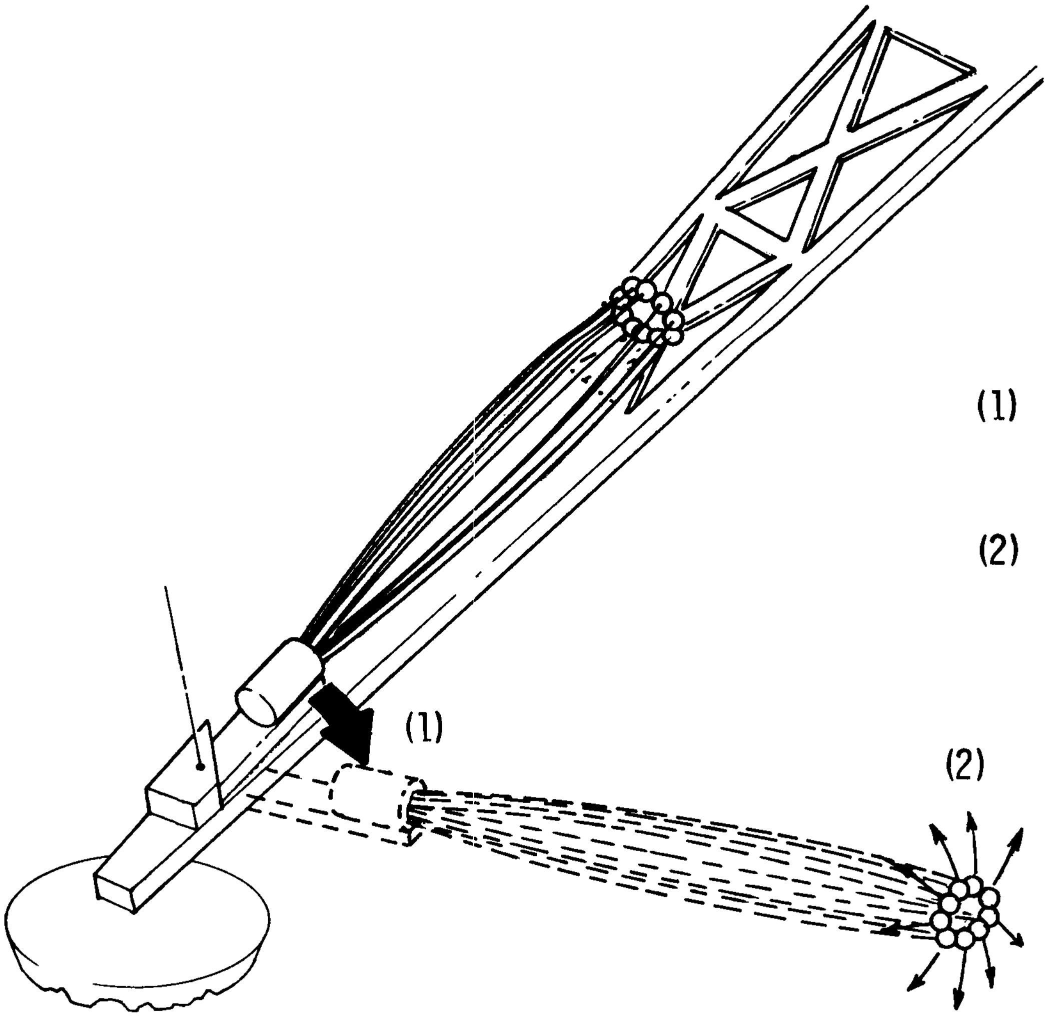

DEPLOYMENT SEQUENCE:

(1) Rotate Folded Wheels out From Landing Legs & Lock in Position

(2) Open Wheels While Operating Drivemotors

Figure VI-3 Wheel Storage/Deployment

Configuration Characteristics

Wheel Diameter	2.0 m
Center of Mass Elevation Above Wheel Hubs	1.0 m
Overall Length (Wheels Deployed)	8.8 m
Overall Width (Wheels Deployed)	6.8 m
Overall Height (Wheels Deployed)	3.0 m

The performance characteristics are discussed in the following paragraphs.

a. Slope Climbing Capability - Assuming sufficient available drive-motor output power, the maximum slope that can be climbed for a soft, noncohesive surface is close to the natural angle of repose of the surface material which is closely related to the angle of internal friction. The Phobos/Demios Engineering Model predicts angles of friction between 25 and 40 degrees. Thus the lower limit of slope climbing capability may be less than 25 degrees. The upper limit could be greater than 40 degrees if the surface is cohesive and active grousers were added to the wheels. If the latter case exists, slope climbing capability might be limited by pitch stability which is discussed later.

b. Ground Clearance - For the concepts considered, the ground clearance is a minimum of one wheel radius near the wheels, increasing as the body is approached. Thus the ground clearance will be greater than one meter.

c. Mobility Power - Because of the low gravity of Phobos and Deimos, the energy required for mobility will be small. Although the "umbrella" wheel is designed for performance rather than for minimum power consumption; the power will be small. By extrapolating results of mobility tests performed by the U. S. Army Waterways Experiment Station and assuming an inefficient wheel, an energy consumption of 0.3 w·hr/km·nt can be assumed for level surfaces. For a 450 kg payload, g = 3 cm/sec^2, and a 15 degree average upslope, the total energy expended will be about 10 w·hr/km, assuming 50% efficiency in the drive system. The power will then be a function of velocity which, in turn, will be dependent upon dynamic performance and stability requirements. For a nominal velocity of 0.1 km/hr, the required input power will be 1 watt.

d. Depression Spanning Capability - The ability to cross over an infinitely deep depression is expressed in terms of the maximum width which can be successfully spanned. For Configuration I the worst case will occur when the wheels 2 and 3 are trailing and go into a depression simultaneously. For this case, the load on wheel 1 (L_1) can be approximated from:

$$L_1 = (L_2 + L_3)\ (\ell/2 - R) \qquad \text{where } \ell = 4.5 \text{ m}$$

$$L_1 = (L_2 + L_3)\ (1/2 - R/\ell\ ) \qquad R = 1 \text{ m}$$

$$L_1 = .28\ (L_2 + L_3)$$

The traction produced by wheels 2 and 3 is:

$$F_t \approx \mu^2 L_1 \text{Sin}\phi + \mu\ (L_2 + L_3)\ \text{Cos}\phi + L_1 \text{Cos}\phi$$

where μ = pull coefficient

ϕ = wheels contact angle

For the depression to be crossed, the net force, $F_t - (L_2 + L_3)\text{Sin}\phi$, must be greater than zero. Assuming a pull coefficient of 0.6, the following condition for successful depression negotiability is defined for configuration I.

$$0.36\ L_1 \text{Sin}\phi + .6\ \left[(L_2 + L_3)\text{Cos}\phi + L_1 \text{Cos}\phi\ \right] - (L_2 + L_3)\text{Sin}\phi > 0$$

Since $L_2 + L_3 = 3.6\ L_1$, the inequality becomes:

$$2.8 \cos\phi > 3.24 \sin\phi$$

or

$$\phi < 41^{\circ}$$

The width of the depression may now be determined from the relationship:

$$\sin\phi = W/2R$$

Thus for configuration I, W_{max} is 1.3 meters.

Employing the same analysis technique, the depression spanning capability of Configuration II may be determined. The load ratios will be $L_1 = .71\ (L_2 + L_3)$. For $\mu = 0.6$ the inequality will be:

$$\phi < 53^{\circ}$$

This results in value of W_{max} of 1.6 meters.

The third configuration will have the best depression scanning capability of all three since when any wheel is in a depression the other two are providing traction. The limiting contact angle is 74 degrees which gives a maximum crevice spanning capability of 1.92 meters at a pull coefficient of 0.6. This value of 1.92 meters also represents the maximum depression width that can be spanned by one wheel of configurations I and II at $\mu = 0.6$.

e. Step Climbing Capability - The step climbing capability (maximum negotiable step height) is closely related to the depression spanning. The worst case for configuration I occurs when wheels 2 and 3 are trailing and contact a step simultaneously. The contact angle with $\mu = 0.6$ will be the same as for depression spanning or a maximum of 41°. For steps this angle is defined by:

$\cos\phi = (R - Z)/R$ where Z = step height

Thus, the worst case maximum step that can be climbed by configuration I is approximately 0.25 meter. For configuration II the maximum contact angle is 53 degrees. Thus for $\mu = 0.6$, configuration II will be limited to climbing steps less than 0.35 meters. The third configuration will be able to climb larger steps since it will always have 2 wheels supplying traction. Its maximum step climbing capability will be defined either by ground clearance or the ability of the rear wheel to start up a step. If the step is higher than one wheel radius, the pull coefficient must be greater than 0.9. At $\mu = 0.6$ the limiting value of contact angle is 74 degrees, giving a maximum step height of 0.75 meters.

f. Vehicle Stability - Roll and pitch stability must be maintained during surface traverses. The maximum allowable roll and pitch angles for the three configurations are listed below. In each case the axis of rotation is taken as the line between 2 wheels.

Configuration	Max. Roll Angle	Max. Pitch Angle
I	66°	66°
II	59°	74°
III	66°	66°

These angles must not be exceeded by the sum of the slope angle and angle due to obstacle impact which is a function of obstacle size, wheel dynamics, and operating velocity.

g. Operating Velocity - The operating velocity should be a value which can provide the largest range while maintaining stability. When the rover contacts an obstacle such as a step, there will be angular deflection due to the kinetic energy which is $1/2\ Mv_i^2$. The worst case assumes that this energy changes to rotational energy. This gives an initial angular velocity ($\dot{\theta}_i$) of:

$$\dot{\theta} = \frac{M}{I} v_i$$

Considering configuration I, since it has the lowest pitch stability margin, the inertia about the rear axle will be:

$$I_\theta = \frac{M}{3} (2.25)^2 = 1.7 \text{ M}$$

The moment due to gravity opposing this rotation will produce an angular deceleration of 2.25 Mg/I_θ or $1.32 \times 10^{-2} g$. This acceleration must overcome the initial velocity before the stability limit angle is reached. If the vehicle is going up a slope the angular deflection is less than the limit. For this analysis a slope of 30 degrees will be assumed, making the maximum angle 36 degrees or approximately 0.6 radian. Using the following relationships and a g of 1 cm/sec^2, the maximum allowable velocity can be found: At

$$.77 \, v_i - 1.32 \times 10^{-2} t = 0 \qquad \text{(E-1)}$$

$$.77 \, v_i t - 0.66 \times 10^{-2} t^2 = 0.6 \qquad \text{(E-2)}$$

At the point that the velocity is zero the maximum displacement occurs. Thus as in equation E-1, t may be expressed in terms of v_i. This value of t is then substituted in E-2 to find the value of v_i which satisfies the inequality. For this case the maximum value of v_i is 16 cm/sec.

The worst case for roll stability is configuration II with the roll axis represented by a line between wheels 1 and 2 or 1 and 3. Assuming a 30° lateral slope, the stability limit angle is 29 degrees or 0.51 radian. Performing an analysis similar to that just used, the maximum velocity for maintaining roll stability for configuration II is 13 cm/sec. The inertia for this case is $I_\phi = 0.92$ M.

For a vehicle which has an elastic wheel, some of the initial energy will be expended as work in compressing the wheel, thereby decreasing the angular displacements and increasing the maximum safe velocity. To point out the effects of gravity upon dynamic performance, the maximum velocity for the same configurations operating on Earth can be determined. For roll stability the velocity limit is 4.1 m/sec and for pitch stability 5 m/sec, again for an inelastic wheel.

3. Wheeled Mobility Simulation

Martin Marietta's digital simulation of unmanned roving vehicle dynamics, Reference VI-1, was used to analyze the performance of a four-wheeled Phobos rover. A four-wheeled configuration was used since it was in the digital program and three-wheel configurations were not.

A detailed discussion of the program including the logic, method, and program listing is provided by reference 7.

The four wheeled rover model has a wheel base of 3 meters and a tread of 2.5 meters. The total body mass is 450 kg. which includes two 10 kg masses placed to locate the combined center of mass at the geometric center. The total body inertia of the three rectangular masses about the yaw axis at the mass center is 615 kg/m^2. The gravitational constant was 0.01 m/sec^2.

The wheels are modeled as flexible with a wheel deflection coefficient of 15 nt/m and internal damping of 28.6 $\frac{nt\text{-}sec.}{m}$ The rover velocity limit per wheel is 0.1 m/sec.

The soil properties include curves for the bearing pressure vs. sinkage and wheel thrust vs. slippage. PHI is the angle of internal friction. The program also stores the Bekker soil constants to allow use of the theoretical curve fit equations. The following computer runs use the Lunar Nominal and Mars - Dune and Lag Gravel soil models.

Table VI-2 gives the vehicle characteristics and soil properties used for the Phobos/Deimos data runs.

The Rover program accepts the step perturbations as a function of the vehicle range from the start. The steps are input for the left and right wheels independent of body yaw. The step height ranges from 2.5% to 40% of the wheel radius. Figure VI-5 shows the obstacle location with respect to the rover body.

The wheel velocity vs time curve in Figure VI-6 shows the acceleration for a soil with cohesion (Run 1) and without cohesion (Runs 2, 3, 4). Thus the available thrust is much greater for a soil with cohesion. The velocity as plotted is a function of wheel slippage, motor rise-time, wheel contact area, wheel load, and sinkage. The relationship is further defined by the wheel slip vs. time curve.

The Rover program determines the body attitude change due to the step based on the net forces on each wheel. These forces are derived from the potential soil thrust, the time duration required to traverse the obstacle, and the vehicle forces which resist the motion. Thus in Run 1 of Figure VI-7, the cohesive soil provides more attitude change than Runs 2, 3 and 4. The vehicle "sees" the step at wheel 1 and begins to yaw negative. The vehicle then "sees" the step at wheel 2. There is a period of time that, dependent on the vehicle velocity and step height, the vehicle "sees" both steps. The vehicle clears the first step but is still negotiating the last step.

Table VI-2 Rover Digital Simulation Model-Inputs

1. VEHICLE CHARACTERISTICS

Total Mass	450 kg
Gravitational Acceleration	0.01 m/s^2
Mass Center At Geometric Center	
Body Yaw Axis Inertia	615 kg/m^2
Wheel Base	3 m
Tread	2.5 m
Number of Wheels	4
Wheel Width at Surface	0.01 m
Wheel Damping	28.6 nt-s/m
Wheel Deflection Coef.	15 nt/m
Velocity Limit	0.1 m/s

2. SOIL PROPERTIES

Lunar Nominal (Run 1)	Thrust vs Wheel Slip Curve Bearing Pressure vs Sinkage Curve Phi - 35° (Angle of Internal Friction) Cohesion - 500 nt/m^2 Density - 1500 kg/m^3
Mars - Dune + Lag Gravel (Run 2, 3, 4)	Thrust vs Wheel Slip Curve Bearing Pressure vs Sinkage Curve Phi - 35° Cohesion - 0 Density - 1500 kg/m^3

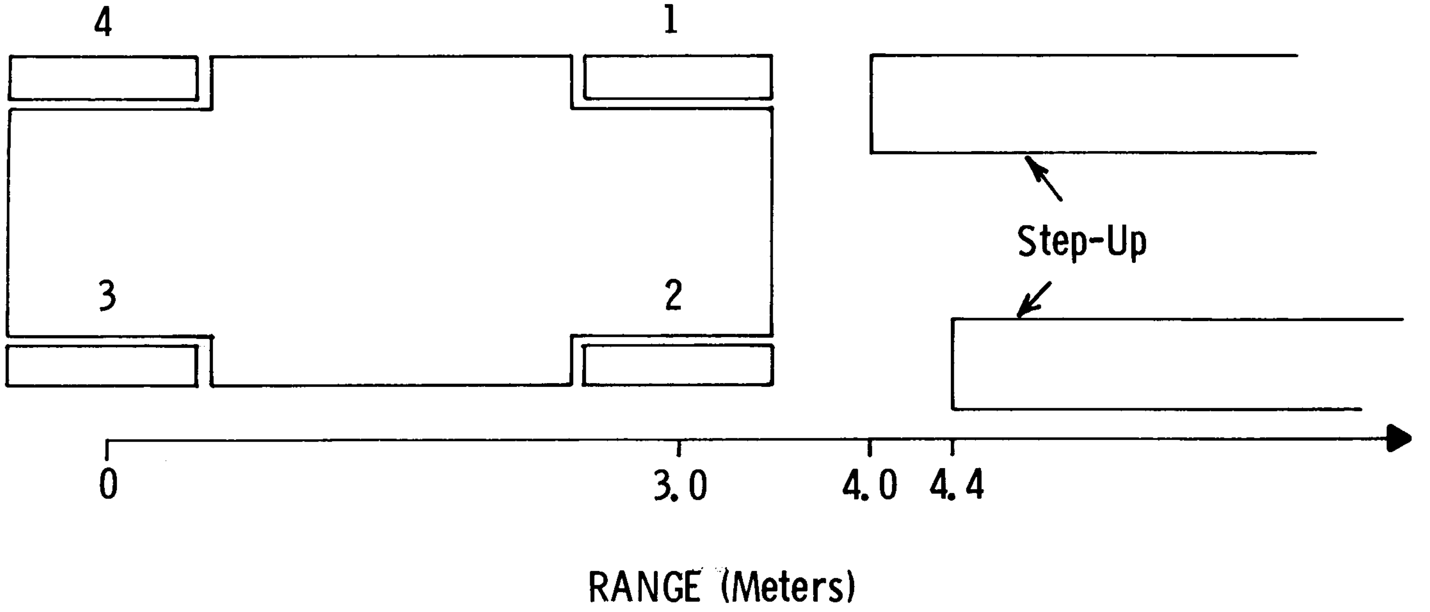
4
1
3
2
Step-Up
0
3.0
4.0
4.4
RANGE (Meters)

	Surface Step
Run 1	2.5% Wheel Rad.
Run 2	2.5%
Run 3	6.5%
Run 4	40%

Figure VI-5 Problem Configuration for Digital Simulation

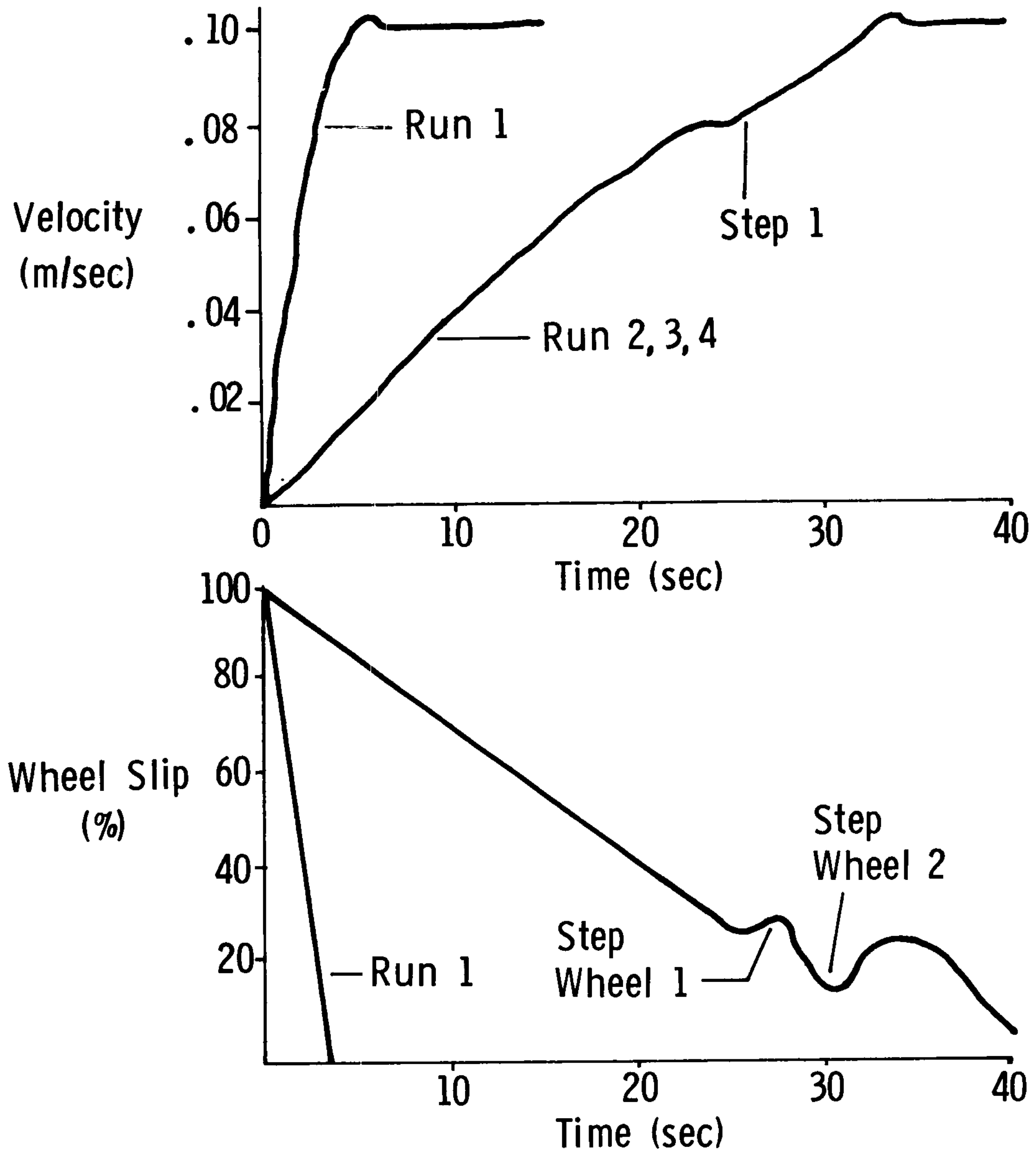

Figure VI-6 Velocity and Slip Outputs

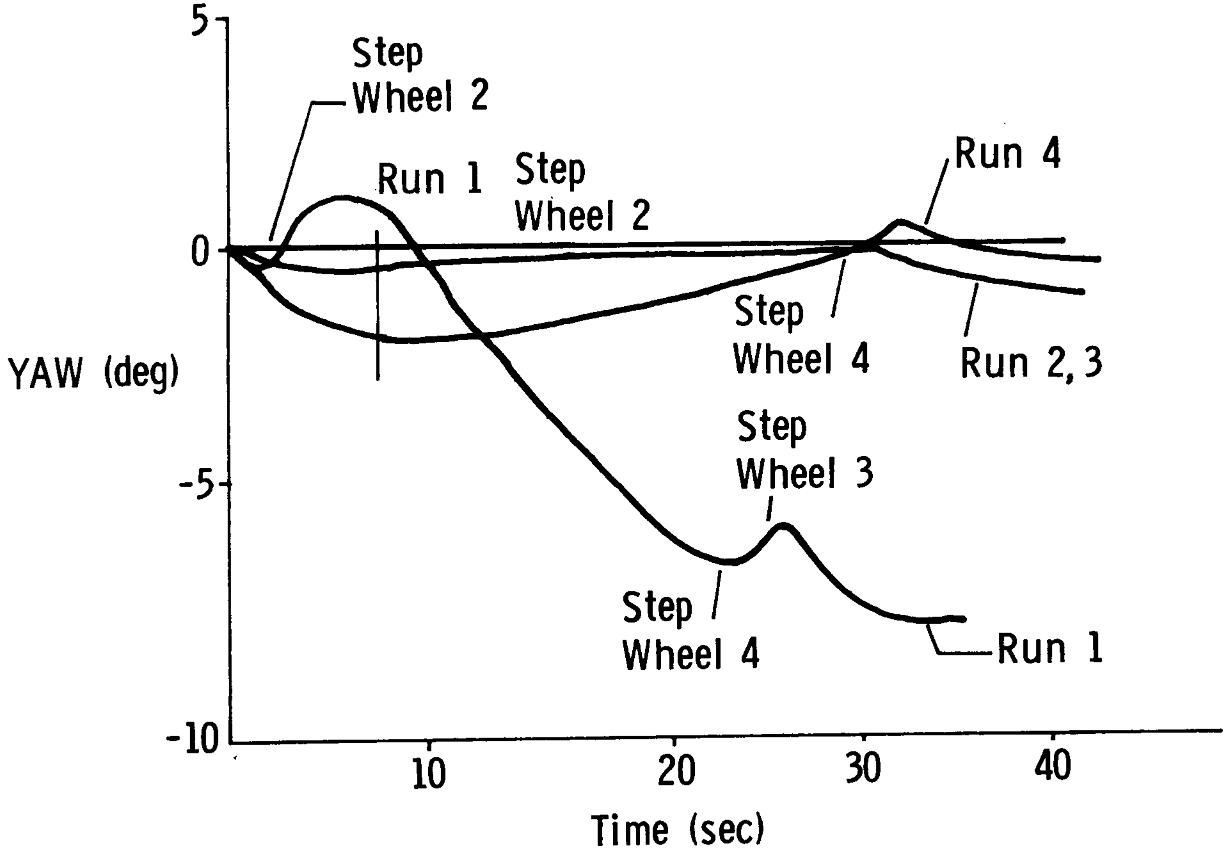

Figure VI-7 Yaw Perturbations at Obstacle

Run 1 provided unexpected acceleration (greater than gravitutional input) and yaw perturbations which can be explained by the thrust differential caused by the varying wheel contact area at the step and the soil cohesion.

B. PHOBOS/DEIMOS FLYING ROVER

The flying rover shown in Figure VI-8 appears essentially the same as the baseline lander shown previously. The only visible change is the larger tankage required for mobility fuel. The one-shot shock absorbers in the baseline system would be replaced by reusable shock absorbers using electrical or gas actuators.

As developed in Phase I, Figure VI-9 depicts the vertical velocity required to reach Altitude (H) and Flight Duration (T) in gravity fields ranging from the lowest Deimos level to the highest Phobos level projected in the Phobos/Deimos Engineering model. Once launched off the surface with the necessary ΔV_Z, the indicated flight sequence is followed.

An example of a flying rover traverse segment is illustrated in Figure VI-10. This example used a nominal Phobos gravitational level of 0.01 m/sec^2 and calls for traversing over a 100 m obstacle on the way to a destination 800m away and 50m lower than the launch site. Using the curves in Figure VI-9, 1.5 m/sec provides clearance over the 100m obstacle and a flight time of 300 seconds to point number (3) on the trajectory. The flight sequence (steps 1 through 4) requires 7.7 m/sec of ΔV and 1.9 kg of fuel, neglecting gravity losses. Many variations on this sequence are possible including one designed to minimize landing

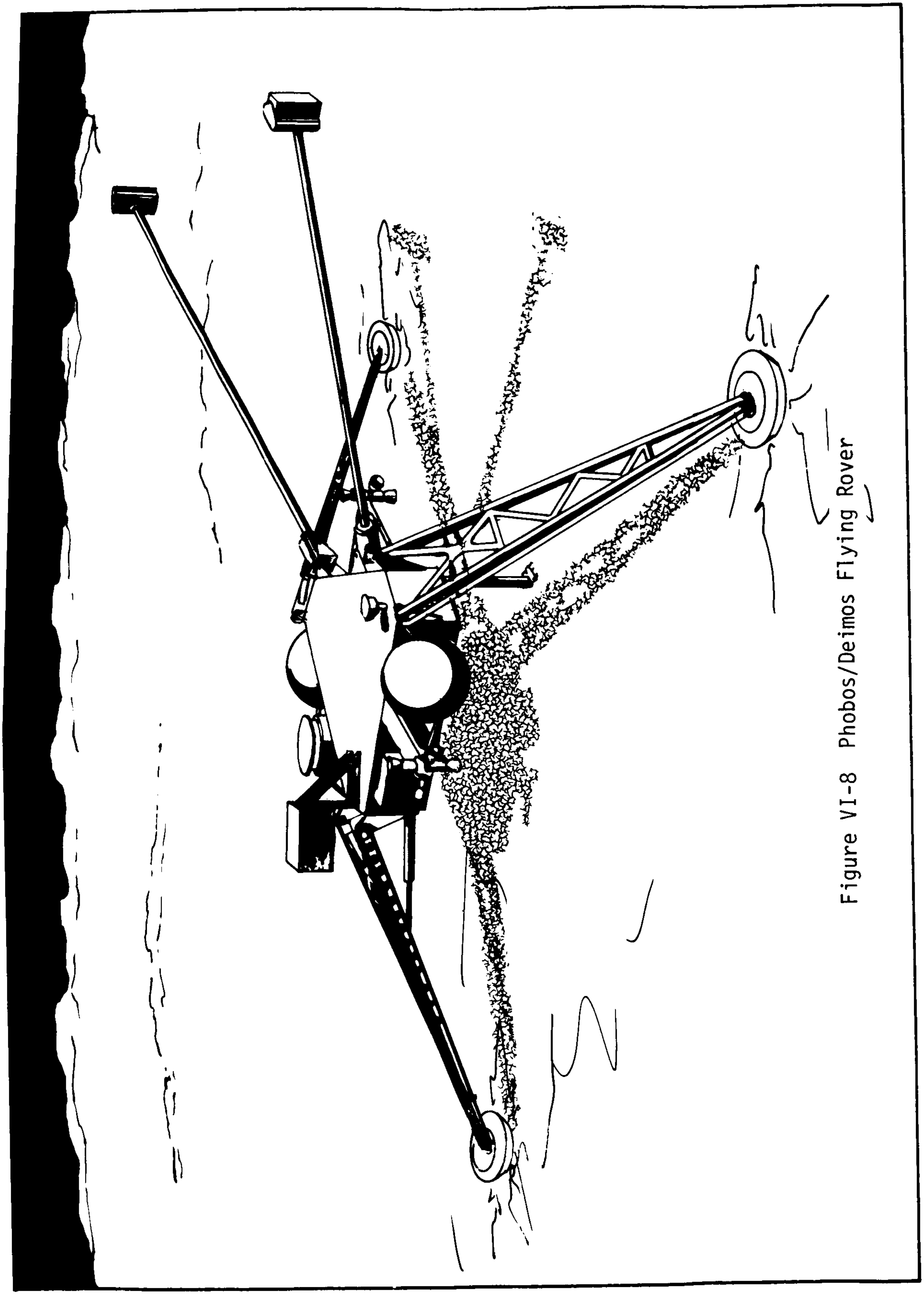

Figure VI-8 Phobos/Deimos Flying Rover

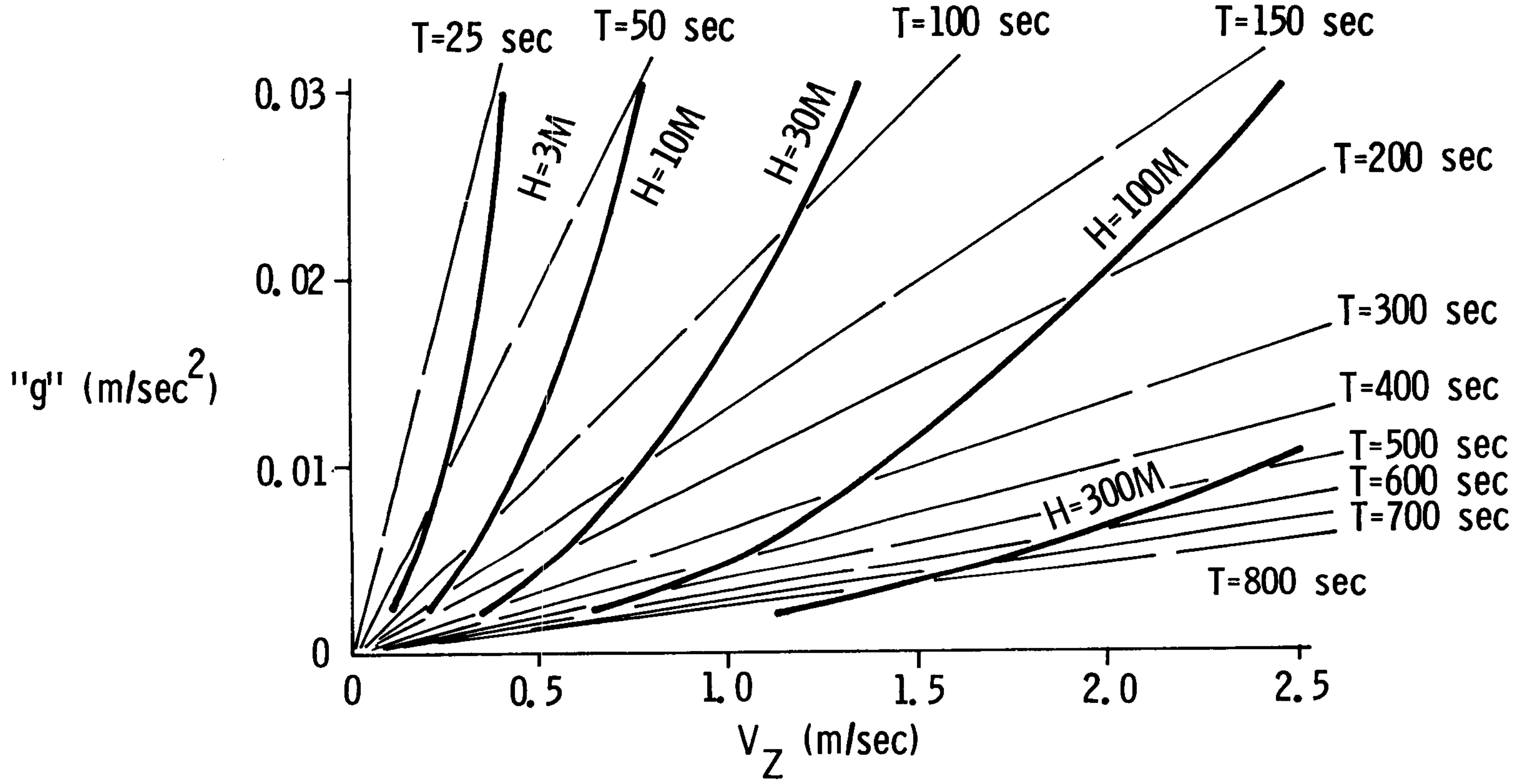

Sequence:

(1) Input V_Z Sufficient to Achieve Altitude (H) That Will Clear Terrain Obstacles in Path

(2) Input V_X Sufficient to Reach Destination Before T Elapses

(3) Input - V_X to Stop V_X at Destination

(4) Input Retro V_Z to Reduce Landing V_Z to Permissible Level

(5) Maintain Attitude Control Throughout

Figure VI-9 Velocity/Altitude/Time Curves for Phobos/Deimos Flying Rover

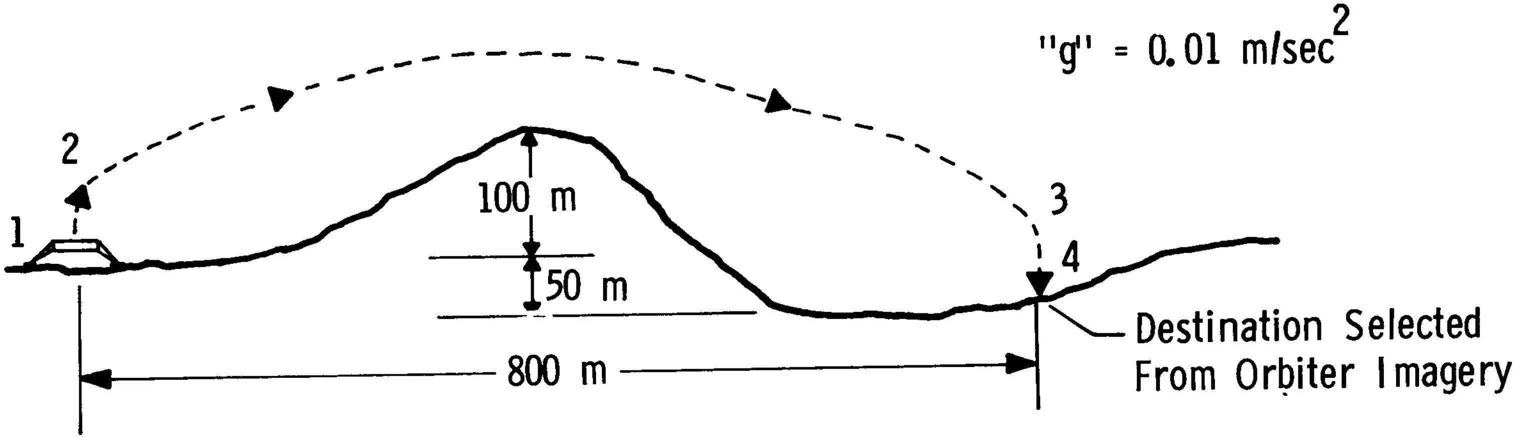
"g" = 0.01 m/sec^2
1
2
3
4
100 m
50 m
800 m
Destination Selected From Orbiter Imagery

(1) ΔV_Z = 1.5 m/sec To Clear 100 m Obstacle (Gives T=300 sec)
(2) ΔV_X = 2.7 m/sec To Traverse 800 m During T
(3) ΔV_X = 2.7 m/sec To Stop V_X Over Destination (Descent Velocity is Now 1.5 m/sec at an Altitude of 50m Over Destination. Descent Velocity Will Increase to 1.8 m/sec During 50m Drop)
(4) ΔV_Z = 0.8 m/sec to Reduce Landing Velocity to 1.0 m/sec

Total ΔV = 7.7 m/sec (1.9 kg of Fuel)

Figure VI-10 Flying Rover Example

site alteration by the main vertical thrusters. For this type of operation, an additional ΔV_Z of 1.5 m/sec would be used to stop descent at point 3 in the Figure VI-10 example. The rover would then free-fall to the surface, impacting 100 seconds later with a velocity of 1 meter per second. This sequence eliminates the final ΔV_2 shown, giving a new increase of 0.7 m/sec form a total ΔV of 8.5 m/sec and consumption of 2.1 kg of fuel.

C. DEPLOYABLE BOOM INSTRUMENT MOBILITY

Several extendible/retractible boom constructions have been developed over the past decade. For multiple extension/retraction cycles reel stored configurations have demonstrated good performance characteristics. Typical of these configurations is the Bi-stem configuration developed by SPAR Aerospace Corporation. Table VI-3 presents structural characteristics of different size booms constructed from beryllium copper and stainless steel. These two materials are commonly used for extendible booms since they exhibit a high ratio of yield strength to Modulus of Elasticity. The stainless steel construction provides a stronger structural member for less weight than the correspoinding BeCu construction. Thus, the following discussion will consider only stainless steel booms.

For science instrument deployment at the end of a boom, it is assumed that no roll torque will be produced. The critical parameters for defining maximum extension length are the critical bending moment at the boom root (M_{cr}) and the tip deflection (δ). It will not be desirable for the boom to push against the

Table VI-3 Extendible Boom Parameters

	CONFIGURATION		
	I	II	III
Tube Diameter (cm)	2.2	3.4	5.1
Critical Bending Moment (nt. m)	27.9	122.0	406.0
Mass Per Unit Length (kg/m)	0.13	0.3	0.6
Flexural Stiffness (nt. cm^2)	2.0×10^6	8.6×10^6	57.6×10^6
Extension Force (nt)	29.9	54.1	99.3
Energy Expenditure Per Unit Length (w. hr/m)	0.05	0.08	0.15
Power Required Per Unit Extension Velocity (w. sec/m)			
Average	42	76	136
Peak	49.4	90	164

surface since column buckling might occur or the force exerted by the boom might push the lander across the surface or tip it over. This the boom tip must be maintained above the surface.

1. Bending Moment

The bending moment at the boom root will be the sum of the moments due to the instrument mass, the boom mass, and the mass of the instrument cable. The instrument cable will be assumed to consist of ten #30 leads resulting in a mass of 7.5×10^{-3} kg/m. The boom mass is given in Table VI-3. The resultant moment expression is:

$$M_{tot} = M_i gL + M_{bc} gL^2/2.$$

Where: M_i = instrument mass (kg)

M_{bc} = boom + cable mass per unit length (kg/m)

L = boom extension length (m)

g = gravitational acceleration (m/sec^2)

In actual practice, the value of M_{tot} should not exceed 80% of the critical bending moment.

2. Deflection Characteristics

The tip deflection of extendible booms loaded with an instrument should be kept reasonable small to maximize the actual reach. Deflection of the tip due to load and boom weight may be determined from the expressions:

$\delta_1 = \frac{PL^3}{3}$; $_2 = \frac{WL^4}{8}$ where δ_1 = deflection due to tip load (cm)

δ_2 = deflection due to boom and cable load (cm)

λ = flexural stiffness (nt cm^2)

W = weight per unit length (nt/m)

P = instrument load (nt)

Boom tip deflection as a function of length for instrument mass up to 10 kg is shown in Figure VI-11. In order to keep the boom tip from contacting the surface, the boom deployment mechanism must be rotated up as the boom is extended. The pitch angle required at the boom root may be approximated by assuming that the deflected boom represents an arc of a circle. The tip slope angle (α) may be determined from the expression:

$$\alpha = \frac{WL^3}{6} + \frac{PL^2}{2}$$

Referring to the diagram below, this angle will be the angle subtended by the deflected boom. Using this angle the chord length (C) may be calculated as:

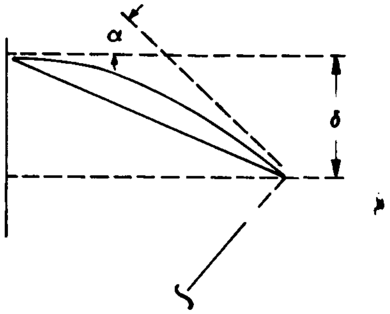

$$\alpha = L/R$$
$$C = 2R\,\mathrm{Sin}\,(\alpha/2)$$

$$C = \frac{2L}{\alpha}\,\mathrm{Sin}\,(\alpha/2)$$

The required base evaluation angle will then be:

$$\theta_r = \mathrm{Sin}^{-1}(\delta/C)$$

This angle is shown in Figure VI-11 as a function of boom length for a 10 kg instrument mass.

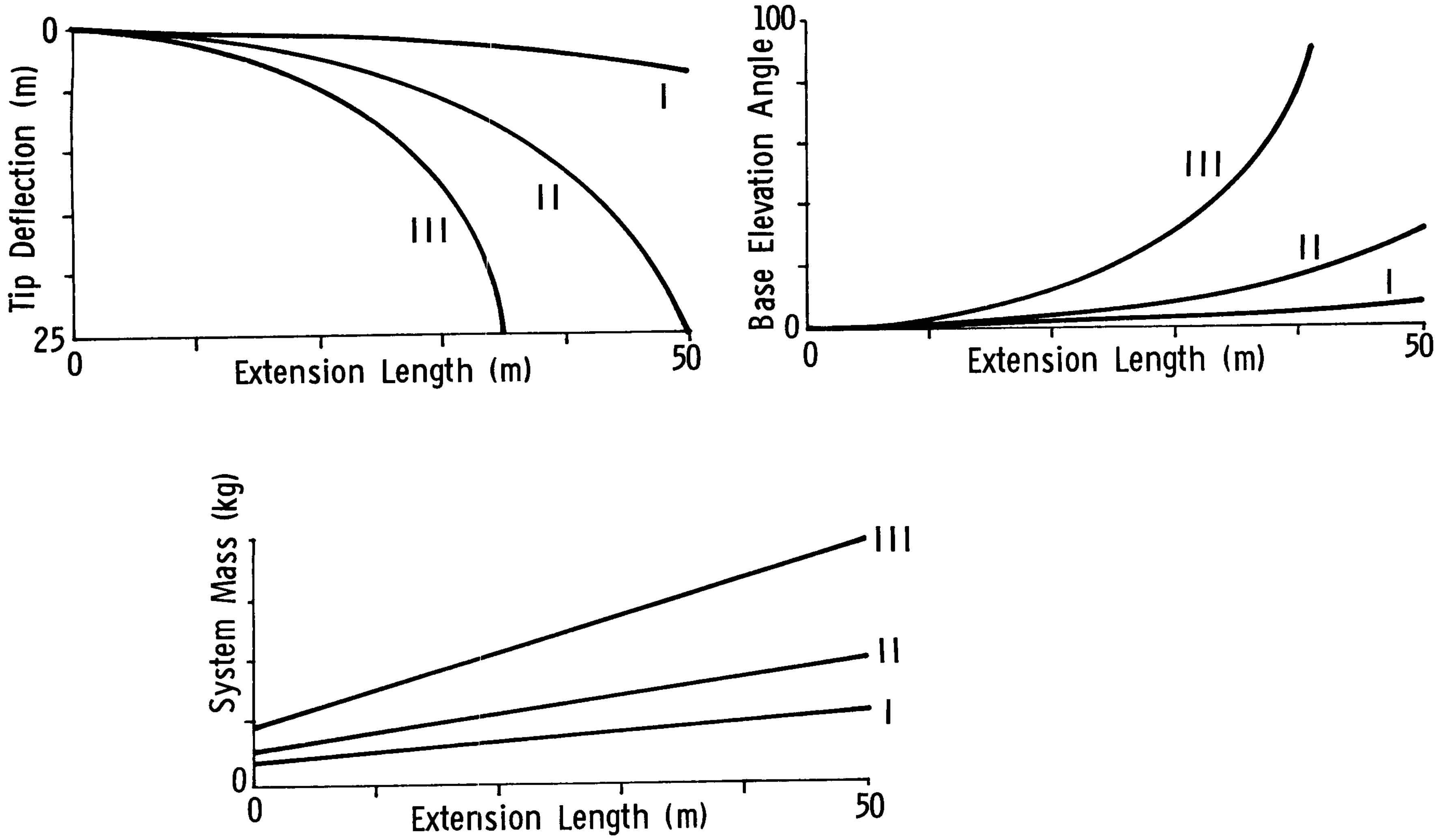

Figure VI-11 Extendible Boom Characteristics

3. Power Requirements

The energy expended during each deployment cycle will equal the product of a total extension length times the sum of retraction and extension forces. It will be assumed that the forces associated with the cable will be one tenth of the boom forces. Energy associated with elevating the boom will be negligible. The energy required will vary from 1.1 w•hr to 3.8 w•hr for boom diameters between 2.18 and 5.1 cm. Power required can be obtained by multiplying energy times desired extension velocity.

4. Weight Impact

The payload mass increase due to incorporation of a boom included the cable deployment mechanism, cable, boom, and boom deployment mechanism. Estimated mass of the cable deployment system is 10 kg. The cable mass is assumed to be 7.5×10^{-3} kg/m as stated previously. The boom deployment mechanism mass varies as a function of boom diameter. The total delta mass of boom systems as a function of length is shown in Figure VI-11.

D. PHOBOS/DEIMOS ROVER NAVIGATION CONCEPT

In the design of a Phobos/Deimos Rover navigation system, it would be of great advantage from a reliability, cost, and time viewpoint if Viking Lander/Orbiter hardware could be used. Since this hardware includes inertial navigation equipment and imaging equipment, it appears to meet the state sensing requirements. That is, it will be able to sense changes in velocity in an inertial coordinate system and update that system from an external source. Most of the hardware that comprises the navigation system discussed herein is Viking equipment.

The Phobos/Deimos rover navigation system concept presented here consists of two vidicon cameras, an inertial measurement unit, an odometer, a computer, and a communication system, configured as depicted in the block diagram, Figure VI-12.

Each of the two cameras has two uses. One camera is used for stellar imaging and as one element in the range finder. The other camera is used for science and as the other element in the range finder. The stellar sensor vidicon camera is rigidly fixed to the inertial measurement unit truss. The truss assembly, however, can be gimballed to provide viewing access to a large region of the sky. The stellar data technique employed enables the readout of the presence of a star, its magnitude and location on the vidicon without having to process data on an empty region of the sky. The system is compatible with the data rate limitations implied by RF communication or onboard data processing. The readout beam is driven via a D to A converter using a clock to generate the frame scan. When the threshold detector is crossed by a star the beam position in digital format is gated into a register. The peak level obtained is converted to a digital word, and the address and magnitude stored in temporary memory. Finally the data is either applied to the star catalog or communicated to Earth.

If suitable stars are not detected in the course of the scan, the truss (and camera) are rotated and the scan process repeated. Waiting a short time would also bring the other stars into the field of view. Shutter and lens controls will be applied (probably from earth) to negate the effect of smear due to Phobos high rotation rate and to permit the sensing of the

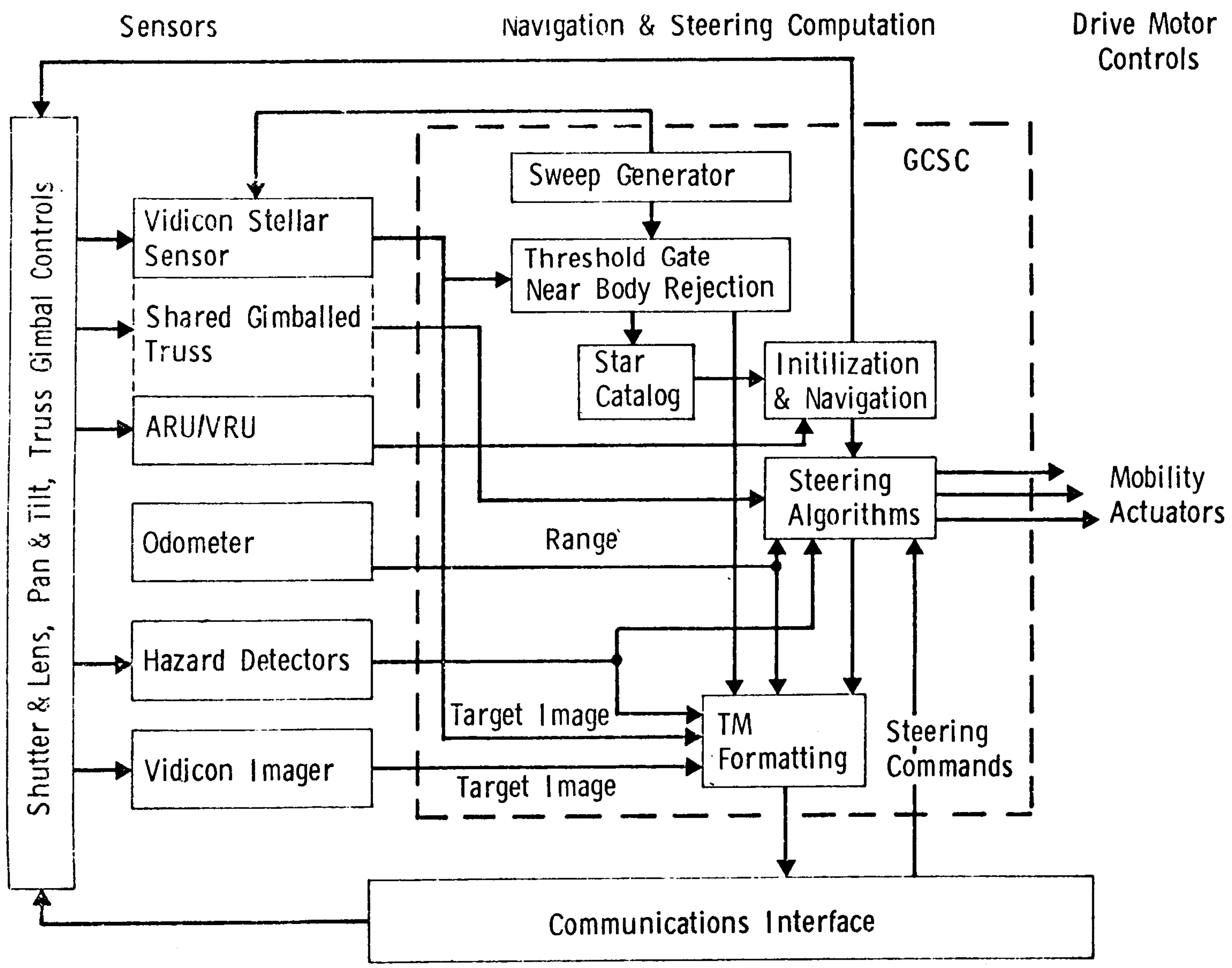
Sensors
Navigation & Steering Computation
Drive Motor Controls
GCSC
Shutter & Lens, Pan & Tilt, Truss Gimbal Controls
Vidicon Stellar Sensor
Shared Gimballed Truss
ARU/VRU
Odometer
Hazard Detectors
Vidicon Imager
Sweep Generator
Threshold Gate Near Body Rejection
Star Catalog
Initilization & Navigation
Steering Algorithms
Mobility Actuators
Range
Target Image
Target Image
TM Formatting
Steering Commands
Communications Interface

Figure VI-12 Rover Navigation System Block Diagram

bright Mars disk itself for navigational purposes. Several vidicons are currently under investigation; however, the Orbiter "A" camera system which will have been used as a stellar sensor in 1976 is baselined with the TV scan modified as discussed above. Figure VI-13 provides a sample of areas of the celestial sphere which were interrogated with this camera (Ref. VI-2).

The Attitude Reference Unit (ARU) and Velocity Reference Unit (VRU) are used as a strapped down inertial measurement unit (IMU) as in a normal Viking Lander operation. The VRU is also used as a gravitometer on Phobos. However, the gravitational attraction of Phobos is so low (assumed .003 to .0004 g) that the null uncertainty in these accelerometers may make them unsuitable for this purpose. However, higher quality space-qualified units are readily available. In traverse operations, the noise environment may swamp the changes in velocity from the VRU making it unsatisfactory as the source for obtaining range data. It may be more feasible to use the VRU as a vertical sensor and compute range as the swept out great circle range angle, or change in direction of local vertical, as obtained from the processed ARU data or from stellar data. A tactile or wheel odometer might aid in distance measurements. Track errors can be obtained as attitude errors by stopping and solving for special location of the local vertical vector.

The stereo range finder uses both cameras, a known base leg, and the required camera covergence angles (or electronic equivalent) to compute range. The operator on Earth controls the system and selects a distant target for traverse. (Using this system as an automatic area correlator navigation system while moving does not appear feasible, due to the varying light levels encountered over the slow traverse.)

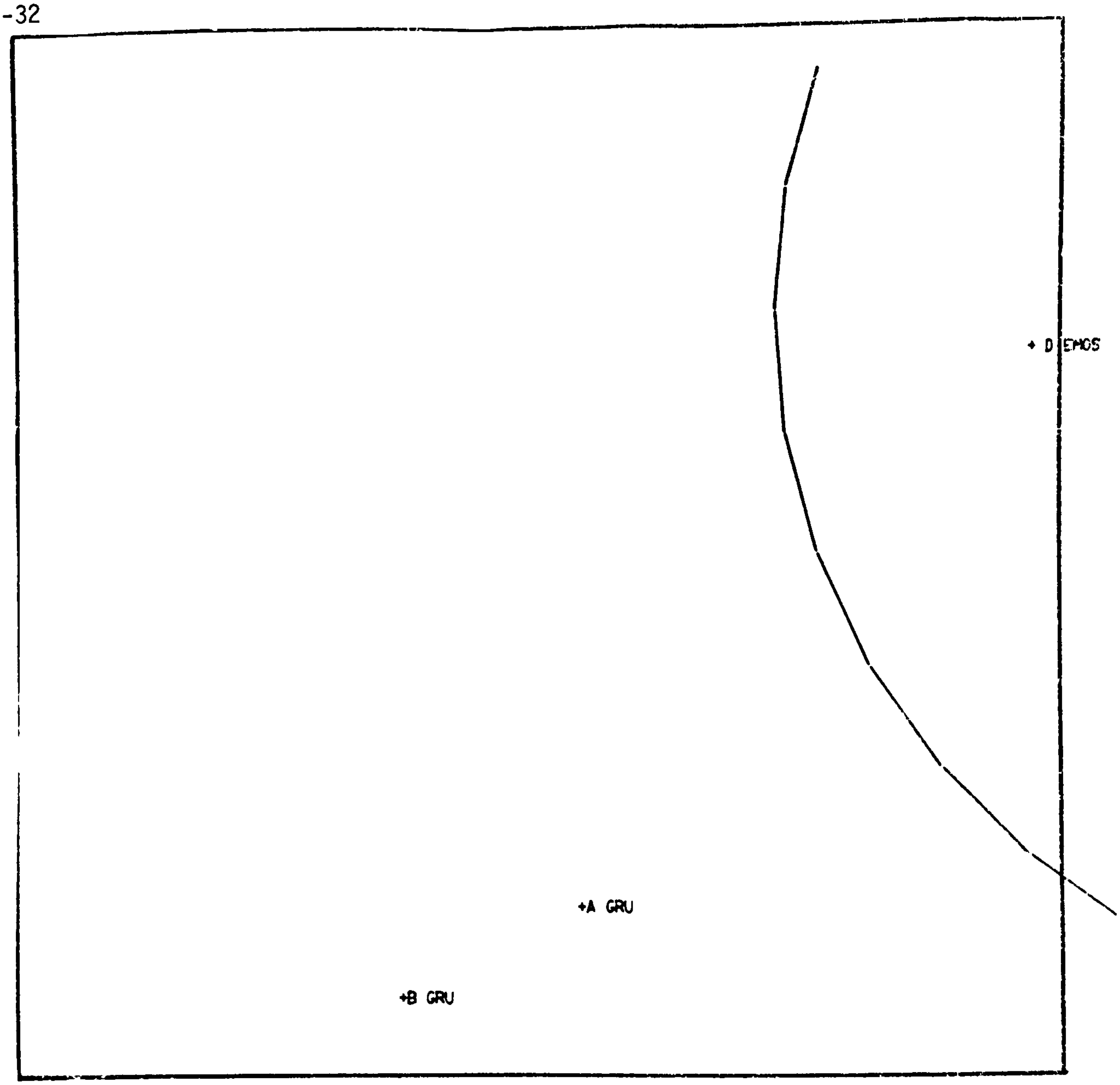

```
PICTURE NO.    2JULIAN DATE 2444514.5000000
```

```
CONE    90.0000 CLOCK    30.0000 TIME 2444514.5000000
VIEW VECTOR  6.74761752E-01      -6.33523451E-01      -3.78441410E-01
SATELLITE  DIEMOS     IS IN FIELD OF VIEW
STAR A GRU       HAS MAGNITUDE OF   2.2D
STAR B GRU       HAS MAGNITUDE OF   2.2D
```

Figure VI-13 Sample of Celestial Sphere from Phobos Surface

The steering logic is based upon commanded great circle traverse. The steering will compute range-to-go and heading errors. The steering logic block output will be signals to control the mobility system to drive range-to-go to zero and remove the effect of track errors. Track errors are probably best resolved by solving for a new great circle course which terminates at the target rather than returning to the old course.

The operational sequence would begin before landing when the camera is used to provide an attitude update to the inertial guidance system. This is done by obtaining a picture of Phobos against a stellar background and using the star data to update the direction cosine matrix stored in the airborne digital computer. (The direction cosine matrix is the electronic gimbal algorithm which makes a strapped down IMU appear to be a gimballed platform.) A position update is made via the deep space net.

The rover navigation sequence begins shortly after landing, as follows: The accelerometer triad, which constitutes the VRU, is used to establish the magnitude and direction of the Phobos local gravity vector; the direction is defined as vertical. The celestial sphere is then interrogated to establish the angles between three known stars and local vertical. The vidicon used is rigidly mounted to the truss which contains the accelerometers so that the angular relationship between the vidicon axis and each accelerometer input axis is known and preserved. The intersection of the position circles derived from the stellar data provided a unique position solution as shown in Figure VI-14. The stellar angular data is again used to update the direction cosine matrix stored in the onboard computer. The stellar data can also be used to determine the direction and magnitude

ESTABLISH INITIAL CONDITIONS
- Update Attitude Reference
- Locate Phobos Spin Axis
- Define Local "g" Direction & Magnitude
- Find Position on Phobos

SELECT TARGET
- Via Video Image -or- Preselected Sites -or to- Communication Region

COMMAND TRAVERSE
- Transform Target Coordinates to Heading Angle and Range to go
- Compute Compensation Coefficients,
- Steer Great Circle Using ARU, VRU, Optical & Odometer Feedback

UPDATE
- Stellar Update for Attitude & Position
- Video Update to Desired Target

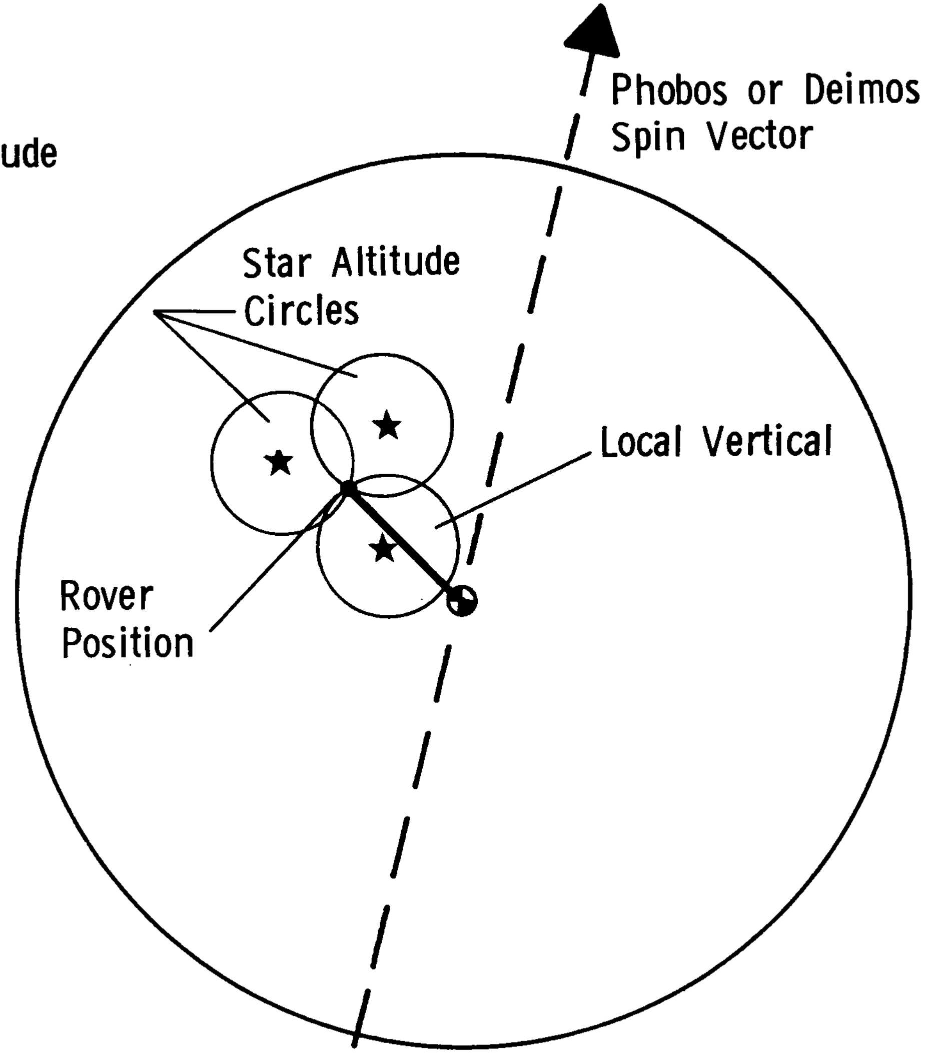
Phobos or Deimos Spin Vector
Star Altitude Circles
Local Vertical
Rover Position

Figure VI-14 Rover Navigation Functional Description

of Phobos' spin vector very accurately . Having established initial position on Phobos and updated the inertial guidance system, the system can proceed to accept guidance commands. Several methods of command are available; preprogrammed traverse, adaptively from local scientific results, or from the Earth based control as the result of a desirable target observed with rover or orbiter camera. For any case the command will be in the form of a great circle path constraining range (or great circle range angle) and nulling track errors. When the inertial navigation system indicates the range traverse has been achieved, the rover will be stopped and a "fine" check made with the stellar vidicon. The attitude reference system will again be updated at this time.

It should be noted that in certain cases the images of the near bodies, Mars and Deimos, will be available and possibly more convenient for navigational purposes than stellar data.

E. PHOBOS/DEIMOS ROVER COMMUNICATIONS

The mission to Phobos was considered to be the baseline mission during the course of this study. Two communications concepts were studied in detail: 1) direct Phobos surface to Earth link, and 2) relay through orbiter. Figure VI-15 summarizes the geometry and assumptions for these links. In each case communications systems evaluated were constrained to basic Viking Lander systems with minimum modifications allowed. Minimum modifications that were allowed were: 1) operation x-band, and 2) variations in antenna configuration. Figure VI-16 illustrates data volumes available per Phobos orbit for the

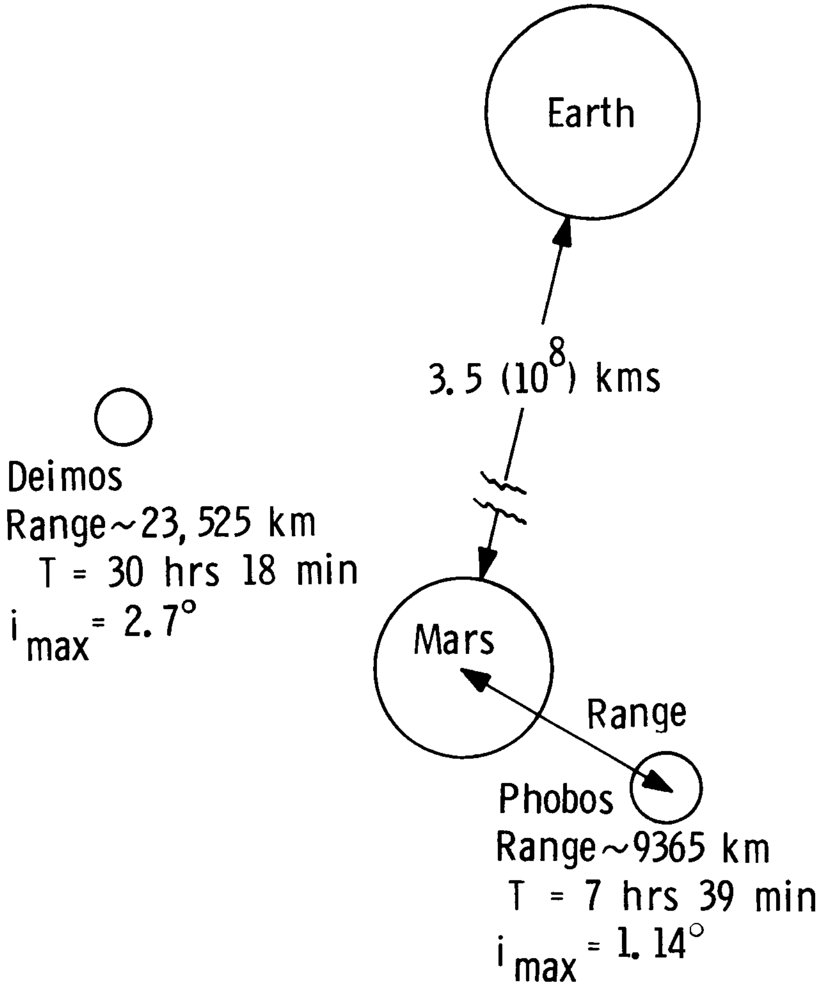
Earth
$3.5\ (10^8)$ kms
Mars
Range
Deimos
Range ~ 23, 525 km
T = 30 hrs 18 min
$i_{max} = 2.7°$
Phobos
Range ~ 9365 km
T = 7 hrs 39 min
$i_{max} = 1.14°$

CONSTRAINTS & ASSUMPTIONS

Landing Date ~ 10/1/80

Maximum Planetary & Satellite Occultation ~ 1.1 Hours/Orbit

Maximum Terrain Look Angle Limitations ~ 25°

DSN Reception

Figure VI-15 Communication System Geometry, Constraints, and Assumptions

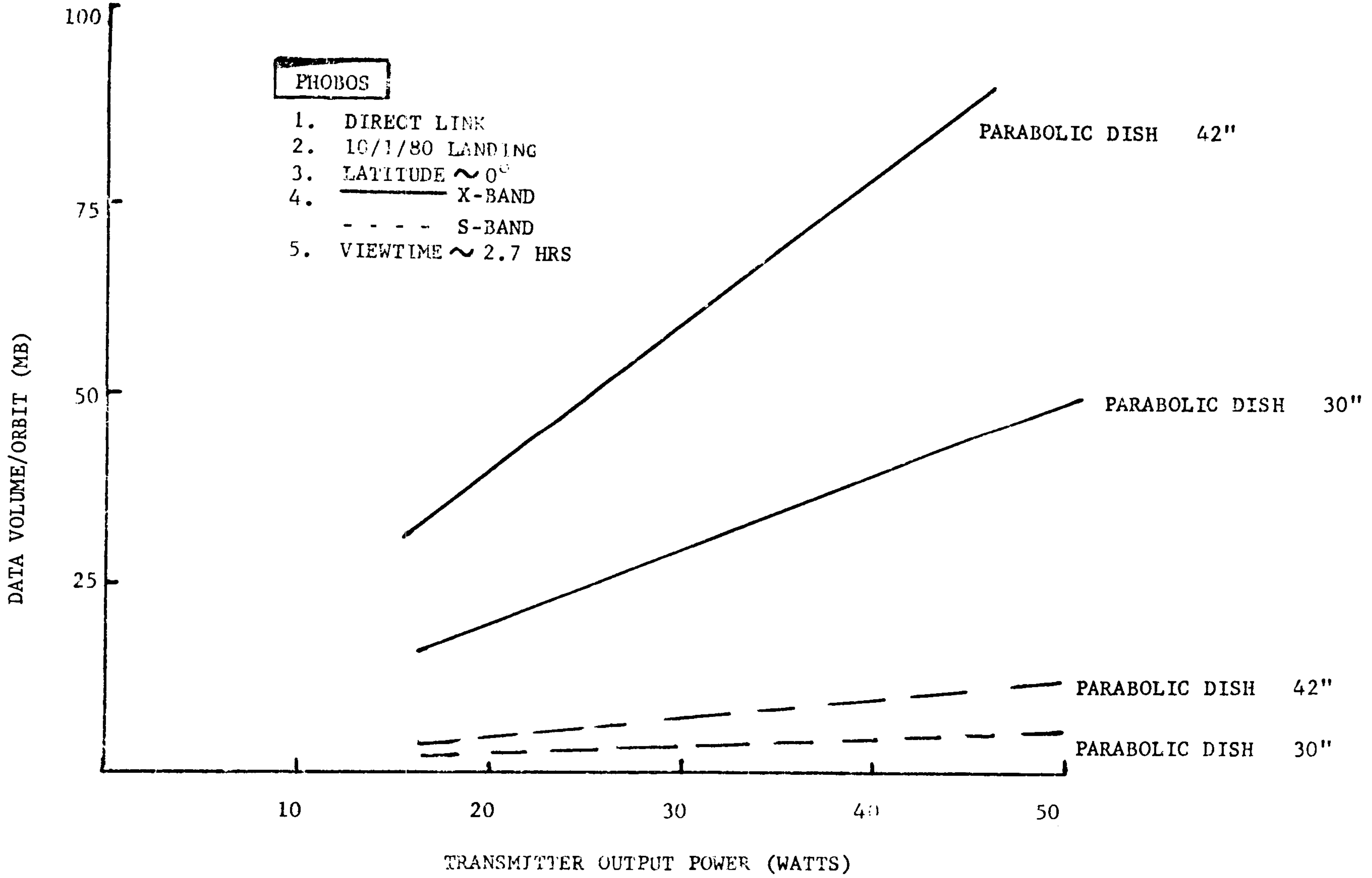

Figure VI-16 Candidate Communication System Performance

baseline system and with the aforementioned modifications in a direct link mode.

The orbital mechanics of the Mars/Phobos/Deimos system present problems when attempting to establish direct link communications from the surface of Phobos. Earth occultation, as seen from the landing site, is largely a function of date and Phobos latitude. Figure VI-17 presents the advantages of rover operations on Phobos over that of a fixed lander when the roving path is planned to optimize Earth view time/orbit.

The analysis performed on the relay through the orbiter was also limited by the desire to operate with baseline Viking systems allowing the same minimum modifications, as presented above, to the orbiter.

The orbiter is placed in an orbit around Mars very similar to that of Phobos. The orbit is such that the orbiter appears to orbit Phobos once every 7.5 hours. A cavity backed cross slot was selected as the URV antenna due to its large HPBW (130°). This antenna and the dynamics of the system allows a two (2) hour communication window between the orbiter and rover each Phobos orbit. The capability of the rover system (power modification) as a function of orbiter range is presented in Figure VI.-18 and the communication systems characteristics are summarized in Table VI-4. If data rates at the three (3) db point are desired, the illustrated values may be divided by eight (8).

The two communications techniques felt most promising are shown in Table VI-5 for the Phobos mission. In the direct link configuration output power is limited to 40 watts due to landed weight considerations. The antenna size was considered

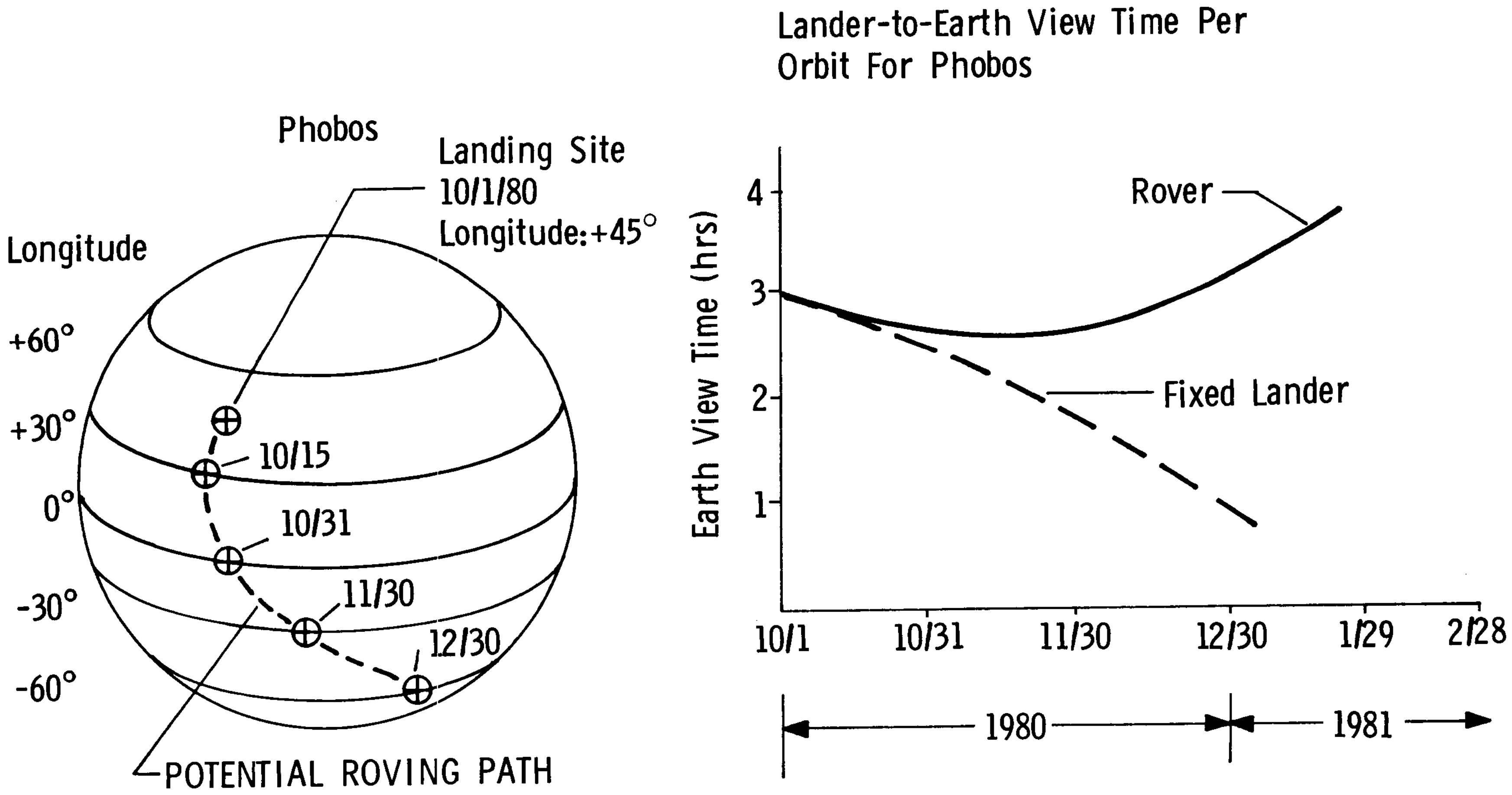
Lander-to-Earth View Time Per Orbit For Phobos

Figure VI-17 Phobos Mobility/Communication Interaction

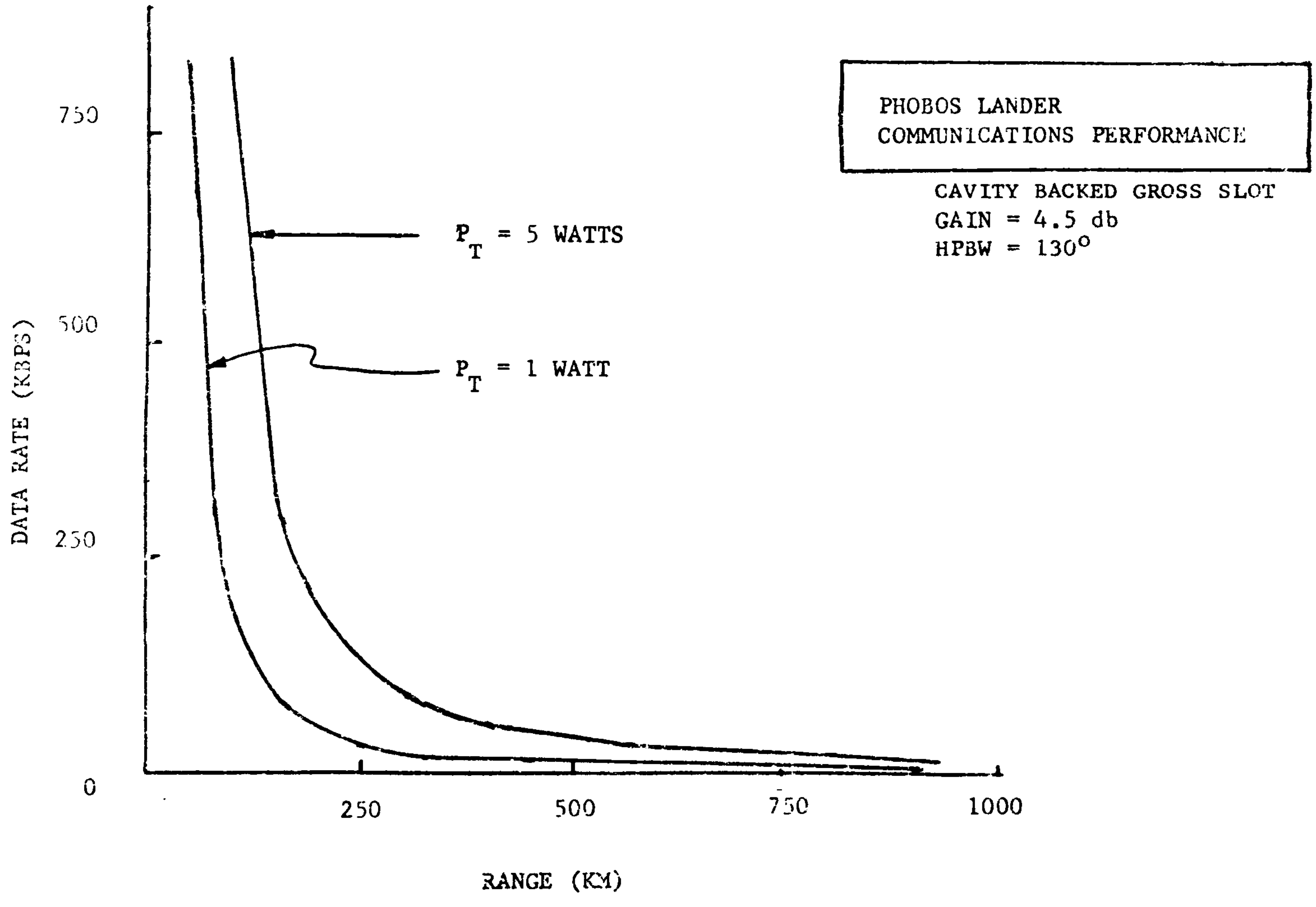

Figure VI-18 Lander/Orbiter Communication System Performance

Table VI-4 Communication System Characteristics

Command Rate ~ 50 Bps
Error Rate: 10^{-6}

Lander Data Rate ~ 160 Kbps (UHF)
Error Rate: 10^{-2}

Orbiter Data Rate ~ 64 Kbps (X-Band)
Error Rate: 10^{-2}

Lander Antenna Type: Cavity
Backed Cross Slot (4 db)

Orbiter Antenna Type:
Parabolic (58" Diameter,
g=41 db)

Lander Antenna Pointing:
HPBW = 130°, Pointing Req'd
if Above Latitude of $|\text{Lat}| = 65°$

Orbiter Antenna Pointing:
HPBW = 1.2°

Lander Communication System
Size: 1350 In^3 (Includes Antenna)

Communications System
Weight: 46.1 lbs

Lander Power Requirements
$\left.\begin{array}{l}\text{In} \sim 5 \text{ Watts}\\ \text{Out: } 1 \text{ Watt}\end{array}\right\}$ ERP= 4.5 db

Orbiter Power Requirements
$\left.\begin{array}{l}\text{In} \sim 200 \text{ Watts}\\ \text{Out: } 40 \text{ Watts}\end{array}\right\}$ ERP= 57 db

DSN Reception

Table VI-5 Comparison of Direct Link vs Relay through Orbiter Communication System Performance

DIRECT LINK

Configuration	Data Rate	
	S-Band	X-Band
(1) Output Power~20 Watts 30" Parabolic Dish	250 Bps	2 KBps
(2) Output Power~40 Watts 30" Parabolic Dish	500 Bps	4 KBps
(3) Output Power~40 Watts 42" Parabolic Dish	1 KBps	8 KBps

Maximum Data Volume/Orbit
From Above ~ 100 MB

RELAY THROUGH ORBITER

Lander/Orbiter

Output Power~1 Watt
Cavity Backed Cross Slot (4db)
Data Rate~160 KBps
Range ~ 125 km
Two Hour Transmission
Data Volume~1150 MB

Orbiter/Earth

X-Band Transmission
58' Parabolic Antenna
Output Power~40 Watts
Data Rate ~ 64 KBps
Earth View Time/Rev~6.65 Hr
Data Volume/Rev~1550 MB

maximum because of resulting pointing requirements (HPBW = 1.8°).

Note that the maximum data rates assume x-band transmission. Earth bound atmospheric conditions may make x-band transmission impractical. Dual feeds (S- and X-band) should be provided. The maximum data volumes at s-band would be approximately 1/8 of those illustrated.

The communications profile in Figure VI-19 illustrates the advantage, in terms of data volume, of utilizing existing orbiter capabilities with modification to operate at x-band. Orbiter relay at s-band is distinctly preferable to direct link performance at x-band due to high direct link power and antenna pointing requirements. Note that orbiter data volumes/orbit exceeding 1200 MB are possible only with simultaneous reception and relay transmission. However, assuming 6.65 hours/orbit available for relay, data volume for the previous system will be limited by a maximum of 1580 MB/orbit.

F. MOBILITY STUDY CONCLUSIONS

Analysis of wheeled, flying, boom-deployed science mobility leads to the conclusion that wheeled mobility is the best mode to incorporate into the landed system. The wheeled rover offers significant advantages over flying in the areas of weight, controllability, and opportunity for adaptive science. The only factor favoring flying is its ability to cross gross terrain obstacles (cliffs, ridges, crevices) that would require major detours with a wheeled system.

Furlable booms offer a practical means of getting short range

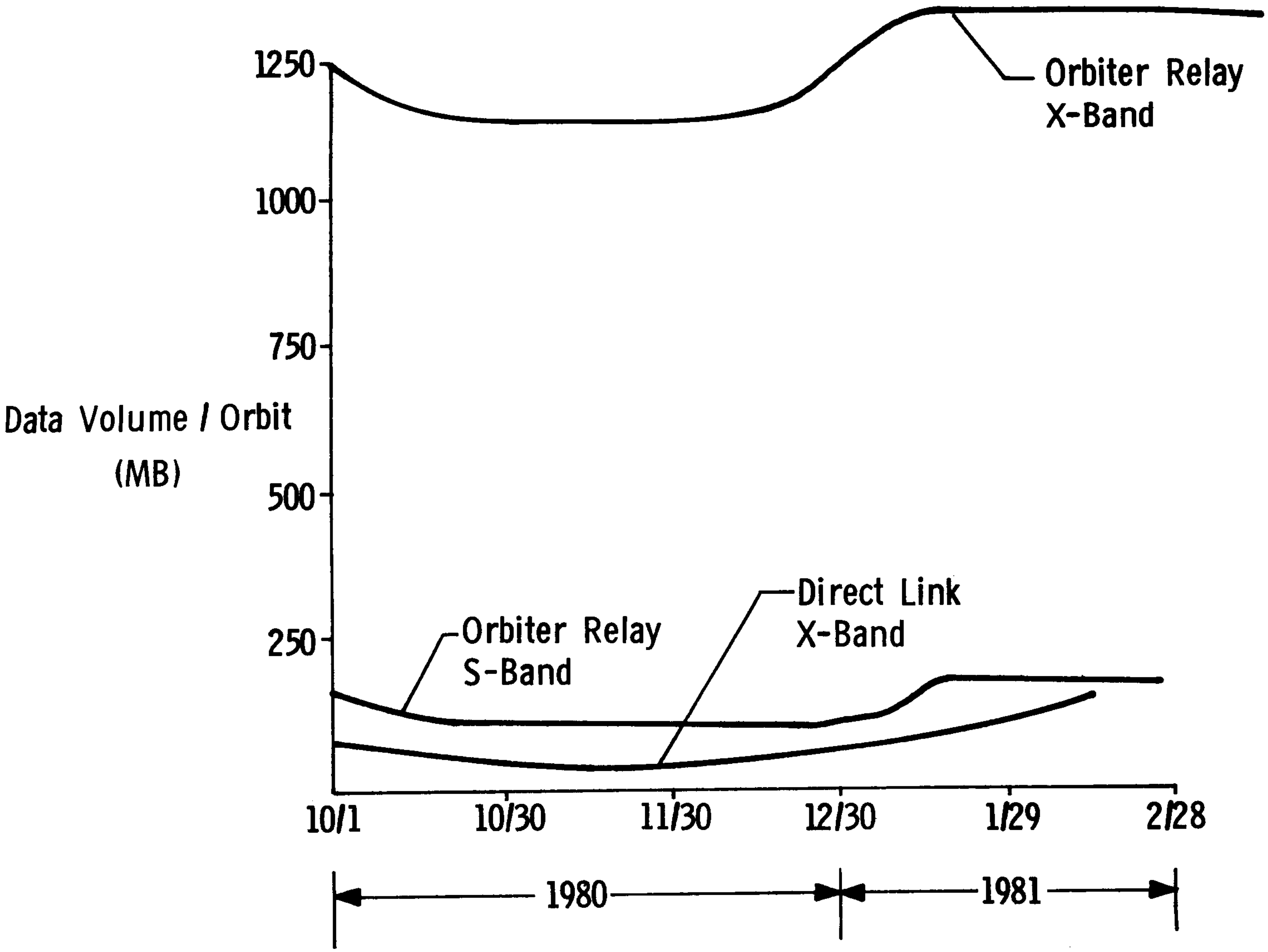

Figure VI-19 Communication Profile/Phobos Rover

(50 m) mobility and could be considered for a stationary lander mission. However, the weight penalty associated with booms is equal to the weight penalty of the wheeled mobility subsystem. Of the many factors influencing the choice of mobility mode, only projected development risk/cost favors booms.

REFERENCES

VI-1 MMC Document S-71-48571-002, Unmanned Roving Vehicle Mobility Dynamics Digital Simulation Model, D. M. Adams, December 1971.

VI-2 MMC Document S-71-48571-003, A Navigation Concept for Unmanned Roving Vehicles on Phobos, A. L. Brooks, December 1971.

VII. Program Costs

VII PROGRAM COSTS

The cost summary for the baseline sample return mission in FY '72 dollars (no escalation factors added) is based on the ground rules listed in Table VII-1. The cost estimate has been built up using a work breakdown structure patterned after the Viking '75 Lander System. This WBS contains over 80 elements of cost. Labor and material estimates were made for each of the WBS elements. Table VII-2 summarizes the baseline sample return program cost. Two previously developed program estimates were used as references and calibrations for this estimate: 1) the Viking '75 program (which should have higher costs for equivalent elements because of the completely new developmental nature of the work), and 2) the Viking '77 program (which should be lower for equivalent elements because it involves minimum modification to existing designs.

A cost summary was also prepared in which the second flight spacecraft and the spare were eliminated. The cost savings that would result are presented in Table VII-3.

Table VII-1 Costing Ground Rules

Two Flight Spacecraft

One Spare Flight Spacecraft

F/Y '72 Dollars

Titan III D/Centaur Launch Vehicle

One System Contractor For Total Spacecraft

Non Interferance With Other Viking Programs

Maximum Inheritance of Technology From Viking and Planetary Explorer Programs

Qual & Proof Test Evaluation Units

Sterilization Not Required

Use Modified V-75 Ground Equipment

Sample Recovery Not Costed

Table VII-2 Cost Summary - Baseline Sample Returm Mission

SPACECRAFT		288
Management and Technical Support	75	
Mission Analysis & Systems Engr & Integr	23	
Subsystem Development & Qualification		
Landed Orbiter	85	
Return Vehicle	66	
Systems Assembly and Test	12	
Launch and Flight Operations	27	
SCIENCE		35
OTHER NASA COST		79
LAUNCH VEHICLES		44
TOTAL		$446

FUNDING BY FISCAL YEARS

77	78	79	80	81	82	83	Total
25	86	112	94	53	40	36	446

Table VII-3 Cost for One Flight Article With Minimum Spares ($ in Millions)

	Baseline	Option Δ	New Cost
SPACECRAFT	288	<38>	250
SCIENCE	35	<3>	32
OTHER NASA COST	79	<9>	70
LAUNCH VEHICLE	44	<22>	22
TOTALS	446	<72>	374

VIII. Program Schedule

VIII PROGRAM SCHEDULE

The summary schedule shown in Table VIII-1 indicates the key milestones and span times for the Phobos/Deimos sample return program from SRT, which begins in January 1974, MA & D long lead, and full go-ahead in the third quarter of 1976, through launch in the fourth quarter of 1981. Mission duration after launch will be approximately 1000 days.

The basic assumptions and groundrules used in the development of this schedule are:

(1) Target launch date is 9 December 1981 with a nominal launch window of 30 days.

(2) Two flight and one spare flight spacecraft

(3) One system contractor for total spacecraft

(4) Use of modified Viking '75 ground equipment

(5) Qualification and Proof Test Evaluation units are used.

The schedule has been patterned after the Viking '75 Project Master Schedule. Major development and development testing activities will be required to accomplish the orbiter modifications, Planetary Explorer modifications, sample collection and protection system, and the return entry capsule.

Table VIII-1 Phobos Sample Return Mission

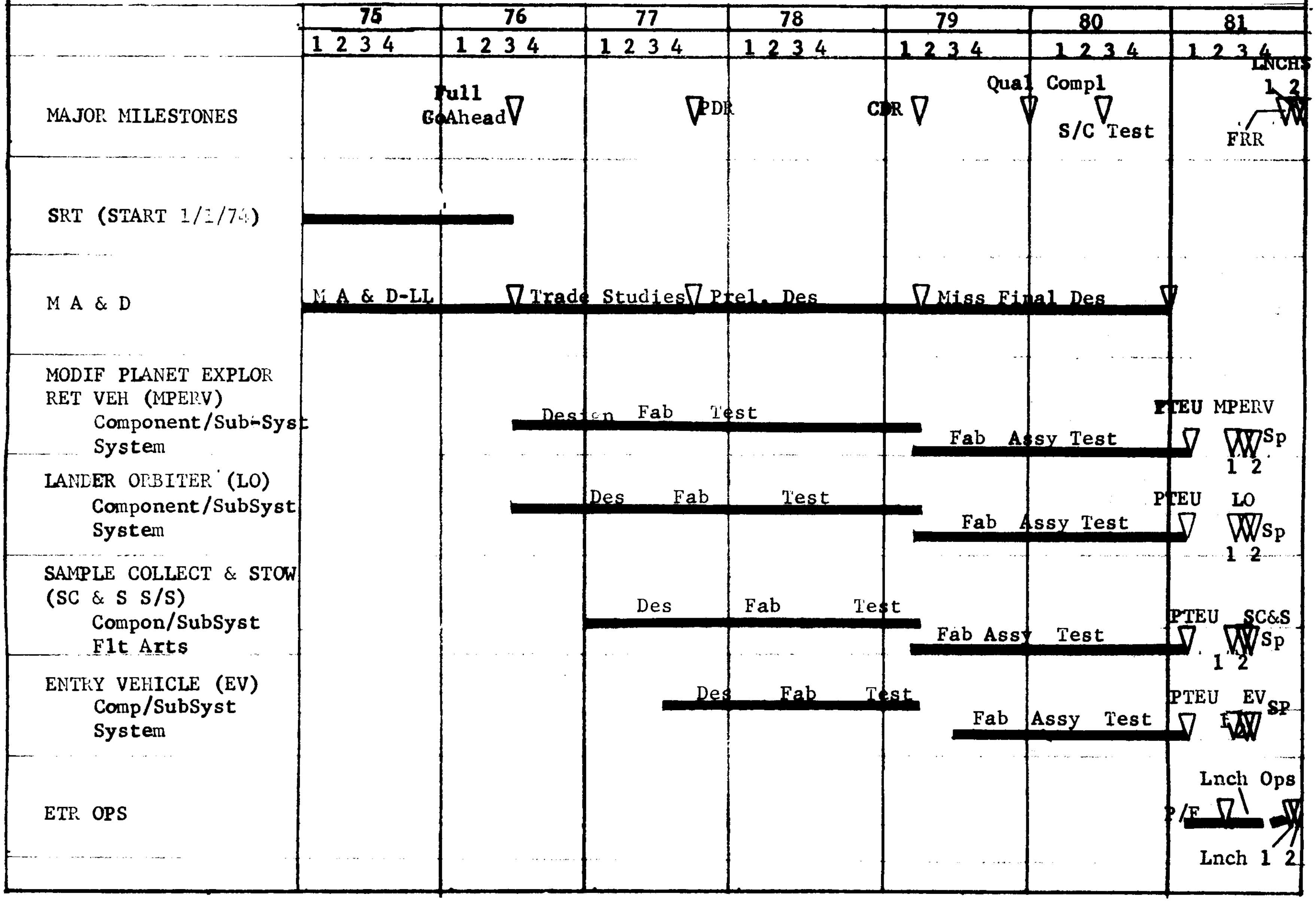

IX. Conclusions

IX. CONCLUSIONS AND TECHNOLOGY REQUIREMENTS

The principal conclusions drawn from the Phase II study are summarized in this section.

This study has demonstrated the feasibility of using a minimally modified Viking Orbiter to deliver a sample return vehicle to Phobos in the 1979-1983 time period. For the baseline mission chosen, a Titan IIIE/Centaur launch vehicle has the capability to launch a sample return spacecraft that can return 5 kg of surface samples via direct Earth entry with sea recovery. Mariner, Planetary Explorer and Mars Viking hardware and technology were found to be adequate to meet all the spacecraft systems and subsystems requirements.

No high-risk technology problems were identified in the various subsystem mechanizations that were examined. During the course of the study, however, several technology requirement areas were identified. Supporting research and technology (SRT) work performed in these areas would be beneficial in building confidence in mission flexibility and reducing possible development risks. These studies are identified in Table IX-1 and described in the following paragraphs.

Table IX-1 Recommendations for Further Study and Technology Requirements

Further Study

Space Shuttle Applications to Sample Return Missions
Navigation Analysis for Sample Return Missions
Communications System Analysis for Sample Return Missions
High Speed Earth Entry Analysis
Long-Life Reliability of Spacecraft Subsystems and Components

Technology Requirements

Light-Weight, Low-Power 3-Axis and Closed-Loop
Spin Stabilized G&C Subsystems
Sample Collection and Protection Subsystems
Automatic Spacecraft Alignment and Ascent Guidance Subsystems

A. SPACE SHUTTLE APPLICATIONS TO SAMPLE RETURN MISSIONS

Use of the Space Shuttle concept would allow greater payloads for the Phobos/Deimos sample return mission. The Space Shuttle could also be used to collect the Phobos/Deimos sample return module from an Earth orbit, thus eliminating any concern for contamination.

B. NAVIGATION ANALYSIS FOR SAMPLE RETURN MISSIONS

The sample return mission from Phobos/Deimos utilizes a light-weight spin-stabilized vehicle. A more extensive navigation analysis would increase the probability of a successful mission and most likely reduce the ΔV expenditure allocated for navigation uncertainties.

C. COMMUNICATION SYSTEM ANALYSIS FOR SAMPLE RETURN MISSION

The use of the spin stabilized, light-weight spacecraft for the Earth return mission presents some difficult design problems for the communication system. An optimum system would have a lower chance of failure and therefore increase the mission success probability.

D. HIGH SPEED EARTH ENTRY ANALYSIS

The sample return mission design utilizes a direct entry mode. This results in entry velocities of approximately 12.65 km/sec as compared to the Apollo program's maximum entry velocities of 11.06 km/sec. This additional velocity at entry would require a comprehensive analysis prior to the final design of the entry capsule. Conservative design guidelines have been used in this study and additional study could decrease ablator weight and increase the probability of success.

E. LONG-LIFE RELIABILITY OF SPACECRAFT SUBSYSTEMS AND COMPONENTS

Phobos/Deimos mission success is obviously dependent on the reliability of the spacecraft and the sample return vehicle. Other factors affecting mission success are the requirements for complex maneuvers, the long term operation of the spacecraft and sample return subsystems, the number of launch opportunities, and the technological developments required. Mission success is thus probablistic in nature and becomes an important study parameter in formulating various spacecraft and sample return design and operational concepts.

Typically, the reliability program plan involves the following steps:

1) Establishment of reliability goals,
2) Allocation of reliability with respect to mission phases,
3) Establishment of subsystem/part reliability allocations and
4) Determination of failure modes effects.

Probably the most important of these steps is the latter. Failure mode identification and its effect on the spacecraft/ sample return vehicle probability of mission success is extremely useful as a criterion for the selection of system operational concepts, use of redundancy, diagnostic and engineering data requirements, and science experiment selection. A full understanding of potential system/subsystem failures and their effects on mission success is essential to optimize the balance of functional and equipment redundancy, command and control backup provisions, and status data requirements.

Since subsystems proposed for use in the Phobos/Deimos missions are being developed for programs presently in being (Viking) or proposed (Planetary Explorer) it is essential that continuing monitoring and sufficient program insight be maintained in order to comprehensively catalog failure modes and their effects in order of importance, together with an evaluation of possible design solutions.

F. LIGHTWEIGHT, LOW POWER, 3-AXIS AND CLOSED LOOP SPIN STABILIZED G&C SUBSYSTEM

The return of a surface sample from Phobos or Deimos to Earth requires a lightweight orbital and interplanetary cruise vehicle. Current small interplanetary vehicles (e.g. Pioneer or Planetary Explorer) use open loop spin-stabilized G&C subsystems with vehicle attitude data processed on the ground. While this approach is adequate for missions requiring very few maneuvers, the more complex Phobos/Deimos return flight could be done more accurately with a lightweight, low power, three-axis stabilized or a closed loop spin stabilized G&C subsystem.

These subsystems could be synthesized from state-of-the-art hardware and technology. SRT work could develop these concepts, and investigate integration, interfacing and operational problems.

G. SAMPLE COLLECTION AND PROTECTION

Techniques and equipment for the acquisition of surface samples are required based on the latest definition of the Mars surface. The objective of this activity is the development and test of planetary surface sample acquisition techniques and associated equipment. In addition, techniques to provide adequate canning and safe storage of the acquired Mars samples must be developed.

H. AUTOMATIC SPACECRAFT ALIGNMENT AND ASCENT GUIDANCE SUBSYSTEMS

A requirement of an unmanned sample return mission, such as one from Phobos or Deimos, is to accurately determine the location and attitude of the landed vehicle so that the ascent of the return vehicle can be successfully carried out. SRT work to design and develop an automatic leveling and training subsystem is recommended. Investigations into lightweight, low-power G&C subsystems to control ascent trajectory would also be beneficial to a Phobos/Deimos sample return mission concept.

Appendix

SRTRK PROGRAM DESCRIPTION

The SRTRK program was designed to simulate the three impulse transfers from Phobos or Deimos to Earth. The program determines the required C3 and DLA for the trans-Earth injection as a function of the launch and encounter date. The parameters for the intermediate orbit are input to the program. These are the circular altitudes of the satellite, the apoapsis altitude of the intermediate orbit, and the desired periapsis altitude for the final injection maneuver. The program uses these inputs and the injection requirements to determine the ΔV requirements for this transfer. In addition to this calculated ΔV, ΔV is allocated for the separation from the satellite, gravity and steering losses, navigation uncertainties and midcourse maneuvers. The sequence of orbital events are as follows:

1) Raise apoapsis to the input value--typically 95000 km.
2) Lower periapsis to the input value desired for the trans-Earth injection.
3) Calculate the required plane change to place the required departure vector in the orbit plane.
4) Increase the velocity at periapsis to yield the required C3.

The ΔV for these maneuvers and the additional ΔV are combined. The propellant required to provide this ΔV for the fixed initial weight is calculated. The propulsion system weight is then calculated and the remaining weight is available for the spacecraft. This information is printed out in addition to the departure conditions. The program now calculates the ΔV to get the spacecraft into a specified capture orbit at Earth and re-calculates the required propellant propulsion system weight and spacecraft weight.

The result is two spacecraft weights for each launch and encounter date, one indicating the spacecraft weight for a direct entry at Earth and the other for capture into a specified Earth capture orbit.

The results of the data generated by this program allow the selection of a launch and encounter space yielding a maximum spacecraft weight.